NEW DIAZO REAGENTS AND APPLICATIONS OF β-LACTONES FOR SYNTHESIS AND BIOLOGICAL EVALUATION OF NATURAL PRODUCTS

A Dissertation

by

SUPAKARN CHAMNI

Submitted to the Office of Graduate Studies of
Texas A&M University
in partial fulfillment of the requirements for the degree of

DOCTOR OF PHILOSOPHY

December 2011

Major Subject: Chemistry

New Diazo Reagents and Applications of β-Lactones for Synthesis and Biological

Evaluation of Natural Products

NEW DIAZO REAGENTS AND APPLICATIONS OF β-LACTONES FOR

SYNTHESIS AND BIOLOGICAL EVALUATION OF NATURAL PRODUCTS

A Dissertation

by

SUPAKARN CHAMNI

Submitted to the Office of Graduate Studies of
Texas A&M University
in partial fulfillment of the requirements for the degree of

DOCTOR OF PHILOSOPHY

Approved by:

Chair of Committee,	Daniel Romo
Committee Members,	David E. Bergbreiter
	Coran M. H. Watanabe
	Thomas McKnight
Head of Department,	David H. Russell

December 2011

Major Subject: Chemistry

ABSTRACT

New Diazo Reagents and Applications of β-Lactones for Synthesis and Biological

Evaluation of Natural Products. (December 2011)

Supakarn Chamni, B.S., Thammasat University

Chair of Advisory Committee: Prof. Daniel Romo

Natural products are essential tools for basic cellular studies leading to the identification of medically relevant protein targets and the discovery of potential therapeutic agents. We have developed a set of second-generation diazo reagents with small steric footprints, namely an α-trifluoroethyl (HTFB) diazo reagent, for simultaneous arming and SAR studies of bioactive natural products. The Rh(II)-catalyzed O−H insertions of several alcohol-containing natural products, including the potent translation inhibitor lactimidomycin, are investigated and useful reactivity and both chemo- and site- (chemosite) selectivities are observed. The α-trifluoroethyl diazo reagents (HTFB) shows clear differences in the IL-2 reporter assay with FK506 derivatives and provides greater retention of biological activity in a hMetAP2 proliferation assay of fumagillol derivatives compared to the first generation *p*-bromophenyl diazo reagent (HBPA). The synthetic utilities of the new α-trifluoroethyl diazo reagent (HTFB) provide a great new tool for basic cellular studies facilitating the discovery of new drug candidates for human disease.

Furthermore, we are interested in methodologies for β-lactone synthesis and transformations. In this study, we demonstrated synthetic versatilities of β-lactones for the synthesis of β-lactam congeners of orlistat as fatty acid synthase inhibitors *via* $SnCl_4$-promoted tandem Mukaiyama aldol-lactonization (TMAL) reaction and a one-pot, mild conversion of β-lactones to β-lactams. The inhibitory activities of the derived β-lactam derivatives are determined in a biochemical fluorogenic assay using recombinant FAS-TE, and the micro-molar range FAS-TE inhibitory activities were observed.

Additionally, we pursued synthetic studies toward the total synthesis of spongiolactone, which is a unique β-lactone-containing marine diterpenoid, isolated from the marine sponge *Spongionella gracilis*. This natural product bears a unique tricyclic β-lactone core possessing four contiguous stereogenic centers and an additional stereogenic quaternary carbon on a cyclohexyl appendage. We completed the total synthesis of 6,15-bis-*epi*-spongiolactone by employing an intramolecular nucleophile-catalyzed aldol-lactonization (NCAL) process as the key step to construct the fused tricyclic β-lactone core. Importantly, we developed a double diastereoselective and, for the first time, a kinetic resolution *via* the NCAL process that enables an enantioselective strategy to the tricyclic β-lactone core of (+)-spongiolactone.

DEDICATION

To my beloved parents, Worranart and Sirin Chamni and sister, Nuanphan Chamni.

ACKNOWLEDGEMENTS

I would like to sincerely thank Prof. Daniel Romo, my advisor, for his guidance and support. It has been an excellent experience to work under his supervision. I really appreciate his time in teaching me not only an intellectual research, but also a life-lesson throughout my time at Texas A&M. Thank you for giving me such a great opportunity to expand my knowledge into several research areas during my Ph.D. studies. This opportunity has given me the wonderful chance to learn so much chemistry and increase my research skill and has given me the vision to support my future career as an academician.

I also would like to thank my committee members, Prof. David Bergbreiter, Prof. Coran Watanabe and Prof. Thomas McKnight, for their guidance and assistance throughout the course of this research. Many thanks also to Prof. Daniel Singleton, Prof. Brian Connell and, once again, Prof. David Bergbreiter for the excellent classes to advance my chemistry knowledge and assist my research.

Thanks also to both former and current Romo group members for their friendship, laughs, helps and discussions. It has been a great memorable moment to share with all of you. I would like to thank Dr. Wei Zhang, my research mentor who taught me excellent laboratory tricks. Much appreciation goes to Dr. Sung Wook Cho and Dr. Satyamaheshwar Peddibhotla for their initial studies toward my research. Thank you to Dr. Ke Kong, Gang Liu and Dr. Yonggang Wang for being great chemist-role models. Thanks to Dr. Henry Nguyen, as known as my uncle, for sincere friendship and

TABLE OF CONTENTS

Page

x

LIST OF FIGURES

LIST OF TABLES

CHAPTER I

INTRODUCTION TO METHODS FOR NATURAL PRODUCT

DERIVATIZATION

Over the past 50 years, the discovery and the study of novel natural products produced from diverse living terrestrial and marine organisms has had a profound impact on human health.[1] Indeed, natural products are an immense source of chemical diversity.[2] These complex molecules are capable of interacting with numerous human cellular proteins and typically have intrinsic cell permeability.[3] As a result, many natural products or natural product-inspired small molecules are currently in clinical use as antibiotics, antitumor agents, immunosuppressants, antiviral drugs, and enzyme inhibitors.[4] For example, Taxol isolated from the Pacific Yew tree, is currently used clinically for the treatment of ovarian and breast cancers.[5] Furthermore, natural products have a rich history as tools for basic cellular studies leading to the discovery of potential cellular targets for intervention of human diseases[6] and in this way contain enormous information content that should be fully exploited.

Gaining an understanding of the detailed mode of action of biologically active natural products, including the identification of putative protein targets, continues to be a highly useful strategy for the discovery of human therapeutics.[7] These studies are greatly facilitated by detailed structure-activity relationship (SAR) studies and the synthesis of

_____

This dissertation follows the style of the *Bioorganic and Medicinal Chemistry Letters.*

cellular probes derived from a particular natural product of interest. The choices of derivatization strategies normally depend on the reactive functional group on natural products. These cellular probes, which typically contain a functional group for *in vitro* or *in vivo* attachment of reporter tags such as biotin or a fluorophore, continue to be of great importance for such studies.[8]

1.1. Basic Technology of Cellular Probe

According to activity-based protein profiling (ABPP) fundamentals, pioneered by Carvatt and Bogyo,[9] the bioactive natural product probe typically consists of three elements (Figure 1.1); (i) a reactive group, (ii) a linker region, and (iii) a reporter tag.
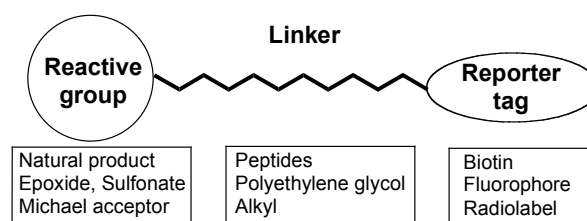
Figure 1.1. Bioactive natural product probe.

The reactive group also referred, as a 'warhead' is the most important piece of the probe design. It is designed to covalently link the probe to the active site of enzyme.

In our study, the reactive group is a bioactive natural product. The linker region is a short hydrophilic polyethylene glycol chain that bridges the reactive group and the marker (tag) together. This element can be used to control the probe specificity such as solubility and prevent steric hindrance between the reactive group and the reporter tag. The tag element is useful for identification or purification such as fluorophore, biotin and radioactive tag. This part also includes the latent analytical handles such as alkynes or azides.

1.2. Methods for Natural Product Derivatization Leading to Cellular Probe Synthesis

Synthetic strategies toward the preparation of natural product probes normally involves the two-step connection of the reactive group and the reporter tag to the linker, which can be done in different synthetic sequences in both *in vitro* or *in vivo* experiments. The most efficient strategy for tag attachment is Sharpless-Hüisgen cycloaddition of the tethered alkyne and azide to deriver a triazole linker (Figure 1.2).[10]
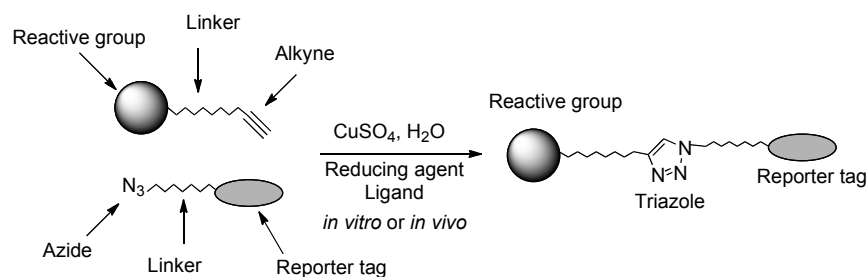
Figure 1.2. Tag attachment *via* Sharpless-Hüisgen cycloaddition.

For the past several years, many methods for natural product derivatization for cellular probe synthesis have been continuously developed, including the development of synthetic methodology to bridge reactive groups to linkers and the development of fluorescent and photoreactive reporter tags. In general, amide and carbamate formations are the common derivatization strategies for alcohol- and acid-containing natural products due to their stability in living cells and practical synthesis (Scheme1.1).[11]

Scheme 1.1

Quinocarmycin probe (**1.1**)

Pladienolide probe (**1.2**)
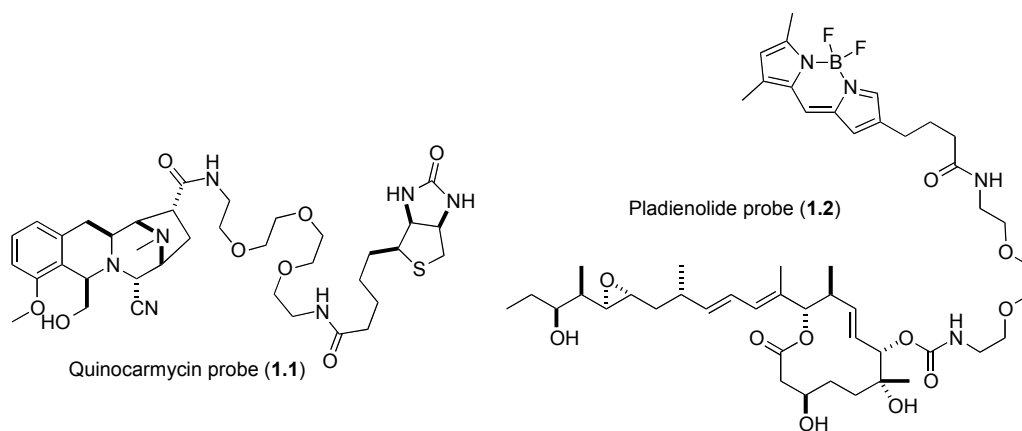
Several synthetic methodologies have been developed for natural product derivatization for linker and tag attachment to deliver natural product conjugates featuring highly retention of biological activity. Carreira and coworkers[12] reported the preparation of amphotericin B probe for biochemical study of mammalian membrane by employing reductive amination of aldehyde and amine to obtain a new piperazine linker in good yield with highly chemoselectivity. This protocol required mild condition, which could be applied to sensitive functional groups such as hemi-acetal, carboxylic acid and

ester. It also showed excellent functional group tolerance toward alcohols and olefins (Scheme 1.2).

Scheme 1.2
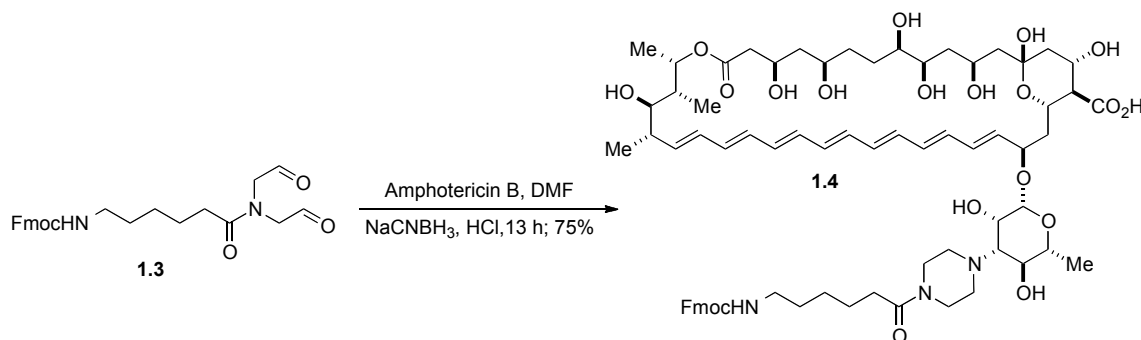
Chemical inducers of protein dimerization (CIDs) are the powerful molecular tools for probing diverse biological processes. CIDs can be used to identify protein targets of natural products by activating gene expression in living yeast cells. In 2004, Peterson and Muddana[13] developed a two-step synthesis of a highly active, and cell-permeable CID of estrone utilizing oxime formation to functionalize the ketone moiety for linker and tag attachment. This method resulted (*O*-carboxymethyl)oxime linker in quantitative yield with the tolerance of unprotected alcohol (Scheme 1.3).

Scheme 1.3
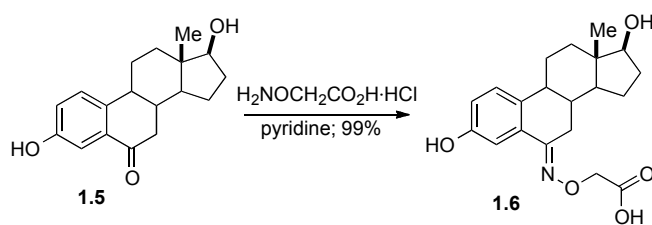
Additionally, metal-mediated coupling reactions have shown the versatility toward the derivatization of sensitive and complex natural compounds. Forsyth and coworkers[14] reported the preparation of phorboxazoles derivatives to elucidate the intracellular processing and targeting of the potent cytostatic/apoptotic anticancer drug. A Sonogashira coupling was employed to couple the terminal alkyne 33-*O*-Me-45,46-dehydrobromophorboxazole A (MDHBPA, **1.7**) and a terminal vinyl iodide derivative of the blue fluorescent dye *N*,*N*,-dimethyl-7-aminocoumarin (DMC, **1.8**) to provide the phorboxazoles-fluorescence probe (**1.9**) in high yield (Scheme 1.4).

Scheme 1.4
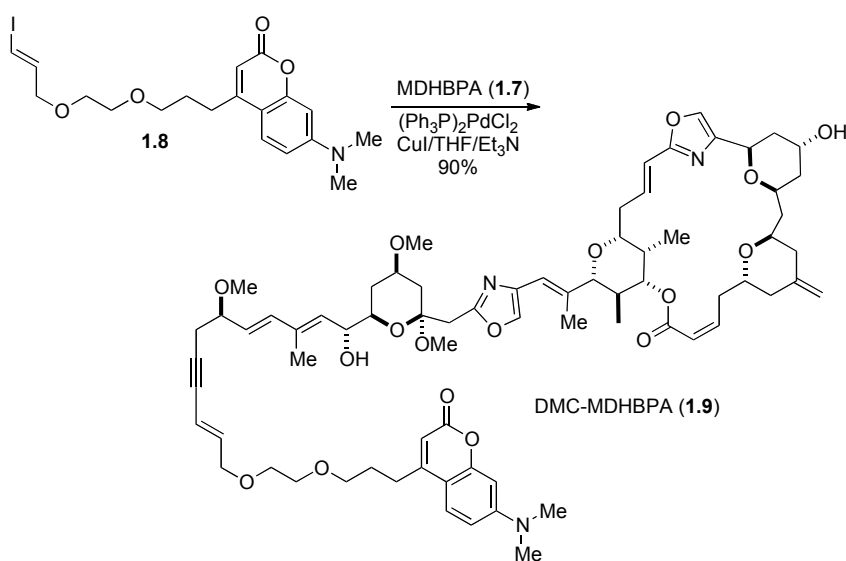
Olefin metathesis also played a role in natural product derivatization and bioactive probe synthesis. Myers and co-workers[15] prepared a dansyl probe of (−)-*ent*-avrainvillamide (**1.12**) to validate the targeting of nucleophosmin using a clever

mutagenesis strategy. They employed olefin metathesis to conjugate (−)-*ent*-avrainvillamide (**1.11**) with biotin **1.10**. The Grubbs second-generation catalyst was used and excellent chemo- and site selectivity were observed. Only the terminal olefin of **1.11** reacted in good yield (Scheme 1.5).

Scheme 1.5
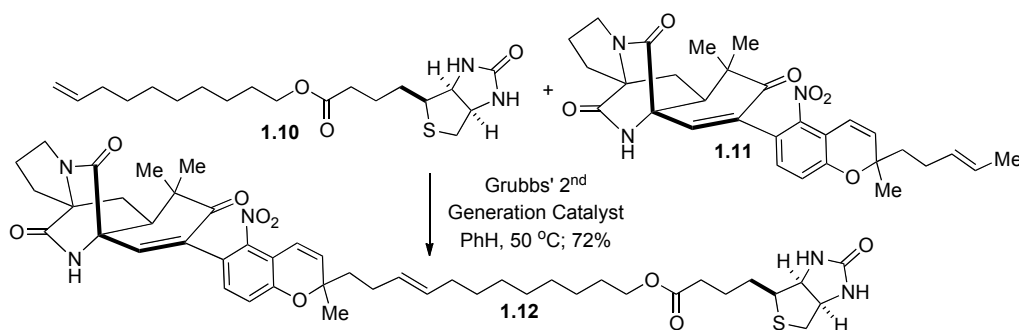
One of the biggest challenges for preparing molecular probes is designing the probe's elements. Choosing suitable linkers and reporter tags facilitates the interaction between natural products and specific protein receptors, while exhibiting minimal indiscriminate bio-reactivity and allows easy visualization, identification and purification of the target enzyme. In 2007, Mizui and co-workers[16] developed a dual crosslinking-affinity probe of pladienolide B as a goal for utilizing photoaffinity labeling and affinity chromatography to verify protein targets in the immunoprecipitation experiments of tumor cells (Scheme 1.6). This probe (**1.13**) was 645-fold less active than pladienolide B but enabled an immunoblotting experiment with streptavidin-horseradish peroxidase and resulted in the identification of a single protein band.

Scheme 1.6
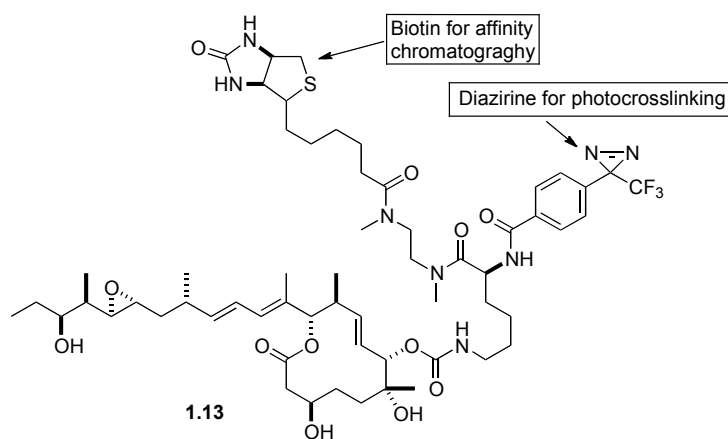
In the Romo group, we have begun the studies toward the development of natural product derivatization methodologies as the goal to develop mild and versatile strategies to functionalize bioactive natural products and prepare natural product probes to facilitate the structure-activity relationship (SAR) studies leading to the discovery of drug candidates. We have developed a couple synthetic methods for mild and monofunctionalization derivatization of natural products, based on natural product's functionalities. Our first publication in this area was report in 2007.[17] We described mild and monofunctionalization of alcohol-containing natural product *via* Rh(II) mediated O–H insertion with new *p*-bromophenyl diazoacetate (Scheme 1.7). Several commercially available natural products and derivatives were functionalized under the reported conditions to achieve the corresponding monoether (**1.16** and **1.17**) in high chemoselectivity with good yield.

Scheme 1.7

gibberellic acid
methyl ester (**1.14**)

1.15 (2.0 equiv)

5 mol% Rh(II) catalyst
CH$_2$Cl$_2$, 22 °C, 1 h

1.16

Rh$_2$(OAc)$_2$; **1.16**:**1.17** >95:5; 55%
Rh$_2$(esp)$_2$; **1.16**:**1.17** ~50:50; 38%

1.17
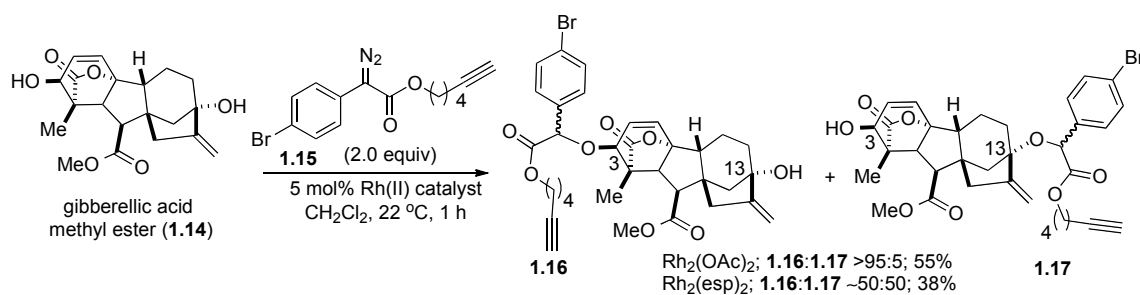
Regarding to the successful establishing scope of mild and monofunctionalization derivatization, this research has been further explored and currently is an ongoing research area in the Romo group. In 2010, we reported another mild and monofunctionalization derivatization of arene containing natural products *via* In(OTf)$_3$ catalyzed iodination.[18] The facile tag attachment *via* variety of metal-mediated coupling reactions highlighted the advantage of this protocol (Scheme 1.8). The regioselectivity was governed by electronic and steric property of substrates. This method provided iodobenzene products in nearly quantitative yield.

Scheme 1.8

NIS (1.1 equiv)

In(OTf)$_3$ (10 mol%)
CH$_3$CN, 23 °C; 97%

1.18

Tag attachment

Sonagashira coupling
Heck coupling
Suzuki coupling

Bioactive
probe

1.19: R^1 = I, R^2 = H; 80%
1.20: R^1 = H, R^2 = I; 7%
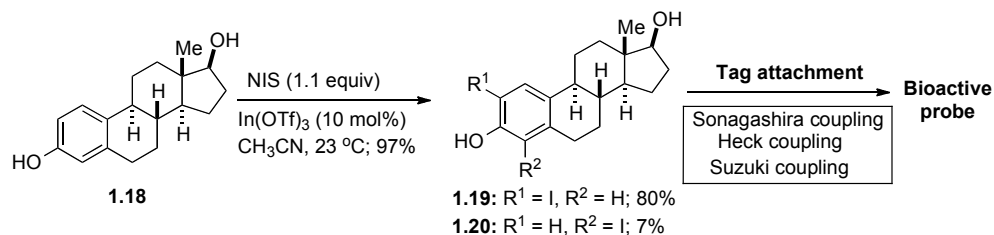
In 2009, White and co-workers[19] reported the development of a use of brønsted base such as *N,N*-diisopropylethylamine for oxidative, Pd(II)/sulfoxide-catalyzed, intermolecular C–H allylic amination. This methodology was utilized in the late-stage oxidation of estrone ((+)-**1.21** and (+)-**1.22**) and cedrene ((−)-**1.25**) derivatives yielding the excellent chemoselectivity toward inactivated terminal olefin in the presence of free alcohol and produced a linear allylic sulfonamide in excellent yield (Scheme 1.9).

Scheme 1.9

(+)-**1.21**; R^1 = TBS, R^2 = Ac
(+)-**1.22**; R^1 = H, R^2 = H

(+)-**1.23**; R^1 = TBS, R^2 = Ac; 72%
(+)-**1.24**; R^1 = H, R^2 = H; 55%

(−)-**1.25**

(−)-**1.26**; 80%
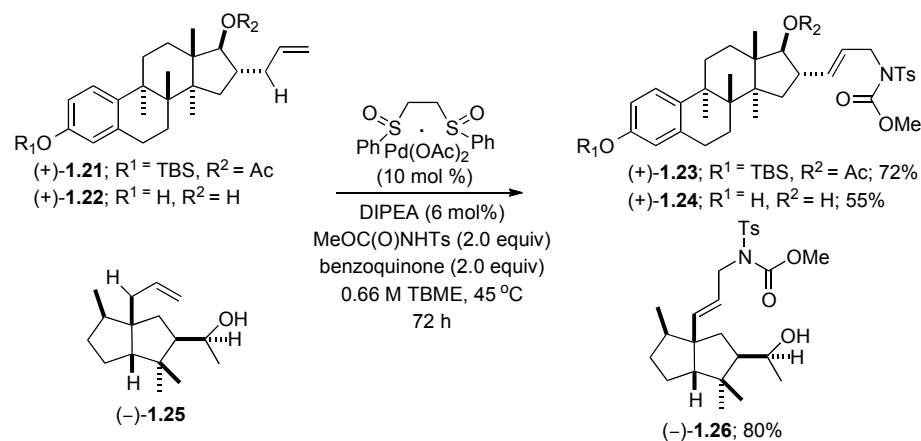
Fluorescence tags have been studied for almost 40 years, since Wieland reported the labeling of phalloidin by fluorescein isothiocyanate in 1967.[20] Since then, fluorescent modifications have continuously emerged as an important tool in the study of natural product biology. In 2006, La Clair and his collaborators[21] established a central strategy for converting natural products into fluorescent probes by labeling a diverse set of natural products with a single dye. By this means, the number of variables displayed within a collection of natural product probes is reduced by the use of single label and a

common set of linkers. As a result, biological data collected from the refined set of probes are homogenized.

Coumarin (**1.27**) was chosen as a central dye for these studies regarding to its lack of biological activity and good photophysical properties. A set of coumarin derivatives was developed with variety of labeling functional groups to enable derivatization the diverse set of bioactive natural products *via* several derivatization methodologies (Scheme 1.10).

Scheme 1.10
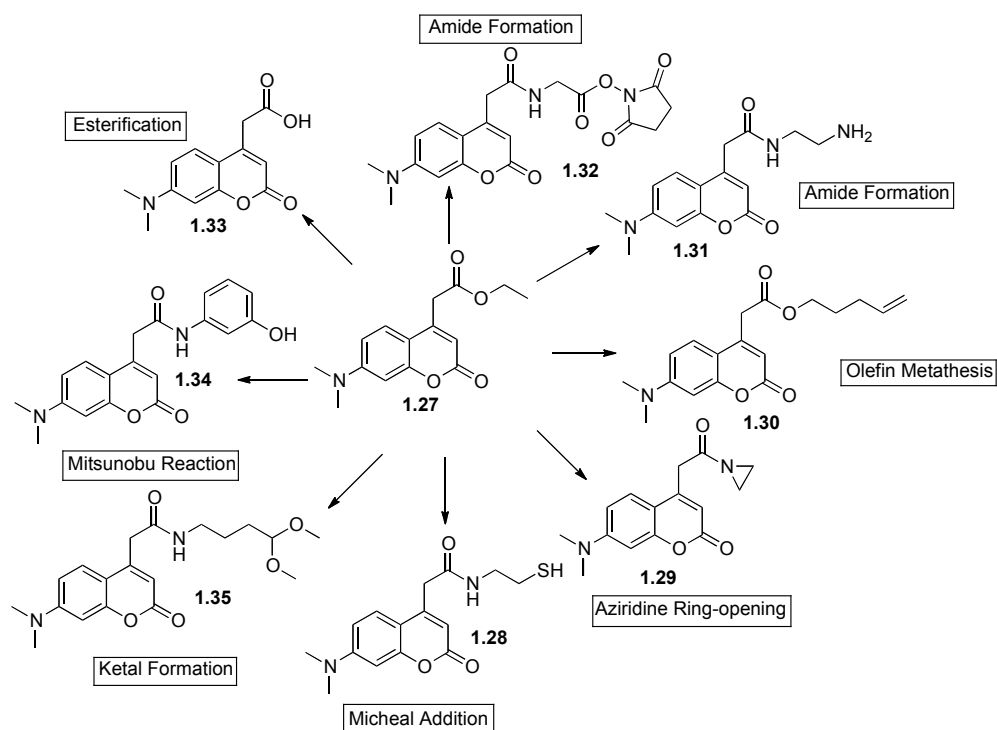
Coumarin labels not only simplifies chromatographic purification but also extend the detection limit. This allows synthetic operations with micrograms of materials and they can be used for live-cell imaging. Additionally, these fluorescent probes provided

reliable retention of natural product's biological activities and gave details of mechanism

of action of natural products leading to drug discovery from natural products.

CHAPTER II

NEW DIAZO REAGENTS WITH SMALL STERIC FOOTPRINTS FOR SIMULTANEOUS ARMING AND STRUCTURE-ACTIVITY RELATIONSHIP STUDIES OF ALCOHOL-CONTAINING NATURAL PRODUCTS*

2.1. Introduction

Natural products and their derivatives have had a long invaluable history as a source of therapeutic agents. Regarding to their structural complexity and interesting biological activity, natural products continue to play a significant role as a tool for protein target discovery and understanding of cellular pathways. Several of bioactive natural products have been used in clinical trial and distributed in the market such as FK506 and orlistat. Numerous of them are currently developed to treat cancer, resistant bacteria and viruses, and immunosuppressive disorders.

In general, following the isolation and purification process, the newly discovered natural products are subjected to a large number of spectroscopic techniques to fully characterize and completely assign stereo structures, which is a time consuming process. The structure elucidation process causes a significantly delay of the basic cellular studies to determine the relevant protein targets, which is an essential knowledge for further

---

synthetic and biomedical research. Additionally, natural product derivatization protocols are typically a formidable approach because a limit quantity of natural products, lack of selectivity and requiring a mild-monofunctionalization reaction.

Many approaches have been developed for preparation of natural product derivatives to afford the novel and unique sites for tag attachment without losing bioactivities.[22] These processes require multi-step syntheses, which are both challenging and time-consuming. Alternatively, random derivatization techniques such as a photo-cross-linking of natural products to an affinity matrix have been developed. However, they cannot rely on any information related to the site of attachment, the retention of bioactivity, and potential design problems in the case of failure to identify the targets.[23] Furthermore, the possibility of natural products degradation, for example by UV irradiation, must be considered.

2.1.1. Simultaneous Arming and Structure-Activity Relationship (SAR) Studies of Natural Products for Chemical Proteomics

Natural products are often challenging to functionalize in chemo- and site ("chemosite")[24] selective manner because of their structural complexity, dense functionality, and limited quantities. We aim to develop a set of chemo- and both site selective and non-site selective reactions that can enable simultaneous arming by attachment of an appropriate functional group (*i.e.,* an alkyne) at various sites on a natural product to provide the diverse set of natural product derivatives, which is an important feature for SAR studies (Figure 2.1).
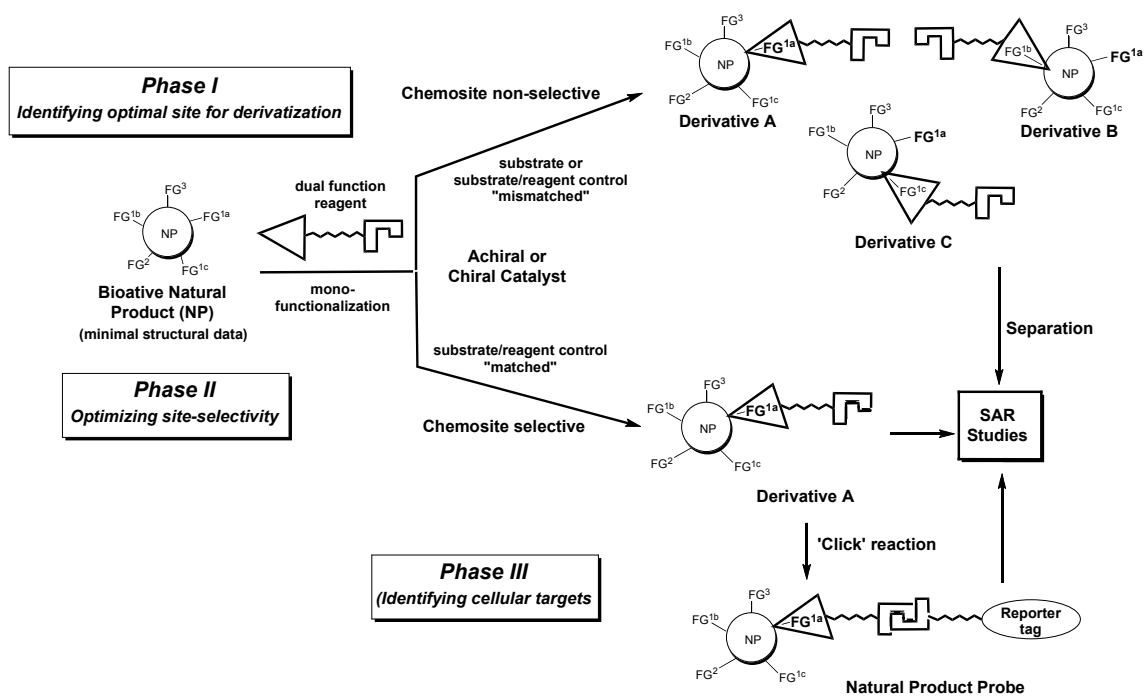
Figure 2.1. General strategy for simultaneous arming and structure-activity relationship studies (SAR) of natural products for chemical genetics.

We are interested in the strategy that relies on metal catalysis, which can facilitate the variation of chemosite selectivity based on catalyst/natural product interaction. In Phase I, substrate and/or reagent control leads to an initial chemoselective but site nonselective reaction to obtain various natural product derivatives (derivatives A, B, and C) from mismatched case. Subsequent separation by robust and versatile methods, such as preparative HPLC and LC-MS, deliver the natural product derivatives for the initial SAR studies to determine the most appropriate site for tag attachment, which provides the greatest retaining bioactivity. In Phase II, the goal is to selectively synthesize natural product derivative that shows the greatest retaining biological activity (Figure 2.1, derivative A) by substrate and reagent control. This matched case leads to a chemosite

selective process to afford only derivative A. In Phase III, subsequent conjugation with reporter tag (*i.e.,* biotin) typically by 'Click' reaction gives rise natural product probes for SAR studies by protein assays and affinity chromatography experiments.

2.1.2. Derivatization of Alcohol-Containing Natural Products *via* Chemo- and Site Selective Rh(II)-Catalyzed O−H Insertions

According to two natural product databases, Dictionary of Natural Product (DNP, Chapman & Hall) and Bioactive Natural Product Database (BNPD, Szenzor), alcohols are one of the most prevalent functional groups found in natural compounds.[25] However, not all alcohols presented in natural products are crucial for biological activity and thus can serve as site for derivatization. To date, there are many approaches for direct derivatization of alcohol containing natural product.[26] However, the reported conditions are typically guided by the knowledge of reactivity and stability of natural products. Additionally, these reactions are conducted under predominantly acidic or basic conditions, which are harsh for many natural products. In contrast, O−H insertions normally take place under mild and neutral conditions, and the diazo ester reagents are stable and easy to prepare. Therefore, O−H insertion proves to be a versatile method for derivatization of alcohol containing natural products.

In the Romo group, we have developed a strategy that enables simultaneous arming and SAR studies for alcohol-containing natural products involving both chemo- and site selective ("chemosite" selective) and site non-selective O−H insertion reactions with rhodium carbenoids derived from alkynyl diazoacetates.[17] In this strategy, the

arming process leads to natural product alkyne-derivatives that are equipped for subsequent conjugation to various tags *via* Sharpless-Hüisgen cycloaddition (Figure 2.2). In this way, the arming step requires only the knowledge of basic functional group presented in natural products, which diminishes the time between natural product isolation and cellular protein receptor isolation. Moreover, metal mediated reaction as Rh(II)-catalyzed O−H insertion is readily performed on small scale and provides a mild and mono-functionalization with high chemo- and site selectivity and potentially some degree of site non-selectivity to obtain the greatest number of derivatives for initial SAR studies. This method can be applied to a diverse set of alcohol-containing natural products for simultaneous arming and SAR studies that also enable subsequent bioactive probe synthesis for chemical genetics.
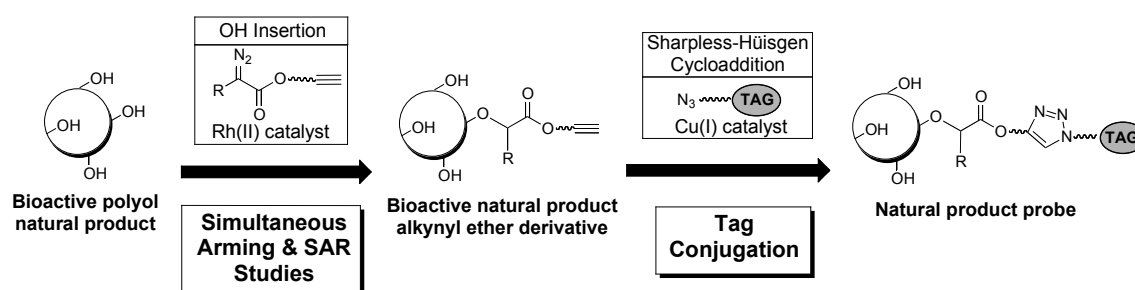
Figure 2.2. Two-step O−H Insertion/Sharpless-Hüisgen cycloaddition sequence for preparation of alcohol-containing natural product probes.

2.1.3. Rh(II)-Mediated O−H Insertion: Mechanism and Carbene Type

Rh(II)-catalyzed O−H insertions were introduced by Tessié and co-workers in 1973[27] and referenced as the most efficient metal-mediated reactions for the

decomposition of α-diazo carbonyl compound. Today, the synthesis and rhodium-mediated O–H insertion reactions of a wide range of diazo compounds are well documented and have become a standard procedure for organic synthesis.[28] Three possible mechanisms have been proposed related to a concerted mechanism, the protonation of a carbene to generate carbocation intermediate, and nucleophilic attack on the electrophilic carbene to form a ylide followed by hydrogen transfer (Figure 2.3).
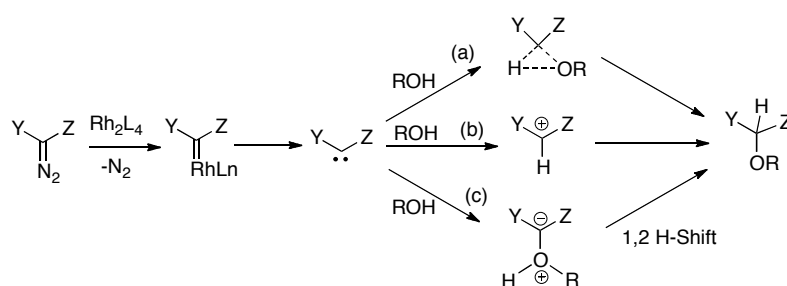
Figure 2.3. Three possible mechanisms of O-H insertion. (a) Concerted mechanism, (b) Protonation of carbene to generate carbocation intermediate, (c) Nucleophilic attack on the electrophilic carbene to form a ylide followed by hydrogen transfer.

However, the detail mechanisms of the C–O bond formation derived from the carbene insertion into the O–H bond are not fully understood. There is no direct experimental evidence to determine the O–H insertion mechanism. Although the concerted pathway (Figure 2.3a) cannot be completely excluded, it was likely that most O–H insertion reactions of carbenes proceed by one of the stepwise processes (Figure 2.3b or 2.3c). Until 2007, Han and co-workers[29] explained the plausible insertion mechanism of Rh(II)-methylene carbene into the O–H bond of alcohols, except phenol[30] by the analysis of the energy barriers using B3LYP functional both in gas phase and in

CH$_2$Cl$_2$. They observed that the energy barrier associated with a concerted mechanism was higher than that of stepwise mechanism. Therefore, they concluded that the insertion of rhodium carbenoid into O−H bond of methanol and ethanol is more likely a stepwise mechanism, while the concerted mechanism is preferred for the O−H insertion of phenols.

A metal carbenoid is a reactive species derived from the decomposition of a diazo precursor. The O−H insertion reactivity and selectivity, including chemoselectivity, regioselectivity, and stereoselectivity normally depend on the metal carbene character, which is classified into three major groups according to the carbenoid substitutents; acceptor, acceptor/acceptor, and donor/acceptor (Figure 2.4).[31]

acceptor substituted carbeniod	acceptor/acceptor substituted carbeniod	donor/acceptor substituted carbeniod
M=⟨ H / EWG	M=⟨ EWG / EWG	M=⟨ EDG / EWG
EWG = CO$_2$R, COR NO$_2$, PO(OR)$_2$ SO$_2$R	EWG = CO$_2$R, COR NO$_2$, SO$_2$R CN	EWG = CO$_2$R, COR EDG = vinyl, alkynyl aryl , heteroaryl
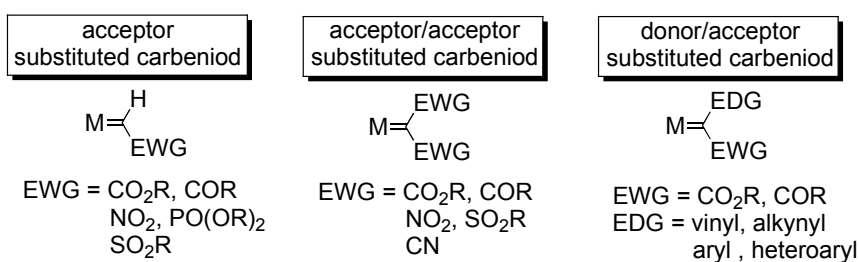
Figure 2.4. Classification of carbenoid intermediates.

In general, reactivity of a particular carbene is governed by substituents and the metal. The terms "donor" and "acceptor" refer to electron donation or withdrawal through resonance effects, respectively. An acceptor group (EWD) generally increases electrophilicity and reactivity, whereas a donor group (EDG) increases stability and chemoselectivity.[32] With regard to selectivity and reactivity of carbenoid in C−H

activation chemistry, the electrophilic carbenoids exhibit poor regio- and stereoselectivity and they are susceptible to other competing reactions such as carbenoid dimerization. However, the carbenoids with insufficient electrophilicity show a lack of reactivity. An electron-withdrawing substituent, typically a carbonyl moiety causes highly electrophilicity. The acceptor carbenoids, which derived from diazo compounds bearing a single electron-withdrawing substituent, are highly reactive metallocarbenoid species, which cause a high degree of carbene self-dimerization. The acceptor/acceptor carbenoids, derived from diazo compounds bearing two electron-withdrawing substituents, are highly stable compared to acceptor carbenoid precursors. In the presence of a second electron-withdrawing group, a highly active metal catalyst is required to decompose these diazo compounds. However, the derived metal carbenoid is highly reactive but less selective. The common side reactions for these carbenoids are carbene self-dimerization and hydride transfer to form zwitterionic intermediates.

The donor/acceptor carbenoids contain a donor substituent, such as vinyl or aryl, which is capable of stabilizing the carbenoid through electron resonance. The donor/acceptor carbenoids are capable of undergoing highly chemoselective processes. As a result, the donor/acceptor carbenoids are often used in metal-catalyzed insertion research.

2.2. Results and Discussion

In the Romo group, we previously described mild and versatile strategies for simultaneous arming (with a reactive functional group or array) and SAR studies that

facilitate mode of action studies of natural products.[17,18] One such method involves chemosite selective and non-selective O−H insertions with rhodium carbenoids derived from hexynyl-α-*p*-bromophenyl diazoacetate (**2.1**, HBPA) as a donor/acceptor carbenoid precursor. The arming process leads to natural product derivatives that are equipped with tethered alkynes for subsequent conjugation to various tags *via* Sharpless-Hüisgen cycloaddition to generate cellular probes (Figure 2.5). The utility of this strategy was demonstrated with a panel of natural products including FK506. An FK506-HBPA-biotin conjugate probe (**2.2**) was employed to successfully pull-down the entire 'immunosuppressive complex' consisting of calcineurins A/B, calmodulin, and FKBP12.
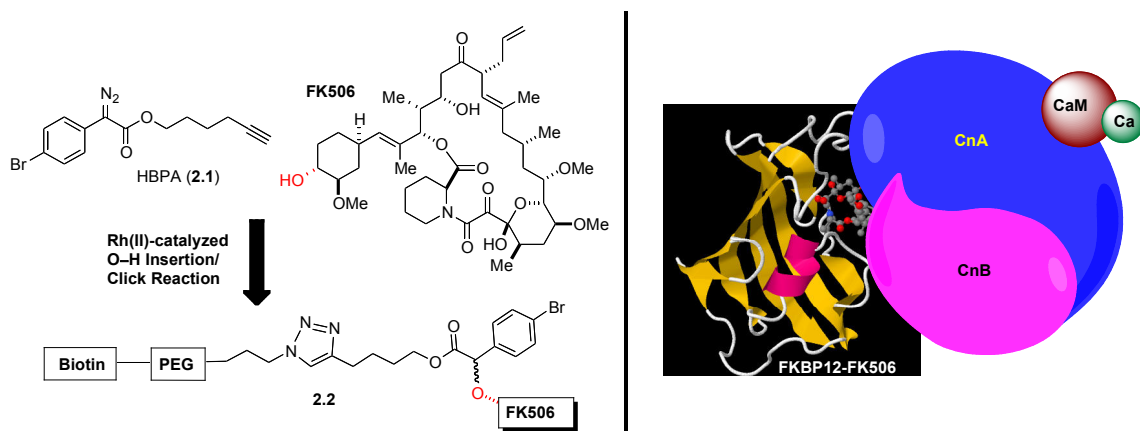
Figure 2.5. Proof of principle affinity experiments with a novel FK506-HBPA-biotin conjugate obtained *via* O−H Insertion/Sharpless-Hüisgen cycloaddition leading to the pull-down of the entire "FK506 Immunosuppressive Complex".

2.2.1. Alteration of Chemosite Selectivity Using Chiral Rh(II) Catalysts

The simultaneous arming and SAR studies of alcohol-containing natural products *via* Rh-catalyzed O−H insertions has provided a versatile tool for the mild and mono-

functionalization derivatization of alcohol containing natural product with high chemosite selectivity. As a goal for obtaining the greatest number of derivatives for initial SAR studies, the development of the O–H insertions was performed by relying on a metal catalysis process. The use of rhodium catalysts bearing chiral ligands to enable a type of "double asymmetric synthesis"[33] potentially leads to the variation of chemosite selectivity toward the O–H insertion of alcohol-containing natural products.

In this study, Doyle's rhodium(II) carboxamidate complexes (Figure 2.6) were interesting since they displayed outstanding enantioselectivity, regioselectivity and stereoselectivity.[34] These carboxamidate catalysts consist of four classes of complexes: pyrrolidinones ($Rh_2(5S\text{-MEPY})_4$), oxazolidinones ($Rh_2(4S\text{-MEOX})_4$), imidazolidinones ($Rh_2(4S\text{-MPPIM})_4$), and azetidinones ($Rh_2(4S\text{-MEAZ})_4$). These catalysts have more structural rigidity than rhodium(II) carboxylates such as $Rh_2(OAc)_4$ and $Rh_2(esp)_2$ (Figure 2.7) and include four bridging amine ligands around the dirhodium core with two oxygen and two nitrogen donor atoms bound to each rhodium in a *cis*-configuration. The chiral center of the enantio-pure ligands is positioned in such a manner that influences the approach of the substrate and the orientation of the carbene, thereby influencing regioselectivity as well as stereoselectivity.
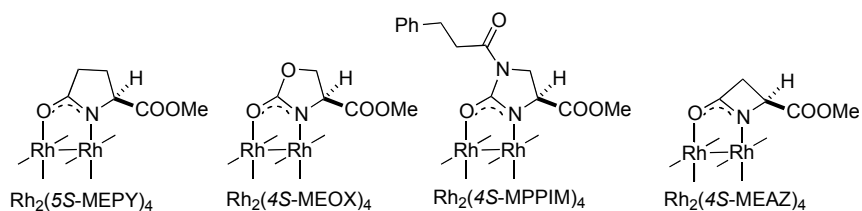
Figure 2.6. Doyle's rhodium chiral catalysts.
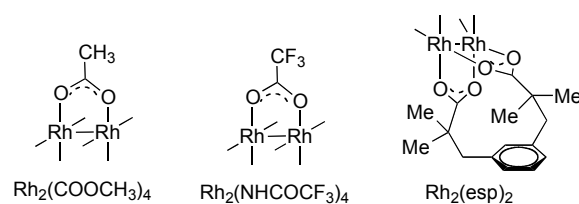
Figure 2.7. Rhodium (II) carboxylated catalysts.

According to this idea, the experiments were preformed to demonstrate the potential of altering chemosite selectivity, while maintaining the mono-functionalization O–H insertion process. The commercially available chiral Rh(II) catalysts developed by Doyle[35] were investigated for O–H insertions with gibberellic acid methyl ester (**2.3**) and brefeldin A (**2.4**). These two natural products served as the model substrates since they contain several potentially reactive sites for alteration of chemosite selectivity (Figure 2.8). Gibberellic acid methyl ester (**2.3**) has an internal and a terminal disubstituted olefin and two sterically differentiated alcohols (secondary and tertiary alcohol), whereas brefeldin A (**2.4**) has the electronically differentiated olefins, and alcohols including α,β unsaturated ester, secondary alcohol and allylic alcohol.

Gibberellic acid methyl ester (**2.3**)   Brefeldin A (**2.4**)

➡ Reactive site for O–H insertion
➤ Reactive site for cyclopropanation
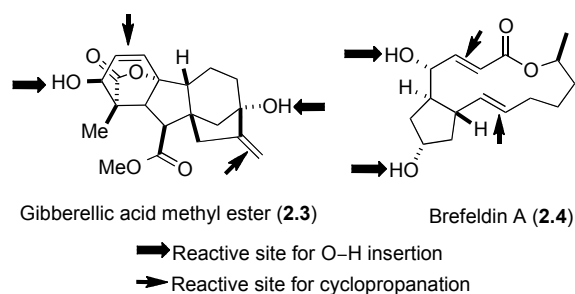
Figure 2.8. Ideal substrates for alteration of chemosite selectivity study.

Exploring the variation of chemosite selectivity of O–H insertion of gibberellic acid methyl ester (**2.3**) with Rh(II) catalyst including achiral and chiral catalysts showed a significant difference in carbene reactivity (Table 2.1). In most case, O–H insertion occurred at the secondary alcohol of gibberellic acid methyl ester to obtain **2.5a** as a major product and no reaction at the olefins leading to cyclopropanation adducts. Rh_2(*4S*-MEAZ)$_4$ (Table 2.1, entry 4) provided the highest yield of **2.5a** (72%) and highest diastereoselectivity (dr, 1:2). However, its enantiomeric catalyst Rh_2(*4R*-MEAZ)$_4$ (Table 2.1, entry 5) provided **2.5a** only 35% yield. These results pointed out to the desired difference in molecular recognition between substrate and catalyst.

Surprisingly, Rh_2(esp)$_2$, which is an achiral catalyst developed by Du Bois,[36] was the only catalyst that provided the alteration of site selectivity (Table 2.1, entry 2). In this case, O–H insertion at the tertiary alcohol of gibberellic acid methyl ester (**2.3**) was observed along with O–H insertion at the secondary alcohol in 1:1 ratio (dr, 1:1). Both diastereomers were separable and obtained in moderate yield. Employing enantiomers of Rh_2(*4S*-MEPY)$_4$, Rh_2(*4R*-MEPY)$_4$, and Rh_2(*4S*-MPPIM)$_4$ (Table 2.1, entries 6, 7 and 9) produced only HBPA dimerization with no observation of O–H insertion products. Interestingly, O–H insertion with Rh(esp)$_2$ at low temperatures (−78 °C) also caused self-dimerization of HBPA and precluded O–H insertion with gibberellic acid methyl ester (**2.3**).

Table 2.1. Alteration of chemosite selectivity employing Rh(II) chiral catalysts process with gibberellic acid methyl ester (**2.3**).
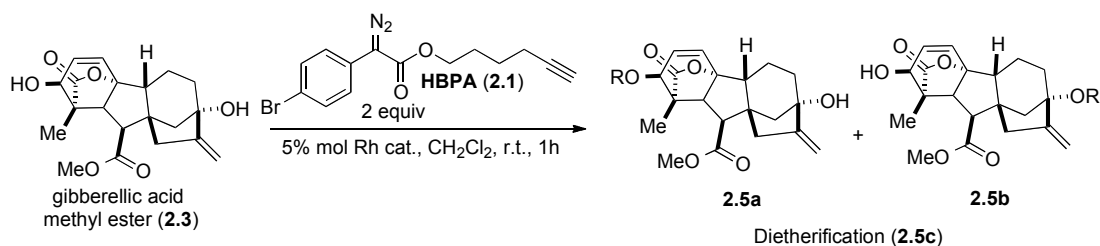
Entry	Rhodium Catalyst	Reaction Condition	**2.5a:2.5b**[a]	%Yield[b]	dr[c]
1	Rh$_2$(OAc)$_4$	23 °C, 1 h	>95:5	62% **2.5a**	1:1
2	Rh$_2$(esp)$_2$	23 °C, 30 min	~50:50	35% **2.5a** 28% **2.5b**	1:1
3	Rh$_2$(esp)$_2$	−78 °C, 1 h then 23 °C, 1 h	Obtained only HBPA dimer	ND[e]	ND
4	Rh$_2$(4S-MEAZ)$_4$	23 °C, 30 min	>95:5	72% **2.5a**	1:2
5	Rh$_2$(4R-MEAZ)$_4$	23 °C, 30 min	>95:5	35% **2.5a**	1:1
6	Rh$_2$(4S-MEPY)$_4$	23 °C, 6 h	Obtained only HBPA dimer[d]	ND	ND
7	Rh$_2$(4R-MEPY)$_4$	23 °C, 6 h	Obtained only HBPA dimer[d]	ND	ND
8	Rh$_2$(4S-MEOX)$_4$	23 °C, 30 min	>95:5	35% **2.5a**	1:1
9	Rh$_2$(4S-MPPIM)$_4$	23 °C, 6 h	Obtained only HBPA dimer[d]	ND	ND

[a]Ratios were determined by ^{1}H-NMR (500 MHz) and no dietherification was observed. [b]Yields refer to isolated yields. [c]Diastereomeric ratios (dr) of **2.5a** at ether α-carbon were determined by ^{1}H-NMR (500 MHz). [d]Reaction was slowly proceeded. [e]ND refers to not determined.

Investigating chemosite selectivity of O–H insertion of brefeldin A (**2.4**) was performed in the same strategy as gibberellic acid methyl ester (Table 2.2). The pairs of

enantiomeric catalysts (Table 2.2, entries 3-8) were studied along with achiral Rh(II) carboxylates (Table 2.2, entries 1 and 2). In this study, we observed only O–H insertion of the secondary alcohol of brefeldin A, no cyclopropanation at the olefins and no dietherification (**2.6c**). Rh$_2$(OAc)$_4$ (Table 2.2, entry 1) provided the highest yield of **2.6a** (62%) with dr, 1:1.

Table 2.2. Alteration of chemosite selectivity employing Rh(II) chiral catalysts with brefeldin A (**2.4**).
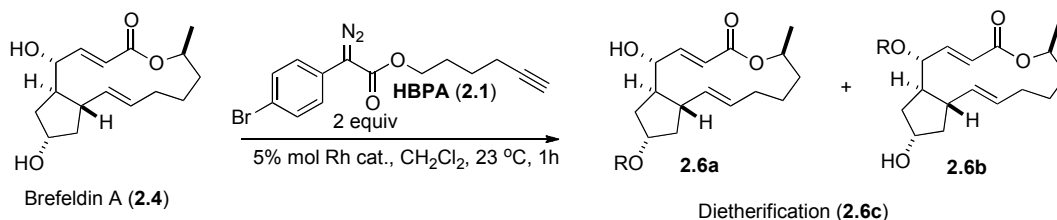
Entry	Rhodium Catalyst	**2.6a**:**2.6b**[a]	% yield of **2.6a**[b]	dr[c]
1	Rh$_2$(OAc)$_4$	>95:5	62%	1:1
2	Rh$_2$(esp)$_2$	>95:5	24%	>19:1
3	Rh$_2$(4S-MEAZ)$_4$	>95:5	29%	1:1
4	Rh$_2$(4R-MEAZ)$_4$	>95:5	23%	1:1
5	Rh$_2$(4S-MEPY)$_4$	Obtained only HBPA dimer[d]	ND[e]	ND
6	Rh$_2$(4R-MEPY)$_4$	Obtained only HBPA dimer[d]	ND	ND
7	Rh$_2$(4S-MEOX)$_4$	>95:5	28%	1:1
8	Rh$_2$(4S-MPPIM)$_4$	Obtained only HBPA dimer[d]	ND	ND

[a]Ratios were determined by ^{1}H-NMR (500 MHz) and no dietherification was observed. [b]Yields refer to isolated yields. [c]Diastereomeric ratios of **2.6a** at ether α-carbon were determined by ^{1}H-NMR (500 MHz). [d]Reaction was slowly proceeded. [e]ND refers to not determined.

Interestingly, an unexpected diastereoselective O–H insertion was observed when Rh$_2$(esp)$_2$ was used (Table 2.2, entry 2). This catalyst gave low yield of **2.6a** (24%) but showed an excellent diastereoselectivity (dr, >19:1). Use of chiral Rh(II) carboxamidates (Table 2.2, entries 3, 4 and 7) significantly lowered the yield of O–H insertion products (**2.6a**) comparing to Rh$_2$(OAc)$_4$ (23-29% *vs.* 62% isolated yield, respectively). In this case, the enantiomeric catalysts Rh$_2$(*4S*-MEAZ)$_4$ and Rh$_2$(*4R*-MEAZ)$_4$ (Table 2.2, entries 3 and 4) provided the same reactivity leading to the low yield of **2.6a** (29% and 23%, respectively) and similar diastereoselectivity (dr, 1:1) was observed. Employing both enantiomers Rh$_2$(*4S*-MEPY)$_4$ and Rh$_2$(*4R*-MEPY)$_4$, and Rh$_2$(*4S*-MPPIM)$_4$ (Table 2.2, entries 5, 6 and 8) produced only HBPA dimerization and no O–H insertion products were observed. These results were similar to O–H insertion of gibberellic acid methyl ester, which were described previously.

Regarding to the results we observed from Tables 2.1 and 2.2, we concluded the idea of altering site selectivity by chiral catalysts *via* a type of "double asymmetric synthesis" that each natural product has specific shape-shape interactions or specific "shape fit" with particular metal carbenoids. Therefore, the overall shape interaction and reactivity of catalyst are more important than chirality's of the catalyst itself.

2.2.2. Development of Second Generation Diazo Reagents

In our initial study, the first generation of diazo reagents, 5-hexynyl-(α-4-bromophenyl) diazoacetate (HBPA, **2.1**) was applied to the Rh(II)-promoted O–H insertion of various types of alcohol-containing natural products.[17] However, the large

steric size of the *p*-bromophenyl group and its close proximity to the point of attachment to the natural product was a potential liability for retaining bioactivity and subsequent affinity chromatography experiments. We thus sought to develop sterically smaller diazo reagents with similar or better reactivity to the *p*-bromophenyl substituted reagent (HBPA) that potentially improve the retention of bioactivity.

Herein, we describe the development of an α-trifluoroethyl (HTFB) substituted carbenoid precursor (**2.7**) that leads to a greatly reduced steric footprint yet provides similar reactivities, including chemosite selectivities, as the previously described *p*-bromophenyl reagent **2.1** (Figure 2.9). Importantly, the α-trifluoroethyl (HTFB) substituted conjugates may offer greater utility for identifying cellular receptors of bioactive natural products due to their smaller steric size. We therefore set out to study the α-trifluoroethyl (**2.7a**), α-trifluoromethyl (**2.7b**), and α-cyano (**2.7c**) diazo reagents that possess different substituents with varied steric sizes and electron withdrawing potential, which would also alter the reactivity of the derived rhodium carbenoids (Figure 2.9). While the proposed diazo reagents would lead to acceptor/acceptor carbenoids,[37] the fluorinated hex-5-ynyl 2-diazo-4,4,4-trifluorobutanoate (**2.7a**, HTFB) and hex-5-ynyl 2-diazo-3,3,3-trifluoropropanoate (**2.7b**) have the added advantage of enabling ^{19}F-NMR analysis of crude natural product derivatization reactions.

In contrast, the hex-5-ynyl 2-cyano-2-diazoacetate (**2.7c**) was expected to provide a highly reactive metallocarbenoid species.[38] Computational studies performed on Spartan '08 v1.2.0 software at the level of theory: DFT-B3LYP/6-31++G(2df,2p) were used for calcutating molecular volumes. These results supported the significant

steric size difference based on calculated molecular volumes that could be expected between the derived natural product derivatives (cyano, 35.10 Å^3; 1,1,1-trifluoroethyl: 65.51 Å^3; *p*-bromophenyl: 117.02 Å^3). In addition, the hex-5-ynyl 2-(4-*p*-azidophenyl)-2-diazoacetate (**2.7d**)[39] was prepared for its potential as a trifunctional linker for photoaffinity labeling of low affinity binding proteins[40] and the derived carbenoid was expected to exhibit similar reactivity to the *p*-bromophenyl reagent **2.1**.
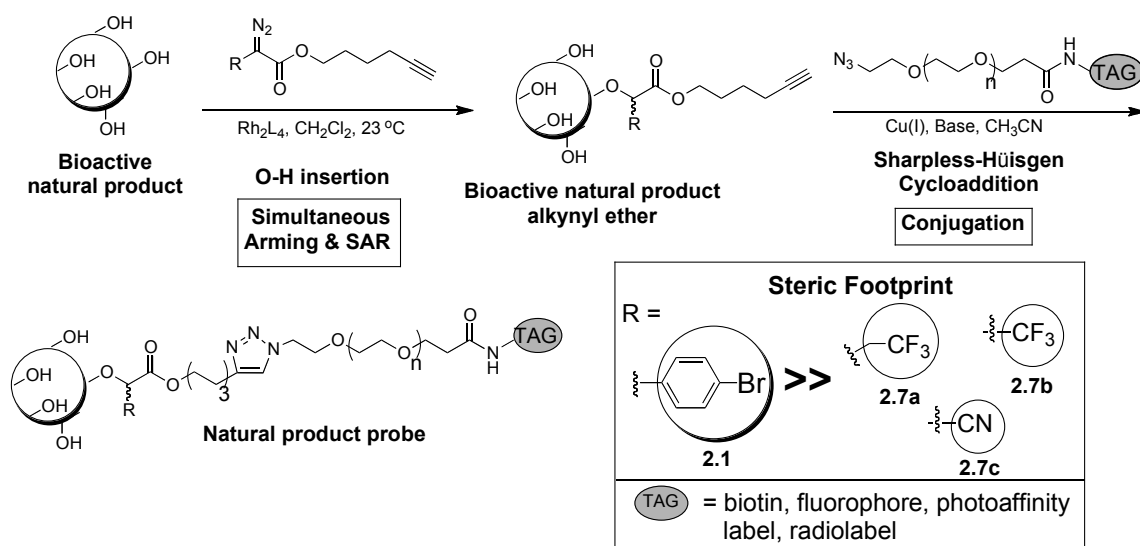
Figure 2.9. Simultaneous arming/SAR studies *via* O–H insertion of polyol natural products using diazo reagents with varied steric footprints and subsequent tag conjugation.

To enable studies of their reactivity, these new diazo reagents were successfully prepared on gram scale (~5 g) by esterification and subsequent base-promoted diazo transfer. We found that diazo reagents **2.7a** (Scheme 2.1), **2.7c** (Scheme 2.2), and **2.7d** (Scheme 2.3) are stable at room temperature, and storable at -10 $^{\circ}$C with no

decomposition after one year. However, the α-trifluoromethyl reagent **2.7b** (Scheme 2.4) is highly unstable and decomposed at room temperature.

Scheme 2.1

4,4,4-trifluorobutanoic acid (**2.7a-1**)

hex-5-yn-1-yl 4,4,4-trifluorobutanoate (**2.7a-2**)

EDCI.HCl, DMAP CH$_2$Cl$_2$, 23 °C, 2h
92%

TiCl$_4$, Et$_3$N, CH$_3$CN reflux, 30 min
91%

hex-5-yn-1-yl 2-benzoyl 4,4,4-trifluorobutanoate (**2.7a-3**)

p-ABSA, DBU
CH$_3$CN, 23 °C, 4h
58%

2.7a (HTFB)

Scheme 2.2

2-cyanoacetic acid (**2.7c-1**)

DCC, CH$_3$CN
23 °C, 6h
90%

hex-5-yn-1-yl 2-cyanoacetate (**2.7c-2**)

Pyridine, CH$_3$CN
23 °C, 24h
48%

2.7c

Scheme 2.3

2-(4-aminophenyl)acetic acid (**2.7d-1**)

i) Conc. HCl, aq NaNO$_2$
0 °C, 15 min

ii) NaN$_3$, 0 °C, 30 min
99%

2-(4-azidophenyl)acetic acid (**2.7d-2**)

i) (COCl)$_2$, DMF, CH$_2$Cl$_2$
23 °C, 4h

ii) HO
Et$_3$N, DMAP, 23 °C, 12h
74%

hex-5-yn-1-yl 2-(4-azidophenyl)acetate (**2.7d-3**)

p-ABSA, DBU
THF, 23 °C, 30 min
68%

2.7d

Scheme 2.4

The reactivity of diazo reagents **2.7a**, **2.7c**, and **2.7d** were initially studied with gibberellic acid methyl ester (**2.3**), which serves as an ideal substrate to study chemosite selectivity. Under the standard O–H insertion conditions with $Rh_2(OAc)_4$, diazo reagents **2.7a** and **2.7d** exhibited similar stability and reactivity compared to the *p*-bromophenyl diazo **2.1** (Table 2.3, entry 1) providing monoethers **2.8a** and **2.8d** derived from O–H insertion with the more accessible secondary alcohol along with recovered ester **2.3** (Table 2.2, entries 2 and 4). However, the more reactive α-cyano reagent **2.7c** gave a complex mixture likely resulting from both O–H insertion and cyclopropanation[41] with no recovery of starting material (Table 2.3, entry 3).

Overall, the α-trifluoroethyl diazo reagent **2.7a** provided the best results with regard to stability, reactivity, and selectivity of derived rhodium carbenoid compared to the *p*-bromophenyl diazo **2.1**. With respect to catalysts, $Rh_2(esp)_2$ described by DuBois,[36] gave optimal conversion to the monoether **2.7a** (66%) and higher diastereoselectivity (dr, 4:1), however, this was accompanied by 25% of diether **2.10** (Table 2.3, entry 5). $Rh_2(OAc)_4$ was the most chemosite selective catalyst favoring the less hindered and nucleophilic secondary alcohol at C3 (Table 2.3, entry 2). We next investigated various known chiral Rh(II) catalysts in conjunction with the α-

trifluoroethyl diazo reagent **2.7a** as a mean to alter chemosite selectivity of the O–H

insertion. Several commercially available chiral rhodium catalysts including those of

Davies[42] and Doyle[35] were investigated.

Table 2.3. Comparison of reactivity and chemosite selectivity of novel diazo reagents **2.7a**, **2.7c-d** with various Rh(II) catalysts.
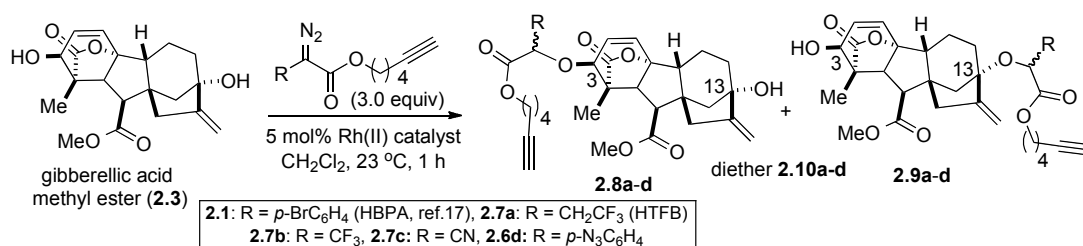
Entry	Diazo reagent	Catalyst	Monoether ratio **2.8:2.9**[b]	Diether **2.10**	% Yield[d]	dr (**2.8**)[e]
1[a]	**2.1**	$Rh_2(OAc)_4$	>95:5	<5[c]	55 (38)	1:1
2	**2.7a**	$Rh_2(OAc)_4$	95:5	<5[c]	45 (32)	2:1
3	**2.7c**	$Rh_2(OAc)_4$	ND[f]	ND	ND	ND
4	**2.7d**	$Rh_2(OAc)_4$	70:30	0	57 (25)	1:1
5	**2.7a**	$Rh_2(esp)_2$	87:13	25	66 (7)	4:1
6	**2.7a**	$Rh_2(OCOCF_3)_4$	50:50	0	28 (44)	2:1
7	**2.7a**	$Rh_2(4S-$	ND	0	<5[c] (74)	ND
8	**2.7a**	$Rh_2(4R-$	ND	25	<5[c] (68)	ND
9	**2.7a**	$Rh_2(4S-$	50:50	0	41 (29)	1:1
10	**2.7a**	$Rh_2(S-DOSP)_4$	85:15	0	75	3:1

[a]Data from ref. 17. [b]Ratios were determined by ^{1}H-NMR (500 MHz). [c]Ethers **2.8-2.10** were detected by LC-MS but not ^{1}H-NMR (500 MHz). [d]Yields refer to isolated yields and numbers in parentheses refer to recovered starting material. [e]Diastereomeric ratios of **2.8** at ether α-carbon were determined by ^{1}H-NMR (500 MHz). [e]ND refers to not determined.

The use of chiral catalysts enables a type of 'double diastereoselectivity' that could in principle alter chemosite selectivity. Of the four chiral catalysts studied (Table 2.3, entries 7-10), Rh_2(S-DOSP)$_4$ provided the highest yield of monoetherification (75%) of ester **2.3** with good diastereoselectivity (dr, 3:1) and a high degree of chemosite selectivity (Table 2.3, entry 10). However, Rh_2(OCOCF$_3$)$_4$ and Rh_2(MEOX)$_4$, which are known to lead to more reactive carbenoids compared to Rh_2(OAc)$_4$' gave lower chemosite selectivity as expected. Thus, these catalysts are ideal for obtaining the greatest number of derivatives for initial SAR studies of a novel polyol natural product.

The scope of this O–H insertion with the new trifluoroethyl diazo ester (**2.7a**) was assessed with several commercially available natural products and derivatives (Table 2.4). In general, O–H insertion with metallocarbenoid is governed by both steric and electronic effects.[43] Despite the smaller steric size of the α-trifluoroethyl group, Rh_2(OAc)$_4$ catalyzed O–H insertions of diazo reagent **2.7a** with the natural products showed similar chemosite selectivity compared to the *p*-bromophenyl reagent **2.1**. These results suggested that the electronic effects play the predominant role for chemosite selectivity.

Brefeldin A (**2.4**) presented two potentially reactive alcohols; however, the more accessible secondary alcohol (C13) was selectively alkylated over the more electron rich allylic alcohol (C1). Paclitaxel (**2.11a**) has two electronically and sterically distinct secondary alcohols and a tertiary alcohol. The more accessible secondary alcohol (C2') was selectively derivatized with no reaction detected at the other alcohols or the amide N–H. To determine the reactivity of amines in comparison to alcohols, ephedrine

(**2.12a**), which bears a secondary alkyl amine and a secondary alcohol, was studied. As expected, the major adduct isolated was that derived from N–H insertion due to greater nucleophilicity; however, some bis-derivatization derived from both N–H and O–H insertion was also detected.

Table 2.4. Scope of $Rh_2(OAc)_4$-catalyzed chemosite selective O–H insertion of HTFB (**2.7a**) with various natural products.
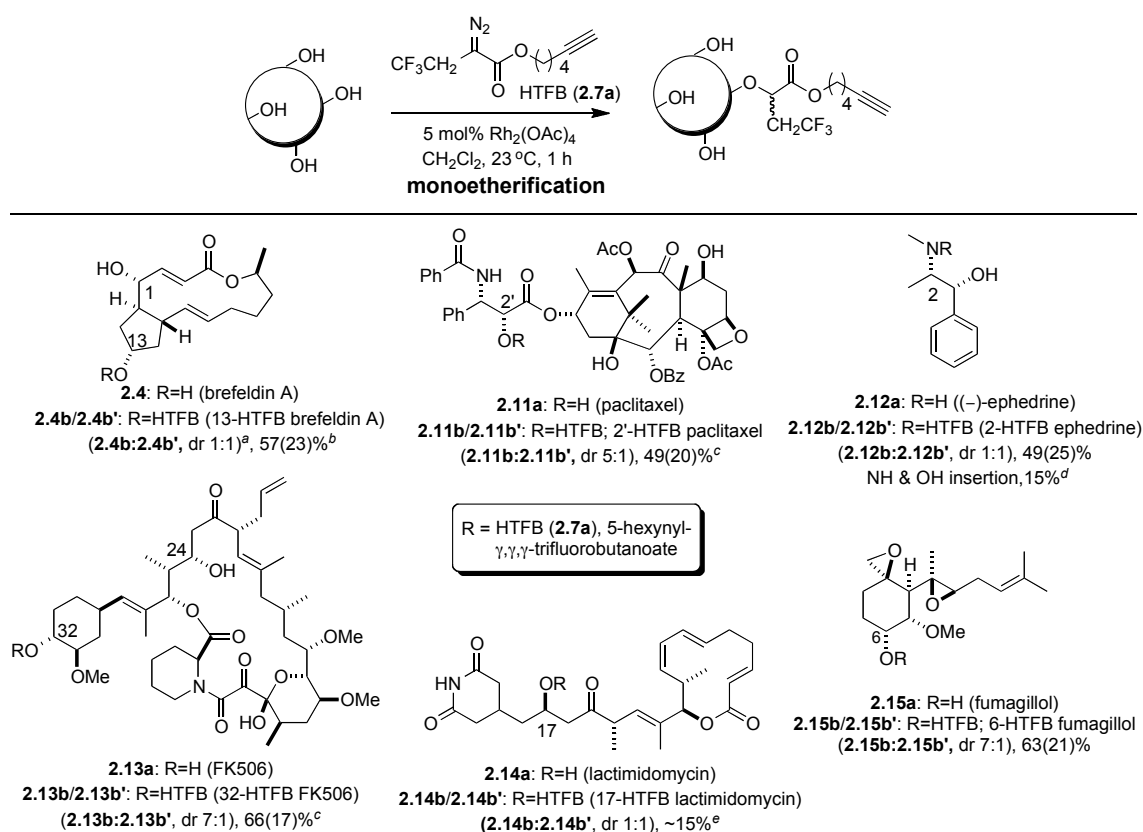
^{a}Diastereomeric ratios (dr) were determined by ^{1}H-NMR (500 MHz) and refer to the mixtures of diastereomers at the ether α-carbon. ^{b}Values refer to isolated yields and numbers in parentheses refer to recovered starting material. ^{c}6.0 equiv of HTFB (**2.7a**) was added via syringe pump over 2 h. ^{d}Bifunctional derivatization involving both O–H and N–H insertion was detected by LC-MS. ^{e}Run on a 2 mg-scale reaction therefore yield is approximate (microbalance) following purification by preparative HPLC with some unreacted lactimidomycin recovered.

In the case of FK506 (**2.13a**), O–H insertion led to chemosite selectivity at the more accessible cyclohexyl secondary alcohol (C32) in 66% yield and with good diastereoselectivity (dr, 7:1). No O–H insertion at the macrocyclic secondary alcohol (C24) or dietherification was observed. Previously, dietherification of FK506 was observed when HBPA (**2.1**) was added in one portion.[17] Therefore, slow addition of 6 equivalents of HTFB (**2.7a**) over 2 h, again prevented dietherification.

Lactimidomycin (**2.14a**) is a macrocyclic natural product with a pendant cycloheximide that has gained much interest due to its potent inhibitory effect on eukaryotic translation and elongation properties leading to dramatic antitumor activities.[44] However, lactimidomycin is highly acid and base sensitive which limits derivatization strategies. Thus, this became an excellent substrate for testing the mildness of this O–H insertion process. Use of HTFB (**2.7a**) provided ~15% yield of isolated, purified (preparative HPLC) ether **2.14b** on a reaction scale of 2 mg at 50% conversion with some loss of material attributed to degradation during purification. The successful derivatization of such a sensitive natural product demonstrates the utility of the described derivatization strategy as it proceeds under essentially neutral conditions, works efficiently on small scale (~1-2 mg), and allows for the recovery of unreacted starting material.

Fumagillol (**2.15a**) is a natural product in fumagillin family, which is known to inhibit angiogenesis through irreversible inhibition of human type 2 methionine aminopeptidase (MetAP2).[45] The O–H insertion of fumagillol employing HTFB provided ether **2.15b** in good yield (63%) without cyclopropanation and epoxide

decomposition.

Overall, these results are consistent with chemoselectivities previously observed for O–H insertion with Rh(II)-carbenoids derived from HBPA (**2.1**) and while not all O–H environments were explored, the same reactivity patterns (primary alcohol ≈ secondary alkyl amine > secondary alkyl alcohol > secondary allylic alcohol ≥ aryl amine > phenolic alcohol > tertiary alkyl alcohol > indole and no reaction with N–H of amide or alkenes) would be expected based on observations to date.

2.2.3. Proof of Principle Protein Assays and Affinity Experiments

We were next interested in studying the effect of having sterically different α-substituents leading to the retaining or improving of biological activities. Our studies focused on the effect of the α-trifluoroethyl substituent (HTFB) that displayed a smaller steric footprint in comparison with the bulky *p*-bromophenyl substituent (HBPA) on the ethers obtained from O–H insertion of natural products in the cellular assays and also affinity chromatography experiments with derived biotin conjugates.

Lactimidomycin conjugates **2.14b/2.14b′** and **2.16/2.16b′** which derived from O–H insertion with the α-trifluoroethyl substituted diazo reagent (**2.3a**) and *p*-bromophenyl substituted reagent (**2.1**) respectively (Scheme 2.5) were assayed in the *in vitro* translation assays performing in rabbit reticulocyte lysates (Promega Flexi RRL). Although, lactimidomycin (**2.14a**) was enabled to derivatize by mild and mono-functionalization O–H insertion with first- and second-generation diazo reagents (**2.1** and **2.3a**, respectively), we observed ~50% conversion and obtained low yield of

2.14b/2.14b′ (15%) and **2.16b/2.16b′** (13%) along with recovery of starting material (**2.14a**) by preparative HPLC separation.

Unfortunately, the SAR studies of **2.14b/2.14b′** and **2.16/2.16′** in cell-proliferation and RNA translation of rabbit reticulocyte lysates assay showed a tremendous loss of inhibitory activity (Table 2.5). The lactimidomycin-HBPA derivatives **2.16/2.16′** showed lower inhibitory activity in cell-proliferation >1000-fold compared to lactimidomycin (IC_{50} >3000 and 2.8 nM, respectively).

Scheme 2.5
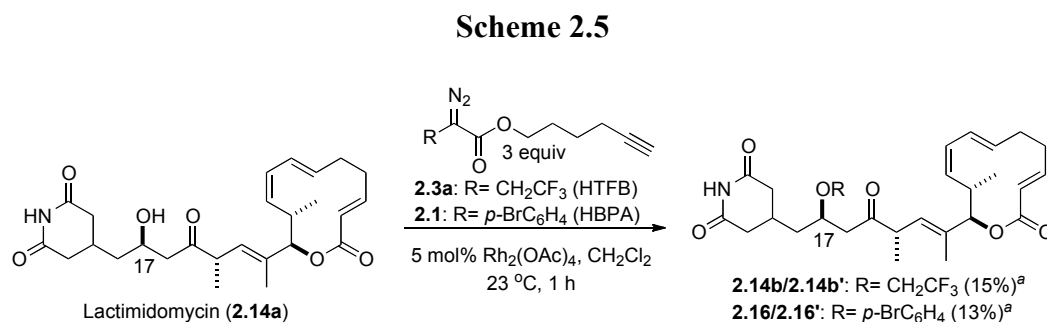
[a]Run on a 2 mg-scale reaction followed by preparative HPLC purification that causes loss and decomposition of desired product therefore yield is approximate (microbalance).

Table 2.5. IC_{50} values of lactimidomycin (**2.14a**) and derivatives **2.14b**, **2.14b′**, and **2.16/2.16′** for *in vitro* proliferation and translation of rabbit reticulocyte lysate assay.

Compound	IC_{50} proliferation (nM)	IC_{50} *in vitro* translation (μM)
Lactimidomycin (**2.14a**)	2.8	0.73
2.14b	ND[a]	98.2
2.14b′	ND	228.7
2.16/2.16′	>3000	63.7

[a]ND = means not determined.

Unexpectedly, lactimidomycin-HBPA derivatives **2.16/2.16′** showed better inhibitory activity in the translation assay compared to lactimidomycin-HTFB derivatives **2.14b** and **2.14b′** (IC_{50} 98.2, 228.7 and 63.7 μM, respectively). However, all resulted lactimidomycin derivatives exhibited lower inhibitory activity in RNA-translation ~100-300 folds compared to lactimidomycin. Since, we know that hydroxyl group on lactimidomycin is not crucial for biological activity. We assumed that the loss of potency resulted from an interference of α-substituent that diminished natural product and protein target interaction. Additionally, the diastereomeric FK506-derived ethers **2.13b/2.13b′** and **2.18/2.18′** were prepared and purified by preparative TLC, which enable to separate each diastereomer. An FK506-HTFB-biotin probe (**2.19**) was prepared by Sharpless-Hüisgen cycloaddition of the major diastereomeric HTFB ether **2.13b** and commercially available biotin azide **2.17**. The FK506-HBPA-biotin conjugate **2.20** was also prepared in a similar fashion (Scheme 2.6).

Scheme 2.6

[a]Ethers **2.13b** and **2.18** are the major diastereomers and ethers **2.13b′** and **2.18′** are minor diastereomers. [b]Biotin probes **2.19** and **2.20** were derived from isolated **2.13b** and **2.18** as single diastereomers, respectively.
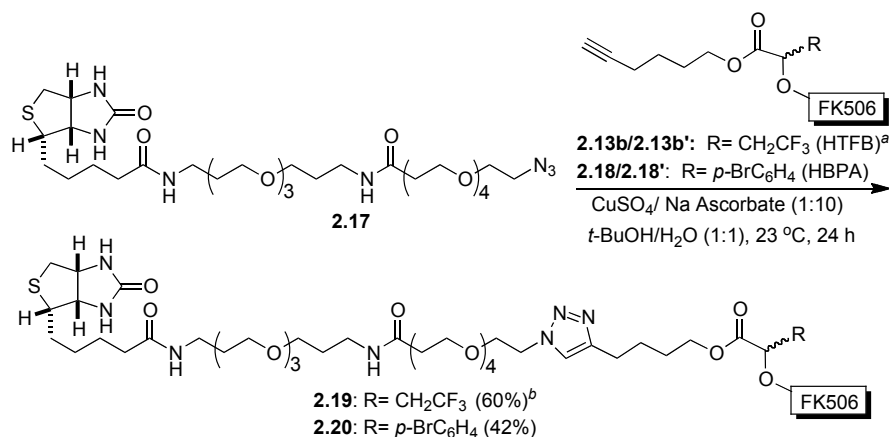
In our previous study, the use of an FK506-HBPA-biotin probe (**2.2**) led to pull-down of the entire immunosuppressive complex including FKBP12, calcineurin A/B, and calmodulin.[17] In the IL-2 reporter assay, the FK506-HTFB derivatives **2.13b** and **2.13b′** showed diminished inhibition of IL-2 production (~2-fold, IC_{50} 15.9±2.8 and 19.8±14.5 nM, respectively) compared to the FK506-HBPA derivatives **2.18** and **2.18′** (IC_{50} 10.2±3.8 and 7.3±0.6 nM, respectively) (Table 2.6). A similar trend was observed when the biotin conjugates were assayed in the IL-2 reporter assay with the FK506-HTFB-biotin probe **2.19** showing a >4-fold decrease in IC_{50} value compared to the corresponding FK506-HBPA-biotin conjugate **2.20**.

Table 2.6. IC_{50} values for IL-2 inhibition of Jurkat T cells by the diastereomeric FK506/HTFB ethers (**2.13b**/**2.13b′**) and FK506-HPBA ethers (**2.18**/**2.18′**) and biotin conjugates **2.19** and **2.20**.

Compound	IC_{50} (nM)[a]
2.13a	1.8±0.2
2.13b	15.9±2.8
2.13b′	19.2±14.5
2.18	10.2±3.8
2.18′	7.3±0.6
2.19	97.4±17.5
2.20	27.9±10.6

[a]Standard deviations provided for assays performed in triplicate.

In the most dramatic demonstration of the impact of a smaller steric footprint, side by side comparison of the two FK506-biotin probes **2.19** and **2.20** showed that the

smaller α-trifluoroethyl conjugate only led to pull-down of FKBP12, while the *p*-bromophenyl conjugate led once again to pull-down of the entire ternary complex containing both FKBP12 and calcineurin (Figure 2.10).
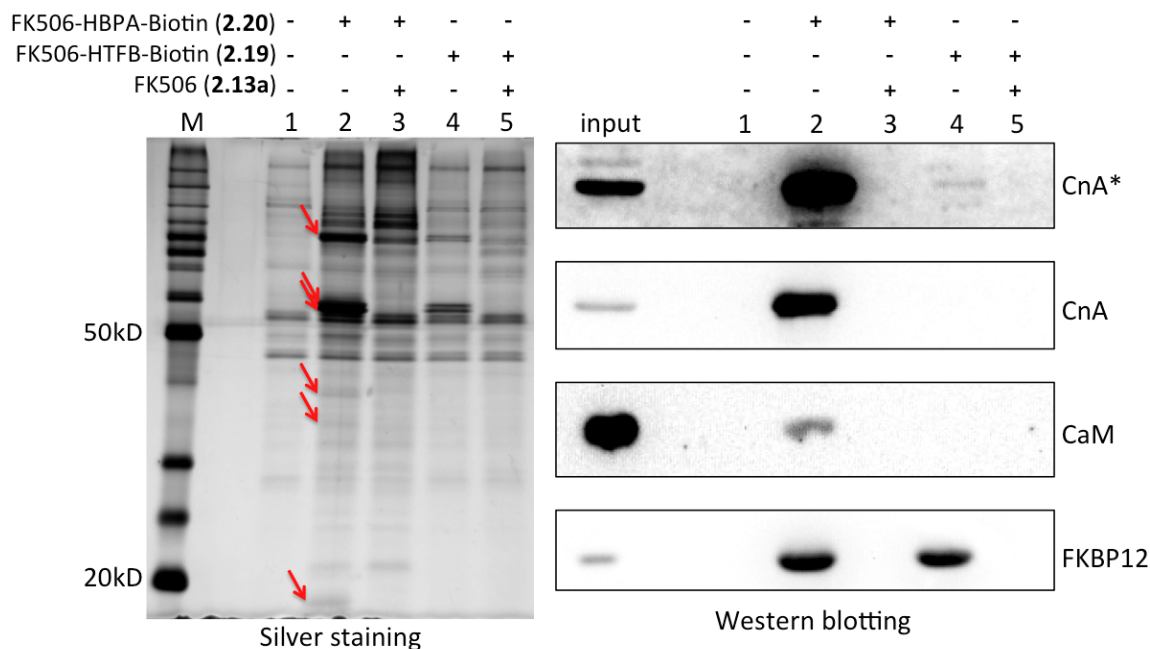
Antibodies are abbreviated as: CnA, calcineurin A; CaM, calmodulin; FKBP12, FK506 binding protein 12 (*means long time exposure). Red arrows indicate proteins that specifically bind to the FK506 probes including CnA, CaM, and FKBP12.

Figure 2.10. Proof of principle affinity chromatography experiments with FK506-HBPA-biotin conjugate (**2.19**) and FK506-HTFB-biotin conjugate (**2.20**). Conjugates were incubated with Jurkat T cell lysates with or without pre-incubation with FK506 (left panel: silver staining of all retained proteins; right panel: Western blotting by indicated antibodies).

These results demonstrated the profound effect of a smaller α-trifluoroethyl *versus* a larger *p*-bromophenyl substituent in pull-down experiments and is consistent with C32-aryl substituted FK506 derivatives, which were previously reported to increase

binding to calcineurin.[46] This previous study also described the increased IL-2 inhibition by C32-aryl *versus* C32-trifluorethyl substituted FK506 derivatives proposed to be due to favorable π-π interactions with calcineurin.

Fumagillol (**2.15a**, Table 2.4) is a natural product known to inhibit angiogenesis through irreversible inhibition of human methionine aminopeptidase type 2 (hMetAP2). The O–H insertions proceeded in good yield to provide HTFB-fumagillol **2.15b/2.15b′** (63%) and HBPA-fumagillol **2.21/2.21′** (58%) without competing cyclopropanation or epoxide degradation (Scheme 2.7).

Scheme 2.7
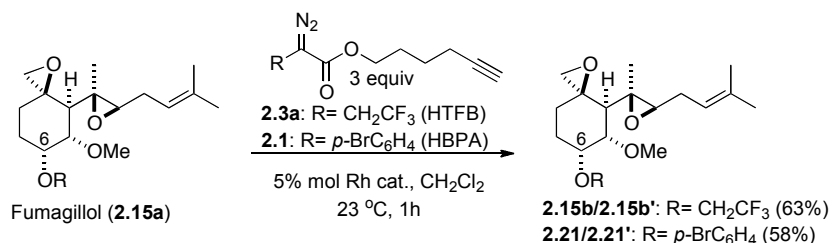
Previous SAR studies have shown that the structure of the C6-substituent can dramatically affect bioactivity.[47] We thus set out to evaluate the difference between trifluoroethyl and *p*-bromophenyl-substituted fumagillol derivatives obtained from O–H insertion of the C6-alcohol of fumagillol. Docking experiments with HTFB- and HBPA-fumagillol (**2.15b/2.15b′** and **2.21/2.21′**) using the X-ray structure of hMetAP2 suggested that the *p*-bromophenyl derivative (**2.21/2.21′**) would suffer from greater

unfavorable interactions upon binding to hMetAP2 compared to the α-trifluoroethyl

derivative (**2.15b**/**2.15b′**) (Figure 2.11).
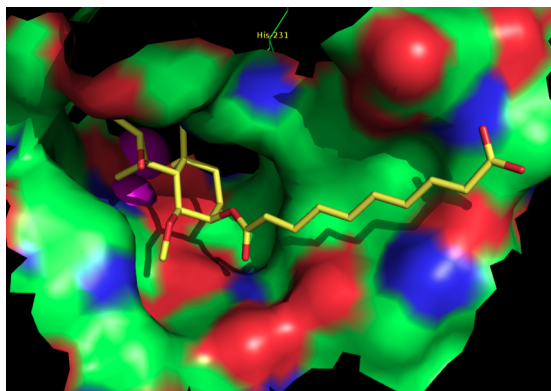
a) Structure of fumagillin bound hMetAP2
(PDB ID: 1BOA).
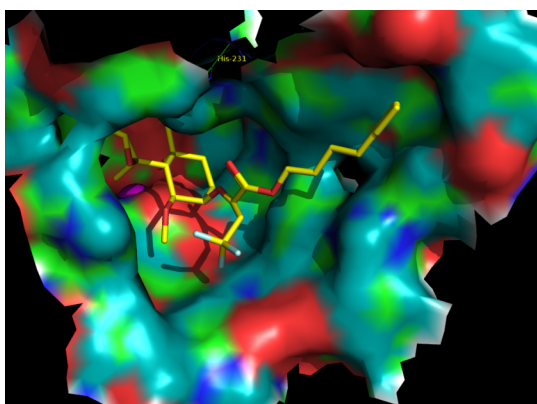
b) Putative structure of **2.15b/2.15b'**, sculpted from PDB ID: 1BOA.
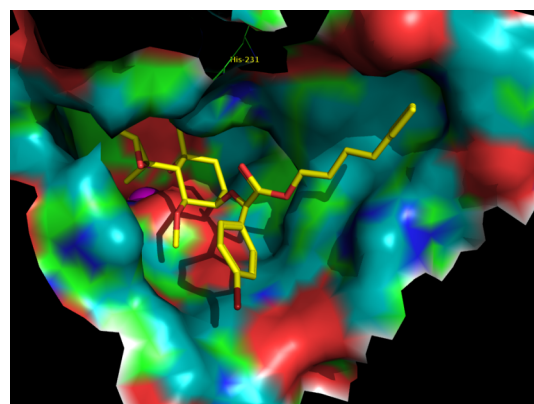
c) Putative structure of **2.21/2.21'**, sculpted from PDB ID: 1BOA.

Figure 2.11 Side-by-side comparison of docked fumagillol-HBPA (**2.21/2.21'**) and fumagillol-HTFB (**2.15b/2.15b'**) and the crystal structure of fumagillin-bound hMetAP2. Cobalt atoms are shown in purple, His-231 (the residue forming the covalent linkage) is marked, and a 5Å zone around fumagillin is rendered as a Connolly surface.

Based on molecular modeling and docking,[48] both HTFB and HBPA derivatives

of fumagillol (Figures 2.11a-c) appear to fit into hMetAP2's substrate binding pocket.

However, the *p*-bromophenyl group of HBPA did not have as much conformational

flexibility as the α-trifluoroethyl of HTFB within the pocket. Furthermore, the *p*-bromophenyl group might be a liability since the fumagillol-HBPA derivative (**2.21/2.21′**) would appear to require larger entrance into the binding pocket through the 'exit tunnel'. Thus, the interaction of fumagillol with hMetAP2 was chosen as a second test system to test the differences that could result between *p*-bromophenyl and α-trifluoroethyl derivatives, which possibly generalized the effect of α-substituent steric footprint for several natural products.

The derived diastereomeric fumagillol ethers **2.15b/2.15b'** and **2.21/2.21'** were not readily separated; therefore, they were used as a mixture of diastereomers for *in cellulo* protein profiling (Scheme 2.8). Side-by-side assays with fuma-alkyne (**2.22**) and TNP470 (**2.23**) were performed for comparison. The affinity experiments with fumagillol-HTFB (**2.15b/2.15b′**) led to greater pull-down of MetAP2 than that of fumagillol-HBPA (**2.21/2.21′**) (Figure 2.12). Consistent with these results, fumagillol-HTFB **2.15b/2.15b′** also showed greater inhibitory activity in a human umbilical vein endothelial Cells (HUVEC) proliferation assay compared to the fumagillol-HBPA derivatives **2.21/2.21′** (~5-fold decrease, IC$_{50}$ 115.3±35.4 and 568.2±215.1 nM, respectively).

Scheme 2.8
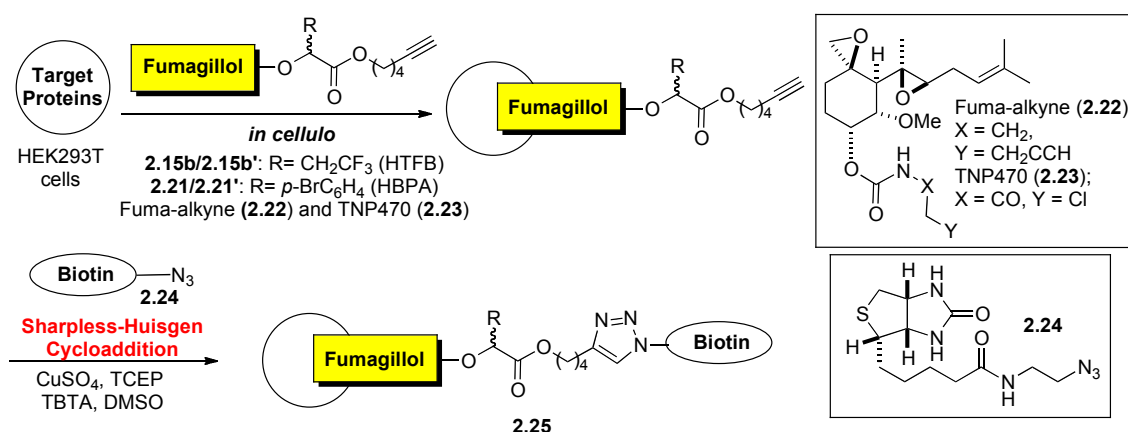
TCEP=tris-(2-carboxyethyl) phosphine; TBTA=Tris[(1-benzyl-1*H*-1,2,3-triazol-4-yl)methyl] amine. A mixture of diastereomers **2.15b/2.15b′** and **2.21/2.21′** were used for the affinity experiments and Sharpless-Hüisgen cycloaddition.

Lane 1: 10% input; Lane 2: DMSO; Lane 3: Fumagillol-alkyne (**2.22**) in competition with TNP470 (**2.23**); Lane 4: Fumagillol-alkyne (**2.22**); Lane 5: Fumagillol-HTFB (**2.15b/2.15b′**); Lane 6: Fumagillol-HBPA (**2.21/2.21′**). Bottom: Western blotting to confirm hMetAP2 (human methionine aminopeptidase type 2). The arrow points to MetAP2.
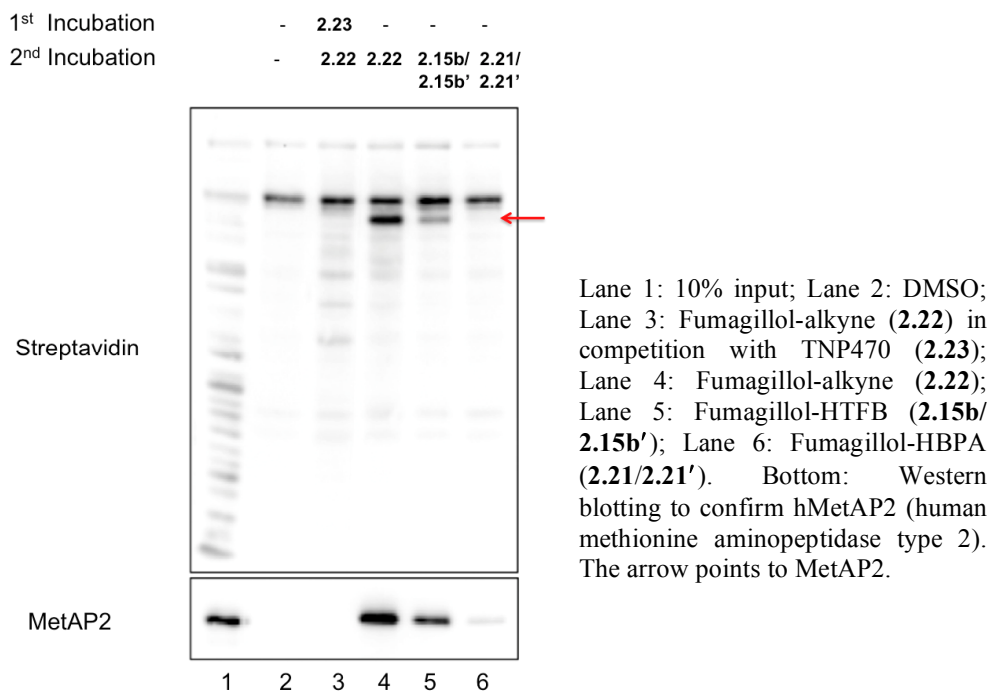
Figure 2.12. Affinity chromatography experiments with fumagillol derivatives **2.15b/2.15b′**, **2.21/2.21′**, **2.21** and **2.23**. Click reactions to catch the fumagillol targets were performed *in vivo* using azide **2.24** to afford biotinylated fumagillol derivatives. The target of fumagillol was analyzed by blotting membrane with streptavidin horseradish peroxidase or antibody against hMetAP2.

A similar trend was observed when **2.15b/2.15b′** and **2.21/2.21′** were assayed in the MetAP2 enzymatic assay (Table 2.7). The fumagillol-HTFB **2.15b/2.15b′** showed ~4-fold increase in EC_{50} value compared to fumagillol-HBPA **2.21/2.21′** (EC_{50} 0.27±0.03 and 0.95±0.23 µM, respectively). Thus, the comparative results of both fumagillol and FK506-HBPA and HTFB alcohol derivatives highlighted the significance of the smaller steric footprint and demonstrate the utility of the novel α-trifluoroethyl diazo reagent **2.3a** for natural product derivatization.

Table 2.7. IC_{50} values in HUVEC cells and the EC_{50} values from hMetAP2 assay of fumagillol (**2.15a**), fumagillol-HTFB (**2.15b/2.15b′**) and fumagillol-HBPA (**2.21/2.21′**).

Compound	IC_{50} Proliferation $(nM)^a$	EC_{50} MetAP2 $(µM)^a$
2.15a	ND	0.06±0.01
2.15b/2.15b′	115.3±35.4	0.27±0.03
2.21/2.21′	568.2±215.1	0.95±0.23
2.22	0.47±0.07	ND
2.23	0.16±0.06	ND

^{a}Standard deviations provided for assays performed in triplicate. ND = not determined. hMetAP2 = human methionine aminopeptidase type 2.

2.3. Conclusion

In conclusion, the variation of chemo- and site selectivity of O−H insertion protocol for derivatization of alcohol-containing natural products was described by employing Rh(II) catalysts including achiral and chiral catalysts. The results suggest that each natural product has specific shape-shape interactions or specific "shape fit" with particular metal carbenoids. Therefore, the overall shape interaction and reactivity of

catalyst are more important than chirality of the catalyst itself. Furthermore, we have developed two new diazo reagents, the α-trifluoroethyl diazo reagent **2.3a** (HTFB) and a *p*-azidophenyl diazo **2.3d** reagent for simultaneous arming and SAR studies of bioactive natural products *via* O–H insertion. HTFB (**2.3a**) possesses a reduced steric footprint compared to the *p*-bromophenyl reagent (**2.1**) and enables the use of ^{19}F-NMR to facilitate small-scale, crude derivatization reaction analysis. Furthermore, this reagent showed comparable reactivity and good chemosite selectivity compared to HBPA (**2.1**). The difference in steric footprint and binding affinity of an HTFB-FK506 derivative for FKBP12 was demonstrated by measurement of IC$_{50}$ values in the IL-2 reporter assay; in addition, affinity chromatography experiments in side-by-side comparisons of FK506-HTFB-biotin (**2.19**) and FK506-HBPA-biotin (**2.20**) led to dramatic differences in proteins captured. Furthermore, HTFB- and HBPA-fumagillol derivatives prepared by these methods also demonstrated the advantage of the α-trifluoroethyl substituent in terms of smaller steric footprint leading to increase the binding to hMetAP2. The *p*-azidophenyl diazo reagent **2.3d** should prove useful for photoaffinity experiments with low affinity natural product receptors. Further applications of these reagents to natural product derivatization and their subsequent use for receptor isolation are under active investigation.

CHAPTER III

SYNTHESIS OF β-LACTAM CONGENERS OF ORLISTAT AS FATTY ACID SYNTHASE INHIBITORS*

3.1. Introduction

In the past several decades, cancer research has continuously been an ongoing study due to its complicated metabolic pathway and uncontrolled tumor growth. Cancer has long been known as a malignant disorder in human diseases. Based on the GLOBOCAN, about 12.7 million cancer cases were reported and 7.6 million cancer patients died in 2008.[49] Disordered intermediary metabolism in human cancer cell has been well documented[50] since Warburg reported the first observation of high levels of anaerobic metabolism in cancer cells (known as the "Warburg effect") in1924.[51] Increased anaerobic glycolysis has become an indication of the transformed phenotype of cancer cell lines, since the glycolytic pathway is an essential energy source for tumors (Figure 3.1).[52] In the 1950s, Greenstein[50] and Medes[53] observed an elevated level of fatty acid synthesis in tumor tissue, which suggested affiliation between glycolytic pathway and fatty acid synthesis. However, little attention was given to endogenous fatty acid synthesis in human cancer cell lines. Thirty years later, Beaker[54] described the *de novo* synthesis of fatty acids in tumor cells that could be a significant source of fatty acid for

---

*Reprinted with permission from "β-Lactam Congeners of Orlistat as Inhibitors of Fatty Acid Synthase" by Zhang, W.; Richardson, R. D.; Chamni, S.; Smith, J. W.; Romo, D. *Bioorg. Med. Chem. Lett.* **2008**, *28*, 2491-2494. Copyright 2008, Elsevier, See Appendix B.

tumor growth, despite having adequate nutritional lipid supply from outer sources. Recently, Kuhajda[55] revealed the association between fatty acid synthesis towards poor prognosis in breast cancer and the inhibition of fatty acid synthesis effectively and selectively killing cancer cells. Regarding these observations, fatty acid synthesis has slowly emerged as a cancer chemoprevention and continues to be of significant interest in tumor biology.
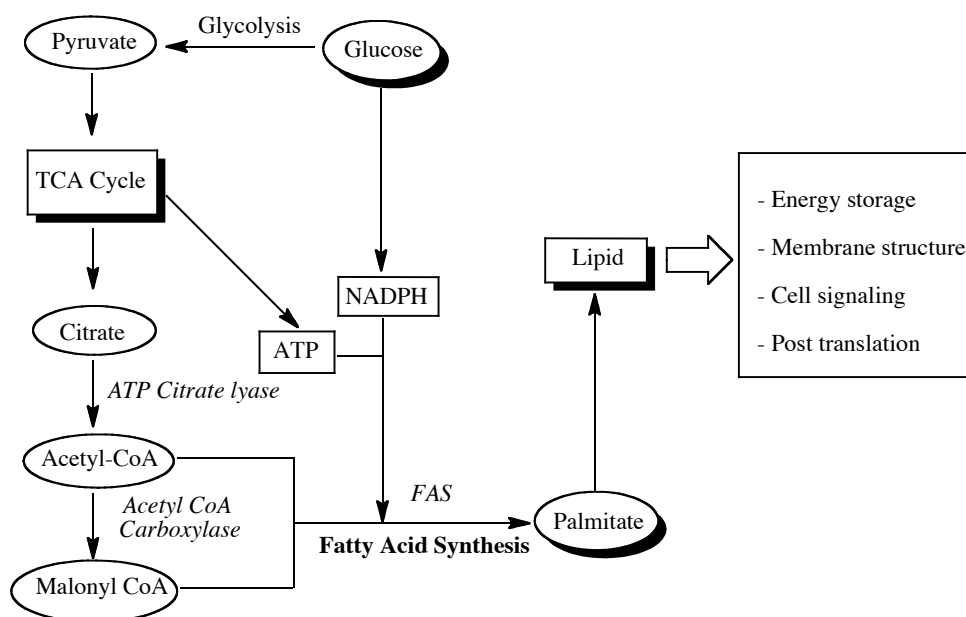
Figure 3.1. Fatty acid synthesis and its functions in mammalian tissues.

3.1.1. Structure and Function of Mammalian Fatty Acid Synthase

Fatty acid synthase (FAS) is a 272 kDa multi-complex enzyme that plays an essential role in fatty acid synthesis leading to the formation of palmitate, a 16-carbon saturated free fatty acid (Scheme 3.1).[56] FAS can be found in all plants and animals and

it is classified into two principal classes. The FAS I is a single, large, multifunctional polypeptide that controls the formation of palmitic acid, while FAS II is the monofunctional enzyme that associates with FAS I to generate a range of lipids for mitochondria functions.[57] The FAS I has recently been found to be an important target for oncology since it showed oncogenic activity[58] and its inhibition effectively and selectively kill cancer cells, with low cytotoxicity to normal cells.[59]

The structure of mammalian FAS consists of two identical multifunctional polypeptides, which contain 6 catalytic domains and 1 protein carrier that arrange in an intertwined, X-shaped, head-to-head homodimer with a buried surface area of 5400 $Å^2$ (Figure 3.2).[60]

The two polypeptide-chains are associated with each other through hydrophobic interactions between the KR, ER and DH domains of the two subunits, which is located at the center of the FAS structure. Each domain adopts a coiled conformation that allows multiple intra- and inter-subunit interactions between the functional domains. The FAS structure can be divided into two portions involving the condensing portion (KS and MAT domains) and the β-carbon modifying portion (DH, ER, and KR domains). The N-terminal domains are β-ketoacyl synthase (KS), malonyl/acetyltransferase (MAT), and dehydrogenase (DH), and the C-terminal domains are enoyl reductase (ER), β-ketoacyl reductase (KR), acyl carrier protein (ACP), and thioesterase (TE).
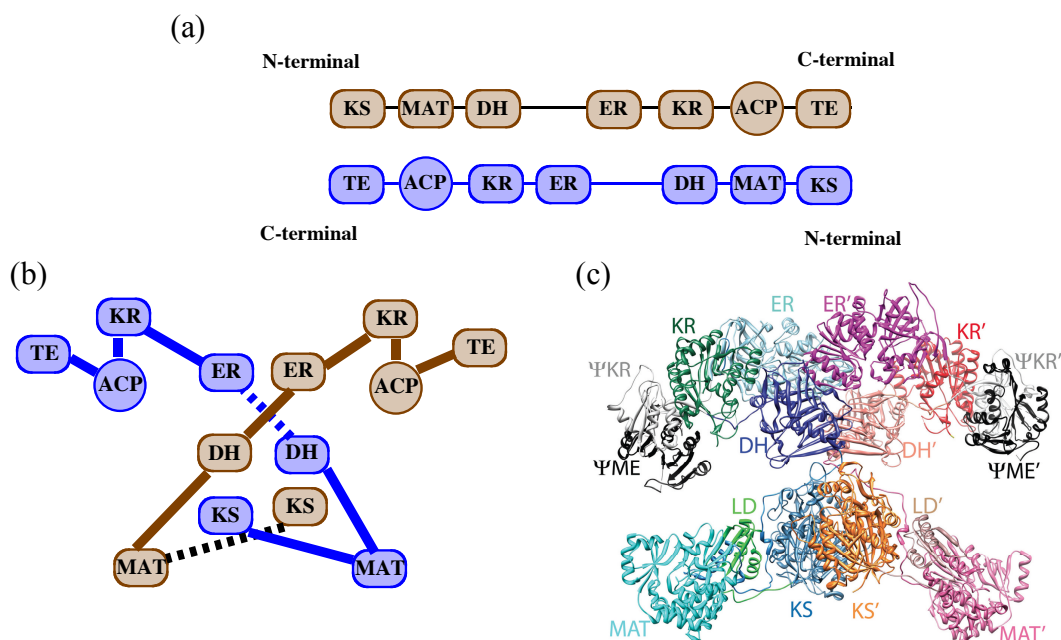
Figure 3.2. Structure and domain organization of fatty acid synthase (FAS). (a) Conventional dimeric model: head-to-tail organization, (b) Revised X-shaped dimeric model: head-to-head organization, (c) 3.2 Å crystal structure of fatty acid synthase (FAS). KS=ketoacyl synthase; MAT=malonyl/acetyltransferase; DH=dehydrogenase; ER=enoyl reductase; KR=ketoacyl reductase, ACP=acyl carrier protein; TE=thioesterase; The two non-enzymatic domains, ΦKR=pseudo-ketoreductase and ΦME=pseudo-methyltransferase.

In normal tissues, more than 25 enzymes are involved in the metabolism of glucose to fatty acids. However, the fatty acid synthetic pathway conducted by FAS involves three crucial steps that happen respectively:[61] (1) the condensation of malonyl-CoA and acetyl-CoA catalyzed by MAT, (2) elongation, a 7-repeating cycle of reduction and dehydration to extend 2 carbons in each cycle, resulting in the elongating of the fatty acid chain catalyzed by KS, DH, ER, and KR, and (3) termination to release palmitate from ACP catalyzed by TE (Figure 3.3).
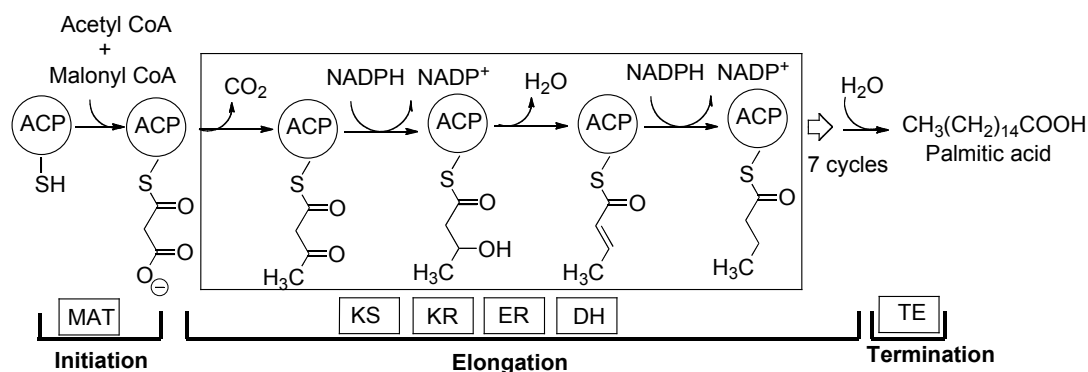
Figure 3.3. Synthesis of palmitic acid by fatty acid synthase.

This process consumes 1 acetyl-CoA, 7 malonyl-CoA, 7 ATP, and 14 NADPH molecules to produce one molecule of palmitate. In highly lipogenic tissues such as liver, lactating breast and adipose tissue of well-nourished adults, the primary role of fatty acid synthesis is energy storage by converting excess carbohydrates to fatty acids, followed by esterification to store as triacylglycerol. Furthermore, fatty acid synthesis has specialized functions such as lactation to produce fatty acids that are easily digested by infant.

3.1.2. Fatty Acid in Tumorigenesis and Fatty Acid Synthase Inhibitors

In normal human tissues, the down-regulation of FAS is normally observed because of sufficiently high levels of fat consumption.[62] A number of studies have shown the over expression of FAS in tumor cells including carcinomas of the colon[63], prostate,[64] ovary,[65] endometrium[66] and breast.[67] The *de novo* fatty acid synthesis of cancer cells results in palmitate, which is similar to the product from normal liver and lipogenic tissues, though FAS is up-regulated in cancer cells and the resulted palmitate is

predominantly incorporated into phospholipids, not triacylglycerol. Furthermore, fatty acid synthesis in tumor cells is transcriptionally generated either by hormones or oncogenes that are operated through kinase pathways, not by food consumption as occurring in normal lipogenic tissue. Additionally, the level of FAS can be detected in patient's blood. The mechanism for FAS up-regulation in cancer cells has not yet been discovered. However, the over expression of FAS, resulting high levels of phospholipids, points to the sufficient energy for promoting tumor growth. This hypothesis has been supported particularly in breast and prostate cancer, where clinical studies found an association between FAS expression and cancer prognosis.[68]

The inhibition of FAS has been studied by employing a diverse array of natural products as FAS inhibitors (Table 3.1). Each FAS inhibitor has a different inhibiting mechanism and inhibits different FAS domains.[69] According to pharmacological studies, FAS inhibitors exhibit anticancer activity by blocking tumor cell proliferation, eliciting tumor cell death, and preventing tumor growth in animal models. Together, these details highlight FAS as a therapeutic target for diagnosis and prognosis of human cancer, and the studies of FAS inhibition potentially lead to new anticancer therapeutics and chemoprevention protocols.

Table 3.1. Fatty acid synthase (FAS) inhibitors and their protein targets.

FAS Inhibitors[a]	FAS Domain targets[b]
Cerulenin	KS
C75	KS, ER and TE
C93	KS
Orlistat and β-lactone derivative	TE
5-(furan-2-ylmethylene) pyrimidine 2,4,6-trione	TE
Tea polyphenol (EGCG and ECG)	KR
EGCG hydrolytic product	MAT
Flavonoid	KR
Triclosan	ER

[a]See Ref. 47d and references cited for details. [b]Fatty acid domains: KS=ketoacyl synthase; MAT=malonyl/acetyltransferase; ER=enoyl reductase; KR=ketoacyl reductase; TE=thio-esterase.

3.1.3. Orlistat, a Fatty Acid Synthase Inhibitor with Antitumor Activity

Orlistat (Tetrahydrolipstatin) is one of the well-known FAS inhibitors as an antiobesity drug with potential antitumor activities. It is the first Food and Drug Administration (FDA)-approved, over-the-counter weight loss medication under the trade name 'Xenical' by Roche and 'Alli' by GlaxoSmithKline that is distributed to many countries including United States. This antiobesity drug primarily inhibits pancreatic and gastric lipases within the gastrointestinal (GI) tracts by blocking hydrolysis of triglycerides, thus no fatty acid uptake from diet.[70] In 2004, orlistat was also found to inhibit the thioesterase domain (TE) of fatty acid synthase (FAS), which is an important enzyme for cancer growth.[71] The FAS-TE mechanism of inhibition by orlistat involves a tight-binding, irreversible inhibition by formation of a new covalent

bond at the active site of serine *via* acylation by the β-lactone (Figure 3.4).[72]
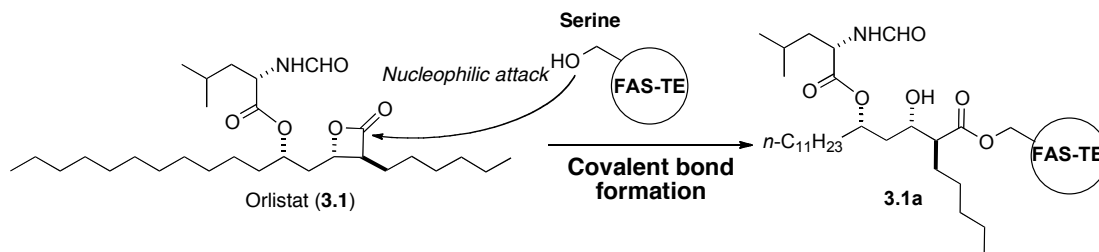
Figure 3.4. Orlistat (**3.1**) and inhibition of FAS-TE mechanism.

Regarding to the effective blocking of cellular FAS activity, orlistat induces endoplasmic reticulum stress and apogenesis in tumor cells, inhibits endothelial cell proliferation and angiogenesis.[58] Several studies toward FAS inhibitors have shown an antitumor activity including prostate, breast, ovary, and melanoma cancer cells without adverse effects on normal cells. However, the clinical application of orlistat for systematic use in cancer chemotherapy is very limited due to poor solubility and oral bioavailability. Indeed, one important aspect of orlistat is observed in the determination of the orlistat-FAS-TE co-crystal structure[59] to confirm the binding mode and inhibiting mechanism (Figure 3.5).

The crystal structure displays the binding pocket in the FAS-TE domain that can be divided into three portions: a cavity that holds the *N*-formyl-*L*-leucine moiety of orlistat, the specificity channel where the 16-carbon palmitate core binds, and the short-chain pocket that accommodates the hexanoyl tail. In FAS-TE active sites, orlistat exists in two forms: a serine adduct derived from a covalently bounded acyl-enzyme

intermediate (Figure 3.5a) and a hydrolyzed product derived for β-lactone hydrolysis by water yielding the hydroxy acid moiety (Figure 3.5b). These findings, together with molecular docking studies, provide useful information for structure-based drug design for drug development and SAR studies of orlistat and other orlistat-like analogues as promising anticancer therapeutics.
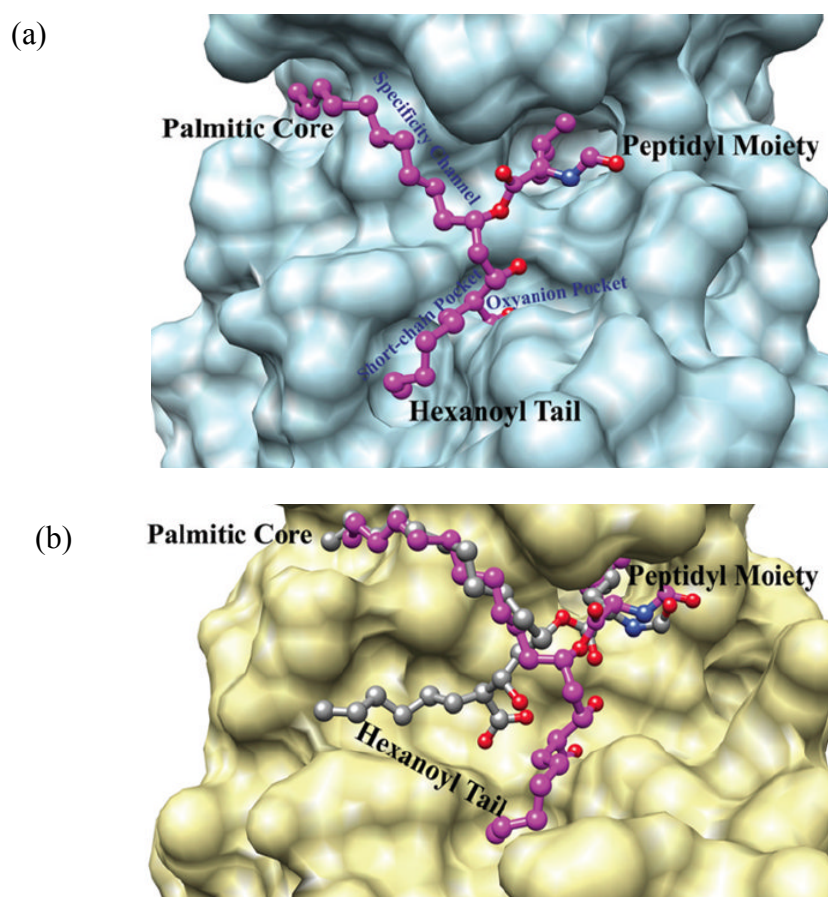
Figure 3.5. Binding mode of orlistat in the TE domain of FAS. (a) a serine adduct intermediate, (b) a hydrolyzed product (gray ball and stick,) with superimposed serine intermediate (pink ball and stick) to show the shifts and changes in the hydrolyzed product.

3.1.4. Synthesis of β-Lactones *via* Tandem Mukaiyama Aldol-Lactonization (TMAL)

β-Lactones is a versatile synthetic intermediates that can undergo a variety of transformations in stereospecific functionalization to achieve the key intermediates for various natural product syntheses.[73] Several direct approaches leading to asymmetric synthesis of β-lactone have been reported[74] including a highly diastereoselective route to racemic *trans*-3,4-disubstituted β-lactones based on a tandem Mukaiyama aldol-lactonization (TMAL). In 1994, Hirai and co-workers reported the first example of β-lactone formation *via* a Mukaiyama aldol-lactonization.[75] The *cis*-β-lactone was produced in low yield from the reaction of *p*-nitrobenzaldehyde and thiopyridyl ketene acetal with ZnCl$_2$ (Scheme 3.1). Building on Hirai's protocol, the Romo group developed a diastereoselective β-lactone synthesis through a tandem Mukaiyama aldol-lactonization (TMAL) to access both *trans*- and *cis*-β-lactone from various aliphatic aldehydes and thiopyridyl ketene acetals by employing ZnCl$_2$[76] and SnCl$_4$[77], respectively to achieve the desired-β-lactones in good to moderate yields with high diastereoselectivity (Scheme 3.2)

Scheme 3.1
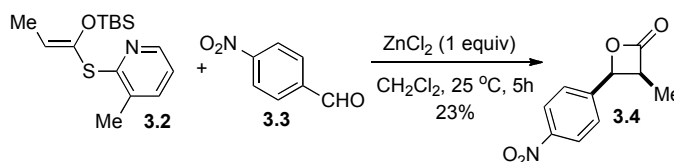
Scheme 3.2
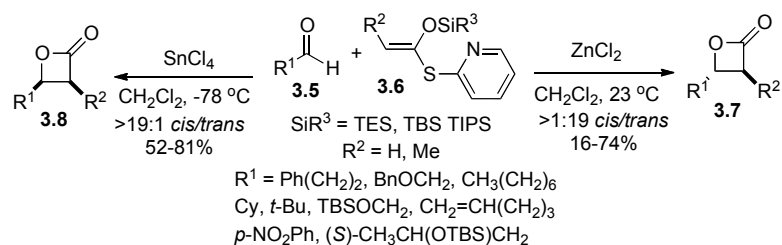
Throughout the course of optimization, various parameters were studied including Lewis acids, substituents and silyl protecting groups on ketene acetals. Several important results were observed to enable highly efficient β-lactone formation *via* TMAL process.[78] To date, ZnCl$_2$ was the only Lewis acid that delivered *trans*-β-lactones (**3.7**). Regarding the substituent on the ketene acetal, the thiopyridine moiety was found to be crucial for β-lactone formation due to the coordination of zinc to sulfur and nitrogen atom on thiopyridine moiety assisting the formation of the zinc complex. Furthermore, the steric bulkiness of the silyl group of the ketene acetal played an important role in the outcome of the TMAL process. We found that less bulky silyl groups increased the yield of β-lactone products. The experimental evidence also suggested that the Mukaiyama aldol was the rate-limiting step because no typical aldol products were observed from the reaction. Based on our observations, we proposed a mechanism of ZnCl$_2$-mediated TMAL reactions, which associated to the highly ordered, boat-like transition state arrangement leading to *trans*-β-lactones (Scheme 3.3).

Considering the nature of thiopyridyl ketene acetal **3.6**, the poor overlapping between sulfur atom and the adjacent carbon atom leads to a high degree of sp^3 character

that facilitates the formation of a cyclic transition state arrangement. The sulfur atom has an available site to coordinate with zinc(II) and forms 4-membered, tetrahedral zinc(II) thiopyridyl chelate **3.6a** (Scheme 3.3). Then, an aldehyde (**3.5**) chelates to zinc(II) and forms the diastereomeric trigonal bipyramidal zinc(II) complexes (*Z*)- and (*E*)-**3.9a**. The formation of a carbon-carbon bond leads to the intermediate (*Z*) and (*E*)-**3.9b** that adopts the boat-like transition stage arrangement, which then undergo facile transannular lactonization ((*Z*) and (*E*)-**3.9c**), followed by Zn–O bond dissociation to release the ring strain yielding silylated β-lactones (*Z*) and (*E*)-**3.9d**. Desilylation by the liberated chloride ion derived from **3.10b** delivers *trans*-β-lactones **3.7**.[79]

Scheme 3.3
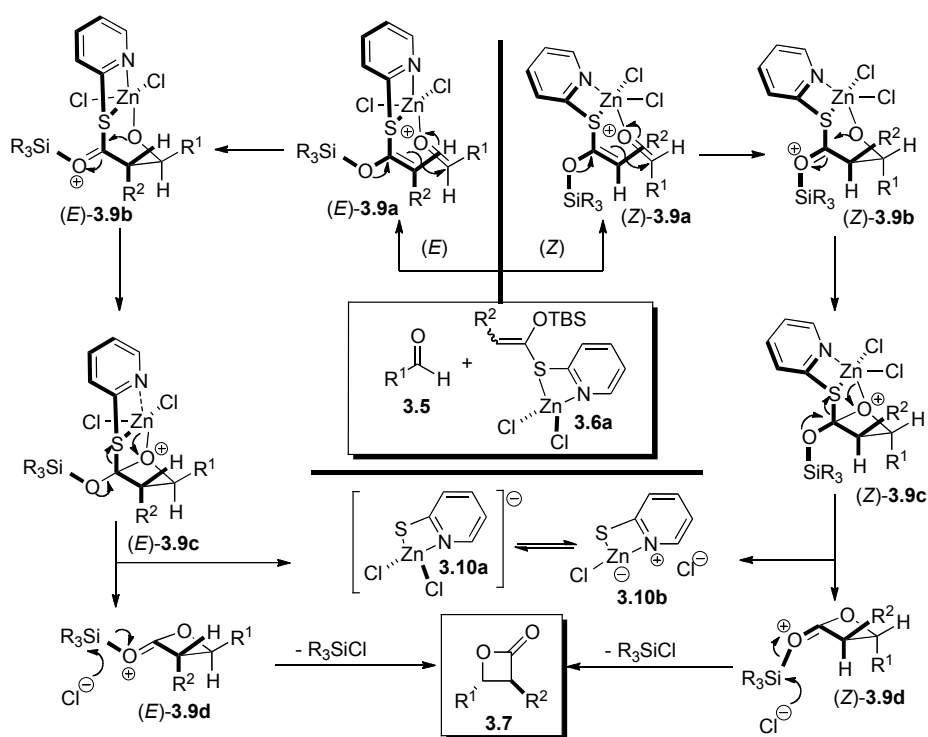
In the case of SnCl$_4$-mediated tandem Mukaiyama aldol-lactonization (TMAL), SnCl$_4$ is known to form a bidentate chelating with the 2-mercaptopyridine moiety of ketene acetal, which facilitates the formation of silylated ketene. Therefore, we proposed the [2+2] cycloaddtion mechanism between aldehyde and *in situ* generated silylated ketenes for SnCl$_4$-mediated TMAL process to achieve *cis*-β-lactones (Scheme 3.4). Nucleophilic attack by aldehyde **3.5** to the highly activated ketene **3.12**, followed by ring closure, delivers the silylated β-lactone intermediate (**3.13**). Subsequent desilylation by the liberated chloride ion yields *cis*-β-lactones **3.8**.[80]

Scheme 3.4
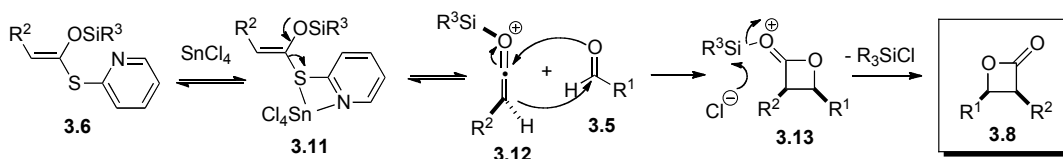
The ZnCl$_2$ and SnCl$_4$-mediated tandem Mukaiyama aldol-lactonization (TMAL) has been used to access a variety of racemic and optically active β-lactones including several natural products.[81]

3.1.5. A Single-pot, Mild Conversion of β-Lactones to β-Lactams

A β-lactam is a four-membered cyclic amide that is commonly found in several antibiotics such as penicillin and amoxicillin.[82] This heterocycle has emerged as an important synthetic target and is employed as a versatile intermediate in synthesis.[83] The

first synthetic β-lactam was reported by Staudinger in 1907 from the [2+2] cycloaddition of diphenylketene (**3.15**) and Schiff base **3.14** (derived from aniline and benzaldehyde) to yield β-lactam **3.16**.[84]

Scheme 3.5
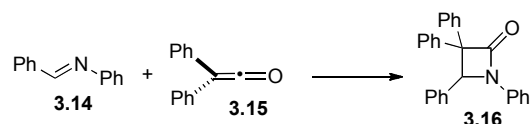
In the Romo's group, we have developed several strategies for β-lactone transformation and extension of its utility in synthesis.[85] Building on Miller's protocol,[86] we reported an indirect route to optically active β-lactams *via* one-pot conversion of β-lactones to β-lactams, involving β-lactone ring opening and intramolecular Mitsunobu cyclization.[87] Acyl C–O ring opening of β-lactone **3.17** by hard-nucleophile such as *O*-benzyloxyamine delivered β-hydroxy amide **3.18** followed by Mitsunobu cyclization to achieve the corresponding β-lactam **3.19** with inversion of configuration at the β-carbon. The *cis*-β-lactones resulted *trans*-β-lactams. In most cases, high diastereoselectivity of the derived β-lactams were observed. However, less satisfactory results were obtained when the α-carbon was substituted with heteroatom such as OBn and $SiMe_3$.

Scheme 3.6

R^1 = alkyl, R^2 = Me, H, OBn, TMS

cis-β-lactone → $trans$-β-lactam; >19:1 $cis/trans$
$trans$-β-lactone → cis-β-lactam; >1:19 $cis/trans$
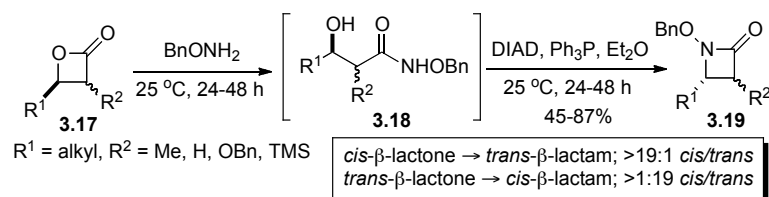
3.1.6. Synthesis of β-Lactone Congeners of Orlistat and SAR Studies

In previous synthetics studies toward FAS inhibitors, a variety of orlistat congeners were prepared using our $ZnCl_2$-mediated tandem Mukaiyama aldol-lactonization (TMAL) process as a key step (Scheme 3.7).[81g,h,j]

Scheme 3.7

Orlistat (**3.1**); R^1 = $C_{10}H_{21}$, R^2 = C_6H_{13}, R^3 = $CH_2(CH_3)_2$
Valilactone (**3.1a**); R^1 = C_5H_{11}, R^2 = C_6H_{13}, R^3 = $CH_2(CH_3)_2$
Panclicin D (**3.1b**); R^1 = C_7H_{15}, R^2 = $C_{10}H_{21}$, R^3 = H
Lipstatin (**3.1c**); R^1 = C_5H_{11}-(cis-CH=CH)-CH_2-(cis-CH=CH)
R^2 = C_6H_{13}, R^3 = $CH_2(CH_3)_2$
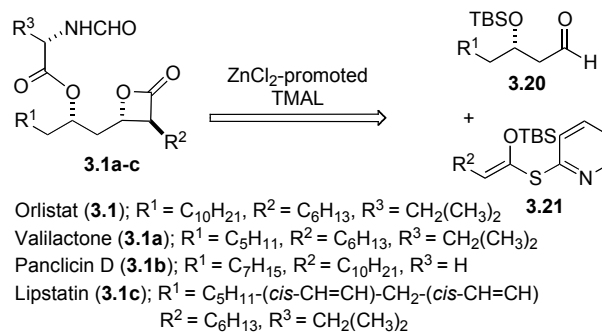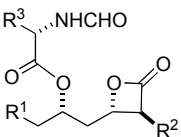
Comparative antagonistic activity of derived orlistat derivatives toward a recombinant form of FAS-TE was reported along with comparative activity-based profiling. Several novel β-lactone based orlistat analogs showed the improved potency toward FAS-TE inhibitor, an increased potency toward tumor cells, and greater selectivity for tumor cells over fibroblasts. However, the structural requirements for inhibition of

FAS-TE and factors for improving solubility, potency, and selectivity were delineated (Table 3.2).[81j] These results provided an important fundamental aspect for structure-based design of β-lactones with optimal cytotoxicity profiles, and it has been suggested that the orlistat congeners can be optimized for use in preclinical drug design and clinical drug development in carcinomas treatment.

Table 3.2. Orlistat congeners that displayed enhanced FAS-TE inhibitory but different cellular selectivity.[a]

Entry		FAS-TE IC$_{50}$ (μM)	MDA-MB-231 IC$_{50}$ (μM)	Hs58.Fs IC$_{50}$ (μM)
1	$R^1 = C_{10}H_{21}$, $R^2 = C_6H_{13}$ $R^3 = (CH_3)_2CH_2$; (Orlistat)	1.35	16.8	70.2
2	$R^1 = C_4H_9$, $R^2 = C_6H_{13}$ $R^3 = (CH_3)_2CH_2$; (Valilactone)	0.03	10.5	>100
3	$R^1 = C_{10}H_{21}$, $R^2 = C_2H_5$, $R^3 = H$	0.23	1.3	10.0
4	$R^1 = (CH=CH)CH_2$, $R^2 = C_6H_{13}$ $R^3 = (CH_3)_2CH_2$	0.28	3.3	29.6
5	$R^1 = C_4H_9$, $R^2 = C_6H_{13}$, $R^3 = H$	0.10	48.0	52.2
6	$R^1 = C_7H_{15}(CH=CH)CH_2$ $R^2 = C_6H_{13}$, $R^3 = (CH_3)_2CH_2$	0.12	>100	43.9
7	$R^1 = C_{12}H_{25}$, $R^2 = C_6H_{13}$, $R^3 = H$	0.21	26.9	37.3
8	$R^1 = C_{12}H_{25}$, $R^2 = C_6H_{13}$ $R^3 = PhCH_2$	0.29	>100	>100

[a]MDA-MB-231 is the breast carcinoma cells and Hs58.Fs is the foreskin fibroblasts. These two cell lines were used to distinguish mechanism based cell death that elicited by inhibition of FAS from general cytotoxicity.

3.2. Results and Discussion

As part of ongoing efforts to develop new β-lactone based transformations, we previously reported a mild, efficient two-step, one-pot method for conversion of β-lactones to β-lactams based on the method of Miller.[86] In conjunction with our ongoing SAR studies of orlistat targeting FAS-TE, we envisioned that conversion of the β-lactone core to a β-lactam would lead to the discovery of a new class of FAS inhibitors with improved solubility and similar or greater potency and selectivity.

Herein, we report the first synthesis of β-lactam derivatives of orlistat that exhibit inhibitory activity toward thioesterase domain of FAS. The synthetic strategy toward the synthesis of β-lactam congener of orlistat synthesis involved stereocomplementary SnCl$_4$-promoted tandem Mukaiyama aldol-lactonization (TMAL) reaction leading to the cis-β-lactone. Subsequent conversion of the cis-β-lactone to the trans-β-lactam was performed via a one-pot β-lactone ring opening followed by intramolecular Mitsunobu reaction to obtain the desired β-lactam (Scheme 3.8).[88]

Scheme 3.8
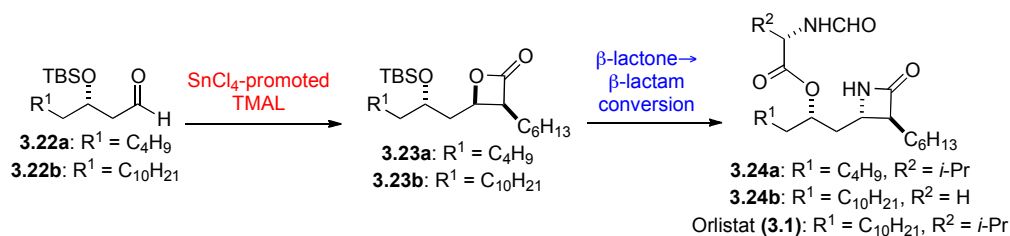
The first target was β-lactam **3.24a**, which directly mimics the stereochemistry

and substituent pattern of orlistat, except the shorter β-substituent. The aldehyde **3.22a** was prepared from dianion alkylation[89] of methyl acetoacetate (**3.25**) leading to **3.26**. A stereogenic center was elaborated from asymmetric Noyori reduction[90] to afford optically active β-hydroxy ester **3.27** followed by silylation and ester reduction to obtain enantiopure aldehyde **3.22a** in good yield (Scheme 3.9).

Scheme 3.9
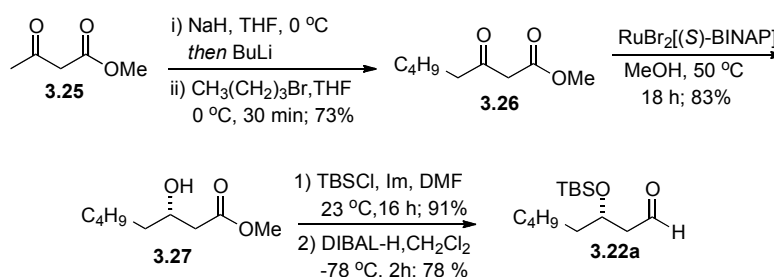
The known ketene acetal **3.28** was prepared from thioesterification of octanoyl chloride (**3.28a**) and 2-mercaptopyridine (**3.28b**) to obtained thioester **3.28c**. Subsequent stereoselective deprotonation[91] followed by treatment with *tert*-butyldimethylsilyl chloride (TBSCl) afforded (*E*)-silyl ketene acetal selectively (Scheme 3.10).

Scheme 3.10
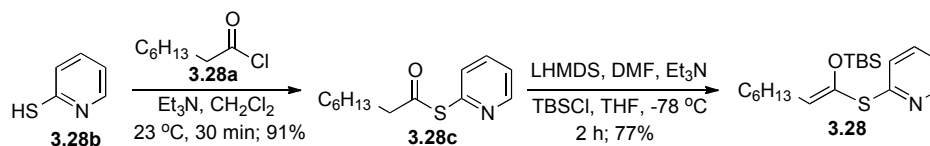
The crucial sequences commenced with $SnCl_4$-promoted TMAL reaction with aldehyde **3.22a** and (*E*)-silyl ketene acetal **3.28** to predominantly deliver the desired *cis*-β-lactone (+)-**3.23a** as a 6:1 mixture of *syn/anti* diastereomers (Scheme 3.11). Complete *cis*-selectivity of β-lactone core was verified by analysis of the coupling constant, which showed J_{H_α,H_β} = 7.0 Hz corresponding to our previous report.[77] The relative stereochemistry with respect to the δ-center was confirmed, based on our previous observations,[74a,81h,81j] and it was consistent with Evans's 1,3-asymmetric induction model for Mukaiyama aldol addition of β-siloxy aldehyde.[92] The facial selectivity *via* 1,3-induction involved internal chelation between Lewis acid and both carbonyl and β-oxygen substituent to deliver a conformationally locked, which promoted the nucleophilic-attack on the less hindered face leading to *anti*-adduct (+)-**3.23a**, respected to δ-siloxy group and β-lactone.

Scheme 3.11
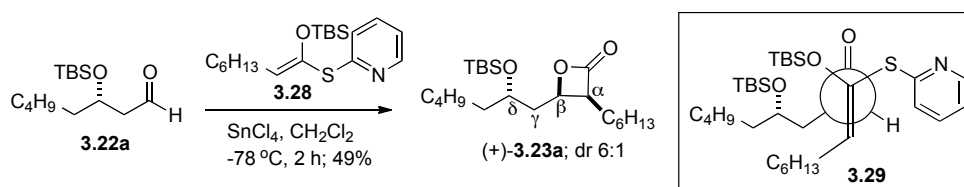
Followed an application of a one-pot conversion of *cis*-β-lactone to *trans*-β-lactam by β-lactone ring opening with benzyloxy amine and intramolecular cyclization through Mitsunobu reaction leaded to the formation of β-lactam (−)-**3.31** with preserved diastereoselectivity (Scheme 3.12).

Scheme 3.12
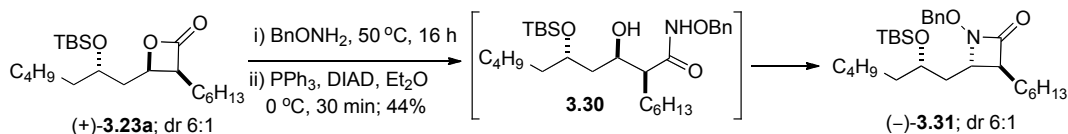
Subsequent desilylation of (−)-**3.31** yielded δ-hydroxy-β-lactam (−)-**3.32**. Finally,

acylation with *N*-formyl-*L*-valine to mimic the ester side chain of orlistat, followed by

SmI$_2$-promoted reductive N−O bond cleavage of the *N*-benzyloxy-β-lactam yielded β-

lactam congener of orlistat (−)-**3.24a** in 9 steps with 8% overall yield (Scheme 3.13).

Scheme 3.13
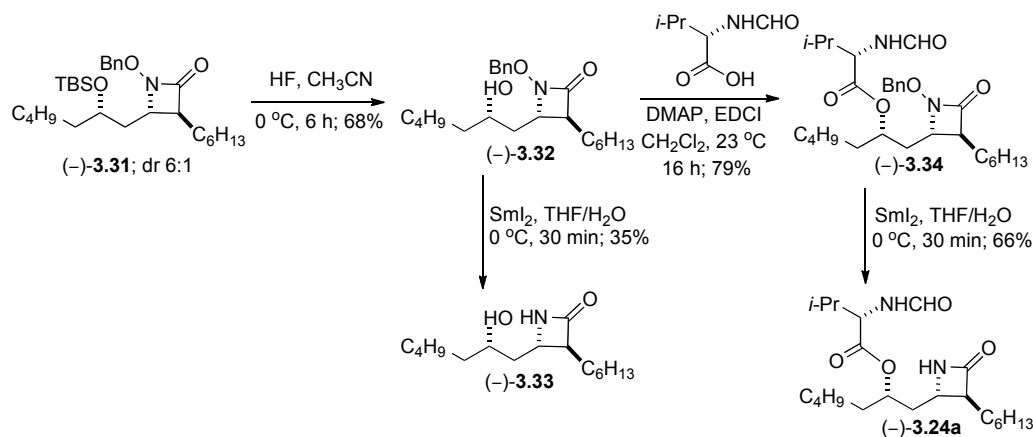
For SAR study, we also targeted the synthesis of β-lactam **3.24b** bearing

different amino acid in ester side chain (Scheme 3.14) by employing similar synthetic

strategy as previously explained. The SnCl$_4$-promoted TMAL reaction of the optically

active aldehyde **3.22b** and thiopyridyl ketene acetal **3.28** provided the *cis*-β-lactone (+)-

3.23b with excellent diastereoselectivity (dr, 15:1). The one-pot conversion of the *cis*-β-lactone (+)-**3.23b** to *trans*-β-lactam (−)-**3.34** followed by desilylation afforded alcohol (−)-**3.35**. Subsequent acylation with *N*-formyl-glycine and reductive N−O bond cleavage by SmI$_2$ completed the synthesis of β-lactam (−)-**3.24b** (dr, 15:1) in 14% overall yield. In addition, the enantiomeric series were also synthesized for SAR comparison employing RuBr$_2$[(*S*)-BINAP] to prepare the enantiomer of aldehyde **3.22b** to obtaining β-lactam (+)-**3.24b** in comparable yields.

Scheme 3.14
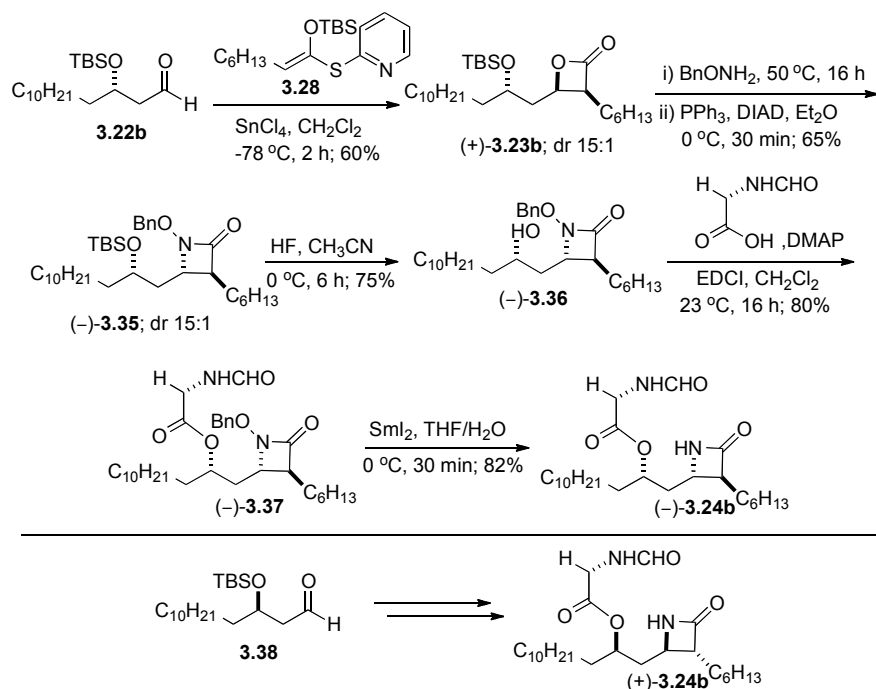
The inhibitory activities of the derived orlistat β-lactam derivatives were determined by the biochemical fluorogenic assay using recombinant FAS-TE (Table

3.3). Not surprisingly, in general, the β-lactam derivatives exhibited lower FAS-TE inhibitory activity compared to orlistat (IC_{50} =1.35 μM) due to the greater stability of β-lactam moiety toward nucleophilic attack by serine active site comparing to β-lactone. Most of *N*-benzyloxy β-lactam derivatives (**3.32**, **3.34**, **3.36** and **3.37**) showed only moderate inhibitory activity toward recombinant FAS-TE with IC_{50} in micromolar range (30-100 μM). Surprising exception was β-lactam (−)-**3.35**, which retained the *N*-benzyloxy group, silyl ether and also shares the same absolute stereochemistry with orlistat. This derivative showed the highest inhibitory activity (IC_{50} = 8.6 μM) among all studied β-lactams.

Table 3.3. Inhibitory properties of β-lactam derivatives of orlistat toward recombinant FAS-TE domain.

Compound	Complement Inhibition IC_{50} (μM)	Compound	Complement Inhibition IC_{50} (μM)
(−)-3.24a[a]	Inconclusive result	(−)-3.35	8.6
(−)-3.24b[b]	No inhibition	(+)-3.35	97.4
(+)-3.24b[b]	No inhibition	(−)-3.36	86.8
(−)-3.32	50.5	(+)-3.36	61.2
(−)-3.33	67.6	(−)-3.37	68.9
(−)-3.34	58.2	(+)-3.37	39.2

[a] dr, 6:1. [b] dr, 15:1.

Unfortunately, inhibitory study of β-lactam (−)-**3.24a**, having a shorter carbon side chain at the β-position, was inconclusive as it failed to exhibit a regular dose-response in the fluorogenic assay. It is also highlighted that a shorter chain at the β-position of the β-lactam relative to the β-lactone of orlistat, did not show significant

improvement in the inhibitory activity toward recombinant FAS-TE, while the improvement in the inhibitory activity was observed in β-lactone derivatives.[81j] Unexpectedly, neither β-lactam (+)-**3.24b** nor its enantiomer, which is structurally most similar to orlistat, showed inhibitory activity; however, this may be due to solubility which is also a problem found in SAR studies of orlistat.

3.3. Conclusion

Several β-lactam congeners of orlistat were successfully prepared for further structure-activity relationship studies (SAR) to evaluate the inhibitory toward thioesterase domain of FAS. The synthetic approach toward β-lactam congeners of orlistat involved SnCl$_4$-mediated tandem Mukaiyama aldol-lactonization (TMAL) reaction and a one-pot conversion of the β-lactone to the β-lactam as the key steps to deliver the desired β-lactam target. The inhibitory activities of the derived β-lactam derivatives were evaluated against a recombinant form of FAS-TE. In general, these derivatives showed lower potency toward FAS-TE compared to their β-lactone analogs. However, the β-lactam (−)-**3.35** possessing a *N*-benzyloxy-β-lactam was discovered to have a good potency (IC$_{50}$ = 8.6 μM). This significant finding suggests that this class of compounds should be further investigated as the potential FAS inhibitors.

CHAPTER IV

SYNTHETIC STUDY TOWARD THE TOTAL SYNTHESIS OF

SPONGIOLACTONE

4.1. Introduction

Spongiolactone (**4.1**) is a marine diterpenoid natural product discovered by Sica and co-workers in 1986 from the extraction of Mediterranean sponge *Spongionella gracilis* which was found in Italy (Figure 4.1).[93] This natural product displays a unique structure that resulted from a heavily rearrangement of spongian diterpene carbon skeleton (**4.2**). Indeed, spongiolactone has partial structural features resembling to the previously isolated gracilin diterpenes.[94] This thus suggested that spongiolactone delivered from a similar precursor but though a different biosynthetic pathway.
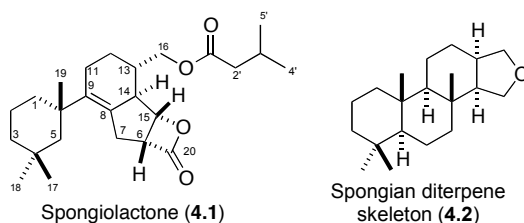
Figure 4.1. Structure of spongiolactone (**4.1**) and spongian diterpene skeleton (**4.2**).

4.1.1. Structural Assignment, Features, and Biological Activity of Spongiolactone and Congeners

As a part of the target re-isolation to accumulate large quantities of the new spongian diterpene family for a variety of biological assays, spongiolactone was isolated and its stereostructure was elucidated on the basis of chemical and physicochemical evidence. Regarding to spectroscopic data and chemical evidence reported by Sica,[84] spongiolactone was isolated as an optically active, colorless oil ($[\alpha]_D$ +67.6, c 1.7, CHCl$_3$) and the IR spectrum showed two carbonyl absorptions at 1830 and 1730 cm^{-1}, which are characteristic absorption of β-lactone and ester functionalities, respectively. In addition, LiAlH$_4$ reduction and subsequent acetylation of spongiolactone gave an expected triacetate **4.3** (Scheme 4.1).

Scheme 4.1
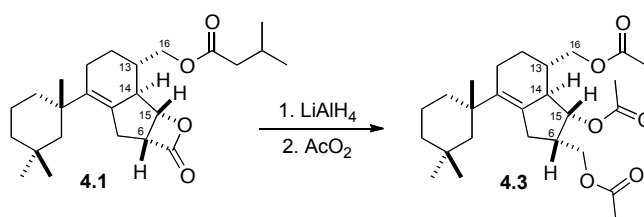
The relative stereochemistry of spongiolactone was revealed based on extensive spin decouple experiments. The results that were obtained from NOE correlations fully corresponded to the proposed structure (Figure 4.2). However, considering the coupling constants of spongiolactone (**4.1**) and its reduced triacetate product (**4.3**) showed the equivocal relative stereochemistry by the unexpected low coupling constant of *trans-*

protons on C14-C15 of **4.1** (J = 4.4 Hz) and identical coupling constants were observed

from *trans*-protons on C14-C15 and *cis*-protons on C6-C15 of **4.3** (J = 8.0 Hz) (Table

4.1).
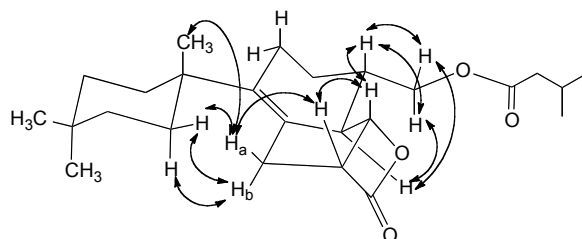
Figure 4.2. The Nuclear Overhauser Effect (NOE) correlations of spongiolactone.[84]

Table 4.1. ^{1}H-NMR and coupling constant (J) data of contiguous stereogenic centers of spongiolactone (**4.1**) and triacetate **4.3**.^{a}

Position	δ_H (J) of **4.1**	δ_H (J) of **4.3**
6	3.90 ddd (6.0, 11.0, 6.0)	2.51 m
7	3.04 dd (16.0, 11.0)	2.80 bdd (16.5, 8.4)
	2.66 dd (16.0, 6.0)	2.29 m
14	2.42 dd (12.0, 4.4)	2.29 m
15	4.77 dd (6.0, 4.4)	4.90 dd (8.0, 8.0)
16	4.14 dd (11.0, 6.6)	4.13 dd (11.0, 4.4)
	4.04 dd (11.0, 6.6)	3.98 dd (11.0, 6.2)

$^a\delta_H$ values are recorded in ppm and J values are recorded in Hz.

Considering all spectroscopic evidence, Sica and co-workers reported the

complete structure of spongiolactone as an unusual tricyclic-β-lactone-containing

diterpenoid possessing four contiguous stereogenic centers, a stereogenic quaternary

carbon on the cyclohexyl appendage, and an isovaleric ester chain. However, the

absence of a single-crystal X-ray structure leaves the relative and absolute stereochemistry of this natural product still in question.

In 2009, Jaspars and co-workers reported the discovery of a demethyl congener of spongiolactone, 3′-norspongiolactone (**4.4**), from the extract of marine sponge *Spongionella porifera* found in West Angaur, the Philippines (Figure 4.3).[95] The spectroscopic data including COSY and HMBC correlations obtained for the diterpene moiety of 3′-norspongiolactone (**4.4**) were virtually identical to those reported for spongiolactone (**4.1**). The only difference between these two compounds was the presence of butyric ester instead of the isovaleric ester found in spongiolactone. Therefore, they assumed that the relative configurations of both compounds are identical, which was consistent with the observed 2D-NOESY data. Here again, the single-crystal X-ray structure of 3′-norspongiolactone was not obtained.

3′-Norspongiolactone (**4.4**)
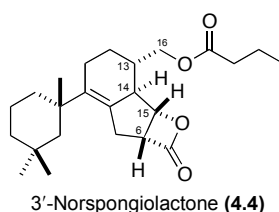
Figure 4.3. Structure of 3′-norspongiolactone (**4.4**).

Interestingly, Jaspars and co-workers reported the biological activities of 3′-norspongiolactone to show cytotoxicity against K562 human chronic myelogenous leukemia cells (IC$_{50}$ 12±1 μM), normal human peripheral blood mononuclear cells (PBMC; IC$_{50}$ 30±10 μM), and 60% EGF-R tyrosine kinase inhibitor. These results

suggested that 3′-norspongiolactone has moderate selectivity toward cancer cell lines compared to human normal cell lines. Due to this low selectivity, 3′-norspongiolactone may not be a good drug candidate for cancer therapy. Because of close structural similarities between spongiolactone and 3′-norspongiolactone, it can be inferred that their biological activities are resemble and points out that spongiolactone is likely toxic to both cancer and normal cell lines.

Importantly, the relative stereochemistry of both spongiolactone and 3′-norspongiolactone is still questionable, especially the stereochemistry of the contiguous stereogenic centers on C13-C14-C15. The ambiguous relative stereochemistry of the spongiolactone core was shown not only in the coupling constants reported by Sica (Table 4.1)[93] and 2D-NOESY reported by Jaspars,[95] but also observed from structural comparisons of spongiolactone and another spongian diterpenes (Figure 4.4).[96] Most of these natural products show a similar cyclohexane baring a quaternary carbon moiety with an α-face proton on the carbon (C13) five atoms away from the quaternary carbon center (C10). These questions lead us to the primary goal for the total synthesis of spongiolactone to confirm its relative and absolute stereochemistry.

Although the first isolation was reported nearly 25 years ago, the synthetic study toward spongiolactone has never been reported neither the biological activities nor the biosynthetic pathway. The presence of the β-lactone, in analogy to other β-lactone-containing natural products, denotes to the acylating potential of this natural product toward cellular targets. Therefore, further bioactive probe synthesis and biological study may disclose modes of actions and protein targets of spongiolactone.
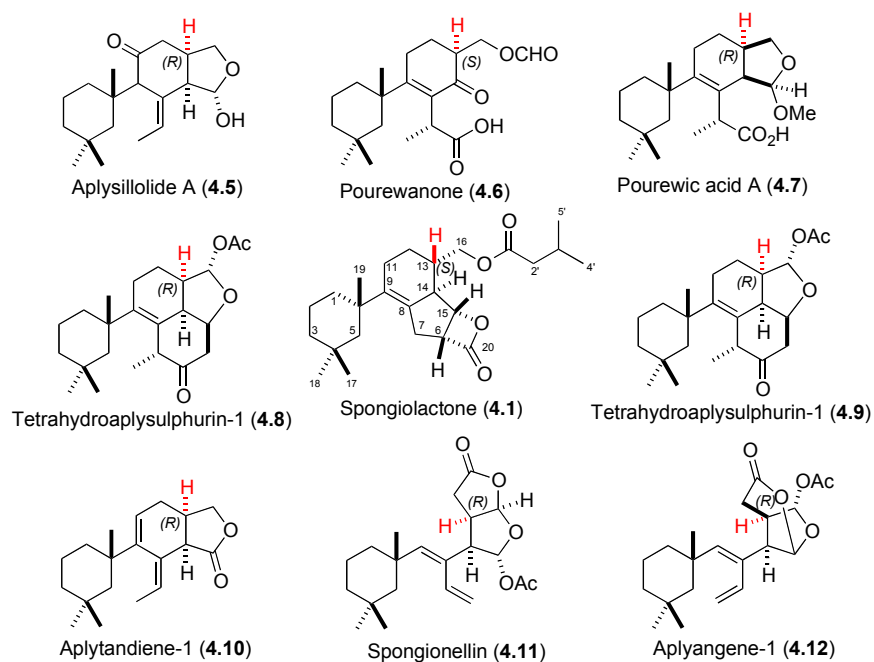
Figure 4.4. Structural comparison of spongiolactone (**4.1**) and spongian diterpenes.

4.1.2. Intramolecular Nucleophile-Catalyzed Aldol-Lactonization (NCAL) Process

β-Lactones have emerged as versatile synthetic intermediates due to their inherent reactivity derived from ring strain.[73] As the masked aldehyde functionality, β-lactones undergo a variety of transformations in stereospecific fashions and are employed as the key intermediates in many natural product syntheses. In recent years, several methodologies have been reported for the asymmetric synthesis of β-lactones and continue to be an active research area.[74]

One of the first practical, catalytic asymmetric β-lactone syntheses was developed by Wynberg and co-workers in 1982 and its utility was demonstrated by the large-scale synthesis of optically active malic and citramalic acid.[97] In this process, the highly reactive aldehyde **4.13** was treated with ketene **4.14** in the presence of cinchona

alkaloids, such as quinidine (**4.16**) and quinine (**4.17**), which were employed as the catalysts to deliver β-(trichloromethyl)-β-propiolactone **4.15a** and **4.15b** in good to moderate yields with excellent to moderate enantioselectivities (Scheme 4.2).

Scheme 4.2

quinidine (**4.16**)→(−)-**4.15**, 95 %yield, 98 %ee
quinine (**4.17**)→(+)-**4.15**, 65 %yield, 76 %ee
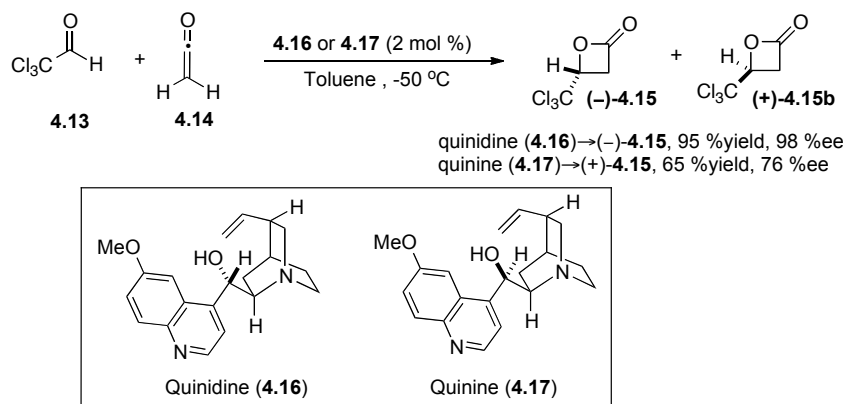
Although the utility of Wynberg β-lactone synthesis is well documented and stands as a benchmark for further development in this area, there are some limitations to this methodology including the need for a ketene generator and the requirement of highly activated aldehyde substrates (*i.e.*, α-chlorinated).

As part of our program to develop a concise, asymmetric route to β-lactones,[85] we described the development of a protocol that allowed the use of an *in situ* generated ketene that was delivered from acetyl chloride (**4.19**) and Hunig's base providing a variety of optically active β-lactones in similar yields with excellent enantioselectivities compared to Wynberg's protocol (Scheme 4.3). However, the highly electrophilic aldehydes remained a prerequisite for the preparation of β-lactones.

Scheme 4.3

4.18   4.19

R = Cl or alkyl

4.16 (2 mol%)

i-Pr$_2$NEt (1.45 equiv)

toluene , -25 °C

4.20

40 - 85 %yield
93 - 98 %ee
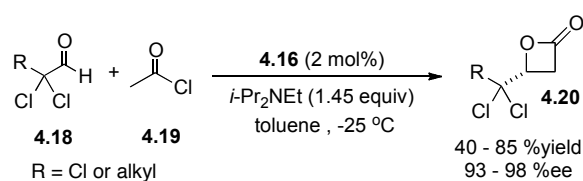
After extensive optimization to overcome the limitations of Wynberg β-lactone synthesis, we investigated the use of unactivated, non-α-chlorinated, aliphatic aldehydes in an asymmetric route to β-lactones and reported the initial development of an intramolecular nucleophile-catalyzed aldol-lactonization (NCAL) process of aldehyde acid that led to a variety of novel β-lactone-fused bicyclic systems.[99]

In 2001, we reported the first example of an intramolecular, asymmetric NCAL reaction employing aldehyde acids as the advanced substrates. These aldehyde acids contained non-activated aldehydes and enabled *in situ* generation of ketene from carboxylic acids by utilizing acid activating reagent and Hünig's base. The slow addition of aldehyde acid to the mixture of nucleophile (in this case *O*-acetyl quinidine and *O*-acetyl quinine) and Mukaiyama's reagent (acid activating agent) gave the bicyclic β-lactones in excellent enantioselectivities (Scheme 4.4).

Scheme 4.4

4.18

R = H, CH$_3$, CO$_2$Me

10 mol % *O*-Actyl Quinidine (**4.20a**)

Cl (3.0 equiv) (**4.21a**)

i-Pr$_2$NEt (4.0 equiv)
CH$_3$CN, 25 °C, 108 h

(+)-**4.19**
(45-55% yield; 90-92% ee)
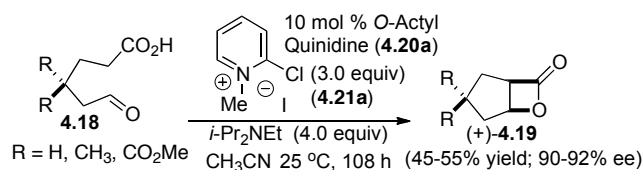
This method merges the catalytic, asymmetric β-lactones synthesis with carbocycle construction *via* organocatalysis. The optimization and exploration of the scope of the intramolecular nucleophile-catalyzed aldol-lactonization (NCAL) reaction lead to significant findings including the development of modified Mukaiyama's reagents,[100] investigation of nucleophiles as organic catalysts and the use of keto acids as the substrates for NCAL process (Scheme 4.5).[101]

Scheme 4.5

n = 1, 2; R¹ = H, OTBS, Alkyl
R² = H, Me, CH₂Ph, (CH₂)₃
R³ = H, Me, CH₂Ph, CO₂Et

Mukaiyama's reagents
R = Me; X = Cl; Y = I
R = n-Pr; X = Br; Y = OTf
R = Me; X = Cl; Y = OTf
R = Et; X = Br; Y = BF₄

Nucleophiles

Aldehyde acid: (10 mol%)
O-Ac Qunidine
O-Ac Quinine
O-TMS Qunidine
O-TMS Qunine

Keto acid (1.5 equiv)
Pyridine
DMAP
PPY
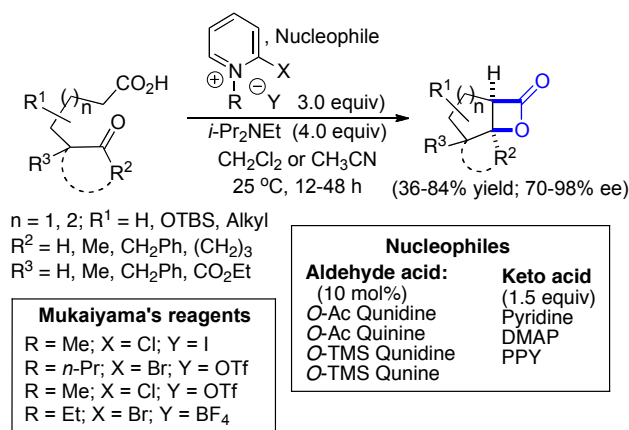
Extension of these studies to keto acid substrates significantly expanded the scope of this process allowing access to bicyclic and tricyclic β-lactone systems that possess up to three stereocenters including a masked tertiary carbinol center and a reactive β-lactone moiety.

After ambitious efforts to improve the NCAL process, the mechanism of the NCAL reaction was proposed (Scheme 4.6).[101,102] This process involves two plausible mechanistic pathways that differ only in the two distinct reactive intermediates; the acyl

ammonium species (**4.25**) derived aldol-lactonization mechanism (*Path A*) and the ketene species (**4.26**) proceeding by a [2+2] cycloaddition mechanism (*Path B*).

Scheme 4.6
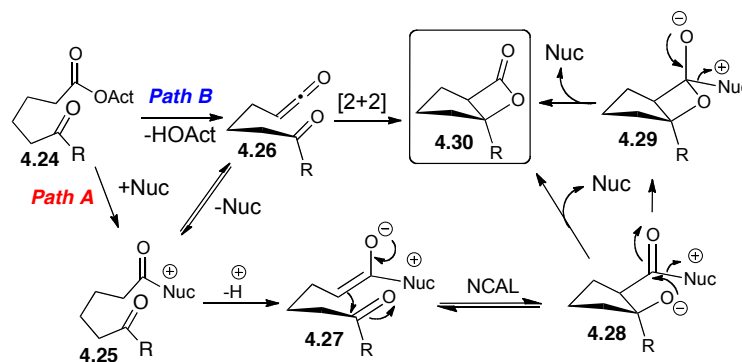
Upon activation of the carboxylic acid by Mukaiyama's reagent, elimination of the hydroxylated activating reagent would lead to ketene **4.26** that would undergo a [2+2] cyclization and deliver β-lactones **4.30**. One other possible mechanistic pathway, which we believe to be the major route to catalytic, asymmetric β-lactones synthesis, is through the formation of an acyl ammonium species *via* nucleophile-promoted transacylation to obtain **4.25**. The loss of nucleophile, which is in equilibrium with acyl ammonium **4.25**, results in the formation of ketene (**4.26**) for [2+2] cyclization. On the other hand, subsequent deprotonation of the acyl ammonium leads to an ammonium enolate **2.27**, which undergoes an intramolecular aldol reaction that is the stereochemical controlling and rate-determining step. Then, lactonization of **4.28** produces the tetrahedral intermediate **4.29** followed by regeneration of the nucleophile, which is employed as a catalyst in this process affords the bicyclic β-lactone **4.30**. Because the

reaction is performed at room temperature, it appears reasonable to assume that either the highly reactive ketene intermediate is slowly generated, and thus only low concentrations are observed, or the acyl ammonium pathway is predominant. Furthermore, due to the ring stain, only *cis*-aldolate **4.27** would be expected to cyclize generating only the *cis*-β-lactone. In the case of the aldehyde acid, the mechanism assuredly involves an aldol-lactonization process due to the observed high level of asymmetric induction. Although the evidence is less conclusive when evaluating the keto acid, to date we believe that an aldol-lactonization mechanism is a major pathway toward organonucleophile-promoted *bis*-cyclization processes.

Recently, we have developed the double diastereoselective, nucleophile-catalyzed aldol-lactonization (NCAL) process for the synthesis of β-lactone fused carbocycles and β-lactone fused tetrahydrofuran using cinchona alkaloid catalysts with enantioenriched aldehyde acids to deliver good to excellent diastereoselectivity (Scheme 4.7).[103]

Scheme 4.7
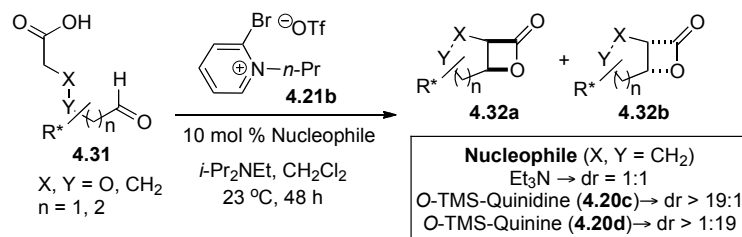
Furthermore, we reported a significant advancement in the NCAL methodology with keto acids involving the use of Birman's chiral cyclic isothiourea as the chiral nucleophile and *p*-toluenesulfonyl chloride as an activating agent (rather than Mukaiyama's reagent) to achieve highly enantioselective bi- and tricyclic β-lactones (Scheme 4.8).[104]

Scheme 4.8
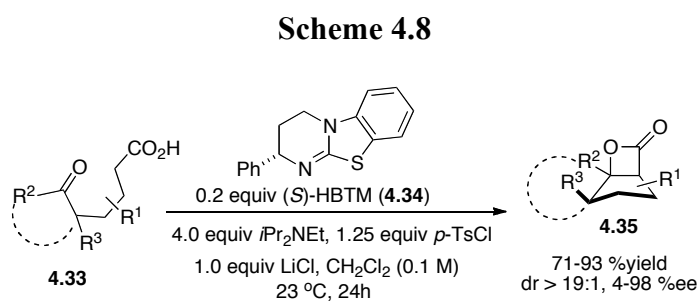
The practical, catalytic, asymmetric NCAL process of aldehyde acids and keto acids has been developed and is an ongoing research area in the Romo group. Optimization and exploration of the scope of asymmetric processes including applications to heterocycles and natural product syntheses are currently underway. The utility of catalytic, asymmetric NCAL process has recently been demonstrated in the total synthesis of (−)-salinosporamide A,[105] (−)-curcumalactone A.[106]

4.1.3. Previous Studies Toward the Total Synthesis of Spongiolactone

In the Romo group, we have been targeting β-lactone-containing natural products since they contain unique structural frameworks and exhibit interesting biological

activities. The utility TMAL and NCAL reactions, which are asymmetric β-lactone forming processes developed in our group have been demonstrated in various total syntheses of β-lactone-containing natural products such as FDA approved antiobesity (−)-orlistat,[81h] (−)-belactocin C,[81i] and the highly potent anticancer (−)-salinosporamide A.[105]

To date, there is no reported evidence of synthetic studies toward spongiolactone. We envisioned applying the NCAL methodology as a key step to construct the β-lactone core structure of spongiolactone. Importantly, this strategy would allow us to investigate the possibility of double asymmetric synthesis in more complex NCAL substrates and expand the scope of reaction conditions.

Previously, several synthetic strategies were studied for the preparation of aldehyde acid substrates for the NCAL process.[107] In the first route, key steps involved an Hajos-Parrish Robinson annulation to achieve decalin **4.37**. Either (−)-proline or (+)-proline were then employed to prepare each enantiomer of spongiolactone since the absolute stereoconfiguration remains unknown. A subsequent Heck coupling with cyclohexene **4.39** to form the stereogenic quaternary carbon, followed by oxidative coupling to obtain aldehyde acid **4.41**. The final step involved the NCAL reaction to afford spongiolactone (Scheme 4.9). Due to the difficulties with selective ketone protection, such as no reaction-taking place or substrate decomposition, this route was abandoned.

Keeping the same synthetic strategy involving a Heck coupling and the NCAL process in the late stages of the synthesis, the aldehyde acid precursor was alternatively

prepared from a Micheal addition/enolate trapping strategy (Scheme 4.10). We decided to begin this synthetic route in racemic fashion to expedite exploration of the full synthesis and then complete an asymmetric synthesis later.

Scheme 4.9
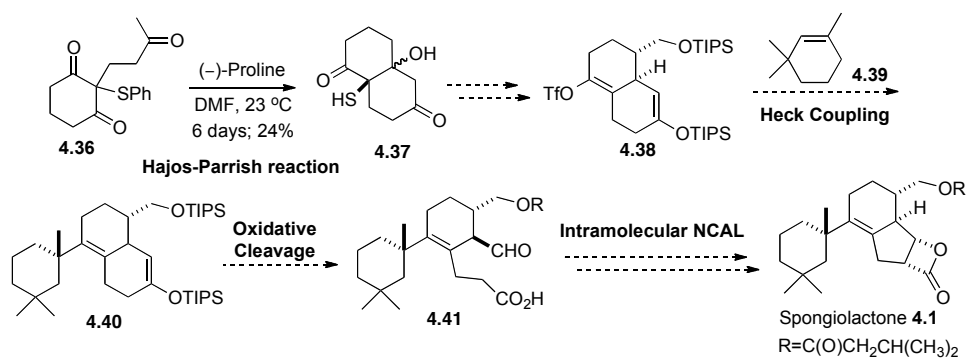
Scheme 4.10
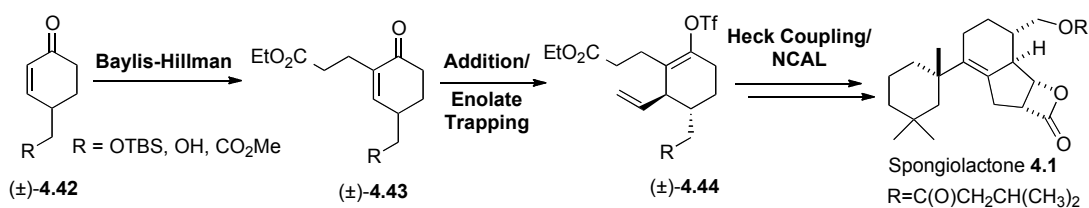
The enone (±)-**4.42** was racemically prepared from a Diels-Alder reaction followed by a Baylis-Hillman alkylation to obtain α-substituted enone (±)-**4.43**. Subsequent, vinyl cuprate addition and electrophilic trapping of the resulting enolate yielded enol (±)-**4.44**, which was set up for the Heck coupling and ultimately preparation of the aldehyde acid as a substrate for NCAL process. This route appeared to be

problematic due to scale up problem found in the preparation of enone (±)-**4.42** and decomposition that took place in Baylis-Hillman reaction. Extensive optimizations were tried, however, no satisfying improvements were observed. Therefore, we decided to peruse an alternative pathway.

Attempts in preparing the aldehyde acid precursor were successful when Stork-Danheiser protocol was employed (Scheme 4.11).[108] The vinylogous ester **4.47** was prepared from a Michael addition between the commercially available 1,3 cyclohexanedione (**4.45**) and *t*-butyl acrylate to afford diketone **4.46**. Subsequent methylation by dimethyl sulfate yielded **4.47** in quantitative yield.

Scheme 4.11
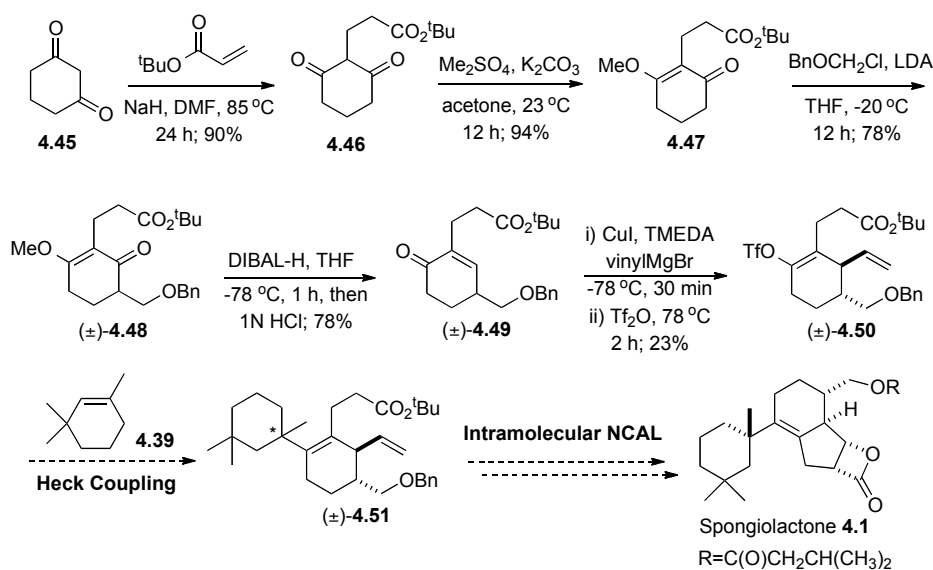
Then, a Stork-Danheiser alkylation of **4.47** with benzyloxy chloromethyl ether provided α-substituted enone (±)-**4.48** followed by reduction and demethylation upon

acidic work up gave enone (±)-**4.49**. To prepare the substrate for Heck coupling, vinyl cuprate addition followed by electrophilic trapping of the enolate yielded enol (±)-**4.50** in low yield. Although enol (±)-**4.50** was successfully prepared, the Heck coupling failed. Several attempts to optimize the Heck coupling were studied but no promising results were found. Due to the difficulties encountered in this strategy, we decided to consider an alternative route.

4.1.4. Retrosynthetic Analysis Toward the Total Synthesis of Spongiolactone

Many routes were tried during our synthetic pursuit of spongiolactone. However, copious amounts of problems were encountered due to the instability of intermediates and impractical scale up conditions. Therefore, the synthetic route was revised to construct the fused tricyclic β-lactone core by the NCAL process in the early stage. In this way, the resulting core structure of spongiolactone is set for substrate control in the late stage functional group manipulations to make this a more concise and feasible strategy. Due to the unsuccessful Heck coupling as was previously described, we envisioned that the installation of the cyclohexyl appendage baring a stereogenic quaternary carbon could be completed by nucleophilic addition, and the formation of stereogenic quaternary center will be induced by substrate and reagent control.

After careful consideration, we planed to begin the full synthetic route by utilizing racemic materials, since the absolute configuration of spongiolactone remains unknown and several diastereomers of spongiolactone will be essential for screening protein targets and their bioactivities in basic cell biological studies. The asymmetric

synthesis will be carried out later. We envisioned that the synthesis of spongiolactone could be accomplished after regioselective dehydration to obtain the tetrasubstituted olefin, and installation of the isovaleric ester of alcohol **4.53**. The key step in the late stage synthesis involves diastereoselective allylic zinc addition, developed by Knochel,[109] to install the pendent cyclohexane moiety and a stereogenic quaternary carbon by the S_E' reaction of novel zincate **4.54** and the β-lactone core **4.52**. The fused tricyclic β-lactone **4.52** that is utilized as the key intermediate can be derived from the NCAL reaction with a corresponding aldehyde acid (±)-**4.51**. The aldehyde acid (±)-**4.51** can be readily prepared from the cheap and commercially available 1,3 cyclohexanedione (**4.45**) *via* Stork-Danheiser kinetic alkylation as explain in the previous synthetic route (Scheme 4.12).

Scheme 4.12
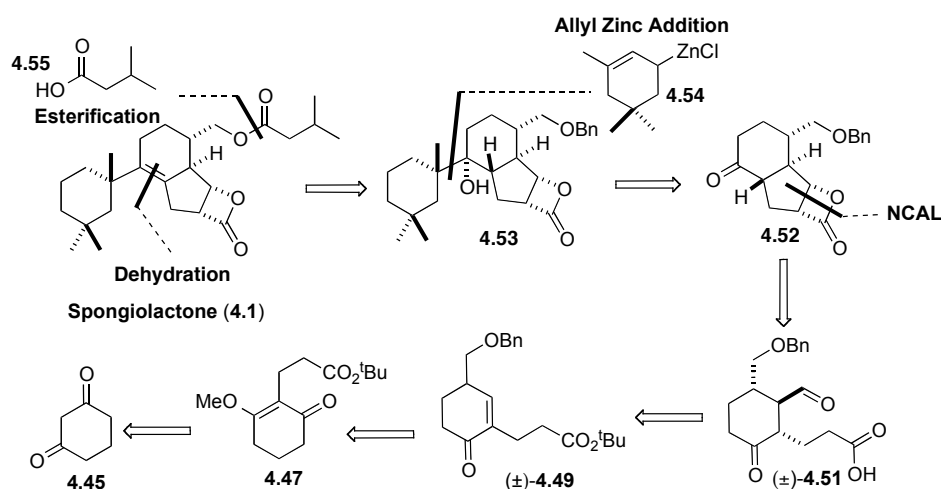
4.2. Results and Discussion

A concise, racemic synthesis toward spongiolactone is envisioned by using inexpensive and commercially available 1,3-cyclohexanedione as the primary substrate. The key steps involve an intramolecular nucleophile-catalyzed aldol-lactonization (NCAL) reaction and diastereoselective allylic zinc addition to construct the fused tricyclic β-lactone core (**4.52**). These steps deliver the diastereoselective setting of four contiguous stereogenic centers and formation of the cyclohexane appendage with a stereogenic quaternary carbon.

4.2.1. Preparation of Aldehyde Acid as NCAL Substrates

Based on previous studies, the aldehyde acid (±)-**4.51** was prepared from 1,3 cyclohexanedione (**4.45**) *via* the Stork-Danheiser kinetic alkylation protocol. Extensive optimizations and synthetic modifications to enable large-scale synthesis of aldehyde acid (±)-**4.51** were studied.

Treatment of 1,3 cyclohexanedione (**4.45**) with *t*-butyl acrylate followed by dimethyl sulfate in DMF successfully provided vinylogous ester **4.47** *via* the two-step, one-pot Michael addition and methylation in quantitative yield (Scheme 4.13). This process improved the synthetic efficiency by one step shortening the overall synthesis of spongiolactone.

Scheme 4.13
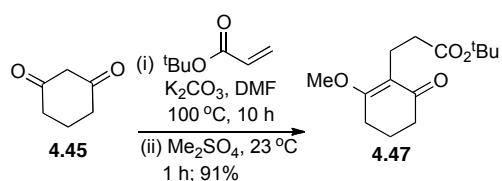
Extensive optimizations of the Stork-Danheiser kinetic alkylation were studied due to the impractical yield and undesired regioselectivity that was observed when LDA/THF conditions were employed. Fortunately, deprotonation of vinylogous ester **4.47** by LHMDS and use of excess benzyloxy chloromethyl ether in toluene delivered desired α-substituted enone (±)-**4.48** in good yield without *O*-alkylation, alkylation at the *t*-butyl ester side chain or γ-alkylation (Scheme 4.14).

Scheme 4.14
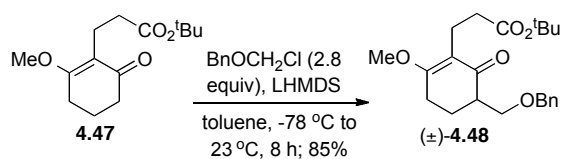
Chemoselective reduction of the α,β-unsaturated ketone *via* a Luche reduction, avoiding the reduction of *t*-butyl ester which observed when DIBAL-H was used, followed by demethylation upon acidic work up furnished γ-substituted enone (±)-**4.49** in good yield (Scheme 4.15).

Scheme 4.15
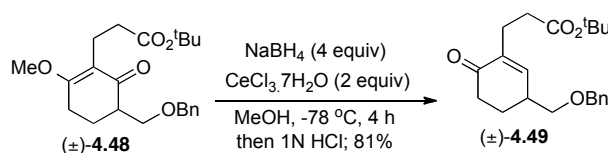
Then, cuprate addition of the enone (±)-**4.49** with 2-methyl-1-propenyl magnesium bromide (R=Me) gave the desired trimethyl silyl enol ether (±)-**4.55** with good diastereoselectity (dr, 10:1), which was better than when vinyl magnesium bromide (R=H) was used (dr, 5:1). The trimethyl silyl enol ether (±)-**4.55** was carried on to the next step without purification. Treatment (±)-**4.55** with TsOH in CH$_3$CN, leading to the one-pot desilylation and deprotection of the t-butyl ester yielded acid (±)-**4.56** in excellent yield (Scheme 4.16).

Scheme 4.16
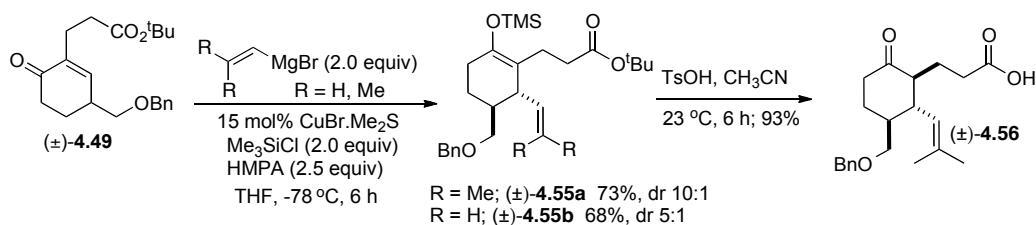
Note that employing TFA/CH$_2$Cl$_2$ or TsOH/CH$_2$Cl$_2$ (Table 4.2) caused the formation of undesired product (±)-**4.56b**, which is derived from deprotection of the benzyl ether under strong acidic conditions to obtain primary alcohol (±)-**4.56a**, followed by nucleophilic addition (Scheme 4.17). The structure of the undesired product

was confirmed by COSY and HMQC. Finally, ozonolysis of alkene acid (±)-**4.56**

afforded aldehyde acid (±)-**4.51** as a substrate for the NCAL process (Scheme 4.18).

Table 4.2. Optimization of one-pot desilylation and deprotection of *t*-butyl ester.

Entry	Condition	(±)-**4.56**	(±)-**4.56a**
1	TsOH (2 equiv), CH$_3$CN, 23 °C, 6 h	93%	0%
2	TsOH (2 equiv), CH$_3$CN, 23 °C, 12 h	79%	10%
3	TsOH (2 equiv), CH$_2$Cl$_2$, 23 °C, 12 h	0%	58%
4	TFA (20 equiv), CH$_2$Cl$_2$, 23 °C, 12 h	82%	13%
5	TFA (30 equiv), CH$_2$Cl$_2$, 23 °C, 12 h	0%	62%
6	SnCl$_4$ (2 equiv), CH$_2$Cl$_2$, 23 °C, 6 h	0%	52%

Yields refer to isolated yield.

Scheme 4.17
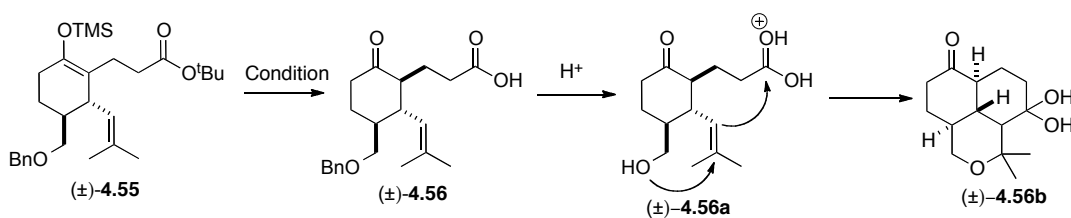
Scheme 4.18
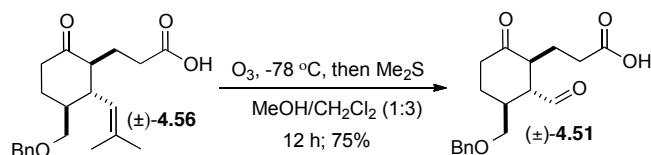
In summary, aldehyde acid (±)-**4.51** was racemically synthesized from a commercially available substrate in six steps with 32% overall yield. Along the course of this study, alternative routes were tried for a more concise strategy starting from commercially available 3-ethoxycyclohex-2-enone (**4.57**) to achieve the desired aldehyde acid (±)-**4.59** in 3 steps. However, the results were unsatisfying (Scheme 4.19).

Scheme 4.19
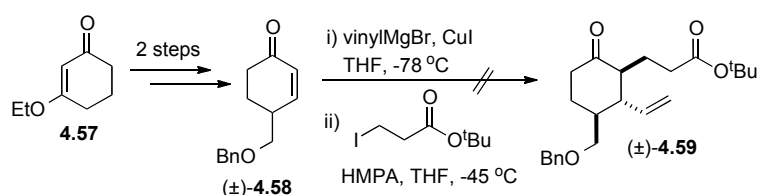
4.2.2. Synthesis of Diastereomeric Tricyclic Cores of Spongiolactone: Double Diastereoselectivity and Kinetic Resolution *via* the NCAL Process with Chiral Lewis Bases

The successful preparation of the aldehyde acid (±)-**4.51** in racemic fashion allowed further studies of the synthesis of the fused tricyclic β-lactone core (**4.52**) employing NCAL process, which has been planned as one of the key step toward the synthesis of spongiolactone. Although the NCAL process had never been attempted in such a complex setting, the *bis*-cyclization process of aldehyde acid (±)-**4.51** with Mukaiyama's reagent and triethylamine underwent smoothly and only required minimal optimization to obtain the bicyclic β-lactone product, which obtained as white crystals. The fully characterization including X-ray crystallographic analysis revealed the relative

stereochemistry of the derived β-lactone (Scheme 4.20).

Scheme 4.20

Spongiolactone (**4.1**)

4.60
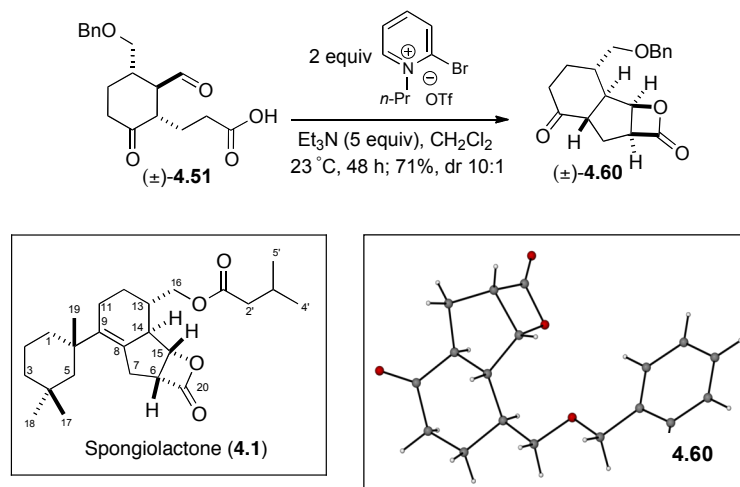
Unfortunately, the relative stereochemistry of β-lactone moiety of (±)-**4.60** did not match with spongiolactone (**4.1**). The resulted β-lactone moiety was formed in the β-face and showed *anti*-relationship with benzyl ether. Additionally, the single X-ray structure confirmed that no epimerization happened in this process.

This result can be rationalized by substrate control and stereoelectronic effect. Since the NCAL reaction of aldehyde acid (±)-**4.51** was performed at 23 $^{\circ}$C, it is reasonable to assume that this process is under thermodynamic control leading to a reversible process to deliver the more stable product. Once *E*-acyl ammonium enolates were generated, ammonium enolates **4.52a** and **4.60a** were in equilibrium *via* bond-rotation. Following an aldol-lactonization process yields β-lactones **4.52a** and **4.60a** (Scheme 4.21).

Scheme 4.21
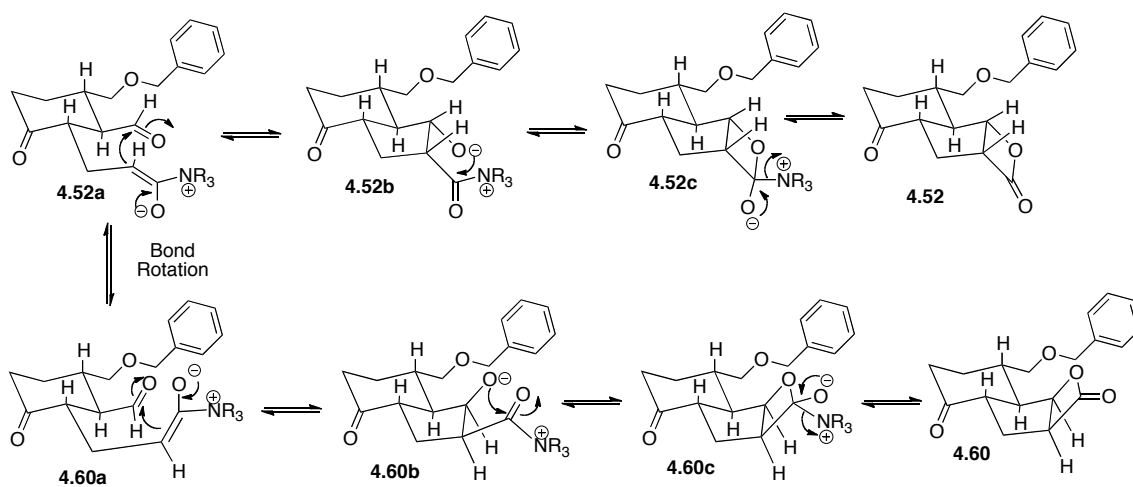
As shown in the transition state arrangement, the formation of ammonium enolate **4.60a** was favored due to less steric hindrance between β-lactone and benzyl ether moiety and lower dipole moment from carbonyl moiety, comparing to ammonium enolates **4.52a** (Scheme 4.22). Even though the ammonium enolate **4.60a** has larger $A^{1,3}$ strain (1,3-allylic strain), the steric effects play an important role, resulting predominantly in the generation of ammonium enolate **4.60a** and β-lactone **4.60** was obtained a single diastereomer.

Scheme 4.22
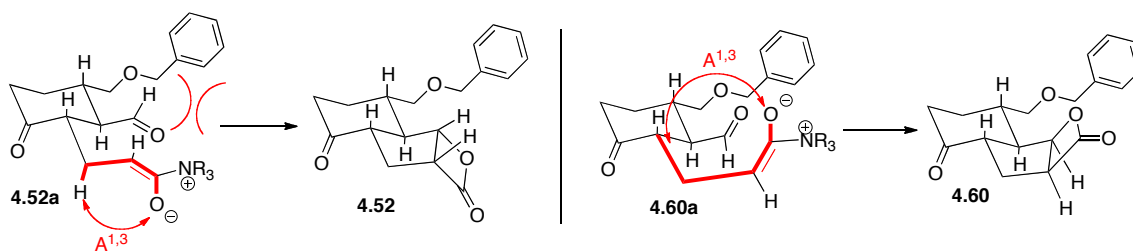
Realizing that the wrong diastereomer was obtained from the key NCAL reaction, governed by substrate control, we have thought about two synthetic ideas. First, we plan to optimize the NCAL reaction of aldehyde acid (±)-**4.51** by employing reagent control to override substrate preference and accomplish the desired β-lactone core **4.52** for the total synthesis of spongiolactone. Second, in consideration of the inconclusive stereoconfiguration of spongiolactone, the fused tricyclic β-lactone **4.60** is continuously employed in late stage of the synthesis to begin the synthetic study of the diastereoselective allylic zinc addition which is one of the key steps in this synthesis to construct a stereogenic quaternary carbon. The resulting products will enable to confirm the relative stereochemistry of spongiolactone.

To accomplish the desired tricyclic β-lactone **4.52**, we envisioned the use of chiral Lewis bases (Figure 4.5) as a chiral reagent to influence stereochemical outcome by overcoming inherent substrate bias through the reagent control in the double diastereoselective NCAL process.
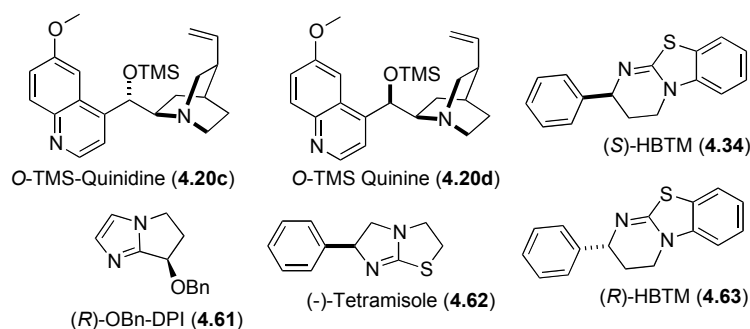
Figure 4.5. Chiral Lewis bases for double diastereoselective NCAL.

Based on our previous studies, various types of chiral nucleophiles such as cinchona alkaloids[101,103] and tetramisole analogs[104] were studied for double diastereodifferentiation of NCAL for both aldehyde acid and keto acid substrates to achieve good to excellent diastero- and enantioselectivity. In the case of complex aldehyde acid (±)-**4.51**, several chiral nucleophiles were studied (Scheme 4.23) and the differences of diastereoselectivities were observed (Table 4.3).

Initial investigation of double diastereoselective NCAL reaction, employing racemic homobenzotetramisole (HBTM) developed by Birman[109] and racemic 7-benzyloxy-6,7-dihydro-5H-pyrrolo-[1,2-a]-imidazole (OBn-DPI) developed by Zhang[110] showed the improvement of diastereoselectivity favoring the desired β-lactone core **4.52**. Fully characterization including 2D-NMR analysis revealed the relative stereochemistry of the derived β-lactone **4.52**. The stereogenic outcome of tricyclic β-lactone **4.52** was confirmed by NOESY (Figure 4.6).

Scheme 4.23
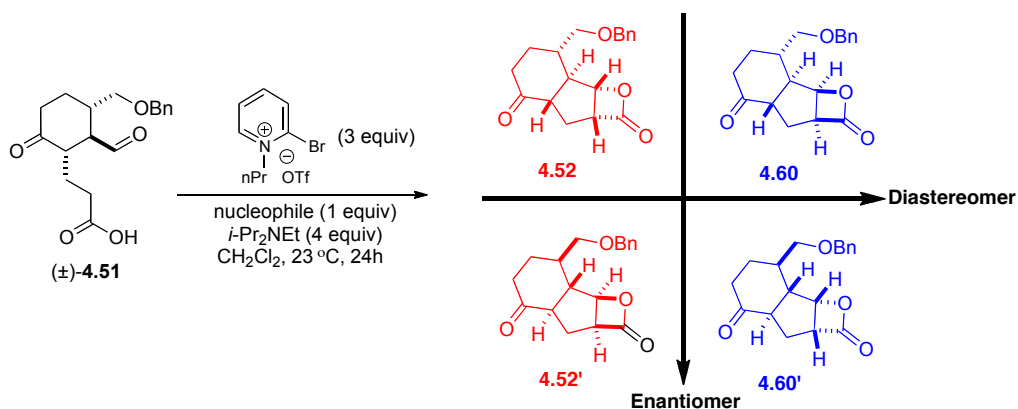
Table 4.3. Investigation of chiral nucleophiles for double diastereoselective NCAL process of aldehyde acid (±)-**4.51**.

Entry	Nucleophile	Yield[a]	dr[b] **4.52**:**4.60**	ee of **4.52**[c]	ee of **4.60**[c]
1	Et$_3$N[d]	71%	1:10	-	-
2	(±)-HBTM	65%	1:2	-	-
3	(±)-*O*Bn-DPI	35%	1:5	-	-
4	*O*-TMS-Quinidine	5%	1:5	>99%	45%
5	*O*-TMS-Quinine	10%	1:7	78%	39%
6	(*S*)-HBTM	42%	1:1	98% (+)-**4.52**	52%
7	(*R*)-HBTM	27%	1:2	96% (−)-**4.52**	38%
8	(-)-Tetramisole	3%	1:6	37%	35%

[a]Reaction was run on 100 mg scale and values refer to isolated yield by Prep-TLC. [b]Enantiomeric excess was determined by Chiral HPLC (OD column, 10% IPA/Hexanes, 0.9 mL/min). [c]Diastereomeric ratio was determined by ^{1}H-NMR (500MHz) of the crude reaction mixture. [d]5 equiv of Et$_3$N was used as a base and nucleophile.

(+)-**4.52**
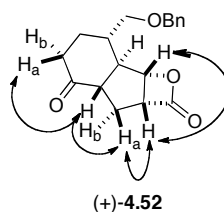
Figure 4.6. Relative stereochemistry and structure analysis by NOESY of (+)-**4.52**.

Since the tricyclic β-lactone (+)-**4.52** was obtained as colorless oil, the conversion of benzyl ether (+)-**4.52** *via* hydrogenation and esterification with commercially available *p*-bromobenzoyl chloride (Scheme 4.24) was successful to achieve a solid *p*-bromobenzyl ester (+)-**4.52b** for the single X-ray crystallographic analysis. However, single X-ray crystallographic studies of ester (+)-**4.52b** failed since only twined crystals were obtained.

Scheme 4.24
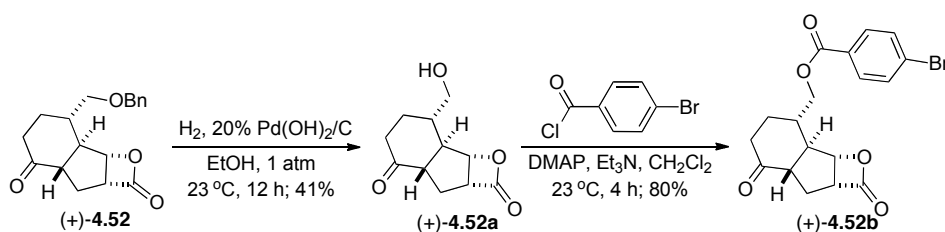
Further investigation of optically active chiral nucleophiles (Table 4.3, entries 4-8) provided the interesting results. (*S*)-HBTM (Table 4.3, entry 6) appeared to be the best nucleophile giving the best yield of bicyclic β-lactone (+)-**4.52** with the highest degree of diastereoselectivity (dr, 1:1 of **4.52**:**4.60)** compared to Et$_3$N (dr, 1:10). On the other hand, (*R*)-HBTM did not increase the level of diastereoselectivity and did not reverse the diastereoselectivity toward the formation of β-lactone (−)-**4.52**. These results showed that (*S*)-HBTM is a matched catalyst. Surprisingly, the desired β-lactone core **4.52**, derived from the enantiopure chiral nucleophiles such as *O*-TMS-Quinidine, (*S*)-HBTM, and (*R*)-HBTM, was obtained in excellent enantioselectivity (Table 4.3, entries 4, 6 and 7). To the best of our knowledge, these results represent the first example of kinetic resolution *via* a double diastereoselective NCAL process. Note that in all cases, 1 equivalent of chiral nucleophile was used to maximize the conversion to the resulting bicyclic β-lactone adduct; although, it was needed at catalytic amounts.

As the purpose to improve diastereoselectivity, extensive optimizations of kinetic resolution and double diastereoselective NCAL process of aldehyde acid (±)-**4.51** were studied using (±)-HBTM as a nucleophile. Note that 3 equivalents of Mukaiyama's

reagent, 1 equivalent of ($\pm$)-HBTM and 4 equivalents of Hünig's base were used as a general condition. Optimizations of reaction conditions were studied by varying the activating agents, solvents, concentrations, additives, and addition methods were studied (Table 4.4).

In summary, the NCAL reaction of aldehyde acid ($\pm$)-**4.51** using ($\pm$)-HBTM was optimal at a concentration of 0.03 M (entry 3) to obtain the highest level of diastereoselectivity toward the formation of the desired β-lactone **4.52** and Mukaiyama's reagent was the best activation agent for this aldehyde acid. TsCl provided low yield (entry 5) and no reaction was observed when using MsCl (entry 6). Polar solvents such as CH_3CN, THF and Et_2O (entries 7-9) did not help increasing the formation of the desired β-lactone core **4.52** and non-polar solvents such as toluene and hexanes (entries 10-12) caused no reaction due to solubility issues. The most interesting results were observed when the additives were added into the reactions. Slow addition of Hünig's base (thermodynamically formed an ammonium enolate) increased the formation of undesired β-lactone **4.60** (Table 4.4, entry 13). Addition of K_2CO_3 to accelerate the reaction tremendously increased the formation of **4.60** (Table 4.4, entry 14). Adding hexamethylphosphoramide (HMPA) as a co-solvent to stabilize the high dipole moment of the transition state arrangement of **4.52** (Table 4.4, entry 15) did not significantly improve the NCAL outcome. Finally, addition of excess amount of Hünig's base (Table 4.4, entry 16) and heating at 50 $^{\circ}$C (Table 4.4, entry 17) significantly assisted the formation of the undesired β-lactone **4.60**.

Table 4.4. Optimizations of kinetic resolution and double diastereoselective NCAL process of aldehyde acid (±)-**4.51** using (±)-HBTM as a nucleophile.

Entry	Activating Agent (3 equiv)	Solvent	Conc.	Yield[a]	dr 4.52:4.60[b]
1	Mukaiyama's reagent	CH_2Cl_2	0.10	51%	1:2.1
2	Mukaiyama's reagent	CH_2Cl_2	0.06	55%	1:2.0
3	Mukaiyama's reagent	CH_2Cl_2	0.03	42%	1:1.7
4	Mukaiyama's reagent	CH_2Cl_2	0.01	10%	1:1.6
5	TsCl	CH_2Cl_2	0.03	25%	1:1.3
6	MsCl	CH_2Cl_2	0.03	NR[c]	--
7	Mukaiyama's reagent	CH_3CN	0.03	1%	1:3.1
8	Mukaiyama's reagent	THF	0.03	7%	1:4.4
9	Mukaiyama's reagent	Et_2O	0.03	NR	--
10	Mukaiyama's reagent	Toluene	0.03	NR	--
11	Mukaiyama's reagent	Benzene	0.03	NR	--
12	Mukaiyama's reagent	Hexanes	0.03	NR	--
13	Mukaiyama's reagent Slow addition of base	CH_2Cl_2	0.03	79%	1:3.8
14	Mukaiyama's reagent 3 equiv K_2CO_3	CH_2Cl_2	0.03	68%	1:30
15	Mukaiyama's reagent 10 equiv HMPA	CH_2Cl_2	0.03	22%	1:2.5
16	Mukaiyama's reagent 50 equiv i-Pr$_2$NEt	CH_2Cl_2	0.03	72%	1:6.5
17	Mukaiyama's reagent Heat at 50 °C	CH_2Cl_2	0.03	53%	1:7.3

[a]Values refers to estimated yield, which calculated from HPLC calibration curve. [b]Diastereomeric ratio determined by ^{1}H-NMR (500 MHz) of the crude reaction mixtures. [c]NR means no reaction.

These results suggested that the undesired β-lactone **4.60** is both the thermodynamic and kinetic product. Therefore, the condition shown in entry 3 (Table 4.4), using (*S*)-HBTM, was the best procedure giving the highest diastereoselectivity (dr, 1:1) for the preparation of the desired β-lactone core (+)-**4.52**.

4.2.3. Cyclohexenyl Zinc Additions: Total Synthesis of 6, 15-Bis-*epi*-spongiolactone

Knochel and coworkers[109] developed a strategy to construct the quaternary carbon in an asymmetric fashion. Addition of allyl zinc to ketones offers a straightforward synthesis of homoallylic alcohols bearing quaternary centers. The advantage of this approach is the use of the allylic zinc reagents, which are stable and easy to prepare. Moreover, this reaction precedes diastereoselectively and regioselectively under mild conditions. Recently, Knochel reported a method for preparation of di- and trisubstituted allylic zinc reagents by using LiCl-mediated insertion of zinc dust into alkyl, aryl, and heteroaryl iodides leading to organozinc reagents in good yields (Scheme 4.25).

Scheme 4.25
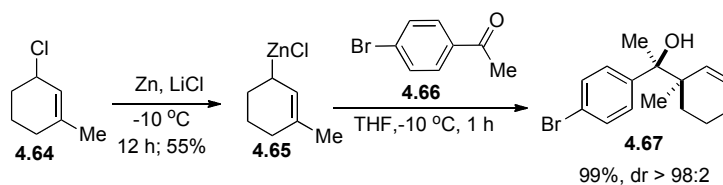
To explore the late stage synthesis and confirm the relative stereochemistry of

spongiolactone, the fused tricyclic β-lactone **4.60** was employed as a substrate for the diastereoselective allylic zinc addition, which is the key step to construct the stereogenic quaternary carbon. The new allylic zinc reagent required for spongiolactone was prepared from an inexpensive commercially available isophorol (3,5,5-trimethylcyclohexn-1-ol) (**4.68**) *via* chlorination and zinc insertion (Scheme 4.26). The chlorination was achieved *via* nucleophilic substitution by treating 3,5,5-trimethylcyclohexn-1-ol (**4.68**) with *N*-chlorosuccinimide in the presence of dimethyl sulfide.[111] The derived allyl chloride **4.69** was employed as the substrate for LiCl-mediated zinc insertion developed by Knochel and co-workers[112] to deliver zincate **4.70**. Concentration of cyclohexnyl zinc reagent **4.70** was determined by iodine titration. Zincate **4.70** was obtained in low yield due to Wurtz coupling, which was the undesired homo-coupling reaction between **4.69** and **4.70** that is usually observed as a by-product in this process. We tried to optimize the zinc insertion to increase the yield of the formation of the desired zincate **4.70**; however, the condition shown in Scheme 4.26 was the best. The zincate **4.70** was stable at 0 °C and slowly decomposed at higher temperatures.

Scheme 4.26
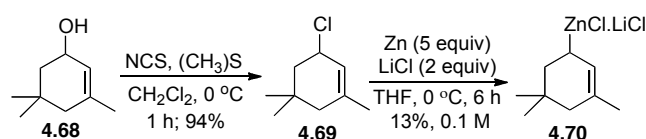
The successful preparation of new zincate **4.70** allowed the further study of the

diastereoselective allylic zinc addition of the fused tricyclic β-lactone **4.60**. To our delight, the diastereoselective allylic zinc addition of new zincate **4.70** to the ketone of fused tricyclic β-lactone (±)-**4.60** in the presence of β-lactone underwent smoothly to achieve homoallylic alcohol (±)-**4.71** as a major diastereomer in quantitative yield (95%) and excellent diastereoselectivity (Scheme 4.27). No trace of β-lactone ring opening was observed.

The derived alcohol (±)-**4.71** was fully characterized and the relative stereochemistry was confirmed by single X-ray crystallographic analysis, disclosing the stereogenic outcome of the all-carbon quaternary center. The X-ray structure showed an *anti*-relationship between methyl group on an all-carbon quaternary center and the adjacent tertiary alcohol.

Scheme 4.27
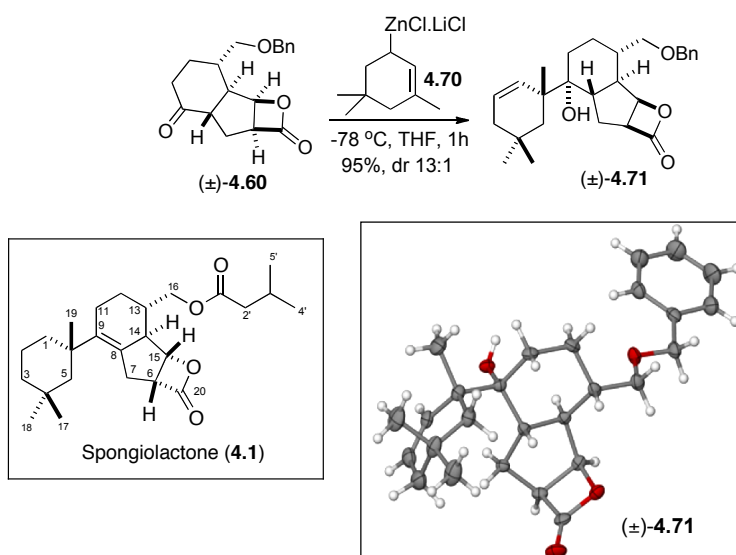
We proposed a transition state arrangement of the diastereoselective allylic zinc addition of zincate **4.70** to the fused tricyclic β-lactone (±)-**4.60** based on Knochel's evidence.[109] The diastereoselectivity was controlled by the cyclic chair-like transition state arrangement (Figure 4.7). The zincate **4.70** generally approached the ketone of (±)-**4.60** on the β-face due to steric hindrance of substrate. The S_E2' mechanism resulted in the formation of two new quaternary centers with an *anti*-relationship yielding methyl group on the β-face and tertiary alcohol on α-face.
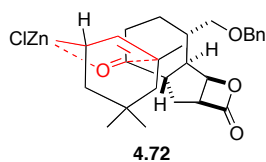
Figure 4.7. Chair-like transition state of allyl zinc addition of ketone (±)-**4.60**.

Comparing to spongiolactone (Scheme 4.27), the relative stereochemistry of all stereogenic centers of (±)-**4.71** was matched with reported structure of natural product, except for the stereochemistry of the β-lactone moiety. Therefore, the synthesis was continued to prove and confirm relative stereochemistry of target molecule **4.1**.

To complete the synthesis, homoallylic alcohol (±)-**4.71** was reduced by employing Pearlman catalyst $(Pd(OH)_2/C)$[113] under hydrogen atmosphere in ethanol to simultaneous hydrogenation of olefin and hydrogenolysis of benzyl group in the same operation to yield saturated alcohol (±)-**4.73**. Finally, selective esterification of primary

alcohol (±)-**4.73** with isovaleric acid (**4.74**) followed by dehydration yielded spongiolactone derivatives (±)-**4.76** and (±)-**4.77** (Scheme 4.28).

Scheme 4.28
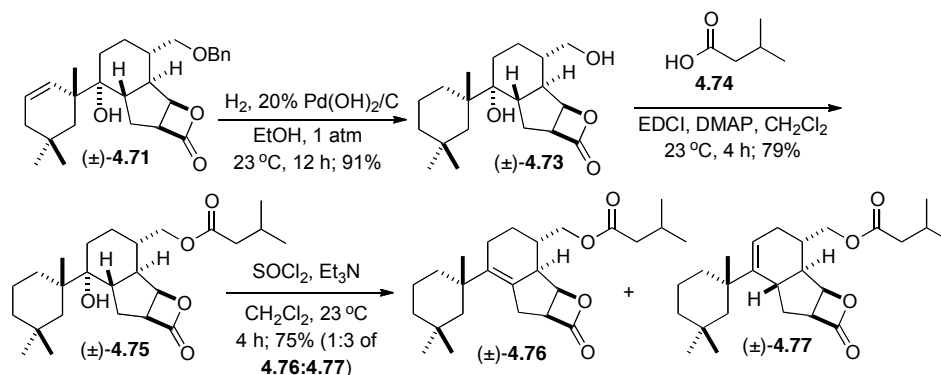
The comparison of ^{1}H-NMR (Figure 4.8) and ^{13}C-NMR (Table 4.5) of (±)-**4.76** and other spongiolactone derivatives ((±)-**4.77** and (±)-**4.77a**) to spongiolactone (**4.1**) and 3′-norspongiolactone (**4.4**) showed different chemical shift patterns, especially at β-lactone moiety. These results suggested that the derived spongian diterpenes (±)-**4.76** was the (±)-6,15- *bis*-epimer of spongiolactone. Additionally, this synthetic study used the benzyl group as the only protecting group. It was incorporated through a commercially available reagent, benzyloxy chloromethyl ether, and removed in the same step with olefin reduction. Therefore, the overall strategy was significantly concise and efficient due to no protection and deprotection step involved in the synthesis. The overall synthetic study toward 6,15-bis-*epi*-spongiolactone ((±)-**4.76**) was completed with a longest linear sequence of 11 steps from commercially available staring material with 4% overall yield.
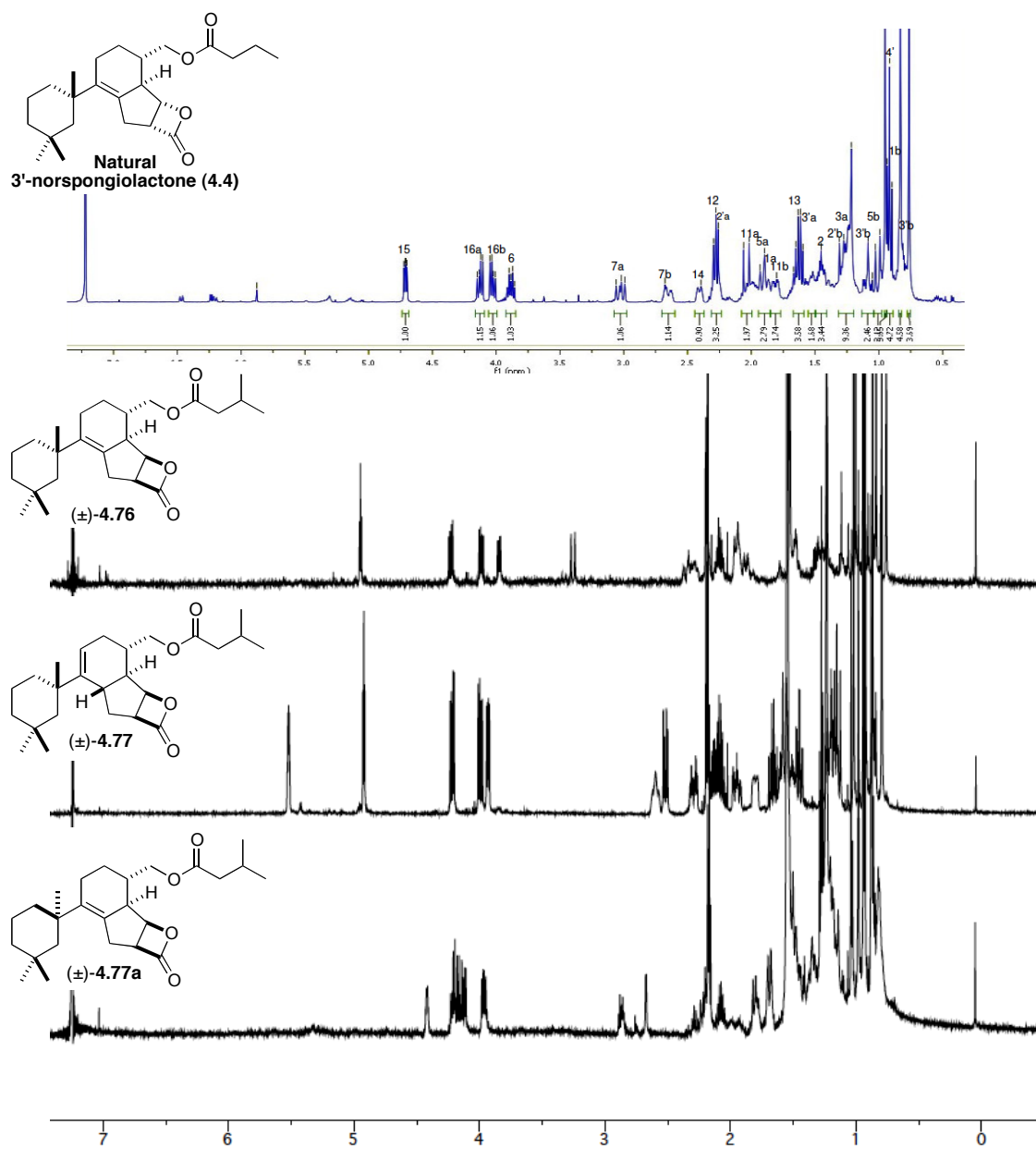
Figure 4.8. Comparison of ^{1}H-NMR of 3′-norspongiolactone (4.4) and 6,15-bis-*epi*-spongiolactone ((±)-4.76) and synthetic spongiolactone derivatives ((±)-4.77 and (±)-4.77a).

Table 4.5 Comparison of ^{13}C-NMR of spongiolactone (**4.1**), 3′-norspongiolactone (**4.4**) and 6,15-bis-*epi*-spongiolactone ((±)-**4.76**).

Position	4.1	4.4	Δ (4.1-4.76)	4.76	Δ (4.1-4.76)
1	38.3	38.3	0.0	38.166	0.13
2	20.9	20.9	0.0	20.919	0.02
3	39.7	39.6	0.1	39.619	0.08
4	31.4	31.4	0.0	31.346	0.05
5	49.9	49.9	0.0	47.680	**2.22**
6	54.3	54.1	0.2	53.650	0.65
7	30.5	30.4	0.1	31.189	0.67
8	133.7	133.5	0.2	126.820	**6.88**
9	139.4	139.0	0.4	142.372	**2.97**
10	39.4	39.2	0.2	39.415	0.02
11	26.3	26.6	0.3	26.787	0.49
12	26.8	26.2	0.6	26.792	0.01
13	36.8	36.6	0.2	33.186	**3.61**
14	50.2	50.2	0.0	50.059	0.14
15	79.9	80.1	0.2	75.737	**4.16**
16	67.6	67.8	0.2	67.404	0.20
17	26.5	26.0	0.5	25.903	0.60
18	32.7	32.9	0.2	33.131	0.43
19	30.3	30.4	0.1	29.727	0.57
20	171.8	172.2	0.4	171.194	**1.50**
1'	172.9	173.7	0.8	173.242	0.61
2'	43.3	36.1	7.2	43.477	0.18
3'	25.6	18.4	7.2	25.669	0.07
4'	22.4	13.7	8.7	22.474	0.07
5'	22.4	-	-	22.474	0.07

4.2.4. Cyclohexenyl Zinc Additions: Synthetic Study Toward the Total Synthesis of

Spongiolactone

The successful preparation of zincate **4.70** and the excellent diastereoselectivity achieved in the allyl zinc addition step in the presence of β-lactone provided the promising synthetic route to spongiolactone. Therefore, we decided to employ the identical late stage strategy to accomplish the total synthesis of spongiolactone. The desired fused tricyclic β-lactone core (+)-**4.52** was functionalized with zincate **4.70** *via* the diastereoselective allyl zinc addition under the same condition described previously (Scheme 4.29).

Scheme 4.29
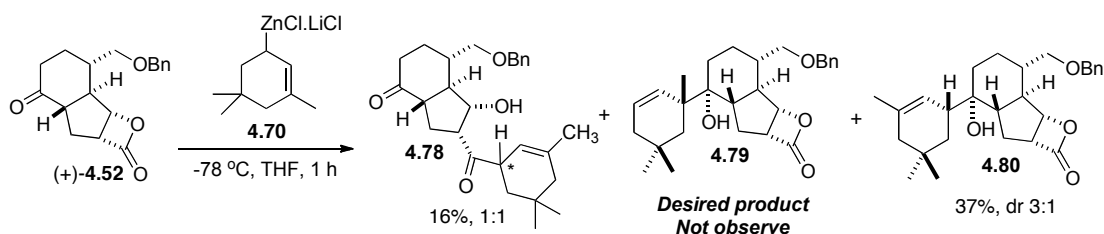
Unfortunately, the desired homoallylic alcohol **4.79** was not formed under this condition. Only α-addition of zincate **4.70** to the ketone yielding **4.80** and β-lactone ring opening (**4.78**) were observed. Several attempts to improve the overall results of the diastereoselective allyl zinc addition of the desired β-lactone core (+)-**4.52** were tried (Table 4.6). However, this reaction was remained unsuccessful. The results showed that raising the temperature, use of non-polar solvents and addition of mild Lewis acid only

led to β-lactone ring opening adduct (**4.78**). These results suggested that the β-lactone moiety of (+)-**4.52** was more reactive than the ketone in this case due to substrate constraints. Furthermore, there was probably no chelation between zincate **4.70** and ketone or β-lactone, since only α-addition adducts were observed.

Table 4.6. Optimizations of diastereoselective allyl zinc addition of the desired β-lactone core (+)-**4.52** with zincate **4.70**.

Entry	Condition[a]	Yield of **4.78**[b]	Yield of **4.80**[b]	Recovery of (+)-**4.52**
1	THF, −78 °C	16%, dr 1:1	37%, dr 3:1	8%
2	THF, 0 °C[c]	75%, dr 1:1	0%	8%
3	Et$_2$O, −78 °C	26%, dr 2:1	0%	59%
4	Toluene, −78 °C	46%, dr 1:1	17%, dr 1:1	28%
5	THF/HMPA (3:1), −78 °C	NR[d]	NR	91%
6	In(OTf)$_3$, THF, −78 °C	73%, dr 3:1	0%	0%
7	Sc(OTf)$_3$, THF, −78 °C	70%, dr 2:1	0%	0%

[a]10 equiv of zincate was added. They were no reaction when using 5 equiv of zincate. [b]Values refers to isolated yield and the diastereomeric ratios were determined by ^{1}H-NMR (500 MHz) of the crude reaction mixtures. [d]NR means no reaction.

We thus sought an alternative reaction that could override substrate constraint. Several methodologies for diastereoselective production of homoallylic alcohols bearing quaternary centers were reported involving In-mediated allylic addition,[114] titanium-catalyzed formation of organozinc[115] and zinc-mediated aqueous Barbier type

reaction.[116] Various conditions were studied (Scheme 4.30) aiming for allylic addition to the ketone of the fused tricyclic β-lactone (+)-**4.52**. However, all attempts failed to provide the desired homoallylic alcohol **4.79**. In all cases, no reaction was observed.

Scheme 4.30

Condition: 1) **4.69**, In, THF, 0 °C to 23 °C
2) **4.69**, In, DMF, 0 °C to 23 °C
3) **4.69**, Zn, THF, Cp$_2$TiCl$_2$, -20 °C to 23 °C
4) **4.69**, Zn, THF, aq. NH$_4$Cl (sat.), -20 °C to 23 °C
5) **4.70**, ZnOTf, THF, -78 °C to 23 °C
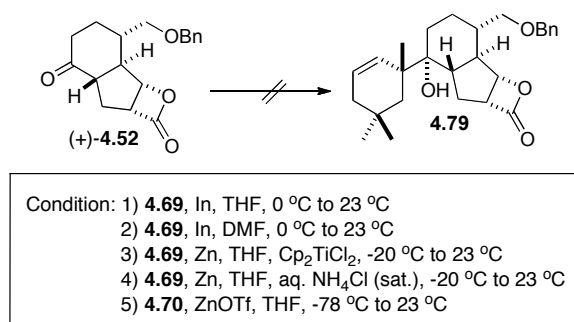
Structural modification of β-lactone (+)-**4.52** by appending the isovaleric ester side chain to increase electrophilicity of the ketone *via* inductive effect was considered to be an alternative route to solve the problem. The β-lactone (+)-**4.52c** was prepared and subjected to the standard diastereoselective allyl zinc addition. However, only the β-lactone ring opening adduct **4.81** was observed as the major product (Scheme 4.31). This reaction was done in small-scale and monitored by LC/MS. We found molecular mass corresponding to **4.81** but no β-lactone absorption on IR spectrum.

Scheme 4.31
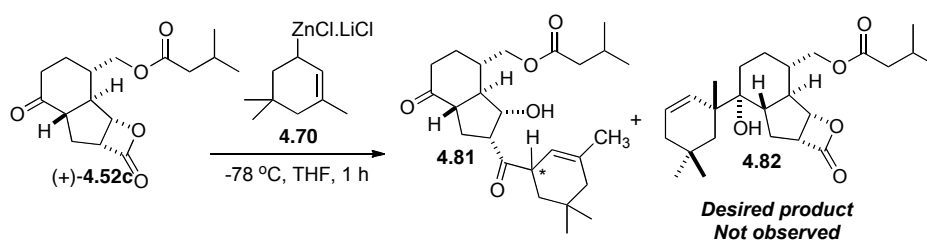
4.2.5. Alternative Strategies Toward the Total Synthesis of Spongiolactone

The successful preparation of 6,15-bis-*epi*-spongiolactone (**4.76a**) generally highlighted the synthetic application of the derived homoallylic alcohol (±)-**4.71** as the intermediate to achieve spongiolactone (**4.1**) *via* β-lactone ring opening and β-lactone reformation. The successful one-pot β-lactone ring opening and epimerization of (±)-**4.71** to obtain hydroxyl acid (±)-**4.83** (Scheme 4.32) allowed the further studies of β-lactone reformation through a Mitsunobu cyclization to correct the stereochemistry of β-lactone.

Scheme 4.32
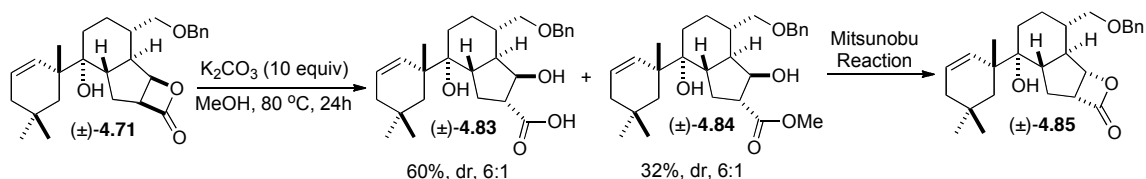
The resulting hydroxyl acid (±)-**4.83** was treated under Mitsunobu condition for the formation of β-lactone (±)-**4.85**, which has the correct β-lactone stereochemistry.

Several conditions were tried (Scheme 4.33) including heating up to 70 °C. However, β-lactone (±)-**4.85** was not formed. Only recovery of starting hydroxyl acid (±)-**4.83** was observed without β-elimination of the secondary alcohol.

Scheme 4.33

Condition: 1) PPh₃, DEAD, THF, 23°C to 70 °C
2) PPh₃, DEAD, Et₃N, THF, 23°C to 70 °C
3) PPh₃, DIAD, Et₂O, 23 °C to reflux
4) PPh₃, DIAD, Et₂O, Et₃N, 23 °C to reflux
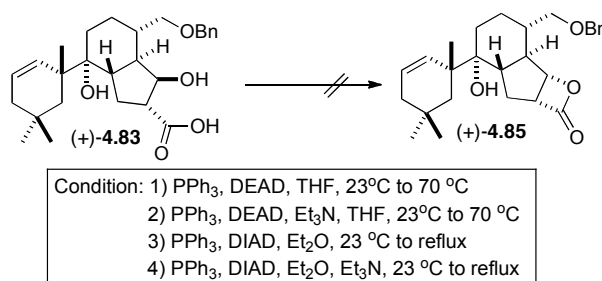
Further optimization by activation of secondary alcohol to a good leaving group *via* tosylation yielded no β-lactone (Scheme 4.34). Only β-elimination product ((+)-**4.86**) was observed along with the remaining starting material ((+)-**4.83**).

Scheme 4.34
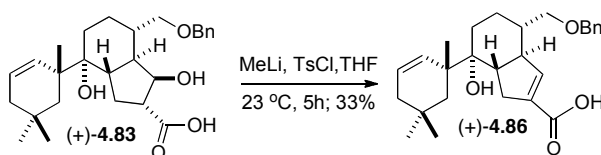
Since diastereoselective allylic zinc addition of β-lactone (+)-**4.52** was problematic, we also considered modifying the synthetic route by installation of cyclohexane appendage and the all-carbon quaternary center in the early stage. Thus,

ketone (±)-**4.87** was treated with a set of alternative methods for allylic addition for the preparation of homoallylic alcohol (±)-**4.88**. Unfortunately, no additional adduct was observed (Scheme 4.35). Further experiments will be studied.

Scheme 4.35
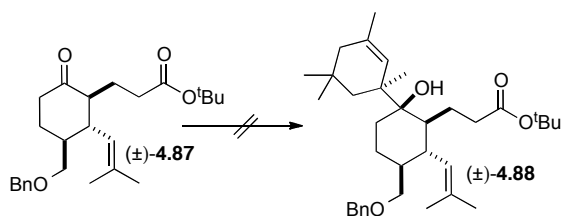
Condition: 1) **4.70**, THF, -78 °C to 23 °C
2) **4.70**, THF, -78 °C to 23 °C
3) **4.70**, In, THF, 0 °C to 23 °C
4) **4.69**, In, DMF, 0 °C to 23 °C
5) **4.69**, Zn, THF, Cp$_2$TiCl$_2$, -20 °C to 23 °C
6) **4.69**, Zn, THF, aq. NH$_4$Cl (sat.), -20 °C to 23 °C
7) **4.70**, ZnOTf, THF, -78 °C to 23 °C

4.3. Conclusion

Several synthetic strategies toward the total synthesis of spongiolactone have been studied by employing the intramolecular nucleophile-catalyzed aldol-lactonization (NCAL) reaction as the key step to construct the fused tricyclic β-lactone core. In this study, we reported the first result of kinetic resolution and double diastereoselective NCAL process catalyzed by (*S*)-HBTM. Furthermore, a highly diastereoselective allyl zinc addition to install an all-carbon quaternary center and pendent cyclohexane was developed. These successful methodologies allowed further functional group manipulations to accomplish the total synthesis of (±)-6,15-bis-*epi*-spongiolactone (**4.76**) in a longest linear sequence of 11 steps from a commercially available staring material with

no protection and deprotection steps. The spongiolactone derivatives (($\pm$)-**4.76**, ($\pm$)-**4.77** and ($\pm$)-**4.77a**) will enable SAR studies to identify the molecular protein target.

Although we could access the desired core β-lactone core of this natural product, the diastereoselective allyl zinc addition to install an all-carbon quaternary center and pendent cyclohexane was unsuccessful. As the results, the total synthesis of spongiolactone is remaining underway and continues to be further developed.

CHAPTER V

CONCLUSIONS

As an interdisciplinary program in nature that entails organic synthesis and chemical biology, we had developed a set of second generation diazo reagents with the smaller steric footprint, namely the α-trifluoroethyl (HTFB), α-cyano and *p*-azidophenyl diazo reagents for simultaneous arming and SAR studies of bioactive natural products *via* O−H insertion protocol for derivatization of the alcohol-containing natural products. Useful reactivity and both chemo- and site (chemosite) selectivities were observed when the α-trifluoroethyl diazo reagent was employed. This diazo reagent (HTFB) provided similar reactivity comparing to the first generation diazo reagent bearing *p*-bromophenyl substituent (HBPA) with the advantage of enabling the use of ^{19}F-NMR to facilitate small-scale, crude derivatization reaction analysis. Modulating natural product-cellular receptor interactions highlighted the profound application of new α-trifluoroethyl diazo reagent (HTFB) as it showed selective protein binding in IL-2 reporter assay of FK506 derivatives and provided the better retention of biological activity in hMetAP2 proliferation assay of fumagillol derivatives comparing to *p*-bromophenyl diazo reagent (HBPA). The synthetic useful of new α-trifluoroethyl diazo reagent (HTFB) and the development of mild and mono-functionalization O−H insertion for derivatization of alcohol-containing natural products have provided a great synthetic tool for basic cellular studies for investigating the information-rich content of complex natural

products leading to the identification of medically relevant protein targets and the discovery of potential therapeutic agents for human diseases.

As the course of synthetic program involving β-lactone chemistry and synthesis of β-lactone containing natural products, the $SnCl_4$-promoted tandem Mukaiyama aldol-lactonization (TMAL) and intramolecular nucleophile-catalyzed aldol-lactonization (NCAL) reaction, which are the synthetic methodologies developed in the Romo group were studied for the synthesis of β-lactam congeners of orlistat and synthetic studies toward the total synthesis of spongiolactone, respectively.

A set of β-lactam derivatives of orlistat was synthesized for structure-activity relationship studies (SAR) to evaluate their fatty acid synthase inhibitory activities in comparison with orlistat. The $SnCl_4$-promoted tandem Mukaiyama aldol-lactonization (TMAL) reaction yielded the *cis*-β-lactone in moderate to excellent diastereoselectivity, followed by conversion of *cis*-β-lactone to the *trans*-β-lactam *via* a one-pot β-lactone ring opening and intramolecular Mitsunobu cyclization furnishing β-lactam analogs. The inhibitory activities of the derived β-lactam derivatives were determined in a biochemical fluorogenic assay using recombinant FAS-TE and the micro-molar range FAS-TE inhibitory activities were observed. Although, these series of β-lactam derivatives showed lower potency compared to the related β-lactone, the enhanced stability of these derivatives suggests that this class of compounds should be further investigated as potential fatty acid synthase inhibitors.

In the synthetic studies toward the total synthesis of spongiolactone, an intramolecular nucleophile-catalyzed aldol-lactonization (NCAL) reaction was

employed as the key step to construct the fused tricyclic-β-lactone core. This synthetic strategy highlighted the useful application of NCAL reaction toward the formation of bicyclic-β-lactones from the complex aldehyde acid. Importantly, we have developed a double diastereoselection and, for the first time, kinetic resolution *via* the NCAL process by using (*S*)-HBTM as a nucleophile, which enabled an enantioselective strategy to access the fused tricyclic β-lactone and set the four contiguous stereogenic centers of spongiolactone core. The quaternary carbon on the pendant cyclohexyl moiety was achieved by a diastereoselective allylic zinc addition that proceeded with high diastereoselectivity and excellent yield. Even though the total synthesis of spongiolactone has not yet been completed, we accomplished the total synthesis of (±)-6,15-bis-*epi*-spongiolactone *via* an 11-step longest linear sequence from commercially available staring materials without protection and deprotection steps emphasizing concise and feasibility of our strategy. The derived spongiolactone derivatives will be further SAR studies to identify the molecular protein targets and mode of action toward cancer cell lines.

REFERENCES

1. (a) Hopkins, A. L.; Groom, C. R. *Nat. Rev. Drug Discovery* **2002**, *1*, 727-730. (b) Meisner, N. C.; Hintersteiner, M.; Uhl, V.; Weidemann, T.; Schmied, M.; Gstach, H.; Auer, M. *Curr. Opin. Chem. Biol.* **2004**, *8*, 424-431. (c) Newman, D. J.; Cragg, G. M. *J. Nat. Prod.* **2007**, *70*, 461-477. (d) Demain, A. L. *Med. Res. Rev.* **2009**, *29*, 821-842.

2. (a) Henkel, T.; Brunne, R. M.; Müller, H.; Reichel, F. *Angew. Chem. Int. Ed.* **1999**, *38*, 643-647. (b) Bajorath, J. *J. Comput.-Aided Mol. Des.* **2002**, *16*, 431-439.

3. (a) Lipinski, C. A.; Lombardo, F.; Dominy, B. W.; Feeney, P. J. *Adv. Drug Delivery Rev.* **1997**, *23*, 3-25. (b) Feher, M.; Schmidt, J. M. *J. Chem. Inf. Comput. Sci.* **2002**, *43*, 218-227.

4. (a) Clardy, J.; Walsh, C. *Nature* **2004**, *432*, 829-837. (b) Butler, M. S. *Nat. Prod. Rep.* **2008**, *25*, 475-516.

5. Rowinsky, E. K.; Donehower, R. C. *New. Eng. J. Med.* **1995**, *332*, 1004-1014.

6. (a) Koehn, F. E.; Carter, G. T. *Nat. Rev. Drug Discovery* **2005**, *4*, 206-220. (b) Paterson, I.; Anderson, E. A. *Science* **2005**, *310*, 451-453. (c) Keller, T. H.; Pichota, A.; Yin, Z. *Curr. Opin. Chem. Biol.* **2006**, *10*, 357-361. (d) Harvey, A. L. *Drug Discovery Today* **2008**, *13*, 894-901.

7. (a) Strausberg, R. L. *Science* **2003**, *300*, 294-295. (b) Burdine, L.; Kodadek, T. *Chemistry & Biology* **2004**, *11*, 593-597. (c) Piggott, A. M.; Karuso, P. *Comb. Chem. High T. Scr.* **2004**, *7*, 607-630. (d) Stockwell, B. R. *Nature* **2004**, *432*, 846-854. (e)

Harvey, A. L.; Clark, R. L.; Mackay, S. P.; Johnston, B. F. *Expert Opin. Drug Dis.* **2010**, *5*, 559-568.

8. (a) Osada, H. *J. Antibiot.* **1998**, *51*, 973-982. (b) Carlson, E. E., *ACS Chem. Biol.* **2010**, *5*, 639-653.

9. (a) Cravatt, B. F.; Wright, A. T.; Kozarich, J. W. *Annu. Rev. Biochem.* **2008**, *77*, 383-414. (b) Berger, A.B.; Vitorino, P.M.; Bogyo, M. *Am. J. Pharmacogenomics* **2004**, 4, 371-381.

10. (a) Kolb, H. C.; Finn, M. G.; Sharpless, K. B. *Angew. Chem., Int. Ed.* **2001**, *40*, 2004-2021. (b) Rostovtsev, V. V.; Green, L. G.; Fokin, V. V.; Sharpless, K. B. *Angew. Chem. Int. Ed.* **2002**, *41*, 2596-2599.

11. (a) Y. Yasaka, M. Tanaka, *J. Chromatogr. B Biomed Appl.* **1994**, *659*, 139-155. (b) La Clair, J. J. *Nat. Prod. Rep.* **2010**, *27*, 969-996.

12. Zumbuehl, A.; Jeannerat, D.; Martin, S. E.; Sohrmann, M.; Stano,P.; Vigassy, T.; Clark, D. D.; Hussey, S. L.; Peter, M.; Peterson, B. R.; Pretsch, E.; Walde, P.; Carreira, E. M. *Angew. Chem, Int. Ed.* **2004**, *43*, 5181-5185.

13. Muddana, S. S.; Peterson, B. R. *Org. Lett.* **2004**, *6*, 1409-1412.

14. Chen, J.; Ying, L.; Hansen, T. M.; Engler, M. M.; Lee, C. S.; La Clair, J. J.; Forsyth, C. J. *Bioorg. Med. Chem. Lett.* **2006**, *16*, 901-904.

15. J. E. Wulff, R. Siegrist and A. G. Myers, *J. Am. Chem. Soc.*, **2007**, *129*, 14444-14451.

16. Y. Kotake, K. Sagane, T. Owa, Y. Mimori-Kiyosue, H. Shimizu, M. Uesugi, Y. Ishihama, M. Iwata and Y. Mizui, *Nat. Chem. Biol.*, **2007**, *3*, 570-575.

17. Peddibhotla, S.; Dang, Y.; Liu, J. O.; Romo, D. *J. Am. Chem. Soc.* **2007**, *129*, 12222-12231.

18. Zhou, C. Y.; Li, J.; Peddibhotla, S.; Romo, D. *Org Lett* **2010**, *12*, 2104-2107.

19. Reed, S. A.; Mazzotti, A. R.; White, M. C. *J. Am. Chem. Soc.* **2009**, *131*, 11701-11706.

20. T. Wieland, Fortschr. *Chem. Org. Naturst*. **1967**, *25*, 214-250.

21. Alexander, M. D.; Burkart, M. D.; Leonard, M. S.; Portonovo, P.; Liang, B.; Ding, X.; Joullié, M. M.; Gulledge, B. M.; Aggen, B. J.; Chamberlin, A. R.; Sandler, J.; Fenical, W.; Cui, J.; Gharpure, S. J.; Polosukhin, A.; Zhang, H.; Evans, P. A.; Richardson, A. D.; Harper, M-K.; Ireland, C. M.; Vong, B. G.; Brady, T. P.; Theodorakis, E. A.; La Clair, J. J. *ChemBioChem* **2006**, *7*, 409-416.

22. (a) Low, W. K.; Dang, Y.; Schneider-Poetsch, T.; Shi, Z.; Choi, N. S.; Merrick, W. C.; Romo, D.; Liu, J. O. *Mol. Cells* **2005**, *20*, 709-722. (b) Nyangulu, J. M.; Galka, M. M.; Jadhav, A.; Gai, Y.; Graham, C. M.; Nelson, K. M.; Cutler, A. J.; Taylor, D. C.; Banowetz, G. M.; Abrams, S. R. *J. Am. Chem. Soc.* **2005**, *127*, 1662-1664. (c) Statsuk, A. V.; Bai, R.; Baryza, J. L.; Verma, V. A.; Hamel, E.; Wender,P. A.; Kozmin, S. A. *Nat. Chem. Biol.* **2005**, *1*, 383-388. (d) Yamaoka, M.; Sato, K.; Kobayashi, M.; Nishio, N.; Ohkubo, M.; Fujii, T.; Nakajima, H. *J. Antibiot.* **2005**, *58*, 654-662. (e) Clardy, *J. ACS Chem. Biol.* **2006**, *1*, 17-19. (f) Hughes, C. C.; Yang, Y.-L.; Liu, W.-T.; Dorrestein, P. C.; Clair, J. J. L.; Fenical, W. *J. Am. Chem. Soc.* **2009**, *131*, 12094-12096. (g) Wang, J.; Zhang, W.; Song, W.; Wang, Y.; Yu, Z.; Li, J.; Wu, M.; Wang, L.; Zang, J.; Lin, Q. *J. Am. Chem. Soc.* **2010**, *132*, 14812-14818.

(h) Nguyen, D. P.; Elliott, T.; Holt, M.; Muir, T. W.; Chin, J. W. *J. Am. Chem. Soc.* **2011**, *133*, 11418-11421.

23. Kanoh, N.; Honda, K.; Simizu, S.; Muroi, M.; Osada, H. *Angew. Chem. Int. Ed.* **2005**, *44*, 3559-3562.

24. Muller, P. *Pure & Appl. Chem.* **1994**, *66*, 1077-1184. The term "chemosite selective" was proposed to describe a reaction that exhibits both chemo and site selectivity.

25. Henkel, T.; Brunne, R. M.; Müller, H.; Reichel, F. *Angew. Chem. Int. Ed.* **1999**, *38*, 643-647.

26. (a) Stewart, I. C.; Bergman, R. G.; Toste, F. D. *J. Am. Chem. Soc.* **2003**, *125*, 8696-8697. (b) Petchprayoon, C.; Suwanborirux, K.; Miller, R.; Sakata, T.; Marriott, G. *J. Nat. Prod.* **2005**, *68*, 157-161. (c) Khan, A. T.; Choudhury, L. H.; Ghosh, S. *Tetrahedron Lett.* **2004**, *45*, 7891−7894. (d) Miller, D. J.; Moody, C. J. *Tetrahedron* **1995**, *51*, 10811-10843. (e) Milioni, C.; Jung, L.; Koch, B. *Eur. J. Med. Chem.* **1991**, *26*, 947-951. (f) Liljeblad, A.; Aksela, R.; Kanerva, L. T. *Tetrahedron: Asymmetry* **2001**, *12*, 2059-2066.

27. Paulissen, R.; Reimlinger, H.; Hayez, E.; Hubert, A. J.; Teyssie´, P. *Tetrahedron Lett.* **1973**, *24*, 2233-2236.

28. Cox, G. G.; Miller, D. J.; Moody, C. J.; Sie, E. R. H. B.; Kulagowski, J. J. *Tetrahedron* **1994**, *50*, 3195-3212.

29. Han, K.; Liu. Z.; Wang, Y.; Yue, X. *Chem. Res. Chinese* **2007**, *23*, 221-225.

30. Qu, Z.; Shi, W.; Wang, J. *J. Org. Chem.* **2003**, *69*, 217-219.

31. Huw, D. M.; Beckwith, R. E. *Chem. Rev.* **2003**, *103*, 2861-2904.

32. Doyle, M.; McKervey, M.; Ye, T. *Modern Catalytic Methods for Organic Synthesis with Diazo Compounds: From Cyclopropanes to Ylides*; Wiley: New York, 1998.

33. For a thorough discussion of the concept of "double-diastereodifferentiation" applied to chiral peptide catalysts and natural products, see: Lewis, C. A.; Miller, S. J. *Angew. Chem. Int. Ed.* **2006**, *45*, 5616-5619.

34. Timmons, D. J.; Doyle, M. P. *J. Organomet. Chem.* **2001**, *617*, 98-104.

35. Doyle, M. P. *J. Org. Chem.* **2006**, *71*, 9253-9260.

36. Espino, G. C.; Fiori, K. W.; Kim, M.; Du Bois, J. *J. Am. Chem. Soc.* **2004**, *126*, 15378-15379.

37. (a) Doyle, M.; McKervey, M.; Ye, T. *Modern Catalytic Methods for Organic Synthesis with Diazo Compounds: From Cyclopropanes to Ylides*; Wiley: New York, 1998. (b) Davies, H. M. L.; Beckwith, R. E. J. *Chem. Rev.* **2003**, *103*, 2861-2904.

38. Denton, J. R.; Cheng, K.; Davies, H. M. L. *Chem. Commun.* **2008**, 1238-1204.

39. Rao, P. N. P.; Uddin, M. J.; Knaus, E. E. *J. Med. Chem.* **2004**, *47*, 3972-3990.

40. Sadakane, Y.; Hatanaka, Y. *Curr. Top. Med. Chem.* **2002**, *2*, 271-288.

41. Marcoux, D.; Azzi, S.; Charette, A. B. *J. Am. Chem. Soc.* **2009**, *131*, 6970-6972.

42. (a) Davies, H. M. L.; Hutcheson, D. K. *Tetrahedron Lett.* **1993**, *34*, 7243-7246. (b) Davies, H. M. L.; Bruzinski, P. R.; Lake, D. H.; Kong, N.; Fall, M. J. *J. Am. Chem. Soc.* **1996**, *118*, 6897-6907.

43. Cox, G. G.; Haighb, D.; Hindleyb, R. M.; Millera, D. J.; Moody, C. J. *Tetrahedron Lett.* **1994**, *35*, 3139-3142.

44. (a) Koko, S.; Yuji, N.; Soichiro, T.; Nobujiro, K.; Masami, H.; Toshio, M.; Yosuke,

S.; Hideo, K.; Masataka, K.; Toshikazu, O. *J. Antibiot.* **1992**, *45*, 1433-1441. (b) Ju, J.; Seo, J.-W.; Her, Y.; Lim, S.-K.; Shen, B. *Org. Lett.* **2007**, *9*, 5183-5186.

45. Chen, X.; Xie, S.; Bhat, S.; Kumar, N.; Shapiro, T. A.; Liu, J. O. *Chemistry & Biology* **2009**, *16*, 193-202.

46. Becker, J. W., Rotonda, J., Cryan, J. G., Martin, M., Parsons, W. H., Sinclair, P. J., Wiederrecht, G., and Wong, F. *J. Med. Chem.* 1999, *42*, 2798-2804.

47. Han, C. K.; Ahn, S. K.; Choi, N. S.; Hong, R. K.; Moon, S. K.; Chun, H. S.; Lee, S. J.; Kim, J. W.; Hong, C. I.; Kim, D.; Yoon, J. H.; No, K. T. *Bioorg. Med. Chem. Lett.* **2000**, *10*, 39-43.

48. Liu, S.; Widom, J.; Kemp, C. W.; Crews, C; Clardy, J. *Science* **1998**, *282*, 1324-1327.

49. (a) Jemal, A.; Bray, F.; Center, M. M.; Ferlay, J.; Ward, E.; Forman, D. *Ca. CANCER J. Clin.* **2011**, *61*, 69-90. (b) Ferlay, J.; Shin, H. R.; Bray, F.; Forman, D.; Mathers, C. D.; Parkin, D.; GLOBOCAN 2008, Cancer Incidence and Mortality Worldwide: IARC CancerBase No. 10. Lyon, France: International Agency for Research on Cancer; Year. Available at: http://globocan.iarc.fr. 2010. Last accessed 8/17/2010.

50. Greenstein, J. P. *Biochemistry of Cancer*. New York: Academic Press, 1954.

51. Warburg, O. *Science* **1956**, *123*, 309-314.

52. Vazquez-Martin, A.; Colomer, R.; Brunet, J.; Lupu, R.; Menendez, J.A. *Cell Prolif.* **2008**, *41*, 59-85.

53. Medes, G.; Thomas, A.; Weinhouse, S. *Cancer Res.*, **1953**, *13*, 27-29.

54. Ookhtens, M.; Kanna, R.; Lyon, I.; Beaker, N. *Am. J. Physiol.* **1984**, *247*, R146-153.

55. Kuhajda, F. P.; Jenner, K.; Wood, F. D.; Hennigar, R. A.; Jacobs, L. B.; Dick, J. D.; Pasternack, G. R. *Proc. Natl. Acad. Sci. USA* **1994**, *91*, 6379-6383.

56. (a) Wakil, S. J. *Biochemistry* **1989**, *28*, 4523-4530. (b) Rangan, V. S.; Joshi, A. K.; Smith, S. *Biochemistry* **2001**, *40*, 10792-10799. (c) Smith, S.; Witkowski, A.; Joshi, A.K. *Prog. Lipid Res.* **2003**, *42*, 289-317. For a review, see: (a) Kuhajda, F. P. *Nutrition* **2000**, *16*, 202-208. (b) Kuhajda, F. P. *Cancer Res.* **2006**, *66*, 5977-5980. (c) Menendez, A. J.; Lupu, R. *Nat. Rev. Cancer* **2007**, *7*, 763-777. (d) Liu, H.; Liu, J.; Wu, X.; Zhang, J. *Int. J. Biochem. Mol. Biol.* **2010**, *1*, 69-89.

57. (a) Zhang, L.; Joshi, A. K.; Smith, S. *J. Biol. Chem.* **2003**, *278*, 40067-40074. (b) Jenke-Kodama, H.; Sandmann, A.; Müller, R.; Dittmann, E. *Mol. Biol. Evol.* **2005**, *22*, 2027-2039.

58. Migita, T.; Ruiz, S.; Fornari, A.; Fiorentino, M.; Priolo, C.; Zadra, G.; Inazuka, F.; Grisanzio, C.; Palescandolo, E.; Shin, E.; Fiore, C.; Xie, W.; Kung, A. L.; Febbo, P. G.; Subramanian, A.; Mucci, L.; Ma, J.; Signoretti, S.; Stampfer, M.; Hahn, W. C.; Finn, S.; Loda, M. *J. Natl. Cancer Inst.* **2009**, *101*, 519-532.

59. (a) Pizer, E. S.; Wood, F. D.; Heine, H. S.; Romantsev, F. E.; Pasternack, G. R.; Kuhajda, F. P. *Cancer Res.* **1996**, *56*, 1189-1193. (b) Pizer, E. S.; Thupari, J.; Han, W. F.; Pinn, M. L.; Chrest, F. J.; Frehywot, G. L.; Townsend, C. A.; Kuhajda, F. P. *Cancer Res.* **2000**, *60*, 213-218. (c) Pizer, E. S.; Pflug, B. R.; Bova, G. S.; Han, W. F.; Udan, M. S.; Nelson, J. B. *Prostate* **2001**, *47*, 102-110. (d) Kridel, S. J.; Axelrod, F.; Rozenkrantz, N.; Smith, J. W. *Cancer Res.* **2004**, *64*, 2070-2075. (e) Alli, P. M.;

Pinn, M. L; Jaffee, E. M.; McFadden, J. M.; Kuhajda, F. P. *Oncogene* **2005**, *24*, 39-46. (f) Liu, H.; Liu, Y.; Zhang, J. T. *Mol. Cancer. Ther.* **2008**, *7*, 263-270. (g) Orita, H.; Coulter, J.; Tully, E.; Kuhajda, F. P.; Gabrielson, E. *Clin. Cancer Res*. **2008**, *14*, 2458-2464.

60. (a) Smith, S. *Faseb J.* **1994**, *8*, 1248-1259. (b) Asturias, F. J.; Chadick, J. Z.; Cheung, I. K.; Stark, H.; Witkowski, A.; Joshi, A. K; Smith S. *Nat. Struct. Mol. Biol.* **2005**, *2*, 225-232.

61. Goodridge, A. G. *Fatty Acid Synthesis in Eucaryotes*. Amsterdam: Elsevier Science, 1991.

62. Weiss, L.; Hoffman, G.; Schreiber, R.; Andres, H.; Fuchs, E.; Korber, E.; Kolb, H. *Biol. Chem.* **1986**, *367*, 905-912.

63. Rashid, A.; Pizer, E. S.; Moga, M.; Milgraum, L. Z.; Zahurak, M.; Pasternack, G. R.; Kuhajda, F. P; Hamilton, S. R. *Am. J. Pathol.* **1997**, *150*, 201-208.

64. (a) Epstein, J. I.; CarMichael, M.; Partin, A. W. *Urology* **1995**, *45*, 81-86. (b) Shurbaji, M. S.; Kalbfleisch, J. H; Thurmond, T. S. *Hum. Pathol.* **1996**, *27*, 917-921.

65. Gansler, T. S.; Hardman, W., III; Hunt, D. A.; Schaffel, S.; Henninger, R. A. *Hum. Pathol.* **1997**, *28*, 686-693.

66. Pizer, E.; Lax, S.; Kuhajda, F.; Pasternack, G.; Kurman, R. *Cancer* **1998**, *83*, 528-537.

67. (a) Alo, P. L.; Visca, P.; Marci, A.; Mangoni, A.; Botti, C.; Di Tondo, U. *Cancer* **1996**, *77*, 474-482. (b) Milgraum, L. Z.; Witters, L. A.; Pasternack, G. R.; Kuhajda, F. P. *Clin.Cancer Res.* **1997**, *3*, 2115-2120. (c) Alo, P. L.; Visca, P.; Trombetta, G.;

Mangoni, A.; Lenti, L.; Monaco, S.; Botti, C.; Serpieri, D. E.; Di Tondo, U. *Tumori* **1999**, *85*, 35-40.

68. (a) Van de Sande, T.; Roskams, T.; Lerut, E.; Joniau, S.; Van Poppel, H.; Verhoeven, G.; Swinnen, J. V. *J. Pathol.* **2005**, *206*, 214-219. (b) Zhang, D.; Tai, L. K.; Wong, L. L.; Chiu, L. L.; Sethi, S. K.; Koay, E. S. *Mol. Cell Proteomics* **2005**, *4*, 1686-1696.

69. (a) Zhou, W.; Simpson, P. J.; McFadden, J. M.; Townsend, C. A.; Medghalchi, S. M.; Vadlamudi, A.; Pinn, M. L. Ronnett, G. V.; Kuhajda F. P. *Cancer Res.* **2003**, *63*, 7330-7337. (b) Menendez, J. A.; Colomer, R.; Lupu, R. *Oncol. Rep.* **2004**, *12*, 411-422. (c) Menendez, J. A.; Mehmi, I.; Atlas, E.; Colomer, R.; Lupu, R. *Int. J. Oncol.* **2004**, *24*, 591-608.

70. (a) Borgström, B. *Biochim. Biophys. Acta* **1988**, *962*, 308-316. (b) Hadvary, P.; Lengsfeld, H.; Wolfer, H. *Biochem. J.* **1988**, *256*, 357-361.

71. (a) Knowles, L. M.; Axelrod, F.; Browne, C. D.; Smith, J. W. *J. Biol. Chem.* **2004**, *279*, 30540-30545. (b) Menendez, J. A.; Vellon, L.; Lupu, R. *Ann. Oncol.* **2005**, *16*, 1253-1267. (c) Menendez, J. A.; Vellon, L.; Lupu, R. *Exp. Biol. Med.* **2005**, *230*, 151-154. (d) Browne, C. D.; Hindmarsh, E. J.; Smith, J. W. *FASEB J.* **2006**, *20*, 2027-2035. (e) Menendez, J. A.; Vellon, L.; Lupu, R. *Int. J. Gynecol Cancer* **2006**, *16*, 219-211. (f) Kridel, S. J.; Lowther, W. T.; Pemble, C. W. *Expert Opin. Investig. Drugs* **2007**, *16*, 1817-1829. (g) Little, J. L.; Wheeler, F. B.; Fels, D. R.; Koumenis, C.; Kridel, S. J. *Cancer Res.* **2007**, *67*, 1262-1269. (h) Menendez, J. A.; Lupu, R. *Nat. Rev. Cancer* **2007**, *7*, 763–777. (i) Carvalho, M. A.; Zecchin, K. G.; Seguin, F.;

Bastos, D. C.; Agostini, M.; Rangel, A. L. C. A.; Veiga, S. S.; Raposo, H. F.; Oliveira, H. C. F.; Loda, M.; Coletta, R. D.; Graner, E. *Int. J. Cancer* **2008**, *123*, 2557-2565. (j) Knowel, L. M.; Yang, C.; Osterman, A.; Smith, J. W. *J. Biol.Chem.* **2008**, *283*, 31378-31384. (k) Little, J. L.; Wheeler, F. B.; Koumenis, C.; Kridel, S. J. *Mol. Cancer Ther.* **2008**, *7*, 3816-3824.

72. (a) Hadvary P, Lengsfeld H, Wolfer H. *Biochem. J.* **1988**, *256*, 357-361. (b) Pemble, C. W.; Johnson, L. C.; Kridel, S. J.; Lowther, W. T. *Nat. Struct. Mol. Biol.* **2007**, *14*, 704-709. (c) Cheng, F.; Wang, Q.; Chen, M.; Quiocho, F. A.; Ma, J. *Proteins* **2008**, *70*, 1228-1234.

73. (a) For a review of β-lactone chemistry, see: Pommier, A.; Pons, J. M. *Synthesis* **1993**, 444-449. For reviews of β-lactone-containing natural products, see: (b) Lowe, C.; Vederas, J.*Org. Prep. Proceed. Int.* **1995**, *27*, 305-346. (c) Pommier, A.; Pons, J. M. *Synthesis* **1995**, 729-744. For transformations of β-lactones, see: (d) Palomo, c.; Miranda, J. I.; Linden, A. J. *Org. Chem.***1996**, *61,* 9196-9201. (e) Zemribo, R.; Champ, M. S.; Romo, D. *Synlett* **1996**, 278-280. (f) Shao, H.; Wang, S. H. H.; Lee, C.-W.; Osapay, G.; Goodman, M. J. *Org. Chem.* **1995**, *60,* 2956-2957. (g) Mead, K. T.; Lu, J. *Tetrahedron Lett.* **1994**, *35,* 8947-8950. (h) Mead, K. T.; Pillai, S. K. *Tetrahedron Lett.* **1993**, *34,* 6997-7000. (i) Mead, K. T.; Zemribo, R. *Synlett* **1996**, 1063-1064. (j) Mead, K. T.; Zemribo, R. *Synlett* **1996**, 1065-1066.

74. For a review of the synthesis of optically active β-lactones, see: (a) Yang, H. W. Romo, D. *Tetrahedron* **1999**, *55*, 6403-6434. (b) Paull, D. H., Weatherwax, A; Lectka, T *Tetrahedron*, **2009**, *65*, 6771-6803. For asymmetric methods, see: (c)

Dymock, B. W.; Kocienski, P. J.; Pons, J.-M. *J. Chem. Soc., Chem. Commun.* **1996**, 1053-1054. (d) Arrastia, I.; Lecea, B.; Cossio, F. P. *Tetrahedron Lett.* **1996**, *37*, 245-248. (e) Zemribo, R.; Romo, D. *Tetrahedron Lett.* **1995**, *36*, 4159-4162. (f) Dirat, O.; Berranger, T.; Langlois, Y. *Synlett* **1995**, 935-937. (g) Tamai, Y.; Someya, M.; Fukumoto, J.; Miyano, S. *J. Chem.Soc., Chem. Commun.* **1994**, 1549-1550. (h) Tamai, Y.; Yoshiwara, H.; Someya, M.; Fukumoto, J.; Miyano, S. *J. Chem. Soc., Chem. Commun.***1994**, 2281-2282. (i) Capozzi, G.; Roelens, S.; Talami, S. *J. Org. Chem.***1993**, *58*, 7932-7936. (j) Case-Green, S. C.; Davies, S. G.; Hedgecock, C. J. R. *Synlett* **1991**, 779−780. (k) Bates, R. W.; Fernandez-Moro, R.; Ley, S. V. *Tetrahedron Lett.* **1991**, *32*, 2651. (l) Evans, D. A.; Janey, J. M. *Org. Lett.* **2001**, *3*, 2125-2128. (m) Cortez, G. S.; Tennyson, R. L.; Romo, D. *J. Am. Chem. Soc*. **2001**, *123*, 7945-7946. (n) Nelson, S. G.; Zhu, C.; Shen, X. *J. Am. Chem. Soc.* **2004**, *126*, 14-15. (o) Wilson, J. E.; and Fu, G. C *Angew. Chem.* **2004**, *116*, 6518-6520. (p) Wilson, J. E.; Fu, G. C. *Angew. Chem., Int. Ed.* **2004**, *43*, 6358-6360. (q) Zhu, C.; Shen, X.; Nelson, S. G. *J. Am. Chem. Soc.* **2004**, *126*, 5352-5353. (r) Calter, M. A.; Tretyak, O. A.; Flascheriem.C. *Org. Lett*. **2005**, *7*, 1809-1812 (s) Gnanadesikan, V.; Corey, E. J. *Org. Lett*. **2006**, *8*, 4943-4945. (t) Lin, Y.; Boucau, J.; Li, Z.; Casarotto, V.; Lin, J.; Nguyen, A.N.; Ehrmantraut, J. *Org. Lett*. **2007**, *9*, 567-570.

75. Hirai, K.; Homma, H.; Mikoshiba, K. *Heterocycles* **1994**, *38*, 281-282.

76. Yang, H. W.; Romo, D. *J. Org. Chem.* **1998**, *63*, 1344-1347.

77. Wang, Y.; Zhao, C.; Romo, D. *Org. Lett.* **1999**, *1*, 1197-1199.

78. Zhao, C. A β-Lactone-Based Route to 1,2-Disubstituted Cyclopentanes. Mechanistic Studies of the Tandem Mukaiyama Aldol-Lactonization (TMAL) Reaction; Studies of the Zwitterionic Intermediate in the General Mukaiyama Aldol Reaction. Ph. D. Dissertation, Texas A&M University, College Station, TX, 1999.

79. Mitchell, T. A. Development of a Tandem, Three-Component Synthesis of Tetrahydrofurans *via* Silylated β-Lactone Intermediates in the Tandem Mukaiyama Aldol-Lactonization. Ph. D. Dissertation, Texas A&M University, College Station, TX, 2008.

80. Wang, Y. Development of New Syntheses and Transformations of β-Lactones: Application to a Concise Total Synthesis of (+)-Brefeldin A. Ph. D. Dissertation, Texas A&M University, College Station, TX, 2002.

81. (a) Schmitz, W. D.; Messerschmidt, N. B.; Romo, D. *J. Org. Chem.* **1998**, *63*, 2058-2059. (b) Wang, Y.; Romo, D. *Org. Lett.* **2002**, *4*, 3231-3234. (c) Merlic, C. A.; Doroh, B. C. *J. Org. Chem.* **2003**, *68*, 6056-6059. (d) Trost, B. M.; Papillon, J. P. N.; Nussbaumer, T. *J. Am. Chem. Soc.* **2005**, *127*, 17921-17937. (e) Yin, J.; Yang, X. B.; Chen, Z. X.; Zhang, Y. H. *Chinese Chem. Lett.* **2005**, *16*, 1448-1450. (f) Henry-Riyad, H.; Lee, C. S.; Purohit, V.; Romo, D*. Org. Lett.* **2006**, *8*, 4363-4366. (g) Purohit, V; Richardson, R. D.; Smith, J. W.; Romo *J. Org. Chem.* **2006**, *71*, 4549-4558. (h) Ma, G.; Zancanella, M.; Oyola, Y.; Richardson, R. D.; Smith, J. W.; Romo, D. *Org. Lett.* **2006**, *8*, 4497-4500. (i) Cho, S. W.; Romo, D. *Org. Lett.* **2007**, *9*, 1537-1540. (j) Richardson, R. D.; Ma, G.; Oyola, Y.; Zancanella, M.; Knowles, L. M.; Cieplak, P.; Romo, D.; Smith, J. W. *J. Med. Chem.* **2008**, *51*, 5285-5296. (k) Romo,

D.; Liu, G. *Org. Lett.* **2009**, *11*, 1143-1146. (l) Liu, G.; Romo, D. *Angew. Chem. Int. Ed.* **2011**, *50*, 7537-7540.

82. Southgate, R. *Contemp. Org. Synth.* **1994**, *1*, 417-431.

83. (a) Alcaide, B.; Almendros, P.; Aragoncillo, C. *Chem. Rev.* **2007**, *107*, 4437-4492.

    (b) Van der Steen, F. H.; Van Koten, G. *Tetrahedron* **1991**, *47*, 7503-7524.

84. Staudinger, H. *Justus Liebigs Ann. Chem*. **1907**, *356,* 51-23.

85. For reviews of β-lactone transformation see: (a) Wang, Y.; Tennyson, R.; Romo, D. *Heterocycles* **2004**, *64*, 605-685. (b) Mitchell, T. A.; Romo, D. *Heterocycles* **2005**, *66*, 627-637. (c) Purohit, V. C.; Matla, A. S.; Romo, D. *Heterocycles* **2008**, *76*, 949-979**.** For examples of β-lactone transformation developed in Romo group see (d) Zemribo, R.; Champ, M. S.; Romo, D. *Synlett* **1996**, 278-280. (e) Zhao, C.; Romo, D. *Tetrahedron Lett.* **1997**, *38*, 6537-6540. (f) Tennyson, R.; Romo, D. *J. Org. Chem.* **2000**, *65*, 7248-7252. (g) Yokota,Y.; Cortez, G. S.; Romo, D. *Tetrahedron* **2002**, *58*, 7075-7080. (h) Tennyson, R.; Cortez, G. C.; Galicia, H. J.; Kreiman, C. R.; Thompson, C. M.; Romo, D. *Org. Lett.* **2002**, *4*, 533-536. (i) Duffy, R. J.; Morris, K. A.; Romo, D. *J. Am. Chem. Soc.* **2005**, *127*, 16754-16755. (j) Zhang, W.; Romo, D. *J. Org. Chem.*, **2007**, *72*, 8939-8942. (k) Mitchell, T. A.; Romo, D. *J. Org. Chem.* **2007**, *72*, 9053-9059. (l) Zhang, W.; Matla, A. S.; Romo, D**.** *Org. Lett.* **2007**, *9*, 2111-2114. (m) Mitchell, T. A.; Zhao, C.; Romo, D. *Angew. Chem. Int. Ed.* **2008**, *47,* 5026-5029. (n) Mitchell, T. A.; Zhao, C.; Romo, D. *J. Org. Chem.* **2008**, *73*, 9544-9551. (o) Mitchell, T. A.; Zhao, C.; Romo, D. *Angew. Chem.* **2008**, *120,* 5104-5107. (p) Purohit, V. C.; Matla, A. S.; Romo, D. *J. Am. Chem. Soc.* **2008**, *130*,

10478-10479. (q) Duffy, R. J.; Morris, K.A.; Vallakati, R.; Zhang, W.; Romo, D. *J. Org. Chem*. **2009**, *74*, 4772-4781.

86. Miller, M. J. *Acc. Chem. Res*. **1986**, *19*, 49-56.

87. Yang, H. W.; Romo, D. *J. Org. Chem.* **1999**, *64*, 7657-7660.

88. Zhang, W.; Richardson, R. D.; Chamni, S.; Smith, J. W.; Romo, D. *Bioorg. Med. Chem. Lett.* **2008**, *18*, 2491-2494.

89. Huckin, S. N.; Weiler, L. *J. Am. Chem. Soc.* **1974**, *96*, 1082-1087.

90. Genêt, J. P.; Ratovelomanana-Vidil, V.; Caño de Andrade, M. C.; Pfister, X.; Guerreiro, P.; Lenoir, J. Y. *Tetrahedron Lett.* **1995**, *36*, 4801-4804.

91. Hattori, K.; Yamamoto, H. *J. Org. Chem.* **1993**, *58*, 5301-5303.

92. Evans, D. A.; Dart, M. J.; Duffy, J. L.; Yang, M. G. *J. Am. Chem. Soc.* **1996**, *118*, 4322-4343.

93. Mayol, L.; Piccialli, V.; Sica, D., *Tetrahedron Lett.* **1987**, *28*, 3601.

94. (a) L. Mayol, V. Piccialli and D. Sica *Tetrahedron* **1868**, *42*, 5369-5376. (b) L. Mayol, V. Piccialli and D. Sica *J. Nat. Prod.* **1986**, *49*, 823-828.

95. Rateb, M. E.; Houssen, W. E.; Schumacher, M.; Harrison, W. T.; Diederich, M.; Ebel, R.; Jaspars, M. *J. Nat. Prod.* **2009**, *72*, 1471-1476.

96. (a) Keyzers, R. A., Northcote, P. T., and Davies-Coleman, M. T. *Nat. Prod. Rep.*, **2006**, *23*, 321-334. (b) González, M. A. *Current Bioactive Compounds,* **2007**, *3*, 1-36.

97. Wynberg, H.; Staring, E. G. J. *J. Am. Chem. Soc.* **1982**, *104*, 166-168.

98. Tennyson, R.; Romo, D. *J. Org. Chem.* **2000**, *65*, 7248-7252.

99. Cortez, G. S.; Tennyson, R. L.; Romo, D. *J. Am. Chem. Soc.* **2001**, *123*, 7945-7946.

100. Oh, S. H.; Cortez, G. S.; Romo, D. *J. Org. Chem.* **2005**, *70*, 2835-2838.

101. Henry-Riyad, H.; Lee, C.; Purohit, V. C.; Romo, D. *Org. Lett.* **2006**, *8*, 4363-4366.

102. Cortez, G. S.; Oh, S. H.; Romo, D. *Synthesis*, **2001**, *11*, 1731-1736.

103. Morris, K. A.; Arendt, K. M.; Oh, S. H.; Romo, D. *Org. Lett.* **2010**, *12*, 3764-3767.

104. Leverett, C. A.; Purohit, V. C.; Romo, D. *Angew. Chem., Int. Ed.* **2010**, *49*, 9479-9483.

105. (a) Ma, G.; Nguyen, H.; Romo, D. *Org. Lett.* **2007**, *9*, 2143-2146. (b) Nguyen, H.; Ma, G.; Romo, D. *Chem. Comm.* **2010**, *46*, 4803-4805. (c) Nguyen, H.; Ma, G.; Fremgen,T.; Gladysheva, T.; Romo, D. *J. Org. Chem.* **2011**, *76*, 2-12.

106. Leverett, C. A.; Purohit, V. C.; Romo, D. *Angew. Chem., Int. Ed.* **2011**, *manuscript.*

107. Cho, S. Total Synthesis of β-Lactone Containing Natural Products; I. Total Synthesis of Belactosin C, II. Synthetic Studies Toward Spongiolactone. Ph. D. Dissertation, Texas A&M University, College Station, TX, 2008.

108. (a) Stork, G.; Danheiser, R. L. *J. Org. Chem.* **1973**, *38*, 1775-1776. (b) Kende, A. S.; Fludzinski, P. *Organic Syntheses*, **1986**, *64*, 68.

109. Ren, H.; Dunet, G.; Mayer, P.; Knochel, P. *J. Am. Chem. Soc.* **2007**, *129*, 5376-5377.

109. Birman, V. B.; Li, X. *Org. Lett.* **2008**, *10*, 1115-1118.

110. Zhang, Z.; Xie, F.; Jia, J.; Zhang, W. *J. Am. Chem. Soc.* **2010**, *132*, 15939-15941.

111. Wickham, G.; Young, D.; Kitching, W. *J. Org. Chem.* **1982**, *47*, 4884-4895.

112. Krasovskiy, A.; Malakhov, V.; Gavryushin, A.; Knochel, P. *Angew. Chem., Int. Ed.*
2006, *45*, 6040-6044.

113. Pearlman, W. M. *Tetrahedron Lett.,* **1967***,17*, 1663-1664.

114. Babu, S. A.; Yasuda, M.; Baba, A. *J. Org. Chem.* **2007**, *72*, 10264-10267.

115. Fleury, L. M.; Ashfeld, B. L. *Org. Lett.* **2009**, *11*, 5670-5673.

116. Breton, G.; Shugart, J.; Hughey, C.; Conrad, B.; Perala, S. *Molecules* **2001**, *6*, 655-
662.

APPENDIX A

EXPERIMENTAL AND SELECTED SPECTRAL DATA

General Methods

Reactions were carried out in flame-dried glassware and magnetically stirred under a nitrogen atmosphere, unless otherwise noted. Commercial solvents and reagents were used as received, unless otherwise stated. Anhydrous solvents were dried over neutral alumina and 4Å molecular sieves. Tetrahydrofuran (THF) was distilled immediately prior to use from sodium metal/benzophenone ketyl. Methanol (MeOH) was distilled from magnesium methoxide. Triethylamine (Et$_3$N), diisopropylamine (Hunig's base) were distilled from calcium hydride immediately prior to use. Zinc dust and Lithium chloride (LiCl) were dried by heating at 130 ^{o}C for 15 min under high vacuum prior to use. Brine refers to a saturated aqueous solution of sodium chloride. All reactions were monitored by thin layer chromatography (TLC) performed using glass-backed silica gel 60F254 (Merck, 250 μm thickness) and liquid chromatography-mass spectrometry (LC-MS) on a 3μ C18 column, 150 x 2.0 mm. Acetonitrile and water were used as mobile phase and no acid was added to the mobile phase, unless otherwise noted. Yields refer to chromatographically and spectroscopically pure compounds unless otherwise stated. Flash column chromatography was performed using 60Å silica gel (230-400 mesh) as a stationary phase as described by Still.[1] Preparative TLC was performed using glass-backed silica gel plate (60 Å, 20 x 20 cm, 250 μm, F254) and developed with indicated HPLC-grade solvents. Bands were identified by UV activity. Silica gel was scraped off the plate, and placed into a 15 mL test tube. The organic

[1] Still, W. C.; Kahn, M.; Mitra, A. *J. Org. Chem.* **1978**, *43*, 2923.

residue was extracted by suspending the silica gel in 5% methanol in ethyl acetate, filtering, and repeating three times. The combined organic solvents were filtered through a cotton plug in a pipette and a 0.45 μm nylon disc was used to remove fine particles of silica gel. Preparative HPLC was performed using a 3μ C18 column, 150 x 4.6 mm. Acetonitrile and water were used as mobile phase and no acid was added to the mobile phase, unless otherwise noted. All optical rotation measurements were made at 20 °C in a 10 millimeter cell (length); concentration (*c*) is reported in g/100mL. Infrared spectra were recorded with a Nicolet Impact 410 FTIR and a Bruker VERTEX 27 FTIR spectrometer. ^{1}H-NMR and ^{13}C-NMR spectra were recorded on a Unity Inova 500 and Inova 300 spectrometer. ^{1}H-NMR chemical shifts are reported as δ values in ppm relative to tetramethylsilane (TMS, 0.00 ppm) or residual CHCl$_3$ (7.27 ppm). ^{1}H-NMR coupling constants (*J*) are reported in Hertz (Hz), and multiplicities are indicated as follows: s (singlet), d (doublet), t (triplet), q (quartet), quint (quintet), m (multiplet), dd (doublet of doublets), ddd (doublet of doublet of doublets), dt (doublet of triplets), bs (broad singlet), apparent (app). Unless indicated otherwise, deuterochloroform (CDCl$_3$) served as an internal standard (77.3 ppm) for all ^{13}C spectra. Mass spectra were obtained on a VG analytical 70S high resolution, double focusing, sectored (EB) mass spectrometer at the center for Chemical Characterization and Analysis (Texas A&M). Enantiomeric excess (ee) was determined by normal phase chiral HPLC (Agilent chromatography) analysis using OD and IA columns (Chiralpak, Daicel Chemical Industries, LTD.) and HPLC grade hexanes and isopropanol were used as mobile phase and no acid/base was added to the mobile phase, unless otherwise noted. For tabulated

^{1}H and ^{13}C-NMR data of natural product derivatives, coupling constants (*J*) are shown after the multiplicity in parentheses. The natural product chemical shifts are highlighted in blue while the diazoacetate is highlighted in red. The numbering of carbons in natural products and derivatives was adopted from initial isolation papers. The following abbreviations are used in the experimental section: *p*-ABSA, 4-acetamidobenzenesulfonyl azide; DBU, 8-Diazabicyclo[5.4.0]undec-7-ene; DCC, dicyclohexylcarbodiimide; DMAP, *N,N*-4-dimethylaminopyridine; EDCI, 1-ethyl-3-(3-dimethylaminopropyl)carbodiimide; HTFB, hex-5-ynyl 2-diazo-4,4,4-trifluoro butanoate; HBPA, hexynyl-α-*p*-bromophenyl diazoacetate; DIAD, diisopropyl azodicarboxylate; HMPA, hexamethylphosphoramade.

Chapter II - Modulating Natural Product-Cellular Receptor Interactions: New Diazo Reagents with Small Steric Footprints for Simultaneous Arming and Structure-Activity Studies of Alcohol-Containing Natural Products

2A. Safety Hazards and Precautions for the Use of Diazoesters and Azides[2]

Diazoesters: Diazo compounds are known to be toxic and unstable towards strong protic and Lewis acids and can decompose by prolonged exposure to light and/or contact with metal salts. Even though diazoacetates are known to be more stable than their alkyl counterparts, throughout this study, all diazoesters were stored in the dark at

---

[2] Peddibhotla, S.; Dang, Y.; Liu, J. O.; Romo, D. *J. Am. Chem. Soc.* **2007**, *129*, 11222.

-10 °C in glass vials. Although during this work we did not experience any uncontrollable reactions with the diazo reagents prepared, we suggest that all reactions be carried out in a well-ventilated fume hood and behind a safety shield.

Azides: Due to the heat sensitive nature of azides, distillation or sublimation as purification techniques are not recommended. Column chromatography may contribute to decomposition, especially when using halogenated solvents. During our studies, reactions were conducted on medium scale (1-5 g) and no incidents were encountered with the compounds used. Extra caution must be taken to make certain that waste-containing azides should not come in contact with acid, which may cause the formation of highly toxic hydrogen azide (toxicity similar to that of hydrogen cyanide).

B) Synthesis of Diazo Reagents: 3a-3d

Synthesis of hex-5-ynyl 2-diazo-4,4,4-trifluorobutanoate (2.7a, HTFB)
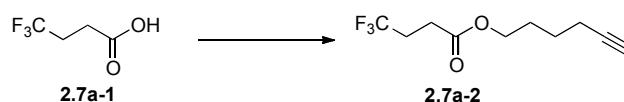
Hex-5-ynyl 4,4,4-trifluorobutanoate (2.7a-2). 4,4,4-trifluorobutanoic acid (**2.7a-1**) (3.40 g, 23.93 mmol) was dissolved in dry dichloromethane (100 mL) in a flame-dried flask under a nitrogen atmosphere. EDCI·HCl (6.88 g, 35.89 mmol) and DMAP (3.48 g, 28.72 mmol) were added and the mixture was stirred at ambient temperature (23 °C) for 10 min. 5-Hexyn-1-ol (3.63 mL, 30.50 mmol) was then slowly added dropwise. The mixture was stirred at ambient temperature for 2 h, and then

quenched with 1% HCl (50 mL). The organic layer was separated and the aqueous layer was extracted with dichloromethane (3 x 50 mL). The combined organic layers were washed with saturated $NaHCO_3$ (50 mL) and brine (50 mL), dried over anhydrous magnesium sulfate and concentrated under reduced pressure (rotary evaporator) to obtain a light yellow oil. The crude ester was purified by flash chromatography on SiO_2 (95:5 of hexanes:EtOAc) to afford hex-5-ynyl 4,4,4-trifluorobutanoate (**2.7a-2**) as a colorless oil (4.9 g, 92%); TLC (80:20, hexanes:EtOAc): R_f = 0.65; IR (thin film) cm^{-1}: 3307, 2113, 1741, 1137; ^{1}H-NMR (500 MHz, CDCl$_3$), δ 4.13 (t, J = 6.3 Hz, 2H), 2.57 (t, J = 8.3 Hz, 2H), 2.50-2.42 (m, 2H), 2.23 (dt, J = 7.1, 2.4 Hz, 2H), 1.96 (t, J = 2.4 Hz, 1H), 1.80-1.72 (m, 2H), 1.62-1.58 (m, 2H); ^{13}C-NMR (125 MHz, CDCl$_3$) δ 170.8, 126.5 (q, J = 273.8 Hz, CF_3), 83.6, 68.8, 64.6, 29.0 (q, J = 30 Hz, CH_2CF_3), 27.4, 26.9 (q, J = 2.5 Hz, CH_2CH_2), 24.8, 18.0; HRMS (ESI+) Calcd for $C_{10}H_{13}F_3O_2Li[M+Li]$: 229.1028, Found: 229.1030.
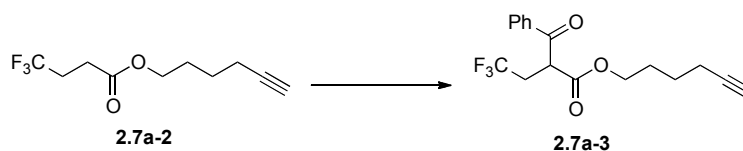
Hex-5-ynyl 2-benzoyl-4,4,4-trifluorobutanoate (2.7a-3). hex-5-ynyl 4,4,4-trifluoro butanoate (**2.7a-2**) (6.0 g, 27.00 mmol) was dissolved in dry acetonitrile (100 mL) in a flame-dried flask under a nitrogen atmosphere. Benzoyl chloride (9.5 mL, 81.81 mmol) and triethylamine (22.50 mL, 161.57 mmol) were added at ambient temperature (23 °C). The mixture was then cooled to 0 °C and stirred for 10 min. Titanium tetrachloride (≥98.0%, Fluka; 5 mL, 45.60 mmol) was slowly added over 30

min via a syringe pump. The brown reaction mixture was warmed to ambient temperature for 15 min, and then heated to reflux at 90 °C for 30 min. Then, the mixture was cooled to ambient temperature, quenched with water and extracted with EtOAc (3 x 50 mL). The combined organic extracts were washed with brine (2 x 50 mL), dried over anhydrous magnesium sulfate and concentrated under reduced pressure (rotary evaporator) to afford a light brown oil. The crude keto-ester was purified by flash chromatography on SiO$_2$ (95:5 of hexanes:EtOAc) to afford hex-5-ynyl 2-benzoyl-4,4,4-trifluorobutanoate (**2.7a-3**) as a yellow oil (7.9 g, 90%) that exists as a mixture of keto/enol forms; TLC (80:20, hexanes:EtOAc): R_f = 0.60; IR (thin film) cm^{-1}: 3304, 3064, 1791, 1744; ^{1}H-NMR (500 MHz, CDCl$_3$) δ 8.17-8.15 (m, 1H), 8.03-8.01 (m, 1H), 7.67-7.61 (m, 1H), 7.54-7.49 (m, 2H), 4.67 (t, J = 6.7 Hz, 1H), 4.12 (t, J = 6.7 Hz, 2H), 2.97-2.89 (m, 2H), 2.10 (dt, J = 2.4, 6.8 Hz, 2H,), 1.92 (t, J = 2.7 Hz, 1H), 1.68-1.62 (m, 2H), 1.43-1.37 (m, 2H); ^{13}C-NMR (125 MHz, CDCl$_3$) δ 192.2, 167.5(enol), 162.2(keto), 153.1, 134.4, 134.0, 130.4, 127.5 (q, J = 210 Hz, CF_3), 128.8, 128.2, 83.4, 68.8, 65.6, 47.7, 32.7 (q, J = 31.3 Hz, CH_2CF_3), 27.1, 24.4, 17.7; HRMS (ESI+) Calcd for C$_{17}$H$_{17}$F$_3$O$_3$Li [M+Li]: 333.1290, Found: 333.1292.
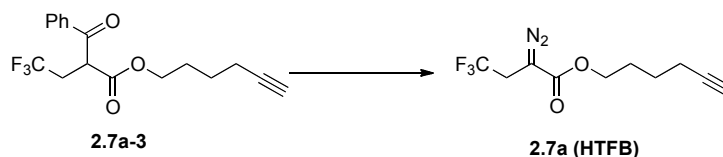
Hex-5-ynyl 2-diazo-4,4,4-trifluorobutanoate (2.7a, HTFB). Hex-5-ynyl 2-benzoyl-4,4,4-trifluorobutanoate (**2.7a-3**) (1.65 g, 5.06 mmol) was weighed into a flame-dried flask and dissolved in dry acetonitrile (50 mL). The reaction mixture was cooled at

0 °C under a nitrogen atmosphere. *p*-ABSA (3.65 g, 15.18 mmol) was added into the reaction mixture followed by DBU (2.27 mL, 15.18 mmol). The mixture was slowly warmed up to ambient temperature (23 °C). The reaction flask was covered by aluminum foil and stirred at ambient temperature for 4 h. After all the starting material was consumed as observed by TLC, all the volatiles were evaporated under reduced pressure (rotary evaporator). The residue was purified by flash chromatography (95:5 of hexanes:EtOAc) and the hex-5-ynyl 2-diazo-4,4,4-trifluorobutanoate (**2.7a**, HTFB) was obtained as a yellow oil (0.73 g, 58%); TLC (80:20, hexanes:EtOAc): R_f = 0.53; IR (thin film) cm^{-1}: 3313, 2096, 1699, 1137; ^{1}H-NMR (500 MHz, CDCl$_3$), δ 4.23 (t, J = 6.8 Hz, 2H), 3.13 (q, J = 16.0 Hz, 2H), 2.26-2.20 (dt, J = 2.5, 6.7 Hz, 2H), 1.96 (t, J = 2.8 Hz, 1H), 1.84-1.74 (m, 2H), 1.64-1.54 (m, 2H); ^{13}C-NMR (125 MHz, CDCl$_3$) δ 165.9, 125.1 (q, J = 271.3 Hz, CF_3), 83.9, 69.1, 65.3, 29.3 (q, J = 58.6 Hz, CH_2CF_3), 28.0, 25.1, 18.3 (C=N$_2$ signal not observed); ^{19}F NMR (300 MHz, CDCl$_3$), δ 67.31 (3F, broad s); HRMS (ESI+) Calcd for C$_{10}$H$_{11}$F$_3$O$_2$N$_2$Li [M+Li]: 255.0933, Found: 255.0919.

Synthesis of hex-5-ynyl 2-diazo-3,3,3-trifluoropropanoate (2.7b)
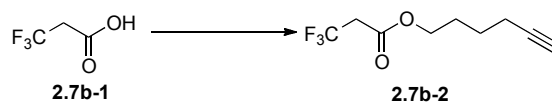
Hex-5-ynyl 3,3,3-trifluoropropanoate (2.7b-2). 3,3,3-trifluoropropanoic acid (**2.7b-1**) (0.50 g, 3.92 mmol) was dissolved in dry dichloromethane (25 mL) in a flame-dried flask under a nitrogen atmosphere. EDCI·HCl (1.13 g, 5.88 mmol) and DMAP
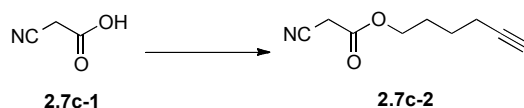
(0.57 g, 4.71 mmol) were added and the mixture was stirred at ambient temperature (23 °C) for 10 min. 5-Hexyn-1-ol (0.6 mL, 5.49 mmol) was then slowly added dropwise. The mixture was stirred at ambient temperature for 4 h, and then quenched with 1% HCl (20 mL). The organic layer was separated and the aqueous layer was extracted with dichloromethane (3 x 50 mL). The combined organic layers were washed with saturated NaHCO$_3$ (20 mL) and brine (20 mL), dried over anhydrous magnesium sulfate and concentrated under reduced pressure (rotary evaporator) to give a light yellow oil. The crude ester was purified by flash chromatography on SiO$_2$ (95:5 of hexanes:EtOAc) to afford hex-5-ynyl 3,3,3-trifluoropropanoate (**2.7b-2**) as a colorless oil (0.67 g, 83%); TLC (80:20, hexanes:EtOAc): R_f = 0.53; IR (thin film) cm^{-1}: 3313, 2117, 1752, 1217; ^{1}H-NMR (500 MHz, CDCl$_3$), δ 4.20 (t, J = 6.7 Hz, 2H), 3.17 (q, J = 10.0 Hz, 2H), 2.24 (dt, J = 2.7, 7.0 Hz, 2H), 1.95 (t, J = 2.7 Hz, 1H), 1.84-1.74 (m, 2H), 1.64-1.54 (m, 2H); ^{13}C-NMR (125 MHz, CDCl$_3$) δ 165.8, 129.4 (q, J = 176.3 Hz, CF_3), 83.8, 68.9, 64.5, 29.1 (q, J = 61.3 Hz, CH_2CF_3), 27.8, 24.9, 18.1; HRMS (ESI+) Calcd for C$_9$H$_{11}$F$_3$O$_2$Li [M+Li]: 215.0871, Found: 215.0867.

Hex-5-ynyl 2-diazo-3,3,3-trifluoropropanoate (2.7b). Hex-5-ynyl 3,3,3-trifluoro propanoate (**2.7b-3**) (0.67 g, 3.23 mmol) was weighed into a flame-dried flask and dissolved in dry acetonitrile (30 mL). The reaction mixture was cooled at 0 °C under nitrogen atmosphere. *p*-ABSA (3.65 g, 15.18 mmol) and DBU (2.27 mL, 15.18 mmol)

were added. The reaction flask was covered by aluminum foil and gradually warmed up to ambient temperature (23 °C) for 2 h. After all the starting material was consumed as observed by TLC, all the volatiles were evaporated under reduced pressure (rotary evaporator) and the crude product was determined by ^{1}H-NMR. However, the desired diazo reagent decomposed during attempted purification by flash chromatography on SiO_2.

Synthesis of hex-5-ynyl 2-cyano-2-diazoacetate (2.7c)

2.7c-1   **2.7c-2**

Hex-5-yn-1-yl 2-cyanoacetate (2.7c-2). 2-cyanoacetic acid (**2.7c-1**) (1.30 g, 15.52 mmol) was dissolved in dry dichloromethane (100 mL) in a flame-dried flask under a nitrogen atmosphere. DCC (3.20 g, 15.52 mmol) was added as a solid and the mixture was stirred at ambient temperature (23 °C) for 10 min. 5-Hexyn-1-ol (0.6 mL, 5.49 mmol) was slowly added dropwise and the mixture was stirred at ambient temperature for 1 h. The reaction was then quenched with 1% HCl (20 mL) and filtered to remove solids. The organic layer was separated and the aqueous layer was extracted with dichloromethane (3 x 50 mL). The combined organic layers were washed with saturated $NaHCO_3$ (50 mL) and brine (50 mL), dried over anhydrous magnesium sulfate and concentrated under reduced pressure (rotary evaporator) to give a red oil. The crude ester was purified by flash chromatography on SiO_2 (90:10 of hexanes:EtOAc) to afford

hex-5-yn-1-yl 2-cyanoacetate (**2.7c-2**) as an orange oil (2.31 g, 90%); TLC (80:20, hexanes:EtOAc): R_f = 0.33; IR (thin film) cm^{-1}: 3305, 2226, 1750, 1154; ^{1}H-NMR (500 MHz, CDCl$_3$), δ 4.23 (t, J = 6.7, 2H), 3.46 (s, 2H), 2.24 (dt, J = 2.7, 7.1 Hz, 2H), 1.96 (t, J = 2.7 Hz, 1H), 1.84-1.79 (m, 2H), 1.75-1.63 (m, 2H); ^{13}C-NMR (125 MHz, CDCl$_3$) δ 162.9, 113.0, 83.4, 68.9, 66.2, 27.1, 24.6, 24.4, 17.8; HRMS (ESI+) Calcd for C$_9$H$_{11}$NO$_2$Li [M+Li]: 172.0905, Found: 172.0921.
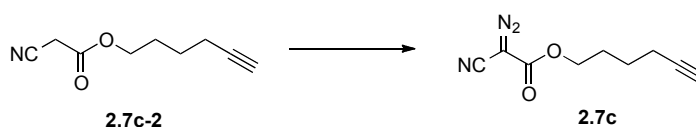
Hex-5-ynyl 2-cyano-2-diazoacetate (2.7c). Hex-5-yn-1-yl 2-cyanoacetate (**2.7c-2**) (1.42 g, 8.60 mmol) was weighed into a flame-dried flask and dissolved in dry acetonitrile (50 mL). Imidazole-1-sulfonyl azide hydrochloride that was freshly prepared by Goddard-Borger's protocol[3] (2.16 g, 10.32 mmol) was added into the reaction mixture at ambient temperature (23 °C) under a nitrogen atmosphere. Pyridine (3.5 mL, 43.0 mmol) was then slowly added and the reaction mixture was stirred at 40 °C for 24 h. After all the starting material was consumed as observed by TLC, the mixture was diluted with EtOAc (50 mL), washed with 1N HCl (50 mL) and brine (50 mL), dried over anhydrous magnesium sulfate and concentrated under reduced pressure (rotary evaporator) to give a yellow residue. The crude product was purified by flash chromatography on SiO$_2$ (80:20 of hexanes:EtOAc) and the diazoacetate **2.7c** was obtained as a yellow oil (0.79 g, 48 %); TLC (80:20, hexanes:EtOAc): R_f = 0.47; IR (thin

---

[3] Goddard-Borger, E. D.; Stick, R. V. *Org. Lett.*, **2007**, *9*, 3797.

film) cm^{-1}: 3292, 2226, 2125, 1720; ^{1}H-NMR (500 MHz, CDCl$_3$), δ 4.26 (t, J = 6.5, 2H),

2.20 (dt, J = 2.4, 7.1 Hz, 2H), 1.94 (t, J = 2.7 Hz, 1H), 1.82-1.76 (m, 2H), 1.59-1.53 (m,

2H); ^{13}C-NMR (125 MHz, CDCl$_3$) δ 161.3, 107.2, 83.3, 68.9, 66.6, 27.3, 24.6, 17.8

(C=N$_2$ signal not observed); HRMS (ESI+) Calcd for C$_9$H$_9$N$_3$O$_2$Li [M+Li]: 198.0855,

Found: 198.0867.

Synthesis of hex-5-ynyl 2-(4-azidophenyl)-2-diazoacetate (2.7d)
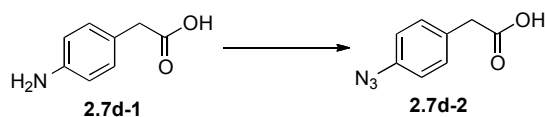
2-(4-azidophenyl)acetic acid (2.7d-2). 2-(4-azidophenyl)acetic acid (**2.7d-2**)

was prepared by the procedure reported by Knaus.[4] 2-(4-aminophenyl)acetic acid (**2.7d-**

1) (2.0 g, 13.23 mmol) was dissolved in a concentrated hydrochloric acid (20.0 mL) at 0

°C. An aqueous solution of NaNO$_2$ (0.92 g, 13.34 mmol; in water 70 mL) was slowly

added over 15 min by an addition funnel. The reaction mixture was stirred at 0 °C for 20

min. An aqueous solution of NaN$_3$ (8.6 g, 132.28 mmol; in water 200 mL) was then

slowly added over a period of 15 min by an addition funnel. The reaction mixture was

then slowly warm to ambient temperature (23 °C). After 30 min, the mixture was

partitioned with EtOAc. The organic layer was separated and the aqueous layer was

extracted with EtOAc (3 x 20 mL). The combined organic layers were dried over

anhydrous magnesium sulfate and concentrated by rotary evaporator to obtain 2-(4-

---

[4] Rao, P.; Uddin, J.; Knaus, E. E. *J. Med. Chem.* **2004**, *47*, 3972.

azidophenyl)acetic acid (**2.7d-2**) as a light yellow-brown crystal (2.30 g, 99%). The material was of sufficient purity to be carried directly to the next step. TLC (50:50, hexanes:EtOAc): R_f = 0.45; IR (thin film) cm^{-1}: 2123, 1696, 1507, 1320; ^{1}H-NMR (500 MHz, CDCl$_3$), δ 7.28-7.24 (d, J = 8.7 Hz, 2H), 7.00-6.93 (d, J = 8.7 Hz, 2H), 3.63 (s, 2H); ^{13}C-NMR (125 MHz, CDCl$_3$) δ 177.6, 139.3, 130.8 (2), 129.8, 119.2 (2), 40.2; HRMS (ESI–) Calcd for C$_8$H$_6$N$_3$O$_2$[M-H]: 176.0460, Found: 176.0468.
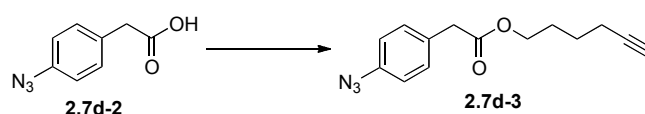
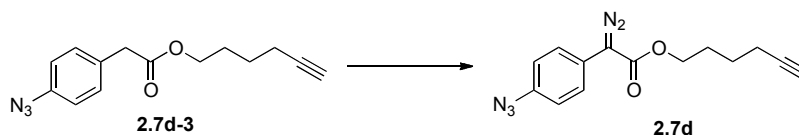**Hex-5-yn-1-yl 2-(4-azidophenyl)acetate (2.7d-3).** 2-(4-azidophenyl)acetic acid (**2.7d-2**) (2.30 g, 12.95 mmol) was dissolved in dry dichloromethane (100 mL) in a flame-dried flask and stirred at ambient temperature (23 °C) under a nitrogen atmosphere. Oxalyl chloride (1.70 mL, 19.42 mmol) was slowly added, followed by DMF (0.2 mL, 2.59 mmol). The reaction mixture was stirred at ambient temperature for 4 h. All volatiles were evaporated under reduced pressure (rotary evaporator). The crude acid chloride was dissolved again in dichloromethane (100 mL) and stirred at ambient temperature. 5-Hexyn-1-ol was added into the reaction followed by Et$_3$N (2.15 mL, 15.54 mmol) and DMAP (0.32 g, 2.59 mmol). The reaction mixture was stirred at ambient temperature for 12 h. The mixture was then quenched with saturated NH$_4$Cl (50 mL) and extracted with dichloromethane (3 x 50 mL). The combined organic layers were washed with water, dried over anhydrous sodium sulfate and concentrated under reduced pressure (rotary evaporator). The crude ester was purified by flash

chromatography on SiO$_2$ (95:5 of hexanes:EtOAc) to afford hex-5-yn-1-yl 2-(4-azidophenyl)acetate (**2.7d-3**) as a light yellow oil (2.48 g, 74%); TLC (90:10, hexanes:EtOAc): R_f = 0.40; IR (thin film) cm^{-1}: 3298, 2117, 1735, 1607; ^{1}H-NMR (500 MHz, CDCl$_3$), δ 7.27-7.25 (d, J = 4 Hz, 2H), 6.99-6.97 (d, J = 8.3 Hz, 2H), 4.11 (t, J = 6.7, 2H), 3.60 (s, 2H), 2.22-2.19 (dt, J = 2.4, 7.0 Hz, 2H), 1.96 (t, J = 2.7 Hz, 1H), 1.77-1.72 (m, 2H) 1.58-1.52 (m, 2H); ^{13}C-NMR (125 MHz, CDCl$_3$) δ 171.4, 138.9, 130.7 (2), 130.6, 119.1 (2), 83.8, 68.7, 64.4, 40.7, 27.5, 24.8, 17.9; HRMS (ESI+) Calcd for C$_{14}$H$_{16}$N$_3$O$_2$ [M+H]: 258.1243, Found: 258.1251.

2.7d-3   **2.7d**

Hex-5-ynyl 2-(4-azidophenyl)-2-diazoacetate (2.7d). Hex-5-yn-1-yl 2-(4-azido phenyl)acetate (**2.7d-3**) (0.44 g, 1.71 mmol) was weighed into a flame-dried flask and dissolved in dry acetonitrile (15 mL). The reaction mixture was stirred at ambient temperature (23 °C) under a nitrogen atmosphere. *p*-ABSA (1.23 g, 5.13 mmol) was then added followed by slow addition of DBU (1.53 mL, 10.26 mmol). The reaction flask was covered by aluminum foil and stirred at ambient temperature for 30 min. After all the starting material was consumed as observed by TLC, all volatiles were evaporated under reduced pressure (rotary evaporator). The residue was purified by flash chromatography on SiO$_2$ (99:1of hexanes:EtOAc) and the diazoacetate **2.7d** was obtained as a yellow oil (0.33 g, 68%): TLC (90:10, hexanes:EtOAc): R_f = 0.63; IR (thin film) cm^{-1}: 3307, 2125, 2075, 1702; ^{1}H-NMR (500 MHz, CDCl$_3$), δ 7.45-7.43 (d, J = 8.8

Hz, 2H), 7.03-7.02 (d, J = 8.8 Hz, 2H), 4.28 (t, J = 6.7, 2H), 2.26-2.22 (dt, J = 2.4, 6.7 Hz, 2H), 1.96 (t, J = 2.7 Hz, 1H), 1.85-1.79 (m, 2H) 1.64-1.59 (m, 2H); ^{13}C-NMR (125 MHz, CDCl$_3$) δ 165.0, 137.5, 125.2 (2), 121.9, 119.6 (2), 83.7, 68.8, 64.5, 27.7, 24.7, 18.0 (C=N$_2$ signal not observed). HRMS (ESI+) Calcd for C$_{14}$H$_{13}$N$_5$O$_2$Li [M+Li]: 290.1229, Found: 290.1252.

(C) General Procedure for O-H Insertion with Gibberellic Acid Methyl Ester (2.3)

Gibberellic acid methyl ester[5] (20 mg, 0.055 mmol) and rhodium catalyst (0.0028 mmol, 0.05 equiv) were weighed into a flame-dried, round-bottomed flask. The solids were suspended in dry dichloromethane (3 mL) and stirred at ambient temperature (23 °C) under a nitrogen atmosphere (Note: some rhodium catalyst did not dissolve). A solution of HTFB diazo reagent **2.7a** (0.165 mmol, 3 equiv,) in dry dichloromethane (1 mL) was prepared and slowly added via a syringe pump over a 1 h period. The reaction mixture was stirred at ambient temperature for 1 h. The solvent was then evaporated under reduced pressure (rotary evaporator), and the residue was purified by preparative TLC (60:40 of hexanes:EtOAc) to afford ethers **2.8a-d**, **2.9a-d** and recovered gibberellic acid methyl ester.

---

[5] Gibberellic acid methyl ester was prepared by a similar procedure as previously described (ref. 1).
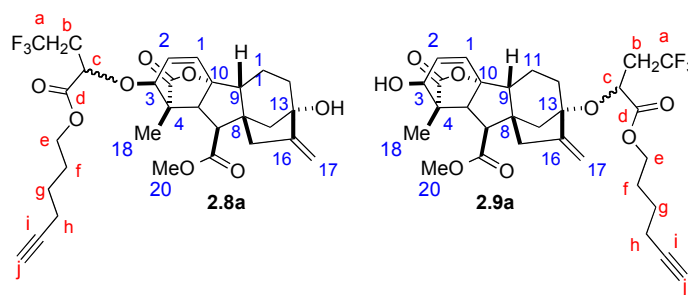
TLC (60:40, hexanes: EtOAc): R_f = 0.40 (**2.8a**) and 0.33 (**2.9a**); HRMS (ESI+)

Calcd for $C_{30}H_{35}F_3O_8Li$ [M+Li]: 587.2444, Found: 587.2456.

Table A-1. ^{1}H-NMR (500 MHz, CDCl$_3$) of **2.8a** and **2.9a**.

Carbon Number	Gibberellic acid methyl ester (**2.3**)[6]	**2.8a**	**2.9a**
1	6.35 (d, 9)	6.40 & 6.39 (d, 9.3)	6.31 & 6.29 (d, 9.3)
2	5.91 (dd, 9, 3.5)	6.00, 5.98 (dd, 3.4,	5.91, 5.87 (dd, 3.3, 9.3)
3	4.16 (d, 3)	4.02 & 4.01(d, 3.4)	-
5	2.80 (d, 10.5)	3.32 & 3.30 (d, 10.7)	3.20 & 3.18 (d, 10.7)
6	3.21 (d, 10.5)	2.76 & 2.74 (d, 10.7)	2.78 & 2.76 (d, 10.3)
17	5.28 & 4.97 (broad s)	5.26 & 4.95 (broad s)	5.21 & 5.03 (broad s)
18	1.25 (s)	1.25, 1.24 (s)	1.24 (s)
20	3.74 (s)	3.72 (s)	3.74 (s)
-----------	HTFB (**2.7a**)	-------------	-------------
a	-	-	-
b	3.13 (q, 16.0)	2.63-2.57 (m)	2.57-2.49 (m)
c	-	4.16-4.12 (m)	4.15-4.11 (m)
d	-	-	-
e	4.23 (t, 6.8)	4.20 (t, 6.9)	4.20 (t, 6.9)

---

[6] Preiss, Adam, G.; Samon, D.; Budesinky, M. *Magn. Reson. Chem.* **1987**, *25*, 239.

**Table A-1.** ^{1}H-NMR (500 MHz, CDCl$_3$) of **2.8a** and **2.9a** (continued).

Carbon Number	Gibberellic acid methyl ester (**2.3**)	**2.8a**	**2.9a**
f	1.84-1.74 (m)	-	-
g	1.64-1.54 (m)	-	-
h	2.26-2.20 (dt, 2.5, 6.7)	2.69-2.54 (m)	2.58-2.49 (m)
i	-	-	-
j	1.96 (t, 2.8)	1.95 (t, 3.0)	1.97 (t, 3.0)

Table A-2. ^{13}C-NMR (125 MHz, CDCl$_3$) of **2.8a** and **2.9a**.

Carbon Number	Gibberellic acid methyl ester (**2.3**)	**2.8a**	**2.9a**
1	132.4	127.6	132.4
2	133.3	134.4	132.7
3	70.0	70.6	67.5
4	53.4	53.4 & 53.0	53.3
5	53.7	53.8	52.7
6	51.3	53.3	50.4
7	172.3	172.19	172.3
8	50.7	50.2	43.4
9	50.9	50.7	50.5
10	90.7	90.5 & 90.3	90.3 & 90.2
11	17.3	17.0	17.0
12	38.5	38.0	29.6
13	78.2	78.2	84.9 & 85.1
14	45.0	44.9	39.0
15	43.3	43.1	36.7

Table A-2. ^{13}C-NMR (125 MHz, CDCl$_3$) of **2.8a** and **2.9a** (continued).

Carbon Number	HTFB (2.7a)	2.8a	2.9a
16	157.1	156.9	152.1 & 151.6
17	108.0	107.5	110.2 & 109.7
18	14.0	14.5	14.3 & 14.0
19	178.3	177.8	178.2
20	52.4	52.1	52.2
--------------	HTFB (2.7a)	-----------------	-------------------
a	125.1 (q, 271.3)	125.1 (q,	127.2 (q, 298.8)
b	29.3 (q, 58.6)	29.3 (q, 58.6)	38.2 (q, 13.8)
c	-	74.7	69.2
d	165.9	169.60	171.2
e	65.3	65.5	65.0
f	28.0	27.4	27.3
g	25.1	24.7	24.5
h	18.3	18.0	17.9
i	83.9	83.4	83.5
j	68.8	69.1	68.9
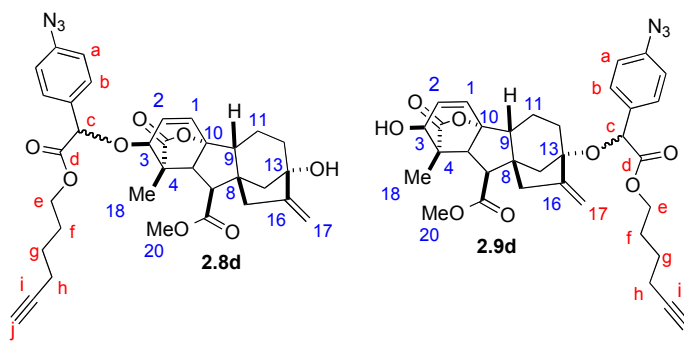
TLC (60:40, hexanes:EtOAc): R_f = 0.31 (**2.8d**) and 0.25 (**2.9d**); HRMS (ESI–)

Calcd for $C_{34}H_{36}N_3O_8$ [M-H]: 614.2502, Found: 614.2530.

Table A-3. ^{1}H-NMR (500 MHz, CDCl$_3$) of **2.8d** and **2.9d**.

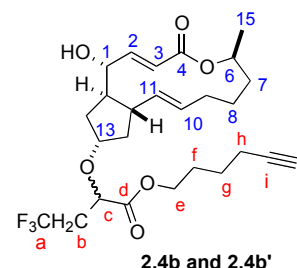| Carbon Number	Gibberellic acid methyl ester (**2.3**)	**2.8d**	**2.9d**
1	6.35 (d, 9)	6.35 & 6.33 (d, 9.8)	6.33 & 6.31 (d, 10.9)
2	5.91 (dd, 9, 3.5)	5.92, 5.90 (dd, 3.6,	6.15, 6.13 (dd, 3.7, 9.7)
3	4.16 (d, 3)	3.74 & 3.73 (d, 3.9)	3.95 & 3.91 (d, 3.4)
5	2.8 (d, 10.5)	3.41 & 3.38 (d, 10.9)	3.40 & 3.38 (d, 10.9)
6	3.21 (d, 10.5)	3.23 & 2.21 (d, 10.7)	3.23 & 2.21 (d, 10.7)
17	5.28 & 4.97 (broad s)	5.27 & 4.96 (broad s)	5.00 & 4.98 (broad s)
18	1.25 (s)	1.24 (s)	1.27 (s)
20	3.74 (s)	3.68 (s)	3.68 (s)
-----------	**2.7d**	-------------------------	-------------------------
a	7.45-7.43 (d, 8.8)	7.43-7.41 (d, 8.8)	7.43-7.41 (d, 8.8)
b	7.03-7.02 (d, 8.8)	7.04-7.02 (d, 7.8)	7.04-7.02 (d, 7.8)
c	-	5.01 (s)	5.01 (s)
e	4.28 (t, 6.7)	4.13 (t, 6.8)	4.13 (t, 6.8)
f	2.26-2.22	-	-

Table A-3. ^{1}H-NMR (500 MHz, CDCl$_3$) of **2.8d** and **2.9d** (continued).

Carbon Number	Gibberellic acid methyl ester (**2.3**)	**2.8d**	**2.9d**
g	1.64-1.59 (m)	-	-
h	1.85-1.79 (m)	2.80-2.72 (m)	2.80-2.72 (m)
j	1.96 (t, 2.7)	1.95 (t, J = 2.9)	1.95 (t, J = 2.9)

This reaction provided a mixture of chemosite isomers and diastereomers.

D) Synthesis of Natural Product/HTFB Ethers; 2.4b-2.15b and Tabulated ^{1}H and ^{13}C-NMR Data

Brefeldin A 13-HTFB ether, 2.4b/2.4′. Brefeldin A
(**2.4a**) (4.8 mg, 0.017 mmol) and rhodium acetate dimer (0.38
mg, 5 mol%) were weighed into a flame-dried, round-bottomed
flask under a nitrogen atmosphere and the solids were
dissolved in CH$_2$Cl$_2$ (1 mL). Then, a solution of hex-5-ynyl 4,4,4-trifluorobutanoate
(HTFB, **2.7a**) (12.8 mg, 0. 051 mmol) in 1 mL of CH$_2$Cl$_2$ was slowly added via a syringe
pump over a 1 h period. After that, the mixture was allowed to stir at ambient
temperature (23 °C) for an additional 1 h. The solvent was evaporated and the residue
was purified by preparative TLC on SiO$_2$ (50:50 of hexanes:EtOAc) to afford 4.9 mg of
diastereomers **2.4b**, **2.4b'** (57% yield) and 1.1 mg of recovered brefeldin A (23% yield).
The 1:1 mixture of diasteromers was further separated by preparative TLC on SiO$_2$
(60:40 of hexanes:EtOAc) to obtain 2.8 mg of **2.4b** and 2.1 mg of **2.4b'**; TLC (60:40 of

hexanes:EtOAc): R_f = 0.41 (**2.4b**) and 0.49 (**2.4b'**); HRMS (ESI+) Calcd for

$C_{26}H_{35}O_6F_3Li$ [M+Li]: 507.2546, Found: 507.2557.

Table A-4. ^{1}H-NMR (500 MHz, $CDCl_3$) of **2.4b** and **2.4b'**.

Carbon Number	Brefeldin A (**2.4a**)[7]	**2.4b**	**2.4b'**
1	4.10 (d, 10)	4.06 (d, 10)	4.08 (d, 10)
2	7.34 (dd, 15.5, 3)	7.34 (dd, 2, 16)	7.35 (dd, 3, 15.5)
3	5.84 (dd, 15.5, 2)	5.91, 5.88 (dd, 2.5, 16)	5.92, 5.89 (dd, 2.0, 16)
6	4.74-4.83 (m)	4.87-4.81 (m)	4.88-4.82 (m)
10	5.60-5.70 (m)	5.72-5.66 (m)	5.73-5.67 (m)
11	5.24 (dd, 15, 10)	5.25-5.22 (dd, 10, 15)	5.28-5.25 (dd, 10, 14.5)
13	4.23 (m)	4.00 (m)	4.03 (m)
15	1.22 (d, 6.5)	-	-
----------	HTFB (**2.7a**)	----------------------------	----------------------------
a	-	-	-
b	3.13 (q, 16.0)	2.60-2.46 (m)	2.64-2.48 (m)
c	-	4.36 (q, 5.0)	4.37 (q, 5.0)
e	4.23 (t, 6.8)	4.22-4.18 (m)	4.22-4.18 (m)
f	1.84-1.74 (m)	1.83-1.79 (m)	1.86-1.79 (m)
g	1.64-1.54 (m)	1.65-1.61 (m)	1.66-1.60 (m)
h	2.26-2.20 (dt, 2.5, 6.7)	2.26-2.22 (dt, 2.4, 6.8)	2.26-2.23 (dt, 3.0, 7.0)
j	1.96 (t, 2.8)	1.97 (t, 2.4)	1.97 (t, 2.2)

[7] (a) Glaser, R.; Shiftan D.; Froimowitz, M. *Magn. Reson. Chem.* **2000**, *38*, 274. (b) Wang, Y.; Romo, D. *Org. Lett.* **2002**, *4*, 3231. (c) Argade, A. B.; Devraj, R.; Vroman, J. A.; Haugwitz, R. D.; Hollingshead, M.; Cushman, M. *J. Med. Chem.* **1998**, 41, 3337.

Table A-5. ^{13}C-NMR (125 MHz, CDCl$_3$) of **2.4b** and **2.4b'**.

Carbon Number	Brefeldin A (2.4a)	2.4b	2.4b'
1	76.0	Overlap with solvent peak	Overlap with solvent peak
2	151.5	151.5	151.3
3	117.6	117.8	117.6
4	166.5	166.2	165.9
6	71.8	71.7	71.8
7	34.1	34.2	34.0
8	26.7	27.7, 26.9	27.5, 26.7
9	31.8	32.0	31.8
10	130.5	131.1 & 130.8	130.6
11	136.5	136.2	136.1
11a	44.3	39.5	40.5
12	43.2	38.8	37.1
13	72.6	76.1	75.9
14	41.3	44.1	43.9
14a	52.0	51.9	51.8
15	20.9	20.9	20.9
----------	HTFB (2.7a)	--------------------------	--------------------------
a	125.1 (q, 271.3)	Low intensity	Low intensity
b	29.3 (q, 58.6)	37.5 (q, 28.8)	37.1 (q, 31.3)
c	-	80.62	80.3
d	165.9	171.1	171.19
e	65.3	65.3	65.1
f	28.0	29.9	29.7
g	25.1	25.0	24.8
h	18.3	18.2	18.0

Table A-5. ^{13}C-NMR (125 MHz, CDCl$_3$) of **2.4b** and **2.4b'** (continued).

Carbon Number	Brefeldin A (2.4a)	2.4b	2.4b'
i	83.9	84.9	84.7
j	68.8	69.1	68.9

Paclitaxel 2′-HTFB ether, 2.11b/2.11b′. Paclitaxel (**2.11a**) (5.7 mg, 0.0067 mmol) and rhodium acetate dimer (0.15 mg, 5 mol%) were weighed into a flame-dried, round-bottomed flask under a nitrogen atmosphere and the solids were dissolved in CH$_2$Cl$_2$ (1 mL). Then, a solution

2.11b/2.11b'
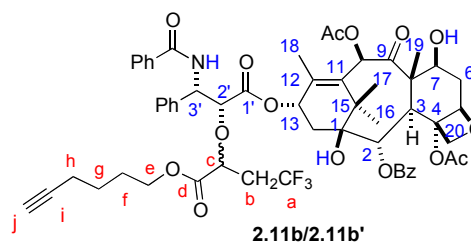
of hex-5-ynyl 4,4,4-trifluorobutanoate (HTFB, **2.7a**) (6.7 mg, 0.040 mmol) in 1 mL of CH$_2$Cl$_2$ was slowly added via a syringe pump over a 2 h period. The mixture was then allowed to stir at ambient temperature (23 °C) for an additional 1 h. The solvent was evaporated and the residue was purified by preparative TLC on SiO$_2$ (50:50 of hexanes:EtOAc) to afford 5.3 mg of a 5:1 mixture of diastereomers **2.11b/2.11b′** (49% yield) and 1.1 mg of paclitaxel (20% yield) was recovered. TLC (90:10, CH$_2$Cl$_2$:acetone): R_f = 0.31; HRMS (MALDI) Calcd for C$_{26}$H$_{35}$O$_6$F$_3$K [M+K]: 1112.3652, Found: 1112.3616.

Table A-6. ^{1}H-NMR (500 MHz, CDCl$_3$) and ^{13}C-NMR (125 MHz, CDCl$_3$) of **2.11b**.

Carbon Number	^{1}H-NMR data Palitaxol (**2.11a**)	^{1}H-NMR data **2.11b** (mixture of diastereomers)	^{13}C-NMR data Palitaxol	^{13}C-NMR data **2.11b** (mixture of diastereomers)
NH	6.99 (d, 9)	7.15 (d, 10)	-	-
NHBz	-	-	167.0	167.0
1	-	-	79.0	79.2
2	5.67 (d, 7)	5.67 (d, 7)	74.9	75.0
3	3.80 (d, 7)	3.79 (d, 7.5)	45.6	45.5
4	-	-	81.1	81.0
4-OAc	-	-	170.3	169.1
4-OAc	-	-	22.6	22.8
5	4.94 (dd, 2, 9.5)	4.96 (dd, 1.5, 10.0)	84.4	84.4
6	-	-	35.6	35.5
7	4.40 (ddd, 4, 7, 11)	4.43 (broad t, 9)	72.2	71.7
8	-	-	58.6	58.5
9			203.6	203.7
10	6.27 (s)	6.28 (s)	75.5	76.5
10-OAc	-	-	171.3	170.1
10-OAc	-	-	20.8	20.8
11	-	-	133.1	133.7
12	-	-	142.0	142.5
13	6.23 (dt, 1, 9)	6.26 (broad t, 10)	72.3	72.1
14	-	-	35.7	35.7
15	-	-	43.2	43.2
16	-	-	26.9	26.8
17	-	-	21.8	22.3

Table A-6. ^{1}H-NMR (500 MHz, CDCl$_3$) and ^{13}C-NMR (125 MHz, CDCl$_3$) of **2.11b** (continued).

Carbon Number	^{1}H-NMR data Palitaxol (**2.11a**)	^{1}H-NMR data **2.11b** (mixture of diastereomers)	^{13}C-NMR data Palitaxol	^{13}C-NMR data **2.11b** (mixture of diastereomers)
18	-	-	14.8	14.86 & 14.13
19	-	-	9.5	9.6
20	-	-	76.5	76.7
20a	4.30 (d, 8.5)	4.30 (d, 8.5)	-	-
20b	4.19 (d, 8.5)	4.20 (d, 8.5)	-	-
1'	-	-	172.7	171.3
2'	4.79 (dd, 5.5, 3)	4.71 (d, 3)	73.2	74.0
2' OH	3.55 (d, 5.5)	-	-	-
3'	5.79 (dd, 9, 2.5)	5.80 (dd, 1.0, 8)	55.0	54.5
----------	HTFB (**2.7a**)	------------------	HTFB (**2.7a**)	--------------------
a	-	-	125.1 (q, 271.3)	Low intensity
b	3.13 (q, 16.0)	2.58-2.51 (m)	29.3 (q,	29.5 (q, 42.5)
c	-	4.04-4.01 (m)	-	81.4
d	-	-	165.9	169.1
e	4.23 (t, 6.8)	4.16 (t, 6.5)	65.3	65.7
f	1.84-1.74 (m)	Overlap	28.0	27.3
g	1.64-1.54 (m)	Overlap	25.1	24.6
h	2.26-2.20	Overlap	18.3	17.9
i	-	Overlap	83.9	83.5
j	1.96 (t, 2.8)	Overlap	68.8	69.0

Ephedrine 2-HTFB ether, 2.12b/2.12b′. To a solution of hex-5-ynyl 4,4,4-trifluorobutanoate (HTFB, **2.7a**) (135.1 mg, 0.54 mmol) in CH_2Cl_2 (1 mL) was added (–)-Ephedrine **2.12a** (30 mg, 0.182 mmol) and stirred at ambient temperature (23 °C) under a nitrogen atmosphere. Then, rhodium acetate (40.0 mg, 50 mol%) was immediately added. The mixture was allowed to stir at ambient temperature for 1 h. The solvent was evaporated and the residue was purified by preparative TLC on SiO_2 (60:40 of hexanes: EtOAc) to afford 34.2 mg (49% yield) of N–H insertion (**2.12b/2.12b′**) as a 1:1 diastereomeric mixture and 7.5 mg of (–)-Ephedrine (25% yield) was recovered. Bis-derivatization derived from both N–H and O–H insertion was observed by LC-MS (~15%). TLC (50:50, hexanes:EtOAc): R_f = 0.56; HRMS (ESI+) Calcd for $C_{20}H_{27}F_3NO_3$ [M+H]: 386.1943, Found: 386.1940.
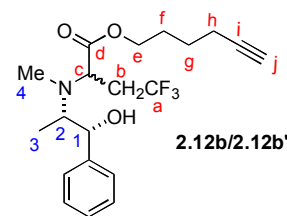
Table A-7. ^{1}H-NMR 500 MHz, $CDCl_3$) and ^{13}C-NMR (125 MHz, $CDCl_3$) of **2.12b**.

Carbon Number	^{1}H-NMR data Ephedrine (**2.12a**)	^{1}H-NMR data **2.12b** (mixture of diastereomers)	^{13}C-NMR data Ephedrine (**2.12**)	^{13}C-NMR data **2.12b** (mixture of diastereomers)
1	4.66-4.7 (m)	4.47-4.45 (dd, 3,7)	73.1	74.9 & 74.5
1-OH	-	4.81 (broad s)	-	-
2	2.66-2.77 (m)	4.27-4.25 (t, 6)	60.4	61.5 & 61.0
3	0.79 (d, 7)	0.84 (d, 6)	14.1	11.5 & 11.4
4	2.39 (broad s)	2.52 (broad s)	33.9	34.5 & 34.0

Table A-7. ^{1}H-NMR 500 MHz, CDCl$_3$) and ^{13}C-NMR (125 MHz, CDCl$_3$) of **2.12b** (continued).

Carbon Number	^{1}H-NMR data Ephedrine (**2.12a**)	^{1}H-NMR data **2.12b** (mixture of diastereomers)	^{13}C-NMR data Ephedrine (**2.12**)	^{13}C-NMR data **2.12b** (mixture of diastereomers)
1-phenyl	7.23-7.30 (4H, m)	7.33-7.33 (4H, m)	141.7, 127.0, 128.0, 126.1	141.8 &141.6, 127.0 & 126.9 128.0 (2), 126.1 (2)
---------	HTFB (**2.7a**)	------------------	HTFB (**2.7a**)	------------------
a	-	-	125.1 (q, 271.3)	129.2 (q, 455.0)
b	3.13 (q, 16.0)	3.12 (q, 10)	29.3 (q, 58.6)	29.6 (q, 33.1)
c	-	2.85 (m)	-	60.3 (2)
d	-	-	165.9	172.3
e	4.23 (t, 6.8)	4.24-4.21 (t, 7)	65.3	64.7 & 64.5
f	1.84-1.74 (m)	1.85-1.76 (m)	28.0	27.8 (2)
g	1.64-1.54 (m)	1.64-1.56 (m)	25.1	24.9 & 24.7
h	2.26-2.20 (dt, 2.5, 6.7)	2.25-2.21 (dt, 3, 5)	18.3	18.0 & 17.8
i	-	-	83.9	83.5
j	1.96 (t, 2.8)	1.96 (t, 3)	68.8	68.5

FK506 32-HTFB Ether, 2.13b/2.13′. FK506 (**2.13a**) (5 mg, 0.0062 mmol) and rhodium acetate (0.15 mg, 5 mol%) were weighed into a flame-dried, round-bottomed flask under a nitrogen atmosphere and the solids were dissolved in CH$_2$Cl$_2$ (1 mL). A solution of hex-5-ynyl 4,4,4-trifluorobutanoate (HTFB, **2.7a**) (9.3 mg, 0.037 mmol) in 1 mL of CH$_2$Cl$_2$ was slowly added via a syringe pump over a 2 h period. The mixture was allowed to stir at ambient temperature (23 °C) for 1 h. The solvent was evaporated and

the residue was purified by preparative TLC on SiO_2 (50:50, hexanes:EtOAc) to afford 4.4 mg of a 7:1 mixture of diastereomers **2.13b** (major diastereomer) and **2.13b′**(minor diastereomer) (64% yield) and 0.85 mg of recovered FK506 (17% yield). The 7:1 mixture of diasteromers were further separated by preparative TLC (60:40 %v/v of hexanes:EtOAc) to obtain a single diastereomer: R_f = 0.43 (**2.13b**) and 0.53 (**2.13b′**); HRMS (MALDI) Calcd for $C_{54}H_{81}F_3NO_{14}$ [M+H]: 1024.5609, Found: 1024.5616.
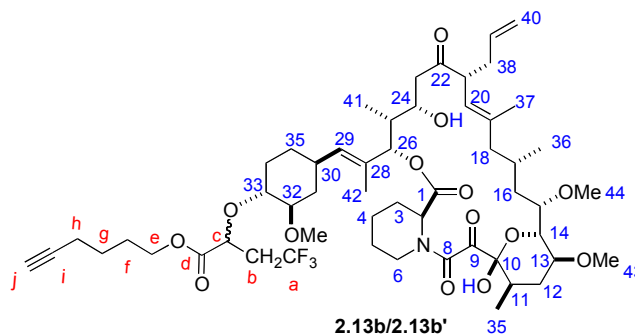
Table A-8. ^{1}H-NMR (500 MHz, CDCl$_3$) and ^{13}C-NMR (125 MHz, CDCl$_3$) of **2.13b**.

Carbon Number	^{1}H-NMR data FK506[8] (**2.13a**) (mixture of rotamers)	^{1}H-NMR data **2.13b** (mixture rotamers)	^{13}C-NMR data FK506 (**2.13a**) (mixture of rotamers)	^{13}C-NMR data **2.13b** (mixture of rotamers)
1	-	-	169.0 & 168.7	169.0 & 168.7
2	4.62 & 5.0 (d, 5)	4.61 & 5.0 (d, 5)	56.5 & 52.7	56.3 & 52.7
3	-	-	27.6 & 26.2	27.5 & 26.2
4	1.28 & 1.69 (m)	Overlap	21.1 & 20.8	21.1 & 22.7
5	-	-	24.5	24.6 & 24.5

[8] Tanaka, H.; Kuroda, A.; Marusawa, H.; Hatanaka, H.; Kino, T.; Goto, T.; Hashimoto, M. *J. Am. Chem. Soc.* **1987**, *109*, 5031. Karuso, P.; Kesseler, H.; Mierke, D. F. *J. Am. Chem. Soc.* **1990**, *112*, 9434. Mierke, D. F.; Schmieder, P.; Karuso, P.; Kessler, H. *Helv. Chim. Acta* **1991**, *74*, 1027.

Table A-8. ^{1}H-NMR (500 MHz, CDCl$_3$) and ^{13}C-NMR (125 MHz, CDCl$_3$) of **2.13b** (continued).

Carbon Number	^{1}H-NMR data FK506 (**2.13a**) (mixture of rotamers)	^{1}H-NMR data **2.13b** (mixture rotamers)	^{13}C-NMR data FK506 (**2.13a**) (mixture of rotamers)	^{13}C-NMR data **2.13b** (mixture of rotamers)
6	4.43 & 3.73 (d, 13)	4.42 & 3.76 (d, 10)	43.8 & 39.2	43.9 & 39.2
8	-	-	165.8 & 164.6	164.6
9	-	-	196.1 & 192.6	196.1 & 192.6
10	-	-	98.6 & 97.0	98.6 & 97.0
11	-	-	34.5 & 33.6	34.3 & 33.6
12	-	-	32.6 & 32.5	32.7 & 32.5
13	3.33 (m)	3.37 (m)	73.5	73.6
14	3.68 (d, 10) 3.85-3.98 (m)	3.59 (dd, 3, 10.5) & 3.89	72.7 & 72.2	73.6 & 73.5
15	3.52-3.60 (m)	3.49-3.43 (m)	76.5 & 75.1	72.4 & 72.1
16	-	-	32.9 & 35.4	32.9 & 35.4
17	-	-	26.2	26.2 & 26.0
18	-	-	48.5 & 48.3	48.5 & 48.4
19	-	-	138.9 & 139.8	139.8 & 138.9
20	4.93 & 4.94 (m)	4.98-5.06 (m)	122.6 & 122.4	122.6 & 122.4
21	3.30 & 3.33 (m)	3.35 (m)	52.9 & 52.7	52.8 & 52.7
22	-	-	212.7 & 212.6	212.8 & 212.6
23	2.1 & 2.7 (m)	2.79 & 2.76 (d, 2.5)	43.8 & 43.2	43.8 & 43.1
24	3.85-3.98 (m)	3.88-3.95 (m)	70.0 & 68.9	70.2 & 68.9
25	-	-	40.3 & 39.8	40.3 & 39.8
26	5.32 & 5.19 (d, 2.0)	5.31 & 5.18 (d, 2.0)	77.8 & 77.1	77.8 & overlap with solvent

Table A-8. ^{1}H-NMR (500 MHz, CDCl$_3$) and ^{13}C-NMR (125 MHz, CDCl$_3$) of **2.13b** (continued).

Carbon Number	^{1}H-NMR data FK506 (**2.13a**) (mixture of rotamers)	^{1}H-NMR data **2.13b** (mixture rotamers)	^{13}C-NMR data FK506 (**2.13a**) (mixture of rotamers)	^{13}C-NMR data **2.13b** (mixture of rotamers)
27	-	-	132.4 & 131.7	132.5 & 131.9
28	4.9-5.2 (m)	4.98-5.06 (m)	129.7 & 129.6	129.5 & 129.4
29	-	-	34.9 & 34.8	35.4 & 35.3
30	-	-	34.8 & 34.7	34.6 & 34.3
31	2.97 (m)	3.17-3.12 (dt, 5.0, 10.0)	84.1	83.2 & 83.1
32	3.35 (broad s)	-	73.6	74.2
33	-	-	31.2 & 31.1	31.9 & 30.7
34	-	-	30.6 (2)	30.0
35	0.89 & 0.93	1.0-0.82 (m)	16.2 & 16.0	16.2
36	0.72 & 0.86	1.0-0.82 (m)	20.4 & 19.4	20.4 & 19.4
37	1.52 & 1.55	1.62 &1.60 (broad s)	15.9 & 15.7	16.0 & 15.8
38	-	-	35.5 & 35.1	85.1 & 35.6
39	5.7 (m)	5.76-5.65 (m)	135.5 & 135.3	135.5 & 135.3
40	4.90-5.20 (m)	4.89-5.06 (m)	116.7	116.7
41	-	-	9.8 & 9.5	9.8 & 9.5
42	1.55 & 1.59	1.64 & 1.63 (broad s)	14.2 & 14.1	14.3 & 14.1
43	3.33 & 3.34	3.39 & 3.38 (broad s)	56.3 & 56.1	56.1 & 55.9
44	3.24 & 3.30	3.29 & 3.25 (broad s)	57.5 & 56.9	57.6 & 57.0
45	3.35	3.33 (broad s)	56.6	56.6
---------	**HTFB (2.7a)**	-------------------	**HTFB (2.7a)**	----------------

Table A-8. ^{1}H-NMR (500 MHz, CDCl$_3$) and ^{13}C-NMR (125 MHz, CDCl$_3$) of **2.13b** (continued).

Carbon Number	HTFB (2.7a)	^{1}H-NMR data 2.13b (mixture rotamers)	HTFB (2.7a)	^{13}C-NMR data 2.13b (mixture of rotamers)
a	-	-	125.1 (q, 271.3)	125.6 (q, 275.0)
b	3.13 (q, 16.0)	3.05-2.98 (m)	29.3 (q, 58.6)	29.4 (q, 21,3)
c	-	4.22-4.15 (m)	-	-
d	-	-	165.9	171.0
e	4.23 (t, 6.8)	4.44 (t, 6.0)	65.3	64.7
f	1.84-1.74 (m)	1.82-1.79	28.0	29.4
g	1.64-1.54 (m)	Overlap	25.1	24.8
h	2.26-2.20 (dt, 2.5, 6.7)	2.26-2.23 (dt, 3, 6.5)	18.3	18.0
i	-	-	83.9	83.6
j	1.96 (t, 2.8)	Overlap	68.8	68.8

Lactimidomycin-HTFB ether (2.14b and 2.14b′). Lactimidomycin (**2.14a**) (1.8 mg, 0.0039 mmol) and rhodium acetate (0.10 mg, 5 mol%) was weighted into a flame-dried, round-bottomed flask under a nitrogen atmosphere and the solids were

2.14b and 2.14b'

dissolved in CH$_2$Cl$_2$ (1 mL). Then, a solution of hex-5-ynyl 4,4,4-trifluorobutanoate (HTFB, **2.7a**) (12.0 mg, 0.047 mmol) in 1 mL of CH$_2$Cl$_2$ was slowly added via a syringe pump over a 1 h period. The mixture was allowed to stir at ambient temperature (23 °C)
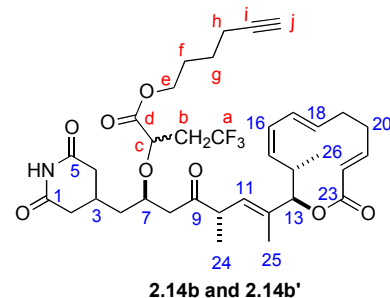
for 1 h. The residue was purified by reverse phase preparative HPLC using Gamini-NX 3μ C18 110A column, 150 x 4.6 mm (gradient 5→30% CH_3CN: H_2O, PDA 168-220 nm) to afford 0.4 mg of a 1:1 mixture of diastereomers **2.14b** and **2.14b′** (15% yield). Each diastereomer was separated and a small amount of unreacted lactimidomycin was recovered. LRMS (MALDI) Calcd for $C_{36}H_{48}F_3NO_8$ [M+H]: 678.3254, Found: 678.3058.
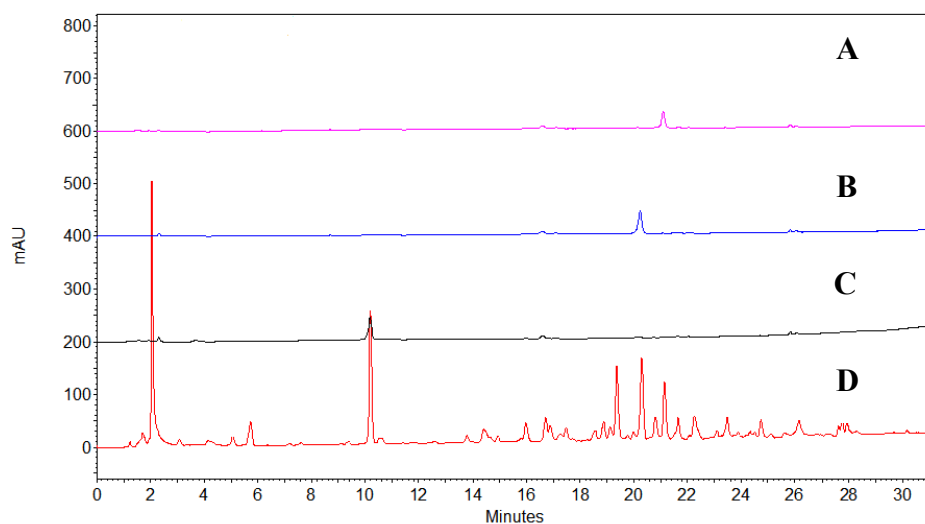
Figure A-1. Preparative HPLC chromatogram for purification of lactimidomycin/HTFB (**2.14a**, **2.14b** and **2.14b′**). (A) purified **2.14b**, (B) purified **2.14b′**, (C) purified lactimidomycin (**2.14a)**, (D) crude reaction mixtures.
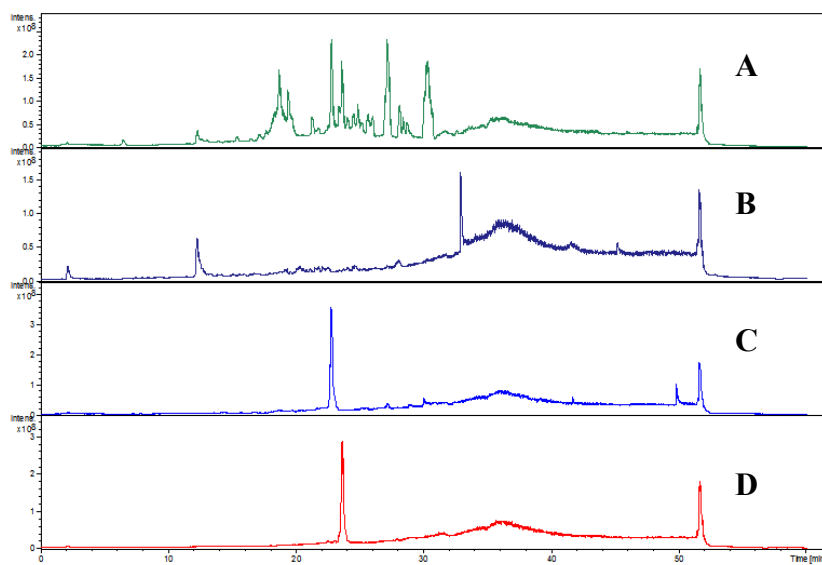
Figure A-2. Total ion count LC/MS chromatogram (positive mode) for purification of lactimidomycin/HTFB (**2.14b** and **2.14b′**). (A) crude reaction mixtures, (B) lactimidomycin (**2.14a**), (C) purified **2.14b′**, (D) purified **2.14**.
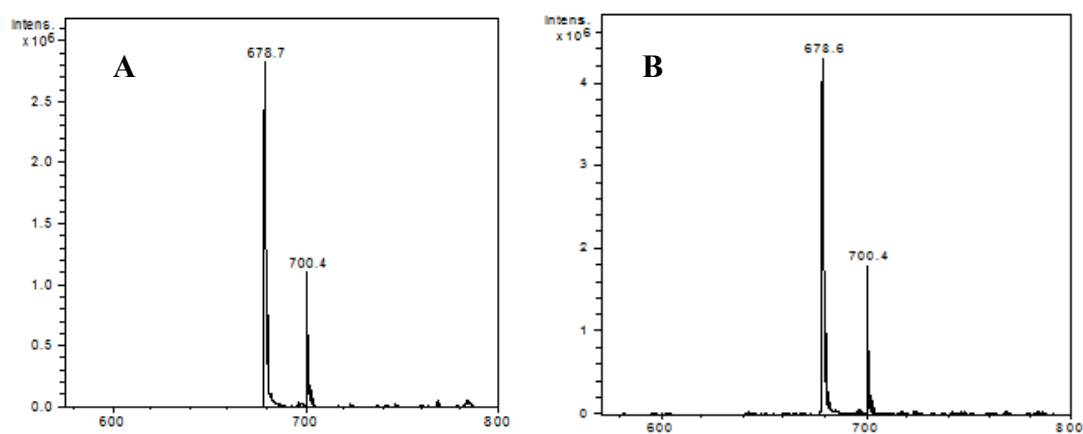
Figure A-3. LC/MS profiles (positive mode) of purified **12b** (A) and purified **2.14b′** (B).

Table A-9. ^{1}H-NMR (500 MHz, CDCl$_3$) and ^{13}C-NMR (125 MHz, CDCl$_3$) of **2.14b′** and **2.14b**.

Carbon Number	^{1}H-NMR data Lactimidomycin (**2.14a**)[9]	^{1}H-NMR data of **2.14b**	^{1}H-NMR data of **2.14b′**
2	5.53 (d, 16.0)	5.56 (d, 15.0)	5.56 (d, 16.0)
3	6.49 (ddd, 16.0, 10.0, 5.0)	6.45 (m)	6.43 (m)
6	5.42 (m)	5.43 (m)	5.42 (m)
7	5.72 (dd, 15.5, 10.5)	5.70 (dd, 16.0, 10.0)	5.70 (dd, 16.0, 10.0)
8	6.06 (t, 11.0)	6.08 (t, 10.0)	5.98 (t, 10.0)
9	5.06 (t, 11.0)	5.10 (t, 10.0)	5.10 (t, 10.0)
10	3.11 (m)	3.10 (m)	3.10 (m)
11	5.34 (m, overlap)	5.37 (m)	5.38 (m)
13	5.34 (m, overlap)	5.37 (m)	5.38 (m)
14	3.44 (m)	3.38 (m)	Overlap with other
16	2.59 (2H, m)	2.57 (2H, m)	2.57 (2H, m)
17	4.12 (m)	4.18 (m)	4.10 (m)
------------	**HTFB (2.7a)**	-----------------------	-----------------------
c	-	4.80 (dd, 3.5, 8.5)	4.72 (dd, 4.0, 8.5)
e	4.23 (t, 6.8)	4.22 (t, 6.8)	4.23 (t, 6.8)
h	2.26-2.20 (dt, 2.5, 6.7)	2.27 (m)	2.27 (m)

Only diagnostic protons that are clearly analyzed by ^{1}H-NMR are included.

[9] Koko, S., Yuji, N., Soichiro, t., Nobujiro, K., Masami, H., Toshio, M., Yosuke, S., Hideo, K., Masataka, K., and Toshikazu, O. *J. Antibiot.* **1992**, *45*, 1433. Ju, J., Seo, J.-W., Her, Y., Lim, S.-K., and Shen, B. *Org. Lett.* **2007**, *9*, 5183.

Fumagillol 6-HTFB ether, 2.15b/2.15′. Fumagillol

(2.15a) (13.2 mg, 0.047 mmol) and rhodium acetate (1.0 mg,

5 mol%) were weighed into a flame-dried, round-bottomed

flask under a nitrogen atmosphere and the solids were

dissolved in CH_2Cl_2 (3 mL). A solution of hex-5-ynyl 4,4,4-

trifluorobutanoate (HTFB, **2.7a**) (34.98 mg, 0.141 mmol) in 2 mL of CH_2Cl_2 was slowly

added via a syringe pump over a 1 h period. The mixture was allowed to stir at ambient

temperature (23 °C) for 1 h. The solvent was evaporated and the residue was purified by

preparative TLC on SiO_2 (70:30, hexanes:EtOAc) to afford 14.7 mg of a 7:1 mixture of

diastereomers **2.15b/2.15′** (63% yield) and 2.8 mg of recovered Fumagillol (21% yield).

TLC (70:30, hexanes:EtOAc): R_f = 0.49; HRMS (MALDI): Calcd for $C_{26}H_{37}O_6F_3Na$

[M+Na] = 525.2440 m/z, Found [M+Na] = 525.2456 m/z.
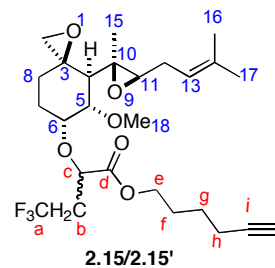
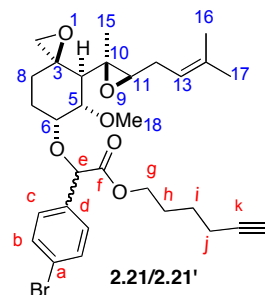**Table A-10.** ^{1}H-NMR (500 MHz, CDCl$_3$) and ^{13}C-NMR (125 MHz, CDCl$_3$) of **2.15b**.

Carbon Number	^{1}H-NMR data Fumagillol (2.15a)[10]	^{1}H-NMR data of 2.15b (mixture of diastereomers)	^{13}C-NMR data Fumagillol (2.15a)	^{13}C-NMR data of 2.15b (mixture of diastereomers)
1	-	-	-	-
2	2.93 & 2.52 (d, 4.3)	2.98 & 2.54 (d, 4.5)	50.7	50.9
3	-	-	58.5	58.4
4	1.91 (d, 11.1)	1.71 (m)	47.0	47.1
5	3.61 (dd, 2.7, 11.1)	3.57 (dd, 2.5, 11.0)	80.9	81.2

[10] Hanson, F. R.; Elbe, T. E. *J. Bacteriol.* **1949**, *58*, 527. Elbe, T. E.; Hanson, F. R. *Antibiot. Chemother.* **1951**, *1*, 54.

Table A-10. ^{1}H-NMR (500 MHz, CDCl$_3$) and ^{13}C-NMR (125 MHz, CDCl$_3$) of **2.15b** (continued).

Carbon Number	^{1}H-NMR data Fumagillol (**2.15a**)	^{1}H-NMR data of **2.15b** (mixture of diastereomers)	^{13}C-NMR data Fumagillol (**2.15a**)	^{13}C-NMR data of **2.15b** (mixture of diastereomers)
6	4.35 (m)	4.33 (dd, 3.5, 9.0)	64.0	64.9
7	1.99 (m) & 1.75 (tdd, 13.9, 2.6,	2.13 (m) & 1.79 (m)	26.5	25.7
8	2.19 (dt, 4.5, 13.6) & 0.96	2.18 (m)	28.5	28.9
9	-	-	-	-
10	-	-	59.8	59.8
11	2.57 (t, 6.5)	2.62 (t, 5.0)	61.2	60.6
12	2.41-2.30 (m) & 2.21-2.09 (m)	2.40-2.35 (m) & 2.20-2.12 (m)	27.3	27.4
13	5.19 (tm, 7.4)	5.22 (tm, 7.0)	118.5	118.8
14	-	-	134.9	134.7
15	1.21 (s)	1.21 (s)	18.0	17.0
16	1.64 (s)	1.67 (s)	13.9	14.2
17	1.73 (s)	1.77 (s)	25.7	25.7
18	3.48 (s)	3.45 (s) & 3.43 (s)	56.5	56.7
----------	**HTFB (3a)**	----------------------	**HTFB (3a)**	-------------------
a	-	-	125.1 (q, 271.3)	124.5 (q, 110.25)
b	3.13 (q, 16.0)	2.60-2.57 (m)	29.3 (q, 58.6)	37.6 (q, 56.3)
c	-	4.19 (t, 6.5) & 4.17 (t, 6.5)	-	-
d	-	-	165.9	170.3
e	4.23 (t, 6.8)	4.24 (m)	65.3	72.9
f	1.84-1.74 (m)	1.84-1.79 (m)	28.0	29.7

Table A-10. ^{1}H-NMR (500 MHz, CDCl$_3$) and ^{13}C-NMR (125 MHz, CDCl$_3$) of **2.15b** (continued).

Carbon Number	^{1}H-NMR data Fumagillol (**2.15a**)	^{1}H-NMR data of **2.15b** (mixture of diastereomers)	^{13}C-NMR data Fumagillol (**2.15a**)	^{13}C-NMR data of **2.15b** (mixture of diastereomers)
g	1.64-1.54 (m)	1.65-1.60 (m)	25.1	24.8
h	2.26-2.20 (dt, 2.5, 6.7)	2.29-2.25 (dt, 3.0, 7.0)	18.3	18.0
i	-	-	83.9	83.7
j	1.96 (t, 2.8)	1.99 (t, 3.0)	68.8	68.8

Fumagillol 6-HBPA ether, 2.21/2.21′. Fumagillol (**2.15a**) (19.2 mg, 0.068 mmol) and rhodium acetate (1.5 mg, 5 mol%) were weighed into a flame-dried, round-bottomed flask under a nitrogen atmosphere and the solids were dissolved in CH$_2$Cl$_2$ (3 mL). A solution of hex-5-yn-1-yl 2-(4-bromophenyl)-2-diazoacetate (HBPA, **2.1**) (65.93 mg, 0.204 mmol) in 2 mL of CH$_2$Cl$_2$ was slowly added via a syringe pump over a 1 h period. The mixture was allowed to stir at ambient temperature (23 °C) for 1 h. The solvent was evaporated and the residue was purified by preparative TLC on SiO$_2$ (70:30, hexanes:EtOAc) to afford 22.8 mg of a 5:1 mixture of diastereomers **2.21/2.21′** (58% yield) and 5.7 mg of recovered Fumagillol (30% yield). TLC (70:30, hexanes:EtOAc): R_f = 0.47; HRMS (MALDI): Calcd for C$_{30}$H$_{39}$O$_6$BrNa [M+Na] = 597.1821 m/z, Found [M+Na] = 597.1806 m/z.

Table A-11. ^{1}H-NMR (500 MHz, CDCl₃) and ^{13}C-NMR (125 MHz, CDCl₃) of **2.21**.

Carbon Number	^{1}H-NMR data Fumagillol (**2.15a**)	^{1}H-NMR data **2.21** (mixture of diastereomers)	^{13}C-NMR data Fumagillol (**2.15a**)	^{13}C-NMR data **2.21** (mixture of diastereomers)
1	-	-	-	-
2	2.93 & 2.52 (d, 4.3)	2.95 & 2.52 (d, 4.0)	50.7	50.9 & 50.8
3	-	-	58.5	58.5 & 58.4
4	1.91 (d, 11.1)	2.19 (d, 11.0)	47.0	47.6 & 47.5
5	3.61 (dd, 2.7, 11.1)	3.57 (dd, 2.3, 11.0)	80.9	82.0 & 81.9
6	4.35 (m)	4.18 (m) & 4.13 (m)	64.0	70.9 & 68.8
7	1.99 (m) & 1.75 (tdd, 13.9, 2.6, 4.5)	2.16-2.11(m) & 1.91-1.88 (m)	26.5	26.5 & 26.2
8	2.19 (dt, 4.5, 13.6) & 0.96 (ddd, 2.5, 4.5, 13.6)	2.18-2.16 (m) & 2.16-2.11(m)	28.5	29.2
9	-	-	-	-
10	-	-	59.8	59.9
11	2.57 (t, 6.5)	2.59 (t, 6.5)	61.2	60.7
12	2.41-2.30 (m) & 2.21-2.09 (m)	2.36-2.30 (m) & 2.28-2.24 (m)	27.3	27.4 & 27.3
13	5.19 (tm, 7.4)	5.20 (tm, 7.5)	118.5	118.7 & 118.6
14	-	-	134.9	134.7
15	1.21 (s)	1.19 (s) & 1.18 (s)	18.0	18.0 & 17.9
16	1.64 (s)	1.64 (s) & 1.63 (s)	13.9	14.2 & 14.1
17	1.73 (s)	1.73 (s) & 1.72 (s)	25.7	25.7
18	3.48 (s)	3.45 (s) & 3.36 (s)	56.5	56.9 & 56.7
----------	HBPA (**2.1**)	-----------------------	HBPA (**2.1**)	------------------

Table A-11. ^{1}H-NMR (500 MHz, CDCl$_3$) and ^{13}C-NMR (125 MHz, CDCl$_3$) of **2.21**(continued).

Carbon Number	HBPA (**2.1**)	^{1}H-NMR data **2.21** (mixture of diastereomers)	HBPA (**2.1**)	^{13}C-NMR data **2.21** (mixture of diastereomers)
a	-	-	119.6	122.5 & 122.4
b	7.50 (d, 9)	7.48 (d, 8.5) & 7.45 (d, 8.5)	125.6	131.6 & 131.4
c	7.36 (d, 9)	7.37 (d, 8.5) & 7.35 (d, 8.5)	124.9	128.9 & 128.8
d	-	-	132.3	136.5 & 136.1
e	-	5.29 & 2.48 (s)	-	-
f	-	-	164.7	171.2 & 170.2
g	4.3 (t, 7)	4.10-4.04 (m)	64.8	64.6 & 64.5
h	1.89-1.79 (m)	1.79-1.67 (m)	28.0	27.5 & 27.4
i	1.58-1.68 (m)	1.47-1.41 (m)	18.3	17.9 & 17.8
j	2.26 (dt, 2.5, 7)	Overlap	25.1	24.9 & 24.7
k	-	-	83.9	83.8 & 83.6
l	1.97 (t, 2.5)	1.93 (t, 3.0)	69.1	79.3 & 78.9

E) Synthesis of FK506-HTFB-Biotin Probe (2.19) by Sharpless-Hüisgen Cycloaddition
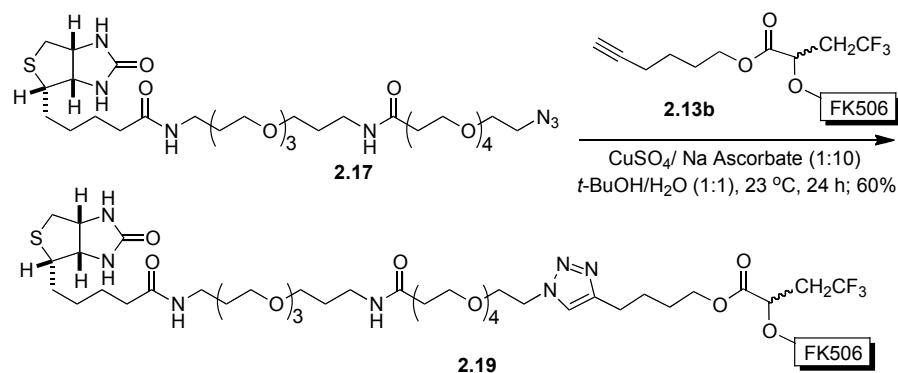
A solution of FK506-HTFB (**2.13b**) (5.5 mg, 0.0054 mmol) in 1.0 mL of dry acetonitrile and a stock solution of (+)-Biotin-(PEO)$_4$-N$_3$ (**2.17**) (93 μL of a 70.0 mM stock solution in dry acetonitrile, 0.0065 mmol, Quanta Bio) was mixed in a vial flushed with nitrogen and equipped with a magnetic stir bar. The reaction mixture was diluted with 1.5 mL of tBuOH/H$_2$O (1:1). A Cu(I) solution was freshly prepared from 2.5 mL of an aqueous solution of CuSO$_4$·5H$_2$O (1 M) and 2.5 mL of an aqueous solution of sodium ascorbate (10 M). The solutions of CuSO$_4$ and sodium ascorbate were mixed and stirred at ambient temperature (23 °C) until the black solution turned light yellow-brown. At this point, the Cu(I) solution (6 μL) was immediately added into the mixture of FK506-HTFB and biotin-azide. The reaction mixture was stirred at ambient temperature for 24 h. The reaction was then filtered through a cotton plug in a glass pipette to remove solid residues and rinsed with 5 mL of EtOAc. The filtrate was concentrated under reduced

pressure and purified by preparative TLC (30:70, MeOH:EtOAc) to afford the FK506-HTFB-biotin probe **2.19** (5.7 mg, 60% yield); TLC (30:70 %v/v of MeOH:EtOAc): R_f = 0.35; HRMS (MALDI): Calcd for $C_{85}H_{137}O_{24}F_3N_8SNa$ [M+Na] = 1765.9309, Found [M+Na] = 1765.9297.

F) Synthesis of FK506-HBPA-Biotin Probe (2.20) by Sharpless-Hüisgen Cycloaddition
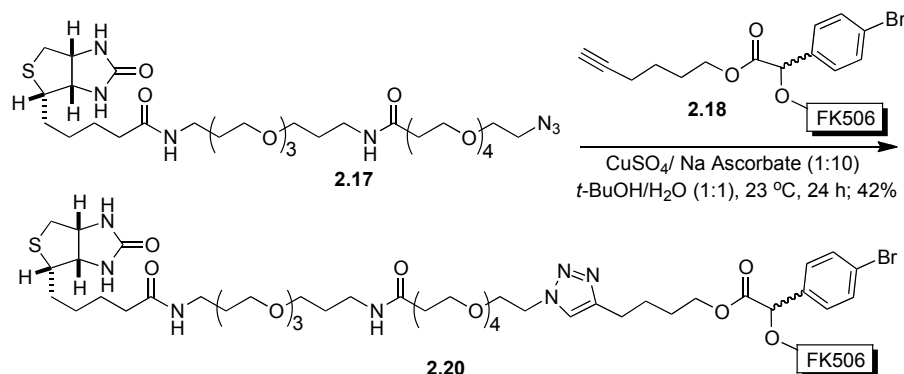
FK506-HBPA (**2.18**) was prepared according to a general O-H insertion method as described in ref. 10. A solution of FK506-HBPA (**2.18**) (41.1 mg, 0.0375 mmol) in dry acetonitrile (1.0 mL) and a stock solution of (+)-Biotin-(PEO)$_4$-N$_3$ (**2.17**) (634 μL of a 70.0 mM stock solution in dry acetonitrile, 0.0444 mmol, Quanta Bio) were mixed in a vial flushed with nitrogen and equipped with a magnetic stir bar. The reaction mixture was diluted with 2.0 mL of tBuOH/H$_2$O (1:1). A Cu(I) solution was freshly prepared from 2.5 mL of an aqueous solution of CuSO$_4$·5H$_2$O (1 M) and 2.5 mL of an aqueous

solution of sodium ascorbate (10 M). The solutions of CuSO$_4$ and sodium ascorbate were mixed and stirred at ambient temperature (23 °C) until the black solution turned light yellow-brown. At this point, the Cu(I) solution (10 μL) was immediately added into the mixture of FK506-HBPA and biotin-azide. The reaction mixture was stirred at ambient temperature (23 °C) for 24 h. The reaction was then filtered through a cotton plug in a pipette to remove all solid residues and washed with 10 mL of EtOAc. The filtrate was concentrated under reduced pressure and purified by preparative TLC (30:70, MeOH:Et$_2$O) to afford the FK506-HBPA-biotin conjugate **2.20** (29.1 mg, 42% yield); TLC (30:70, MeOH:Et$_2$O): R_f = 0.17; HRMS (MALDI) Calcd for C$_{90}$H$_{141}$BrN$_8$O$_{24}$SNa [M+Na] = 1851.8865, Found [M+Na] = 1851.8971.

G) IL-2 Reporter Assay with FK506 Derivatives (2.13b, 2.13b′, 2.18 and 2.18′) and FK506-Biotin Conjugates (2.19 and 2.20)

Jurkat T cells (E6.1) from ATCC were transfected with an IL-2 promoter-driven luciferase reporter plasmid. After 18 h, the cells were aliquotted into 96-well plates at 0.5 million cells per well and incubated with FK506 (**2.13a**), **2.13b, 2.13b′, 2.18, 2.18′**, **2.19** and **2.20** with different concentrations for 30 minutes. The cells were then stimulated with 40 nM phorbol myristate acetate and 1 mM ionomycin for 6 h. Cells were harvested and the luciferase activity was measured. The data were processed with Graphpad Prism software.
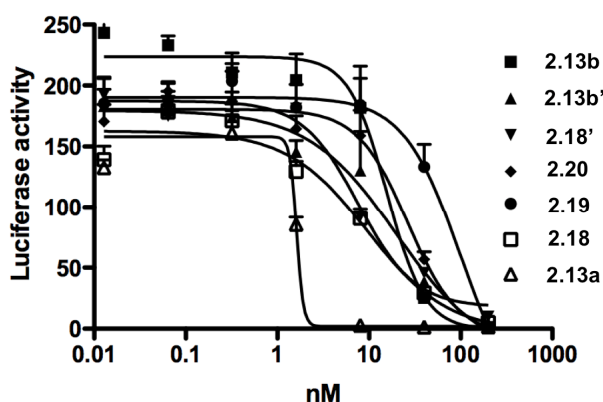
Figure A-4. IC$_{50}$ value plots of IL-2 activation by phorbol myristyl acetate (PMA) plus ionomycin for diastereomeric FK506/HTFB ethers (**2.13b/2.13b′**), FK506-HPBA ethers (**2.18/2.18′**), and biotin conjugate **2.19** and **2.20** in the Jurkat T cells.

H) Affinity Chromatography Experiments with FK506-Biotin Conjugates 2.19 and 2.20

Jurkat T cells (E6.1) were lysed in a lysis buffer containing 20 mM Tris·HCl, pH 7.5, 100 mM KCl, 0.5 mM β-mecaptoethanol, 0.1% Triton X-100 and a protease inhibitor cocktail (Roche Applied Science, Indianapolis, IN). The lysates were aliquoted and incubated with DMSO or FK506 for 30 min, followed by incubation with biotin conjugate **16** or **17** for 1 h. The binding proteins of the FK506-biotin conjugates were captured with 15 ml streptavidin agarose and resolved on SDS-PAGE gel for silver staining or Western blot analysis.

J) 'Click' Reaction and Affinity Chromatography Experiments of Fumagillol Derivatives 2.15b/2.15′, 2.21/2.21′, 2.22 and 2.23

HEK293T cells were first incubated with 20 μM of TNP470 (**2.23**) or DMSO for 30 min, then continued to incubate with 1 μM of **2.15b/2.15′**, **2.21/2.21′**, **2.22** or DMSO

for 1 h. Cells were harvested and lysed with 100 mM phosphate (pH = 8.0) buffer containing protease inhibitor by dounce homogenizer. Cell lysates were subjected to pre-clear with Strepavidin beads for 1h. The total proteins were diluted to the concentration of 2.5 mg/mL. Then, 86 μL of total protein (2.5 mg/mL) was boiled with 0.4% SDS. For click chemistry reaction, other reagents were added, which included 25 μM of biotin-azide 21, 1 mM of Tris(2-carboxyethyl)phosphine hydrochloride (TCEP), 100 μM of tris[(1-benzyl-1H-1,2,3-triazol-4-yl)methyl]amine (TBTA) and 1 mM of $CuSO_4$ to a final volume of 100 μL. The mixture was incubated for 1 h at room temperature. Streptavidin beads were used to capture the final complex and eluted with 2 x SDS sample buffer after extensively washing with washing buffer (100 mM Tris·HCl [pH = 7.5], 500 mM NaCl, and 0.2% SDS). The eluents were separated by SDS-PAGE for western blotting.

K) Proliferation Assay of Fumagillol Derivatives 2.15b/2.15′, 2.21/2.21′, 2.22 and 2.23

HUVEC cells were purchased from Lonza and maintained as suggested. HUVEC cells were plated into 96-well plate for overnight and treated with compounds **2.15/2.15′**, **2.21/2.21′**, **2.22**, and **2.23** with different concentration (0.001, 0.01, 1.0, 10, 100, 1000, 10000 and 20000 nM) for 18 h. The cells were labeled with 0.5 mci ^{3}H thymidine per well for another 6 h and harvested afterwards. The radioactivity of ^{3}H thymidine incorporation were measured by MicroBeta and plotted with GraphPad software.
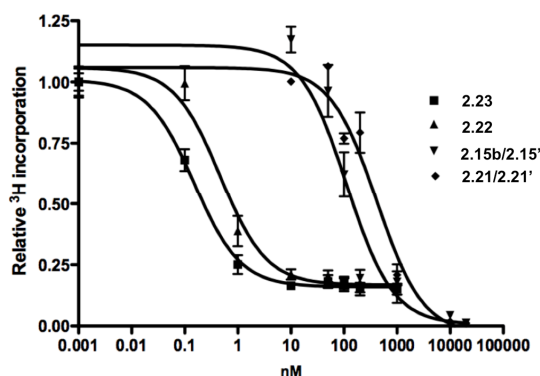
Figure A-5. IC$_{50}$ value plots of fumagillol derivatives **2.15b/2.15b′**, **2.21/2.21′**, **2.22** and **2.23** in HUVEC cells.

L) hMetAP2 Assay of fumagillol derivatives 2.15b/2.15b′ and 2.21/2.21′

Eight different concentrations of fumagillol (2.15a) and fumagillol derivatives (**2.15b/2.15b′** and **2.21/2.21′**) (20, 10, 5, 1, 0.5, 0.1, 0.05 and 0.005 μM) were pipetted into a 96-well plate and they were incubated for 20 min at room temperature with an assay buffer (40 mM HEPES [pH = 7.5], 100 mM NaCl and 10 μM MnCl$_2$) containing 250 nM GST-6×His-ThrCS-HsMetAP2 and 0.02 U proline aminopeptidase as the coupling enzyme. The enzyme reaction was initiated by adding methionylprolyl-*p*-nitroanilide as the substrate (20 μL, 3 mM; such that a final concentration of 600 μM was attained in a 100 μL of total reaction volume in each well) and the change in absorbance at 405 nm was measured using a microplate reader (BMG Labtech, Offenburg, Germany) for a period of 20 min. Reaction progress was computed against the data from the wells containing DMSO alone taken for uninhibited reactions. The data from four independent experiments were combined and the EC$_{50}$ values were determined by plotting the data using the GraphPad Prism software.
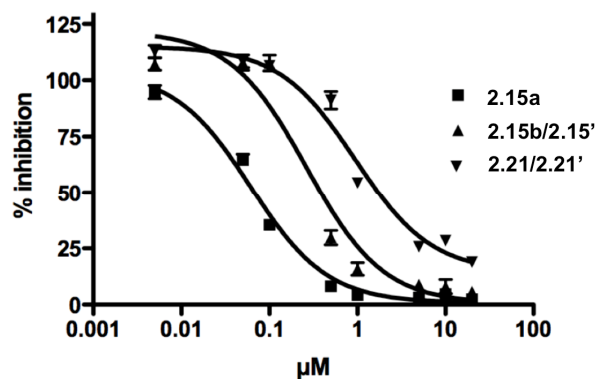
Figure A-6. EC$_{50}$ value plots of fumagillol (**2.15a**), fumagillol-HTFB **2.15b/2.15b′** and fumagillol-HBPA (**2.21/2.21′**) from hMetAP2 assay.

Chapter III - Synthesis of β-Lactam Congeners of Orlistat as Fatty Acid Synthase Inhibitors
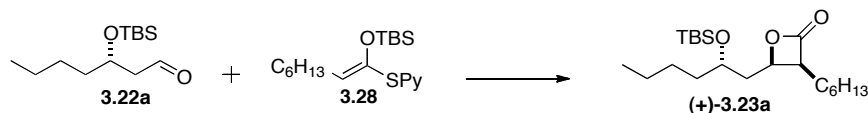
(3*S*,4*R*)-4-((*S*)-2-(tert-butyldimethylsiloxy)-hexyl)-3-hexyloxetan-2-one,   (+)-3.23a. To a solution of aldehyde **3.22a** (555.6 mg, 2.15 mmol) and thiopyridyl ketene acetal **3.28** (1.0 g, 2.87 mmol) in CH$_2$Cl$_2$ (5 ml) at −78 °C was added a solution of SnCl$_4$ (2.0 mL, 2.0 mmol, 1M in CH$_2$Cl$_2$) slowly over 2 h using syringe pump. After 30 minutes, the reaction was quenched with pH 7 buffer solution (5.0 mL) and warmed up to room temperature. The result mixture was filtrated through a plug of celite and the organic layer was separated. The dried (MgSO$_4$) extract was concentrated *in vacuo* and purified by chromatography over silica gel, eluting carefully with 0.3% diethyl ether / hexanes, to give β-lactone (+)-**3.23a** (405.8 mg, 1.05 mmol, 49%) as a colorless oil (dr,

6:1). The major isomer: $[\alpha]_D^{20}$ +30.5 (c 1.05, CHCl$_3$); IR (thin film) 2934, 2863, 1827, 1253, 1063 cm^{-1}; ^{1}H-NMR (500 MHz, CDCl$_3$) δ 4.75 (ddd, J = 2.5, 6.5, 10.5 Hz, 1H), 3.84-3.89 (m, 1H), 3.63 (dt, J = 7.0, 8.5 Hz, 1H), 1.47-1.55 (m, 3H), 1.24-1.36 (m, 18H), 0.88-0.91 (m, 14H), 0.071 (s, 3H), 0.068 (s, 3H); ^{13}C-NMR (125 MHz, CDCl$_3$) δ 172.7, 72.9, 68.6, 52.6, 38.4, 36.8, 32.2, 31.7, 29.3, 27.8, 26.12, 26.07, 26.00, 24.4, 22.8, 22.9, 18.3, 14.3, -4.2, -4.3; LRMS (ESI+) Calcd for C$_{22}$H$_{45}$O$_3$Si (M+H) 385, found 385.
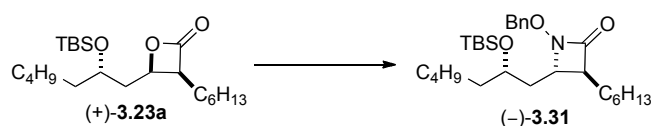
(3S,4R)-1-(benzyloxy)-4-((S)-2-(tert-butyldimethylsiloxy)-hexyl)-3-hexyl azetidin-2-one, (−)-3.31. To a flask with β-lactone (+)-**3.23a** (197.2 mg, 0.46 mmol) was added BnONH$_2$ (123.2 mg, 1.0 mmol). The reaction was warmed to 50 °C for overnight. Next, the reaction was diluted with Et$_2$O (5.0 mL) and cooled to 0 °C. To this solution was added PPh$_3$ (268.7 mg, 1.0 mmol) and DIAD (208.0 mg, 0.2 mL, 1.0 mmol). After 30 minutes, the reaction was warmed to room temperature and concentrated in *vacuo* and purified by chromatography over silica gel, eluting with 1% EtOAc/hexanes, to give β-lactam (−)-**3.31** (111.7 mg, 0.228 mmol, 44%) as a colorless oil (dr, 6:1). The major isomer: $[\alpha]_D^{20}$ −37.8 (c 1.11, CHCl$_3$); IR (thin film) 2934, 2854, 1768, 1466, 1066 cm^{-1} ; ^{1}H-NMR (500 MHz, CDCl$_3$) δ 7.40-7.45 (m, 5H), 5.0 (d, J = 11.0 Hz, 1H), 4.96 (d, J = 11.0 Hz, 1H), 3.71-3.76 (m, 1H), 3.31 (ddd, J = 1.5, 4.5, 9.0 Hz, 1H), 2.55 (dt, J = 2.0, 6.5 Hz, 1H), 1.87 (dt, J = 5.0, 14.0 Hz, 1H), 1.57-1.62 (m, 2H), 1.48-1.54 (m, 1H), 1.21-1.40 (m, 17H), 0.91-0.95 (m, 4H), 0.89 (s, 10H), 0.06 (s,

3H), 0.04 (s, 3H); ^{13}C-NMR (125 MHz, CDCl$_3$) δ 166.9, 135.6, 129.7, 129.2, 128.8, 78.2, 70.0, 61.4, 52.3, 39.3, 37.1, 32.1, 31.8, 29.5, 28.5, 27.1, 26.1, 25.1, 22.86, 22.80, 18.27, 14.31, 14.29, -4.2, -4.3; LRMS (ESI+) Calcd for C$_{29}$H$_{52}$NO$_3$Si (M+H) 490, found 490.
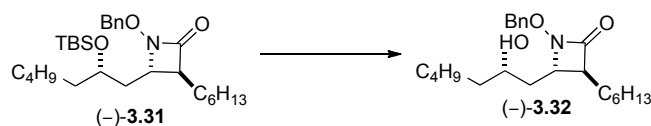
(3S,4R)-1-(benzyloxy)-3-hexyl-4-((S)-2-(hydroxyhexyl)azetidin-2-one, (−)-3.32. To a solution of β-lactam (−)-**3.31** (187.7 mg, 0.38 mmol) in CH$_3$CN at 0 °C was added HF (0.46 mL, 48% w/w in H$_2$O). After 20 minutes, the reaction was warmed up to room temperature. After 6 h, the reaction was carefully quenched with sat. aq. NaHCO$_3$ (3.0 mL) and the mixture was extracted with Et$_2$O. The dried (MgSO$_4$) extract was concentrated in *vacuo* and purified by chromatography over silica gel, eluting with 1% EtOAc/hexanes, to give β-lactam (−)-**3.32** (97.4 mg, 0.259 mmol, 68%) as a colorless oil (dr, 6:1). The major isomer: [α]$_D^{20}$ −28.9 (c 0.97, CHCl$_3$); IR (thin film) 3437 (br), 3032, 2928, 1756, 1460 cm^{-1}; ^{1}H-NMR (500 MHz, CDCl$_3$) δ 7.40-7.46 (m, 5H), 4.99 (d, J = 11.0 Hz, 1H), 4.95 (d, J = 11.0 Hz, 1H), 3.52-3.61 (m, 1H), 3.37 (ddd, J = 2.0, 5.5, 7.5 Hz, 1H), 2.54 (ddd, J = 2.0, 6.0, 8.5 Hz, 1H), 1.66-1.70 (m, 4H), 1.26-1.38 (m, 17H), 0.87-0.91 (m, 6H); ^{13}C-NMR (125 MHz, CDCl$_3$) δ 166.7, 135.4, 129.8, 129.3, 128.9, 78.4, 69.6, 62.9, 51.8, 40.1, 38.3, 31.80, 31.78, 29.4, 28.6, 27.4, 25.4, 22.85, 22.81, 14.32, 14.29; LRMS (ESI+) Calcd for C$_{23}$H$_{38}$NO$_3$ (M+H) 376, found 376.

(–)-**3.32** → (–)-**3.33**
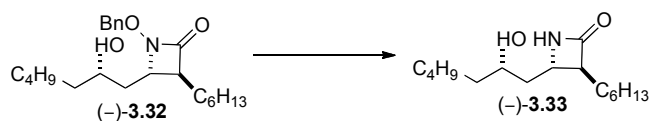
(3*S*,4*S*)-3-hexyl-4-((*S*)-2-hydroxyhexyl)azetidin-2-one, (–)-3.33. To a solution

of alcohol (–)-**3.32** (21.8 mg, 0.06 mmol) in THF (0.9 mL) was added H_2O (30 μL).

Next, this solution was treated with freeze-pump-thawn process at $-78\ ^\circ C$ (twice) before

warmed to $0\ ^\circ C$. A freshly prepared solution of SmI_2 (0.07 M in THF) was added to the

reaction solution dropwise till a persistent deep-blue color formed. After 5 minutes, the

reaction was quenched with sat. aq. $NaHCO_3$ (2.0 mL), and the mixture was extracted

with EtOAc (3 x 20 mL). The dried ($MgSO_4$) extract was concentrated *in vacuo* and

purified by chromatography over silica gel, eluting carefully with 40% EtOAc/hexanes,

to give (–)-**3.33** (5.5 mg, 0.02 mmol, 35%) as a colorless oil (dr, 6:1). The major isomer:

$[\alpha]_D^{20}$ –14.5 (c 0.55, $CHCl_3$); IR (thin film) 3423 (br), 3284 (br), 2925, 2851, 1753 cm^{-1};

^{1}H-NMR (500 MHz, $CDCl_3$) δ 6.09 (s, 1H), 3.66-3.74 (m,1H), 3.42-3.44 (m, 1H), 2.73-

2,76 (m, 1H), 1.60-1.66 (m, 4H), 1.40-1.48 (m, 2H), 1.25-1.35 (m, 15H), 0.90-0.86 (m,

6H); ^{13}C-NMR (125 MHz, $CDCl_3$) δ 171.1, 72.0, 57.5, 54.1, 42.2, 38.8, 31.9, 31.8, 29.9,

29.5, 28.7, 27.5, 25.3, 22.8, 14.32, 14.25; LRMS (ESI+) Calcd for $C_{16}H_{32}NO_2$ (M+H)

270, found 270.
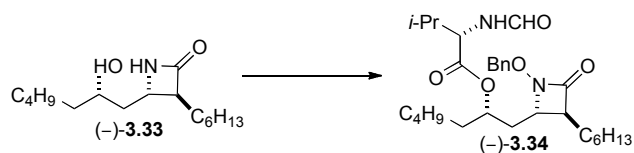
(S)-((S)-1-((2S,3S)-1-(benzyloxy)-3-hexyl-4-oxoazetidin-2-yl)hexan-2-yl) 2-methan amido-3-methylbutanoate, (−)-3.34. To a solution of alcohol (−)-**3.33** (129.5 mg, 0.34 mmol) in CH_2Cl_2 (2.0 mL) at room temperature was added DMAP (125.1 mg, 1.02 mmol), EDCI (151.9 mg. 0.79 mmol) and *N*-formyl-*L*-valine (98.4 mg, 0.67 mmol). The reaction mixture was stirred for overnight. Then, the reaction was quenched with sat. aq. NH_4Cl (3.0 mL), and the mixture was extracted with Et_2O (3 X 20 mL). The dried ($MgSO_4$) extract was concentrated *in vacuo* and purified by chromatography over silica gel, eluting carefully with 20% EtOAc/hexanes, to give ester (−)-**3.34** (137.8 mg, 0.27 mmol, 80%) as a colorless oil: $[\alpha]_D^{20}$ −24.6 (c 1.22, $CHCl_3$); IR (thin film) 3313 (br), 3032, 2931, 2860, 1764, 1738, 1685 cm^{-1}; ^{1}H-NMR (500 MHz, $CDCl_3$) δ 8.14 (s, 1H), 7.25-7.34 (m, 5H), 6.06-6.14 (br, 1H), 4.86 (d, *J* = 11.5 Hz, 1H), 4.83 (d, *J* = 11.5 Hz, 1H), 4.74-4.80 (m, 1H), 4.47 (ddd, *J* = 4.5, 9.5, 11.5, 1H), 2.98-3.04 (m, 1H), 2.34 (ddd, *J* = 2, 7.5, 13.5, 1H), 1.79-1.86 (m, 1H), 1.30-1.50 (m, 6H), 1.08-1.25 (m, 17H), 0.74-0.80 (m, 9H); LRMS (ESI+) Calcd for $C_{29}H_{47}N_2O_5$ (M+H) 503, found 503.
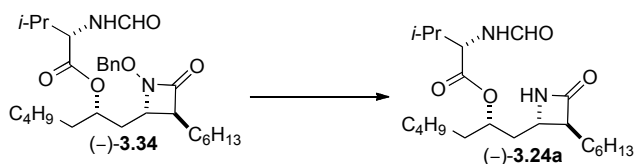
(S)-((S)-1-((2S,3S)-3-hexyl-4-oxoazetidin-2-yl)hexan-2-yl) 2-methanamido-3-methyl butanoate, (−)-3.24a. To a solution of ester (−)-**3.34** (35.2 mg, 0.07 mmol) in

THF (2.8 mL) was added H_2O (90 μL). Next, this solution was treated with freeze-pump-thawn process at −78 °C (twice) before warmed to 0 °C. A freshly prepared solution of SmI_2 (0.07 M in THF) was added to the reaction solution dropwise till a persistent deep-blue color formed. After 5 minutes, the reaction was quenched with sat. aq. $NaHCO_3$ (2.0 mL), and the mixture was extracted with EtOAc (3 X 20 mL). The dried ($MgSO_4$) extract was concentrated *in vacuo* and purified by chromatography over silica gel, eluting carefully with 50% EtOAc/hexanes, to give β-lactam (−)-**3.24a** (18.2 mg, 0.05 mmol, 66%) as a colorless oil: $[\alpha]_D^{20}$ −10.7 (c 0.56, $CHCl_3$); IR (thin film) 3284 (br), 2925, 2851, 1753 cm^{-1}; ^{1}H-NMR (500 MHz, $CDCl_3$) δ 8.22 (s, 1H), 6.82 (br, 1H), 6.33 (br, 1H), 5.03-4.97 (m, 1H), 4.60 (dd, J = 5.0, 9.0, 1H), 3.32 (dt, , J = 5.5, 2.5, 1H), 2.70-2.78 (m, 1H), 2.25-2.19 (m, 1H), 1.94-1.89 (m, 2H), 1.70-1.76 (m, 3H), 1.51-1.67 (m, 4H), 1.23-1.33 (m, 17H), 0.85-0.09 (m, 6H); LRMS (ESI+) Calcd for $C_{22}H_{41}N_2O_4$ (M+H) 397, found 397.

An enantiomeric route was also developed for enatiomers of compound 3.31-3.34. (−)-**3.23a** $[\alpha]_D^{20}$ −36.8 (c 1.1, $CHCl_3$); (−)-**3.31** $[\alpha]_D^{20}$ −28.9 (c 0.97, $CHCl_3$); (−)-**3.33** $[\alpha]_D^{20}$ −14.5 (c 0.55, $CHCl_3$); (−)-**3.34** $[\alpha]_D^{20}$ −24.6 (c 1.22, $CHCl_3$); (−)-**3.24** $[\alpha]_D^{20}$ −10.7 (c 0.56, $CHCl_3$).
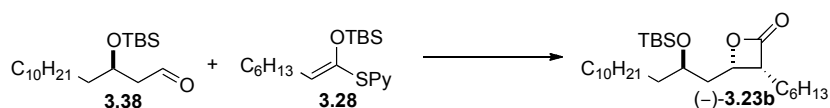
(3R,4S)-4-((R)-2-(*tert*-butyldimethylsilyloxy)tridecyl)-3-hexyloxetan-2-one (-)

-3.23b. To a solution of aldehyde **3.38** (342.4 mg, 1.0 mmol) and ketene acetal **3.28**

(527.0 mg, 1.5 mmol) in CH_2Cl_2 (5.0 mL) at $-78\ °C$ was added a solution of $SnCl_4$ (1.5

mL, 1.5 mmol, 1M in CH_2Cl_2) slowly over 1 h using syringe pump. After 30 min, the

reaction was quenched with pH 7 buffer solution (2.5 mL) and warmed up to ambient

temperature. The resulted mixture was filtrated through a plug of celite and the organic

layer was separated. The dried ($MgSO_4$) extract was concentrated *in vacuo* and purified

by chromatography over silica gel, eluting carefully with 1% EtOAc/hexanes, to give β-

lactone (–)-**3.23b** (280 mg, 0.60 mmol, 60%) as a colorless oil (dr, 14:1). The major

isomer: ^{1}H-NMR (500 MHz, $CDCl_3$) δ 4.76 (ddd, J = 3.0, 6.5, 9.0 Hz, 1H), 3.84-3.90

(m, 1H), 3.64 (dt, J = 6.5, 8.5 Hz, 1H), 1.74-1.86 (m, 2H), 1.46-1.72 (m, 4H), 1.30 (s,

26H), 0.86-0.90 (m, 15H), 0.08 (s, 6H); LRMS (ESI+) Calcd for $C_{28}H_{56}O_3SiLi$ (M+Li)

475, found 475.
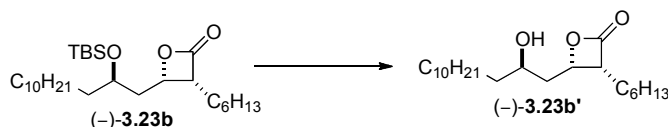
(3R,4S)-3-hexyl-4-((R)-2-hydroxytridecyl)oxetan-2-one **(–)-3.32b′**: To a

solution of β-lactone (–)-**3.23b** (16 mg, 0.034 mmol) in CH_3CN at 0 °C was added HF

(40 μL, 48% w/w in H_2O). After 20 min, the reaction was warmed up to room

temperature After 6 h, the reaction was carefully quenched with sat. aq. $NaHCO_3$ (1.0

mL). After 5 min, the mixture was extracted with Et_2O (3 X 20 mL). The dried ($MgSO_4$)

extract was concentrated *in vacuo* and purified by chromatography over silica gel,

eluting with 15% EtOAc/hexanes, to give alcohol (–)-**3.32b′** (10 mg, 0.028 mmol, 83%)

as a colorless oil: $[\alpha]_D^{20}$ −18.8 (c 0.85, $CHCl_3$); IR (thin film) 3425 (br), 2925, 1821 cm

$^{-1}$; ^{1}H-NMR (500 MHz, $CDCl_3$) δ 4.91 (ddd, J = 2.5, 6.5, 10.5 Hz, 1H), 3.82-3.84 (m,

1H), 3.67 (dt, J = 6.5, 9.0 Hz, 1H), 1.70-1.88 (m, 2H), 1.50-1.64 (m, 2H), 1.22-1.36 (m,

28H), 0.86-0.92 (m, 6H); ^{13}C-NMR (125 MHz, $CDCl_3$) δ 172.4, 72.9, 68.3, 52.8, 38.4,

37.7, 32.2, 31.7, 39.9, 29.88, 29.87, 29.81, 29.7, 29.6, 29.3, 27.7, 25.7, 24.4, 22.9, 22.8,

14.4, 14.3; LRMS (ESI+) Calcd for $C_{22}H_{42}O_3Li$ (M+Li) 361, found 361.

(−)-**3.23b**   (+)-**3.35**
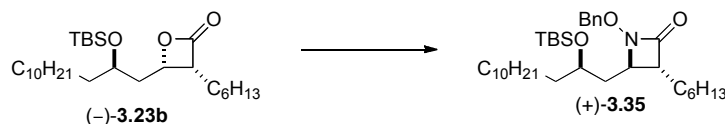
(3R,4R)-1-(benzyloxy)-4-((R)-2-(*tert*-butyldimethylsilyloxy)tridecyl)-3 hexyl

azetidin-2-one, (+)-3.35. To a flask with β-lactone (–)-**3.32b'** (103 mg, 0.22 mmol) was

added $BnONH_2$ (56 mg, 0.44 mmol). The reaction was warmed to 50 °C for 16 h. Next,

the reaction was diluted with Et_2O (2.2 mL) and cooled to 0 °C. To this solution was

added PPh_3 (115 mg, 0.44 mmol) and DIAD (89 mg, 85 μL, 0.44 mmol). After 30 min,

the reaction was warmed up to room temperature and concentrated *in vacuo* and purified

by chromatography over silica gel, eluting with 4% EtOAc/hexanes, to give β-lactam

(+)-**3.35** (70 mg, 0.12 mmol, 56%) as a colorless oil: $[\alpha]_D^{20}$ +24.0 (c 1.00, $CHCl_3$); IR

(thin film) 2925, 2854, 1774, 1465, 1382, 1066 cm^{-1}; ^{1}H-NMR (500 MHz, $CDCl_3$) δ

7.37-7.43 (m, 5H), 4.97 (d, J = 11.0 Hz, 1H), 4.93 (d, J = 11.0 Hz, 1H), 3.69-3.74 (m,

1H), 3.28 (ddd, J = 2.0, 5.0, 9.0 Hz, 1H), 2.53 (dt, J = 1.5, 6.5 Hz, 1H), 1.85 (ddd, J =

5.0, 6.0, 9.0 Hz, 1H), 1.53-1.64 (m, 2H), 1.48 (ddd, J = 5.0, 9.0, 13.5 Hz, 1H), 1.22-1.38

(m, 28H), 0.86-0.92 (m, 15H), 0.04 (s, 3H), 0.03 (s, 3H); ^{13}C-NMR (125 MHz, CDCl$_3$) δ

166.9, 135.7, 129.7, 129.2, 128.8, 78.2, 70.0, 61.5, 52.4, 39.3, 37.1, 32.2, 31.8, 30.0,

29.9, 29.89, 29.86 (2C), 29.6, 29.5, 28.6, 27.1, 26.1, 25.4, 22.9, 22.8, 18.3, 14. 4, 14.3, -

4.2, -4.1; LRMS (ESI+) Calcd for C$_{35}$H$_{64}$NO$_3$Si (M+H) 574, found 574.
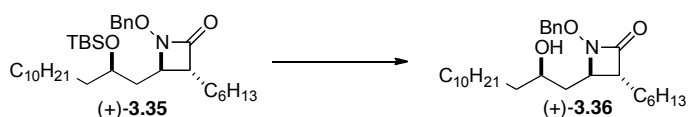
(3R,4R)-1-(benzyloxy)-3-hexyl-4-((R)-2-hydroxytridecyl)azetidin-2-one, (+)-
3.36. To a solution of β-lactam (+)-**3.35** (46 mg, 0.08 mmol) in CH$_3$CN at 0°C was

added HF (96 μL, 48% w/w in H$_2$O). After 20 min, the reaction was warmed up to room

temperature After 6 h, the reaction was carefully quenched with sat. aq. NaHCO$_3$ (1.0

mL), and the mixture was extracted with Et$_2$O (3 X 20 mL). The dried (MgSO$_4$) extract

was concentrated *in vacuo* and purified by chromatography over silica gel, eluting with

20% EtOAc/hexanes, to give alcohol (+)-**3.36** (25 mg, 0.054 mmol, 68%) as a colorless

oil: [α]$_D^{20}$ +26.5 (c 1.13, CHCl$_3$); IR (thin film) 3452 (br), 2923, 2853, 1758, 1456 cm^{-1};

^{1}H-NMR (500 MHz, CDCl$_3$) δ 7.36-7.44 (m, 5H), 4.99 (d, J = 11.0 Hz, 1H), 4.95 (d, J =

11.0 Hz, 1H), 3.54-3.59 (m, 1H), 3.36 (ddd, J = 2.0, 5.5, 9.5 Hz, 1H), 2.52 (ddd, J = 2.0,

6.5, 10.5 Hz, 1H), 1.77 (br, 1H), 1.64-1.76 (m, 2H), 1.45-1.67 (m, 2H), 1.23-1.40 (m,

28H), 0.86-0.92 (m, 6H); ^{13}C-NMR (125 MHz, CDCl$_3$) δ 166.7, 135.4, 129.8, 129.3,

128.9, 78.4, 69.6, 62.8, 51.8, 40.1, 38.2, 32.2, 31.8, 29.9, 29.88, 29.84 (2C), 29.81, 29.6,

29.4, 28.6, 27.4, 25.7, 22.9, 22.8, 14.4, 14.3; LRMS (ESI+) Calcd for $C_{29}H_{49}NO_3Li$ (M+Li) 466, found 466.
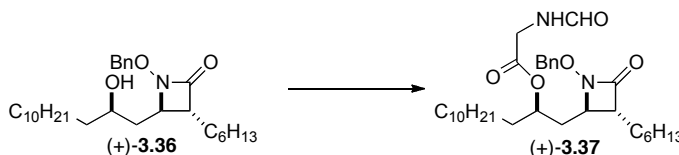
(R)-1-((2R,3R)-1-(benzyloxy)-3-hexyl-4-oxoazetidin-2-yl)tridecan-2-yl 2-methanamidoethanoate, (+)-3.37. To a solution of alcohol (+)-**3.36** (23 mg, 0.05 mmol) in CH_2Cl_2 (1.0 mL) at room temperature was added DMAP (12.2 mg, 0.1 mmol), EDCI (19 mg, 0.1 mmol) and *N*-formylglycine (10.3 mg, 0.1 mmol). After 1.5 h, the reaction was quenched with sat. aq. NH_4Cl (2.5 mL), and the mixture was extracted with Et_2O (3 X 20 mL). The dried ($MgSO_4$) extract was concentrated *in vacuo* and purified by chromatography over silica gel, eluting with 40% EtOAc/hexanes, to give ester (+)-**3.37** (20 mg, 0.037 mmol, 61%) as a colorless oil: $[\alpha]_D^{20}$ +15.4 (c 1.00, $CHCl_3$); IR (thin film) 3322 (br), 2933, 2353, 1754, 1460 cm^{-1}; ^{1}H-NMR (500 MHz, $CDCl_3$) δ 8.23 (s, 1H), 7.39-7.43 (m, 5H), 6.05 (br, 1H), 4.91-4.98 (m, 3H), 4.08 (dd, *J* = 5.5, 19.0 Hz, 1H), 3.94 (dd, *J* = 5.5, 19.0 Hz, 1H), 3.12-3.16 (m, 1H), 2.45 (dt, *J* = 1.5, 7.5 Hz, 1H), 1.92 (ddd, *J* = 5.0, 8.5, 14.0 Hz, 1H), 1.61 (ddd, *J* = 4.0, 8.0, 14.5 Hz, 1H), 1.45-1.53 (m, 2H), 1.20-1.38 (m, 28H), 0.89 (t, *J* = 7.0 Hz, 6H); ^{13}C-NMR (125 MHz, $CDCl_3$) δ 169.3, 166.5, 161.1, 135.4, 129.9. 129.4, 128.9, 78.3, 73.5, 61.5, 52.1, 40.2, 36.9, 34.5, 32.1, 31.8, 29.9, 29.86, 29.84, 29.8, 29.7, 29.6, 29.4, 28.5, 27.3, 25.2, 22.9, 22.8, 14.4, 14.3; LRMS (ESI+) Calcd for $C_{32}H_{53}N_2O_5$ (M+H) 545, found 545.
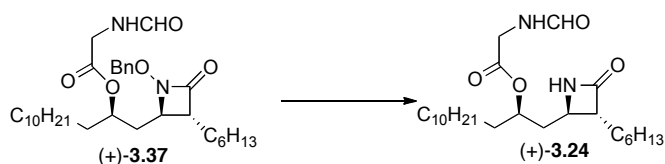
(R)-1-((2R,3R)-3-hexyl-4-oxoazetidin-2-yl) tridecan-2-yl)-2-methan amido ethanoate, (+)-3.24. To a solution of ester (+)-3.37 (17 mg, 0.031 mmol) in THF (1.2 mL) was added H_2O (40 μL). Next, this solution was treated with freeze-pump-thaw process at −78 °C (twice) before warmed to 0 °C. A freshly prepared solution of SmI_2 (0.06 M in THF) was added to the above solution dropwise till a persistent deep-blue color formed. After 10 min, the reaction was quenched with sat. aq. $NaHCO_3$ (2.5 mL), and the mixture was extracted with EtOAc (3 X 20 mL). The dried ($MgSO_4$) extract was concentrated *in vacuo* and purified by chromatography over silica gel, eluting with 80% EtOAc/hexanes, to give β-lactam (+)-3.38 (10.5 mg, 0.024 mmol, 77%) as a colorless oil: $[\alpha]_D^{20}$ +8.3 (c 0.24, $CHCl_3$); IR (thin film) 3422 (br), 2926, 2353, 1743, 1664, 1465 cm^{-1}; ^{1}H-NMR (500 MHz, $CDCl_3$) δ 8.28 (s, 1H), 6.44 (s, 1H), 6.30 (br, 1H), 5.02-5.05 (m, 1H), 4.06 (dd, J = 5.5, 19.5 Hz, 1H), 4.03 (dd, J = 5.5, 19.5 Hz, 1H), 3.37 (dt, J = 2.0, 5.5 Hz, 1H), 2.75 (dt, J = 1.5, 8.0 Hz, 1H), 1.88-1.96 (m, 2H), 1.57-1.78 (m, 2H), 1.22-1.36 (m, 28H), 0.90 (t, J = 6.5 Hz, 6H); ^{13}C-NMR (125 MHz, $CDCl_3$) δ 172.0, 169.6, 169.1, 75.3, 57.6, 53.4, 40.6, 39.8, 35.0, 32.2, 31.8, 29.87, 29.86, 29.8, 29.7, 29.62, 29.59, 29.5, 28.5, 27.4, 25.3, 22.9, 22.8, 14.4, 14.3; LRMS (ESI+) Calcd for $C_{25}H_{47}N_2O_4$ (M+H) 439, found 439.

An enantiomeric route was also developed for enatiomers of compound **3.35**-**3.38**. (–)-**3.35** $[\alpha]_D^{20}$ –26.0 (c 1.0, CHCl$_3$); (–)-**3.36** $[\alpha]_D^{20}$ –27.5 (c 1.7, CHCl$_3$); (–)-**3.37** $[\alpha]_D^{20}$ –21.6 (c 1.0, CHCl$_3$); (–)-**3.24** $[\alpha]_D^{20}$ –8.4 (c 0.7, CHCl$_3$).

Chapter IV - Total Synthesis of Spongiolactone

4.45   **4.47**

Vinylogous ester 4.47. To a solution of 1,3 cyclohexadione (15 g, 133.6 mmol) in 300 mL of dry DMF was added K$_2$CO$_3$ (22.2 g, 160.3 mmol) and the suspension was stirred at room temperature (21 °C) for 10 min. The resulting orange suspension was added *tert*-butyl acrylate (23.3 mL, 160.3 mmol) and stirred at 100°C for 6 h to obtain brown suspension. Then, the reaction was cooled to ambient temperature (21 °C) for 1 h. Another portion of K$_2$CO$_3$ (22.2 g, 160.3 mmol) was added followed by dimethyl sulfate (15.2 mL, 160.3 mmol) and the reaction mixture was stirred at room temperature (21 °C). After 1 h, the light brown suspension was quenched with pH 7 buffer solution (250 mL). The organic layer was separated by separatory funnel and the aqueous layer was extracted with EtOAc (100 mL x 3). The combined organic layers were washed with water (100 mL) and brine (100 mL x 2), dried over anhydrous MgSO$_4$, and concentrated *in vacuo*. Purification of the crude product by flash chromatography on SiO$_2$ eluting with hexanes:EtOAc:Et$_3$N (11:8:1) gave 30.5 g (93%) of vinylogous ester **4.47** as a yellow oil: R$_f$ = 0.42 (1:1-EtOAc:hexanes); IR (thin film) 3271, 2978, 1729, 1649, 1616, 1371,

1163, 1089 cm^{-1}; ^{1}H-NMR (500 MHz, CDCl$_3$) δ 3.79 (s, 3H), 2.55 (t, J = 6.0 Hz, 2H), 2.53 (t, J = 9.5 Hz, 2H), 2.31 (t, J = 6.0 Hz, 2H), 2.22 (t, J = 8.5 Hz, 2H) 1.94-1.99 (m, 2H), 1.42 (s, 9H); ^{13}C-NMR (125 MHz, CDCl$_3$) δ 197.7, 172.9, 172.5, 117.6, 79.5, 55.1, 36.2, 34.1, 28.0(3), 24.7, 20.7, 17.7; HRMS (ESI+) Calcd for C$_{14}$H$_{22}$O$_4$Li [M+Li]: 261.1678. Found: 261.1683.
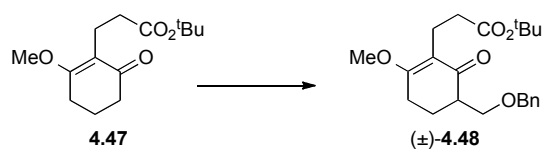
α-Substituted ketone (±)-4.48. To a solution of vinylogous ester **4.47** (17 g, 66.8 mmol) in 200 mL of toluene was cooled to −78 °C. Lithium hexamethyldisilazide (100 mL, 100.3 mmol, 1.0 M in hexanes) was slowly added drop wise. After addition, the reaction mixture was immediately moved from −78 °C bath to 0 °C bath and stirred for 1 h. Then, the orange solution was cooled to −78 °C again and benzyl chloromethyl ether (25.7 mL, 187.2 mmol) was slowly added by syringe pump over an hour period. The reaction was stirred at −78 °C for 4 h and allowed to slowly warm up to ambient temperature (21 °C) for 8 h. The turbid yellow solution was quenched with pH 7 buffer solution (250 mL). The organic layer was separated by separatory funnel and the aqueous layer was extracted with EtOAc (100 mL x 3). The combined organic layers were washed with brine (200 mL), dried over anhydrous MgSO$_4$, and concentrated *in vacuo*. Purification of the crude product by flash chromatography on SiO$_2$ eluting with hexanes:EtOAc:Et$_3$N (15:4:1) gave 21.3 g (85%) of α-substituted ketone (±)-**4.48** as a

yellow oil: $R_f = 0.54$ (1:1-EtOAc:hexanes); IR (thin film) 3061, 3031, 2931, 1723, 1613, 1154 cm^{-1}; ^{1}H-NMR (500 MHz, CDCl$_3$) δ 7.33-7.31 (m, 4H), 4.52 (dd, $J = 11.5$, 19.75 Hz, 2H), 3.88 (dd, $J = 4.0$, 9.5 Hz, 1H), 3.79 (s, 3H), 3.56 (dd, $J = 8.0$, 9.5 Hz, 1H), 2.68 (t, $J = 5.0$ Hz, 1H), 2.65 (t, $J = 5.0$ Hz, 1H), 2.56-2.47 (m, 4H), 2.29-2.20 (m, 1H), 2.22 (t, $J = 8.0$ Hz, 2H), 1.89-1.81 (m, 1H), 1.42 (s, 9H); ^{13}C-NMR (125 MHz, CDCl$_3$) δ 197.2, 173.0, 172.2, 138.4, 128.3 (2), 127.6 (2), 127.5, 117.5, 79.7, 73.2, 69.8, 55.1, 45.0, 34.3, 28.1(3), 24.1, 23.8, 18.0; HRMS (ESI+) Calcd for C$_{22}$H$_{31}$O$_5$ [M+H]: 375.2171. Found: 375.2176.
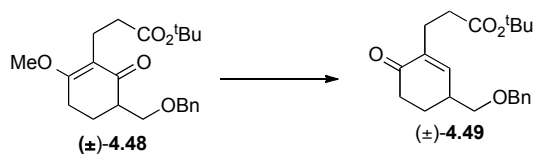
α,β-Unsaturated ketone (±)-4.49. To a solution of α-substituted ketone (±)-**4.48** (7 g, 18.7 mmol) in 200 mL of dry MeOH was added a white powder of CeCl$_3$·7H$_2$O (13.5 g, 37.4 mmol), which was dried at 130 °C for 16h to remove one molecule of H$_2$O and stirred at room temperature (21 °C) for 10 min. The resulted yellow solution was cooled to −78 °C and NaBH$_4$ (2.83 g, 74.8 mmol) was slowly added. The reaction was stirred at −78 °C for 4 h and allowed to slowly warm up to ambient temperature (21 °C) for 8 h to obtain the white suspension. Then, the reaction mixture was treated with 2N HCl (200 mL) and stirred at room temperature (21 °C) until the white suspension turned to a colorless solution. The reaction was extracted with Et$_2$O (100 mL x 3). The combined organic layers were washed with brine (100 mL), dried

over anhydrous MgSO$_4$, and concentrated *in vacuo*. Purification of the crude product by flash chromatography on SiO$_2$ eluting with hexanes:EtOAc (9:1) gave 5.2 g (81%) of α,β-unsaturated ketone (±)-**4.49** as a colorless oil: R$_f$ = 0.21 (1:9-EtOAc:hexanes); IR (thin film) 3091, 3064, 3031, 2978, 1723, 1675, 1359, 1146 cm^{-1}; ^{1}H-NMR (500 MHz, CDCl$_3$) δ 7.38-7.29 (m, 5H), 6.70 (dd, *J* = 1.5, 2.3 Hz, 1H), 4.53 (dd, *J* = 12.0, 14.0 Hz, 2H), 3.44 (ddd, *J* = 7.0, 6.5, 13.5 Hz, 2H), 2.75-2.69 (m, 2H), 2.54 (t, *J* = 5.0 Hz, 1H), 2.51 (t, *J* = 5.0 Hz, 1H), 2.49-2.45 (m, 1H), 2.39-2.32 (m, 2H), 2.11-2.06 (m, 1H), 1.77-1.69 (m, 1H), 1.41 (s, 9H); ^{13}C-NMR (125 MHz, CDCl$_3$) δ 199.2, 172.5, 147.0, 138.6, 138.1, 128.6(2), 127.9, 127.8(2), 80.3, 73.4, 72.9, 37.4, 37.2, 34.5, 28.3(3), 26.2, 25.6; HRMS (ESI+) C$_{21}$H$_{28}$O$_4$Li [M+Li]: 351.2148. Found: 351.2123.
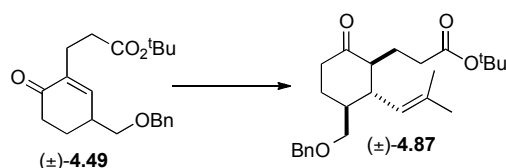
Alkene (±)-4.87. To slurry of copper (I) bromide-dimethyl sulfide complex (0.75 g, 2.9 mmol) in 30 mL of dry THF was added HMPA (6.7 mL, 38.3 mmol) and the mixture was stirred at room temperature (21 °C) for 5 min. The resulted green solution was cooled to −78 °C and 2-methyl-1-propenyl magnesium bromide (115.0 mL, 57.5 mmol, 0.5 M in THF) was added resulting in a yellow slurry. After stirring for 10 min, a solution of α,β-unsaturated ketone (±)-**4.49** (6.6 g, 19.2 mmol) and trimethylsilyl chloride (6.0 mL, 47.9 mmol) in 10 mL of dry THF was added via syringe pump over 1h period. The reaction was stirred at −78 °C for 4 h and allowed to slowly warm up to

ambient temperature (21 °C) for 8 h to obtain the black suspension. Then, the reaction mixture was quenched with a saturated NH$_4$Cl solution (100 mL) and filtered through a Celite with Et$_2$O. The organic layer was separated by separatory funnel and the aqueous layer was extracted with Et$_2$O (100 mL x 3). The combined organic layers were washed with brine (100 mL), dried over anhydrous MgSO$_4$, and concentrated *in vacuo*. Purification of the crude product by flash chromatography on SiO$_2$ eluting with hexanes:EtOAc (19:1) gave 10.8 g (88%; dr, 10:1) of alkene (±)-**4.87** as a yellow oil: R$_f$ = 0.51 (1:9-EtOAc:hexanes); IR (thin film) 3091, 3067, 3028, 2978, 1732, 1711, 1453, 1365 cm^{-1}; ^{1}H-NMR (500 MHz, CDCl$_3$) δ 7.35-7.28 (m, 5H), 4.88 (dt, J = 1.5, 10 Hz, 1H), 4.43 (dd, J = 12.0, 17.0 Hz, 2H), 3.48 (dd, J = 3.0, 9.0 Hz, 1H), 3.23 (dd, J = 7.0, 9.0 Hz, 1H), 2.42-2.38 (m, 2H), 2.36-2.25 (m, 3H), 2.19 (ddd, J = 2.5, 9.0, 12.0 Hz, 1H), 2.15-2.08 (m, 1H), 1.86-1.77 (m, 1H), 1.73 (d, J = 1.5 Hz, 3H), 1.68-1.59 (m, 3H), 1.54 (d, J = 1.5 Hz, 3H), 1.42 (s, 9H); ^{13}C-NMR (125 MHz, CDCl$_3$) δ 211.8, 173.2, 138.5, 134.2, 128.3(2), 127.5, 127.4(2), 126.7, 79.8, 73.2, 72.6, 53.6, 45.9, 42.6, 41.6, 33.6, 30.5, 28.2(3), 25.8, 22.1, 18.6; HRMS (ESI+) C$_{25}$H$_{37}$O$_4$ [M+H]: 401.2692. Found: 401.2683.
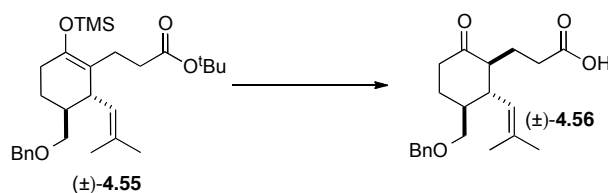
Alkenyl acid (±)-4.56. Followed the cuprate addition of α,β-unsaturated ketone **4.49** as explained above, the crude product ((±)-**4.55**) was directly employed to the next

step after work up without purification over SiO_2. The crude trimethyl silyl enol ether

(±)-**4.55** (104 mg, 0.22 mmol) was dissolved in 10 mL of dry CH_3CN and cooled to 0

^{o}C. *p*-toluenesulfonic acid (83 mg, 0.438 mmol) was slowly added. The reaction was

allowed to warm up to ambient temperature (21 ^{o}C) and stirred for 6 h to obtain the

light-brown solution. The reaction mixture was concentrated *in vacuo* to afford the

brown oil. Purification of the crude product by flash chromatography on SiO_2 eluting

with hexanes:EtOAc (7:3) gave 70.2 mg (93%) of alkene (±)-**4.56** as a colorless oil: $R_f =$

0.50 (1:1-EtOAc:hexanes); IR (thin film) 3339, 3031, 2978, 1732, 1711, 1448, 1362 cm^{-1}; ^{1}H-NMR (500 MHz, CDCl$_3$) δ 7.35-7.28 (m, 5H), 4.88 (dt, J = 1.0, 10 Hz, 1H), 4.43

(dd, J = 12.0, 15.5 Hz, 2H), 3.48 (dd, J = 3.0, 9.0 Hz, 1H), 3.23 (dd, J = 6.5, 9.0 Hz, 1H),

2.49-2.39 (m, 3H), 2.34-2.24 (m, 3H), 2.23-2.18 (ddd, J = 2.5, 9.25, 13.6 Hz, 1H), 1.87-

1.76 (m, 2H), 1.73 (d, J = 1.0 Hz, 3H), 1.71-1.61 (m, 2H), 1.54 (d, J = 1.0 Hz, 3H), No

O-H proton; ^{13}C-NMR (125 MHz, CDCl$_3$) δ 212.1, 179.1, 138.5, 134.6, 128.5(2), 127.7,

127.6(2), 126.5, 73.3, 72.6, 53.6, 45.9, 42.7, 41.6, 32.1, 30.5, 25.9, 21.8, 18.7; HRMS

(ESI+) $C_{21}H_{28}O_4Li$ [M+Li]: 351.2148. Found: 351.2143.
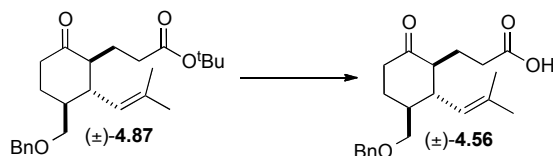
Alkenyl acid (±)-4.56. To a solution of alkene (±)-**4.87** (3 g, 7.5 mmol) in 100

mL of dry CH_2Cl_2 was cooled to 0 ^{o}C. Trifluoroacetic acid (16 mL, 150.0 mmol) was

slowly added dropwise and the reaction was allowed to slowly warm up to ambient

temperature (21 °C) and stirred for 10 h to obtain a brown solution. The reaction mixture

was concentrated *in vacuo* to afford black oil. Purification of the crude product by flash

chromatography on SiO_2 eluting with hexanes:EtOAc (7:3) gave 2.4 g (93%) of alkene

(±)-**4.56** as a brown oil: R_f = 0.50 (1:1-EtOAc:hexanes); IR (thin film), [^1]H-NMR (500

MHz, $CDCl_3$) and [^{13}]C-NMR (125 MHz, $CDCl_3$) were identical to previous explained.
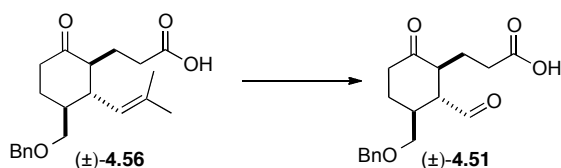
Adehyde acid (±)-4.51. To a solution of acid (±)-**4.56** (2.0 g, 5.8 mmol) in

CH_2Cl_2 (100 mL) and dry MeOH (1.0 mL) was cooled at −78 °C and the ozone was

bubbled through the mixture for several minutes until the blue color persisted. The

remaining ozone was removed by bubbling nitrogen through the solution for 10 min.

Excess dimethyl sulfide (4.5 mL, 58.1 mmol) was added. The mixture was allowed

slowly warm up to ambient temperature (21 °C) and stirred for 12 h. The solvent was

evaporated under reduced pressure and the resulting oil was purified by flash

chromatography on SiO_2 eluting with hexanes/EtOAc (1:1) to afford aldehyde acid (±)-

4.51 (1.5 g, 81%) as a colorless oil: R_f = 0.32 (1:1-EtOAc:hexanes); IR (thin film) 3410,

3037, 2937, 2860, 2724, 1776, 1711, 1456, 1095 cm^{-1}; [^1]H-NMR (500 MHz, $CDCl_3$) δ

9.63 (d, J = 4.0 Hz, 1H), 7.36-7.27 (m, 5H), 4.43 (dd, J = 12.0, 22 Hz, 2H), 3.45 (dd, J =

4.5, 9.5 Hz, 1H), 3.31 (dd, J = 7.0, 9.5 Hz, 1H), 2.73 (ddd, J = 2.5, 9.3, 11.5 Hz, 1H),

2.54-2.33 (m, 7H), 2.14 (ddd, J = 4.0, 13.1, 8.5 Hz, 1H), 1.91-1.84 (m, 1H), 1.65-1.55

(m, 1H), No O-H proton; ^{13}C-NMR (125 MHz, CDCl$_3$) δ 209.7, 200.7, 179.0, 137.7, 128.6(2), 127.9, 127.8(2), 73.4, 72.5, 59.1, 46.7, 40.6, 38.7, 31.5, 29.2, 22.1; HRMS (ESI–) Calcd for C$_{18}$H$_{21}$O$_5$ [M-H]: 317.1389. Found: 317.1375.
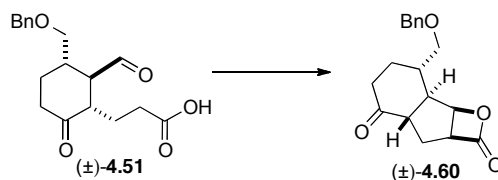
Fused tricyclic β-lactone (±)-4.60. To a solution of Mukaiyama's reagent (1.48 g, 4.2 mmol) in 30 mL of CH$_2$Cl$_2$ was added triethylamine (1.0 mL, 7.1 mmol) and stirred at room temperature (22 ^{o}C). The resulting yellow orange solution was added a solution of aldehyde acid (±)-**4.51** (450 mg, 1.4 mmol) in 10 mL of CH$_2$Cl$_2$ via a syringe pump over 1 h period. After addition, the reaction mixture was stirred at room temperature (22 ^{o}C) for 24 h yielding a dark red solution. The reaction mixture was concentrated *in vacuo* to afford a red-brown oil. Purification of the crude product by flash chromatography on SiO$_2$ eluting with hexanes:EtOAc (1:1) gave 0.33 g (78%; dr, 11:1) of β-lactone (±)-**4.60** as a colorless crystal: R$_f$ = 0.66 (1:1-EtOAc/hexanes); IR (thin film) 3030, 2928, 2863, 1824, 1717, 1453, 1119 cm^{-1}; ^{1}H-NMR (500 MHz, CDCl$_3$) δ 7.37-7.28 (m, 5H), 4.98 (t, J= 3.5 Hz, 1H), 4.53 (dd, J = 12.0, 15.5 Hz, 2H), 3.90 (dd, J = 3.5, 8.0 Hz, 1H), 3.63-3.51 (ddd, J = 4.5, 9.5, 43.3 Hz, 2H), 2.82-2.76 (m, J = 5.5, 12.0 Hz, 1H), 2.45-2.43 (m, 2H), 2.37-2.29 (m, 1H), 2.20-2.14 (m, 2H), 1.89-1.82 (ddd, J = 8.0, 9.0, 17.0 Hz, 1H), 1.78-1.67 (m, 2H); ^{13}C-NMR (125 MHz, CDCl$_3$) δ 209.2, 170.8,

138.1, 128.6(2), 127.9, 127.7(2), 76.1, 73.4, 71.9, 54.5, 51.9, 50.2, 40.6, 37.0, 30.5, 24.8;

HRMS (ESI+) Calcd for $C_{18}H_{21}O_4$ [M+H]: 301.1440. Found: 301.1435.
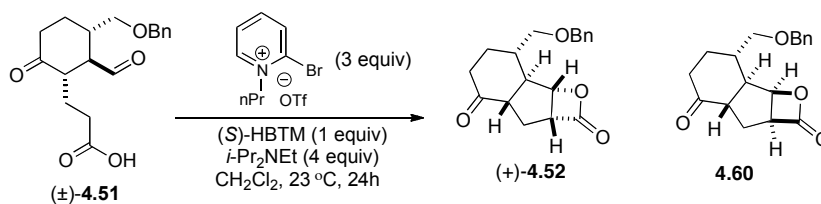
Fused tricyclic β-lactone 4.52. To a solution of Mukaiyama's reagent (1.50 g,

4.3 mmol) and (S)-HBTM[11] (0.76 g, 1.5 mmol) in 30 mL of CH_2Cl_2 was added N,N-

diisopropylethylamine (1.0 mL, 5.7 mmol) and stirred at room temperature (22 °C). The

resulting yellow solution was added a solution of aldehyde acid (±)-**4.51** (450 mg, 1.4

mmol) in 10 mL of CH_2Cl_2 via a syringe pump over 1 h period. After addition, the

reaction mixture was stirred at room temperature (22 °C) for 24 h yielding a dark red

solution. The reaction mixture was concentrated *in vacuo* to afford the red-brown oil.

Purification of the crude product by flash chromatography on SiO_2 eluting with

hexanes:EtOAc (1:1) gave 42%, dr 1:1 of β-lactone products; **4.60** was obtained 92.5 mg

(22%; 52%ee) as a colorless crystal and (+)-**4.52** was obtained 84.3 mg (20%, 96%ee) as

a colorless oil: R_f = 0.52 (2:3-EtOAc/hexanes); $[\alpha]_D^{20}$ +26.7° (c 0.23, $CHCl_3$); IR (thin

film) 2939, 2865, 1826, 1711, 1619, 1423 cm^{-1}; ^{1}H-NMR (500 MHz, $CDCl_3$) δ 7.39-7.31

(m, 5H), 5.19 (d, J= 3.5 Hz, 1H), 4.52 (dd, J = 12.0, 23.0 Hz, 2H), 3.99 (dd, J = 3.5, 8.0

Hz, 1H), 3.55 (dd, J = 4.5, 9.5 Hz, 1H), 3.45 (dd, J = 4.5, 9.5 Hz, 1H), 3.07-3.02 (m, J =

[11] Birman, V. B.; Li, X. *Org. Lett.* **2008**, *10*, 1115.

7.0, 13.0 Hz, 1H), 2.62 (dd, J = 7.0, 12.0 Hz, 1H), 2.51-2.44 (m, 1H), 2.41-2.39 (m, 1H),

2.37 (dd, J = 6.5, 13.0 Hz, 1H), 2.15-2.11 (ddd, J = 3.0, 5.5, 10.0 Hz, 1H), 2.02-1.95 (dt,

J = 8.0, 13.3 Hz, 1H) 1.66-1.61 (m, 2H); ^{13}C-NMR (125 MHz, CDCl$_3$) δ 209.9, 169.8,

137.8, 128.7(2), 128.1, 127.8(2), 79.0, 73.7, 73.2, 54.9, 49.1, 48.2, 37.1, 33.3, 29.9, 28.9;

HRMS (ESI+) Calcd for C$_{18}$H$_{21}$O$_4$ [M+H]: 301.1440. Found: 301.1426.
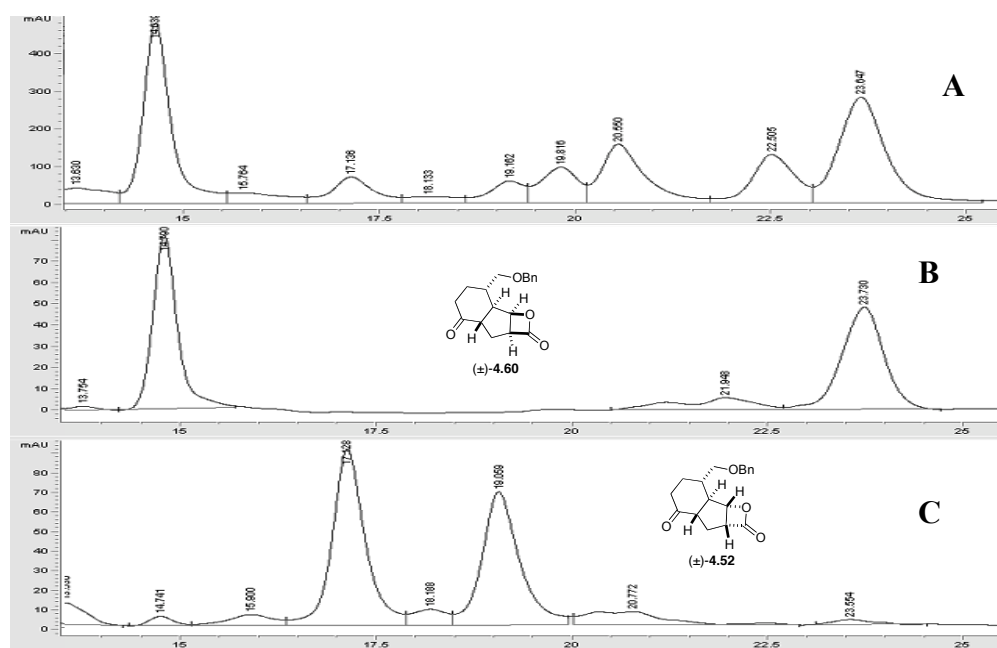
Figure A-7. Chiral HPLC chromatograms of fused tricyclic β-lactone derived from NCAL with (±)-HBTM. Using Chiralpak IA column (Daicel Chemical Industries, LTD.), 0.46 x 25 cm, 10% isopropanol in hexanes, 0.9 ml/min; (**A**) crude reaction mixture, (**B**) purified (±)-**4.60**, (**C**) purified (±)-**4.52**.
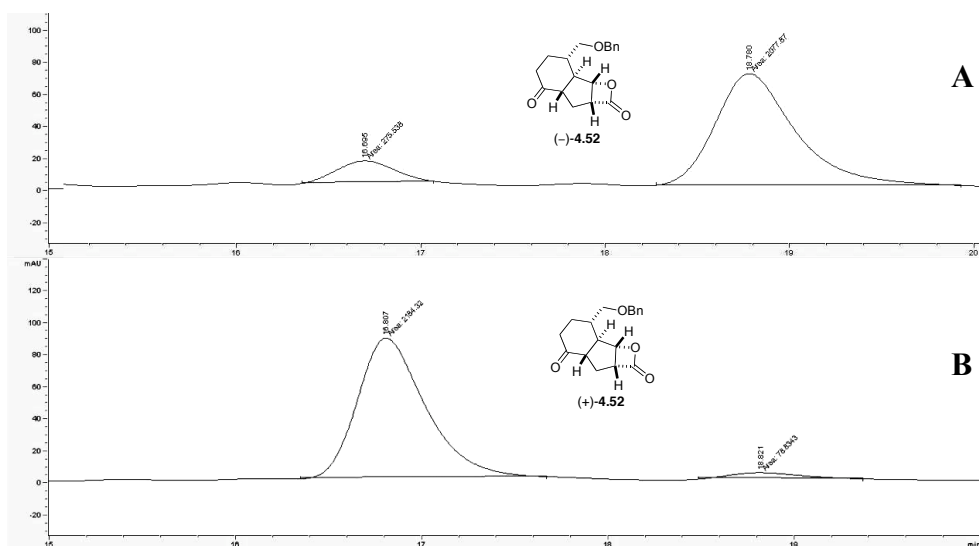
Figure A-8. Chiral HPLC chromatograms of purified **4.52** derived from NCAL process with (*R*)-HBTM (A) and (*S*)-HBTM (B). Using Chiralpak IA column (Daicel Chemical Industries, LTD.), 0.46 x 25 cm, 10% isopropanol in hexanes, 0.9 ml/min.
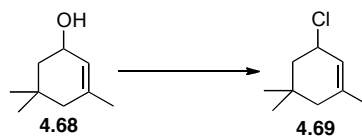
Allyl chloride 4.69. To a solution of *N*-chloro succinimide (7.7 g, 57.5 mmol) in CH$_2$Cl$_2$ was cooled at 0 ^{o}C and dimethyl sulfide (5.0 mL, 66.7 mmol) was slowly added into the reaction mixture. The result white suspension was observed. After 5 min, the resulted white suspension was added 3,5,5-trimethylcyclohex-2-enol (**4.68**) (8.0 mL, 52.3 mmol) and stirred at 0 ^{o}C for 1 h to yield a colorless solution. The reaction mixture was concentrated *in vacuo* to remove all volatiles at 25 ^{o}C. Then, the crude product was dissolved in 100 mL of pentane and cooled at −10 ^{o}C for 3 h. The succinimide, which was a byproduct in this reaction, was precipitated. The solid byproduct was removed by filtration and the filtrate was washed with cold brine (100 mL), dried over anhydrous

MgSO$_4$, and concentrated *in vacuo*. The 3-chloro-1,5,5-trimethylcyclohex-1-ene (**4.69**) was obtain as the colorless oil (98%); bp 40-45 $^{\circ}$C (5 mmHg). Chloride **4.69** was used for the next step without purification and note that **4.69** was decomposed over neutral SiO$_2$, neutral Al$_2$O$_3$ and heating above 90 $^{\circ}$C. IR (thin film) 3043, 2954, 2869, 1658, 1459, 820, 796 cm^{-1}; ^{1}H-NMR (500 MHz, CDCl$_3$) δ 5.49-4.48 (m, 1H), 4.65-4.60 (m, 1H), 1.97-1.92 (m, 2H), 1.69 (s, 3H), 1.66-1.65 (m, 2H), 1.01 (s, 3H), 0.89 (s, 3H); ^{13}C-NMR (125 MHz, CDCl$_3$) δ 137.6, 122.2, 56.9, 45.9, 43.7, 31.9, 30.9, 26.0, 23.8; LRMS (APCI+) Calcd for C$_9$H$_{15}$Cl [M]: 158.0862. Found: 158.
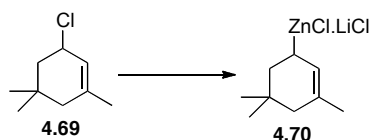
Zincate 4.70: Zinc dust[12](6.4 g, 118.0 mmol) and anhydrous LiCl (1.0 g, 23.6 mmol) were weighted into a flame-dried round-bottomed flask. The solid was dried at 130 $^{\circ}$C (heat gun) under high vacuum for 5 min and cooled down to 23 $^{\circ}$C for 1 h. This process was repeated 3 cycles. The solid mixtures were covered with 10 mL of dry THF and stirred vigorously at 23 $^{\circ}$C. The suspension of zinc and LiCl was activated by adding 1,2 dibromoethane (0.3 mL, 3.5 mmol) and stirred vigorously at 23 $^{\circ}$C for 10 min, followed by addition of TMSCl (0.15 mL, 1.2 mmol). The resulted suspension was generously boiled. The mixture was stirred vigorously for another 30 min to cool down to 23 $^{\circ}$C, and then the reaction was cooled at 0 $^{\circ}$C. A solution of 3-chloro-1,5,5-trimethylcyclohex-1-ene (**4.69**) in 5 mL of dry THF was slowly added into the reaction

---

[12] Commercially available form Aldrich.

mixture *via* a syringe pump over 2 h. The resulting mixture was stirred vigorously under nitrogen atmosphere at 0 °C for 6 h. The zinc suspension was allowed to settle and stored at 0 °C. The concentration and the yield were determined by iodolysis.[13] Iodine (254.0 mg, 1.0 mmol) was placed into a dry 10 mL round-bottomed flask equipped with a magnetic stir-bar and septum under nitrogen. Dry THF (5 mL) was added. The solution of allylic zinc **4.70** was slowly added dropwise with syringe until the red color disappeared for 1 min. The volume of the allylic zinc reagent was determined: molarities of allylic zinc = 1/volumn of allylic zinc reagent. The concentration of the allylic zinc reagent **4.70** was 0.10 mol/l; volume = 16.0 mL; yield: 15%.
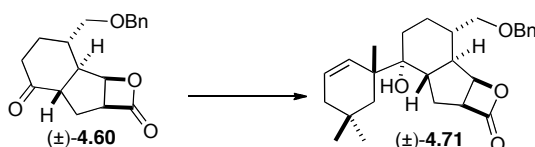
Homoallylic alcohol (±)-4.71. To a solution of fused tricyclic β-lactone (±)-**4.60** (312.7 mg, 1.0 mmol) in 10 mL of dry THF was cooled at −78 °C and a solution of freshly prepared (3,5,5-trimethylcyclohex-2-en-1-yl)zinc(II) chloride **4.70** (9.5 mL, 1.0 mmol, 0.11 M in THF) was slowly added. The reaction mixture was stirred at −78 °C for 1 h. After that, the mixture was quenched with pH 7 buffer solution (50mL) at −78 °C, allowed to warm up to ambient temperature (22 °C) for 30 min and filtered through a Celite with Et$_2$O. The organic layer was separated by separatory funnel and the aqueous layer was extracted with Et$_2$O (50 mL x 3). The combined organic layers were washed with brine (50 mL), dried over anhydrous MgSO$_4$, and concentrated *in vacuo*.

---

[13] Krasovskiy, A.; Knochel, P. *Synthesis* **2006**, *5*, 890.

Purification of the crude product by flash chromatography on SiO$_2$ eluting with hexanes:EtOAc (5:1) gave 421.3 g (95%, dr 13:1) of homoallylic alcohol (±)-**4.71** as a colorless oil: R$_f$ = 0.53 (3:7-EtOAc/hexanes); IR (thin film) 3547, 3028, 2949, 1826, 1453, 1098 cm^{-1}; ^{1}H-NMR (500 MHz, CDCl$_3$) δ 7.37-7.28 (m, 5H), 5.84 (broad s, 1H), 5.67 (broad s, 1H), 4.94 (t, J= 3.5 Hz, 1H), 4.52 (dd, J = 12.0, 20.0 Hz, 2H), 3.75 (dd, J = 3.5, 8.0 Hz, 1H), 3.50 (d, J = 5.0, 2H), 2.54 (dd, J = 7.0, 14.5 Hz, 1H), 2.17(dd, J = 5.5, 13.5 Hz, 1H), 2.01-1.96 (m, 1H), 1.85-1.67 (m, 6H), 1.50 (dd, J = 3.0, 12.0 Hz, 1H), 1.26 (m, 1H), 1.20 (m, 1H), 1.12 (s, 3H), 1.03 (t, J = 7.0, 1H), 0.97 (s, 3H), 0.96 (m, 3H), O–H proton unobservable; ^{13}C-NMR (125 MHz, CDCl$_3$) δ 209.2, 170.8, 138.1, 128.6(2), 127.9, 127.7(2), 76.1, 73.4, 71.9, 54.5, 51.9, 50.2, 40.6, 37.0, 30.5, 24.8; HRMS (ESI+) Calcd for C$_{27}$H$_{36}$O$_4$Li [M+Li]: 431.2774. Found: 431.2781.
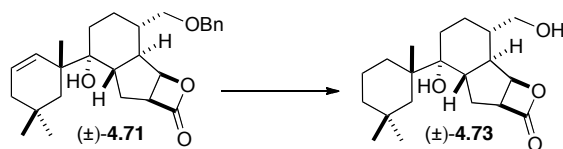
Alcohol (±)-4.73. To a solution of homoallylic alcohol (±)-**4.71** (373.7 mg, 0.88 mmol) in 50 mL of EtOH was added Pd(OH)$_2$ on carbon (75.0 mg, 20% Pd). The reaction was stirred under nitrogen atmosphere and connected to high vacuum. Air was removed under high vacuum and filled with nitrogen gas. This process was repeated 3 cycles. A hydrogen balloon was attached to the reaction flask, evacuated one more time and removed vacuum line. The heterogeneous solution was stirred vigorously at room temperature (22 °C) for 24 h. The reaction was filtered through a pad of Celite with Et$_2$O, dried over anhydrous MgSO$_4$, and concentrated *in vacuo*. Purification of the crude

product by flash chromatography on SiO_2 eluting with hexanes:EtOAc (2:8) gave 240.1 mg (81%) of alcohol (±)-**4.73** as a colorlrss oil: R_f = 0.24 (1:1-EtOAc/hexanes); IR (thin film) 3443, 2951, 2925, 2866, 1821, 1637, 1465, 1388 cm^{-1}; ^{1}H-NMR (500 MHz, CDCl$_3$) δ 5.06 (t, J = 4.0 Hz, 1H), 3.81 (dd, J = 4.0, 8.0 Hz, 1H), 3.67 (ddd, J = 5.0, 11.0, 23.8 Hz, 2H), 2.22 (dd, J = 5.5, 13 Hz, 1H), 1.97-1.91(m, J = 5.5, 12.0 Hz, 1H), 1.75-1.56 (m, 8H), 1.52-1.47 (m, 4H), 1.40-1.35 (m, 3H), 1.19-1.17 (m, 2H), 1.04 (s, 3H), 0.99 (s, 3H), 0.88 (m, 3H); ^{13}C-NMR (125 MHz, CDCl$_3$) δ 172.0, 76.5, 66.5, 53.9, 46.1(2), 44.3, 43.9, 42.1, 39.7(2), 38.8, 36.3, 31.6, 30.9, 28.7, 27.7, 24.9, 21.3, 19.2; HRMS (ESI+) Calcd for $C_{20}H_{33}O_4Li$ [M+Li]: 337.2379. Found: 377.2386.
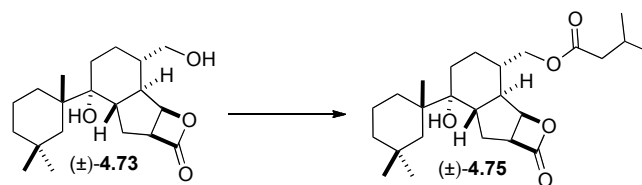
Ester (±)-4.75. To a solution of alcohol (±)-**4.73** (46.7 mg, 0.14 mmol) in 20 mL of dry CH_2Cl_2 was added DMAP (58.5 mg, 0.21 mmol) followed by EDCI·HCl (40.0 mg, 0.21 mmol). The reaction was stirred at ambient temperature (22 ^{o}C) for 10 min until all solids well dissolved and isovaleric acid (**4.74**) (18.5 μL, 0.17 mmol) was added. The mixture was stirred for 4 h and quenched with saturated $NaHCO_3$ solution. The organic layer was separated by separatory funnel and the aqueous layer was extracted with EtOAc (50 mL x 3). The combined organic layers were washed with brine (50 mL), dried over anhydrous $MgSO_4$, and concentrated *in vacuo*. Purification of the crude product by flash chromatography on SiO_2 eluting with hexanes:EtOAc (7:3) gave

44.5 mg (75%) of ester (±)-**4.75** as a colorless oil: R_f = 0.30 (3:7-EtOAc/hexanes); IR

(thin film) 3544, 2946, 2925, 1824, 1720, 1465, 1294, 731 cm^{-1}; ^{1}H-NMR (500 MHz,

CDCl$_3$) δ 4.95 (t, J = 4.0 Hz, 1H), 4.23 (dd, J = 5.0, 11.0 Hz, 1H), 3.97 (dd, J = 6.0, 11.0

Hz, 1H), 3.83 (dd, J = 4.0, 8.0 Hz, 1H), 2.24 (dd, J = 5.5, 13 Hz, 1H), 2.20 (dd, J = 1.5,

7.5 Hz, 2H), 2.14-2.07 (m, 1H), 1.98-1.92 (m, J = 5.5, 12.0 Hz, 1H), 1.86-1.79 (m, 1H),

1.77-1.69 (m, 3H), 1.67-1.56 (m, 2H), 1.52-1.45 (m, 2H), 1.44-1.36 (m, 3H), 1.25 (s,

2H), 1.20-1.15 (m, 3H), 1.04 (s, 3H), 0.99 (s, 3H), 0.96 (d, J = 1.0 Hz, 3H), 0.95 (d, J =

1.0 Hz, 3H), 0.88 (m, 3H); ^{13}C-NMR (125 MHz, CDCl$_3$) δ 173.2, 171.7, 77.5, 76.1,

66.9, 53.9, 46.2, 44.2, 43.8, 43.5, 42.1, 38.8, 36.5, 36.2, 31.6, 31.5, 30.9, 29.8, 28.6,

27.7, 25.7, 25.1, 22.6, 21.2, 19.2; HRMS (ESI+) Calcd for C$_{25}$H$_{41}$O$_5$ [M+H]: 421.2954.

Found: 421.2945.

(+)-**4.52**   (+)-**4.52a**

Alcohol (+)-4.54a. To a solution of benzyl ether (+)-**4.52** (150.0 mg, 0.50 mmol)

in 30 mL of EtOH was added Pd(OH)$_2$ on carbon (30.0 mg, 20% Pd). The reaction was

stirred under nitrogen atmosphere and connected to high vacuum. Air was removed

under high vacuum and filled with nitrogen gas. This process was repeated 3 cycles. A

hydrogen balloon was attached to the reaction flask. The heterogeneous solution was

stirred vigorously at room temperature (22 ^{o}C) for 24 h. The reaction was filtered

through a pad of Celite with Et$_2$O, dried over anhydrous MgSO$_4$, and concentrated *in*

vacuo. Purification of the crude product by flash chromatography on SiO_2 eluting with hexanes:EtOAc (2:8) gave 43.7 mg (41%) of alcohol (+)-**4.54a**. Note that alcohol (+)-**4.54a** slowly decomposed at room temperature (22 °C). $R_f = 0.21$ (7:3-EtOAc/hexanes); $[\alpha]_D^{20}$ +26.7° (*c* 0.23, $CHCl_3$); IR (thin film) 3449, 2931, 2867, 1821, 1711, 1643 cm^{-1}; ^{1}H-NMR (500 MHz, $CDCl_3$) δ 5.20 (d, *J* = 3.5 Hz, 1H), 4.03 (dd, *J* = 3.5, 8.0 Hz, 1H), 3.80 (dd, *J* = 4.5, 11.0 Hz, 1H), 3.66 (dd, *J* = 5.5, 11.0 Hz, 1H), 3.07-3.01 (m, *J* = 7.0, 13.5 Hz, 1H), 2.61 (dd, *J* = 6.5, 12.0 Hz, 1H), 2.52-2.45 (m, 1H), 2.40-2.38 (m, 1H), 2.36 (dd, *J* = 7.5, 14.0 Hz, 1H), 2.17-2.11 (m, 1H), 2.05-1.97 (dt, *J* = 8.5, 13.3 Hz, 1H) 1.67-1.53 (m, 2H), O–H proton unobservable; ^{13}C-NMR (125 MHz, $CDCl_3$) δ 210.1, 169.9, 78.9, 65.4, 54.9, 49.0, 47.5, 37.0, 34.7, 29.9, 28.5; HRMS (ESI–) Calcd for $C_{11}H_{13}O_4$ [M-H]: 209.0814. Found: 209.0821.

(+)-**4.52a**   (+)-**4.52c**
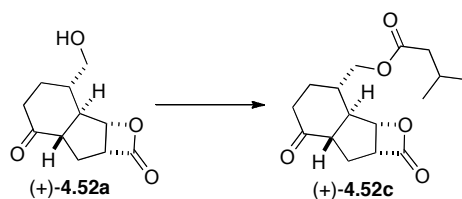
Ester (+)-4.52c. To a solution of alcohol (+)-**4.52a** (120.0 mg, 0.57 mmol) in 50 mL of dry CH_2Cl_2 was added DMAP (180 mg, 0.87 mmol) followed by EDCI·HCl (165.0 mg, 0.87 mmol). The reaction was stirred at ambient temperature (22 °C) for 10 min until all solids well dissolved and isovaleric acid (0.1 mL, 0.87 mmol) was added. The mixture was stirred for 4 h and quenched with saturated $NaHCO_3$ solution. The organic layer was separated by separatory funnel and the aqueous layer was extracted with EtOAc (50 mL x 3). The combined organic layers were washed with brine (50 mL),

dried over anhydrous MgSO$_4$, and concentrated *in vacuo*. Purification of the crude

product by flash chromatography on SiO$_2$ eluting with hexanes:EtOAc (7:3) gave 125.8

mg (81%) of ester (+)-**4.52c** as a colorless oil: R$_f$ = 0.45 (1:1-EtOAc/hexanes); $[\alpha]_D^{20}$

+29.2° (*c* 0.21, CHCl$_3$); IR (thin film) 3544, 2946, 2925, 1824, 1720, 1465, 1294, 731

cm^{-1}; ^{1}H-NMR (500 MHz, CDCl$_3$) δ 4.95 (t, *J* = 4.0 Hz, 1H), 4.23 (dd, *J* = 5.0, 11.0 Hz,

1H), 3.97 (dd, *J* = 6.0, 11.0 Hz, 1H), 3.83 (dd, *J* = 4.0, 8.0 Hz, 1H), 2.24 (dd, *J* = 5.5, 13

Hz, 1H), 2.20 (dd, *J* = 1.5, 7.5 Hz, 2H), 2.14-2.07 (m, 1H), 1.98-1.92 (m, *J* = 5.5, 12.0

Hz, 1H), 1.86-1.79 (m, 1H), 1.77-1.69 (m, 3H), 1.67-1.56 (m, 2H), 1.52-1.45 (m, 2H),

1.44-1.36 (m, 3H), 1.25 (s, 2H), 1.20-1.15 (m, 3H), 1.04 (s, 3H), 0.99 (s, 3H), 0.96 (d, *J*

= 1.0 Hz, 3H), 0.95 (d, *J* = 1.0 Hz, 3H), 0.88 (m, 3H); ^{13}C-NMR (125 MHz, CDCl$_3$) δ

173.2, 171.7, 77.5, 76.1, 66.9, 53.9, 46.2, 44.2, 43.8, 43.5, 42.1, 38.8, 36.5, 36.2, 31.6,

31.5, 30.9, 29.8, 28.6, 27.7, 25.7, 25.1, 22.6, 21.2, 19.2; HRMS (ESI+) Calcd for

C$_{25}$H$_{41}$O$_5$ [M+H]: 421.2954. Found: 421.2945.

(±)-6,15-bis-*epi*-spongiolatone ((±)-4.76). To a solution of alcohol (±)-**4.75**

(15.0 mg, 0.04 mmol) in 2 mL of dry CH$_2$Cl$_2$ was cooled at 0 °C. The reaction mixture

was added triethylamine (30 μL, 0.21 mmol) followed by slow addition of thionyl

chloride (SOCl$_2$) (13 μL, 0.17 mmol). The reaction was allowed to slowly warm up to

ambient temperature (22 °C) and stirred for 12 h. The mixture was then diluted with 5

mL of dry CH_2Cl_2 and quenched with pH 7 buffer solution. The organic layer was separated by separatory funnel and the aqueous layer was extracted with CH_2Cl_2 (10 mL x 3). The combined organic layers were washed with brine (10 mL), dried over anhydrous $MgSO_4$, and concentrated *in vacuo*. Purification of the crude product by preparative thin layer chromatography developing twice with hexanes:EtOAc (9:1) gave 1.6 mg of 6,15-bis-*epi*-spongiolatone ((±)-**4.76**) (20% brsm) as a colorless oil and 7.2 mg of (±)-**4.77** (55% brsm) as a colorless oil, with 2.1 mg of recovered starting material ((±)-**4.75**). (±)-**4.77**; R_f = 0.61 (3:7-EtOAc/hexanes). (±)-6,15-bis-*epi*-spongiolactone ((±)-**4.76**); R_f = 0.61 (3:7-EtOAc/hexanes); IR (thin film) 3064, 2954, 2925, 1821, 1807, 1637, 1267 cm^{-1}; ^{1}H-NMR (500 MHz, CDCl$_3$) δ 4.97 (t, J = 4.0 Hz, 1H), 4.25 (dd, J = 5.0, 11.0 Hz, 1H), 4.01 (dd, J = 6.0, 11.0 Hz, 1H), 3.87 (dd, J = 4.0, 8.0 Hz, 1H), 3.27 (d, J = 15.0 Hz, 1H), 2.41-2.34 (m, 2H), 2.34-2.27 (m, 1H), 2.21 (dd, J = 1.5, 8.0 Hz, 2H), 2.14 (dd, J = 6.5, 13.0 Hz, 1H), 2.09 (dd, J = 6.5, 13.0 Hz, 1H), 2.00-1.94 (m, 2H), 1.92-1.87 (m, 1H), 1.52-1.47 (m, 2H), 1.38-1.32 (m, 2H), 1.31-1.27 (m, 2H), 1.25 (bs, 2H), 1.03 (s, 3H), 0.97 (s, 3H), 0.95 (s, 3H), 0.86 (s, 3H), 0.78 (s, 3H); ^{13}C-NMR (125 MHz, CDCl$_3$) δ 173.2, 171.2, 142.4, 126.8, 75.7, 67.4, 53.6, 50.1, 47.6, 43.5, 39.6, 39.4, 38.2, 33.2, 33.1, 31.3, 31.2, 29.7, 26.7, 26.8, 25.7, 25.9, 22.4 (2), 20.9; HRMS (ESI+) Calcd for $C_{25}H_{38}O_4Li$ [M+Li]: 403.2848. Found: 403.2851.

Crystal and Molecular Structure Determination

X-ray Diffraction Laboratory, Department of Chemistry, Texas A&M University

Data Collection: A Leica MZ 75 microscope was used to identify a suitable colorless multi-faceted crystal with very well defined faces with dimensions (max, intermediate, and min) 0.08 mm x 0.06 mm x 0.03 mm from a representative sample of crystals of the same habit. The crystal mounted on a nylon loop was then placed in a cold nitrogen stream (Oxford) maintained at 110 K. A BRUKER GADDS X-ray (three-circle) diffractometer was employed for crystal screening, unit cell determination, and data collection. The goniometer was controlled using the FRAMBO software, v.4.1.05.[14] The sample was optically centered with the aid of a video camera such that no translations were observed as the crystal was rotated through all positions. The detector was set at 5.0 cm from the crystal sample. The X-ray radiation employed was generated from a Cu sealed X-ray tube (K_α = 1.5418 Å with a potential of 40 kV and a current of 40 mA) fitted with a graphite monochromator in the parallel mode (175 mm collimator with 0.5 mm pinholes). 180 data frames were taken at widths of 0.5° with an exposure time of 15 seconds. These reflections were used in to determine the unit cell using Cell_Now.[15] A suitable cell was found and refined by nonlinear least squares and Bravais lattice procedures. The unit cell was verified by examination of the *h k l* overlays on several frames of data. No super-cell or erroneous reflections were observed.

---

[14] FRAMBO v. 4.1.05 "Program for Data Collection on Area Detectors" BRUKER-Nonius Inc., 5465 East Cheryl Parkway, Madison, WI 53711-5373 USA

[15] Sheldrick, G. M. "Cell_Now (version 2008/1): Program for Obtaining Unit Cell Constants from Single Crystal Data": University of Göttingen, Germany

After careful examination of the unit cell, a standard data collection procedure was initiated using omega and phi scans.

Data Reduction, Structure Solution, and Refinement: Integrated intensity information for each reflection was obtained by reduction of the data frames with SAINTplus.[16] The integration method employed a three dimensional profiling algorithm and all data were corrected for Lorentz and polarization factors, as well as for crystal decay effects. Finally the data was merged and scaled to produce a suitable data set. SADABS[17] was employed to correct the data for absorption effects. Systematic reflection conditions and statistical tests indicated the space group P-1. A solution was obtained readily using SHELXTL (SHELXS).[5] All non-hydrogen atoms were refined with anisotropic thermal parameters. The Hydrogen atoms bound to carbon were placed in idealized positions [C–H = 0.96 Å, $U_{iso}(H) = 1.2$ x $U_{iso}(C)$] and refined using riding model. The structure was refined (weighted least squares refinement on F^2) to convergence.[18] X-seed was employed for the final data presentation and structure plots.[19]

---

[16] SAINT (Version 7). "Program for Data Integration from Area Detector Frames", Bruker–Nonius Inc., 5465 East Cheryl Parkway, Madison, WI 53711-5373 USA

[17] Sheldrick, G.M. "SADABS (version 2008/1): Program for Absorption Correction for Data from Area Detector Frames", University of Göttingen, 2008

[18] Sheldrick, G.M. (2008). Acta Cryst. A64, 112-122.

[19] Barbour, L.J.,(2001) "X-Seed (version 2.0): A Software Tool for Supramolecular Crystallography" *J. Supramol. Chem.* **2001***, 1,* 189-191.

Report: November 02, 2009
Structure: DRB_091030_G ((±)-**4.60**)
Operator: Dr. Nattamai Bhuvanesh
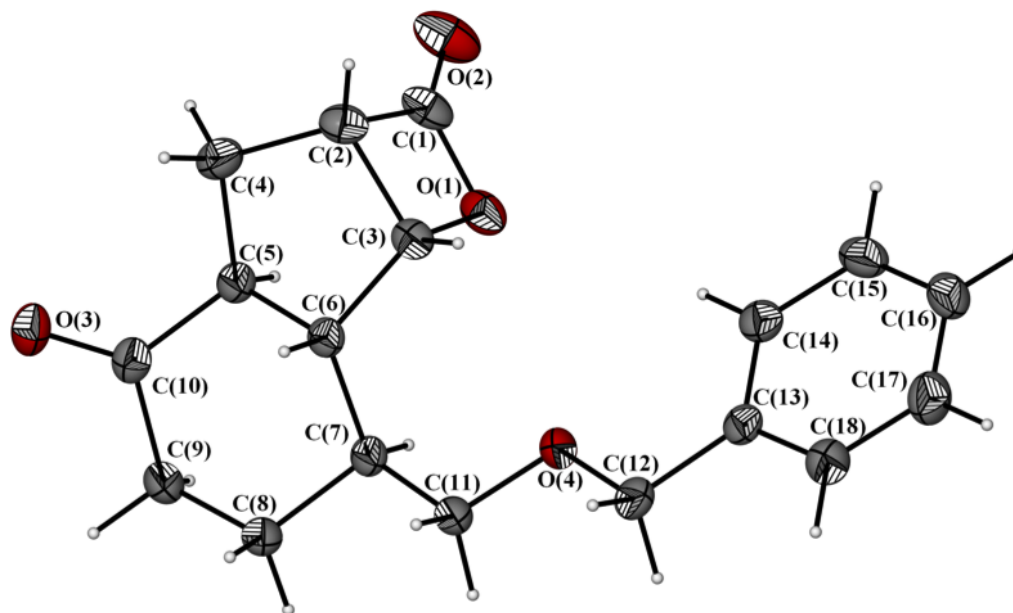
Figure A-9. Single X-ray structure of (±)-**4.60**.

Table A-12. Crystal data and structure refinement for DRB091030_G (($\pm$)-**4.60**).

Identification code	drb1030
Empirical formula	C18 H20 O4
Formula weight	300.34
Temperature	110(2) K
Wavelength	1.54178 Å
Crystal system	Triclinic
Space group	P-1
Unit cell dimensions	a = 5.9726(9) Å a= 70.138(8)°.
	b = 10.9573(16) Å b= 88.964(9)°.
	c = 12.5060(18) Å g = 84.535(9)°.
Volume	766.16(19) Å^3
Z	2
Density (calculated)	1.302 Mg/m^3
Absorption coefficient	0.743 mm^{-1}
F(000)	320
Crystal size	0.08 x 0.06 x 0.03 mm^3
Theta range for data collection	3.76 to 60.00°.
Index ranges	-6<=h<=6, -12<=k<=12, -14<=l<=14
Reflections collected	7535
Independent reflections	2149 [R(int) = 0.0389]
Completeness to theta = 60.00°	93.9 %
Absorption correction	Semi-empirical from equivalents
Max. and min. transmission	0.9780 and 0.9429
Refinement method	Full-matrix least-squares on F^2
Data / restraints / parameters	2149 / 0 / 199
Goodness-of-fit on F^2	1.020
Final R indices [I>2sigma(I)]	R1 = 0.0393, wR2 = 0.0969
R indices (all data)	R1 = 0.0548, wR2 = 0.1060
Largest diff. peak and hole	0.136 and -0.218 e.Å^{-3}

Table A-13. Atomic coordinates (x 10^4) and equivalent isotropic displacement parameters (Å^2x 10^3) for DRB091030_G (($\pm$)-**4.60**). U(eq) is defined as one third of the trace of the orthogonalized U^{ij} tensor.

	x	y	z	U(eq)
C(1)	10152(3)	5262(2)	1188(2)	34(1)
C(2)	8303(3)	4513(2)	1877(2)	30(1)
C(3)	6851(3)	5832(2)	1396(2)	26(1)
C(4)	8577(3)	4222(2)	3159(2)	34(1)
C(5)	8131(3)	5566(2)	3275(1)	27(1)
C(6)	6200(3)	6243(2)	2408(1)	24(1)
C(7)	5772(3)	7692(2)	2264(1)	26(1)
C(8)	5226(3)	7813(2)	3434(1)	30(1)
C(9)	6963(3)	7053(2)	4368(2)	33(1)
C(10)	7538(3)	5660(2)	4414(2)	28(1)
C(11)	3827(3)	8383(2)	1458(1)	28(1)
C(12)	2464(3)	8936(2)	-400(1)	29(1)
C(13)	2950(3)	8883(2)	-1570(2)	27(1)
C(14)	4986(3)	8341(2)	-1839(2)	31(1)
C(15)	5353(3)	8336(2)	-2940(2)	36(1)
C(16)	3698(4)	8863(2)	-3769(2)	37(1)
C(17)	1653(4)	9385(2)	-3493(2)	41(1)
C(18)	1290(3)	9395(2)	-2406(2)	34(1)
O(1)	8892(2)	6438(1)	820(1)	32(1)
O(2)	12073(2)	5049(2)	976(1)	49(1)
O(3)	7526(2)	4728(1)	5289(1)	34(1)
O(4)	4331(2)	8384(1)	340(1)	29(1)

Table A-14. Bond lengths [Å] and angles [°] for DRB091030_G ((±)-**4.60**).

C(1)-O(2)	1.193(2)
C(1)-O(1)	1.365(2)
C(1)-C(2)	1.514(3)
C(2)-C(4)	1.533(3)
C(2)-C(3)	1.547(3)
C(2)-H(2)	1.0000
C(3)-O(1)	1.497(2)
C(3)-C(6)	1.515(2)
C(3)-H(3)	1.0000
C(4)-C(5)	1.526(2)
C(4)-H(4A)	0.9900
C(4)-H(4B)	0.9900
C(5)-C(10)	1.496(2)
C(5)-C(6)	1.546(2)
C(5)-H(5)	1.0000
C(6)-C(7)	1.532(2)
C(6)-H(6)	1.0000
C(7)-C(11)	1.515(2)
C(7)-C(8)	1.540(2)
C(7)-H(7)	1.0000
C(8)-C(9)	1.534(2)
C(8)-H(8A)	0.9900
C(8)-H(8B)	0.9900
C(9)-C(10)	1.514(3)
C(9)-H(9A)	0.9900
C(9)-H(9B)	0.9900
C(10)-O(3)	1.218(2)
C(11)-O(4)	1.424(2)
C(11)-H(11A)	0.9900
C(11)-H(11B)	0.9900
C(12)-O(4)	1.413(2)
C(12)-C(13)	1.505(2)

Table A-14. Bond lengths [Å] and angles [°] for DRB091030_G ((±)-**4.60**) (continued).

C(12)-H(12A)	0.9900
C(12)-H(12B)	0.9900
C(13)-C(18)	1.387(3)
C(13)-C(14)	1.389(3)
C(14)-C(15)	1.391(3)
C(14)-H(14)	0.9500
C(15)-C(16)	1.381(3)
C(15)-H(15)	0.9500
C(16)-C(17)	1.387(3)
C(16)-H(16)	0.9500
C(17)-C(18)	1.377(3)
C(17)-H(17)	0.9500
C(18)-H(18)	0.9500
O(2)-C(1)-O(1)	126.59(18)
O(2)-C(1)-C(2)	137.93(19)
O(1)-C(1)-C(2)	95.47(14)
C(1)-C(2)-C(4)	113.12(15)
C(1)-C(2)-C(3)	84.07(14)
C(4)-C(2)-C(3)	106.96(14)
C(1)-C(2)-H(2)	116.1
C(4)-C(2)-H(2)	116.1
C(3)-C(2)-H(2)	116.1
O(1)-C(3)-C(6)	112.02(13)
O(1)-C(3)-C(2)	88.94(13)
C(6)-C(3)-C(2)	106.09(14)
O(1)-C(3)-H(3)	115.5
C(6)-C(3)-H(3)	115.5
C(2)-C(3)-H(3)	115.5
C(5)-C(4)-C(2)	103.13(14)
C(5)-C(4)-H(4A)	111.1
C(2)-C(4)-H(4A)	111.1
C(5)-C(4)-H(4B)	111.1

Table A-14. Bond lengths [Å] and angles [°] for DRB091030_G ((±)-**4.60**) (continued).

C(2)-C(4)-H(4B)	111.1
H(4A)-C(4)-H(4B)	109.1
C(10)-C(5)-C(4)	119.10(15)
C(10)-C(5)-C(6)	110.14(14)
C(4)-C(5)-C(6)	103.63(14)
C(10)-C(5)-H(5)	107.8
C(4)-C(5)-H(5)	107.8
C(6)-C(5)-H(5)	107.8
C(3)-C(6)-C(7)	120.15(14)
C(3)-C(6)-C(5)	103.17(13)
C(7)-C(6)-C(5)	111.14(14)
C(3)-C(6)-H(6)	107.2
C(7)-C(6)-H(6)	107.2
C(5)-C(6)-H(6)	107.2
C(11)-C(7)-C(6)	112.98(15)
C(11)-C(7)-C(8)	108.16(14)
C(6)-C(7)-C(8)	108.58(13)
C(11)-C(7)-H(7)	109.0
C(6)-C(7)-H(7)	109.0
C(8)-C(7)-H(7)	109.0
C(9)-C(8)-C(7)	113.96(14)
C(9)-C(8)-H(8A)	108.8
C(7)-C(8)-H(8A)	108.8
C(9)-C(8)-H(8B)	108.8
C(7)-C(8)-H(8B)	108.8
H(8A)-C(8)-H(8B)	107.7
C(10)-C(9)-C(8)	112.83(15)
C(10)-C(9)-H(9A)	109.0
C(8)-C(9)-H(9A)	109.0
C(10)-C(9)-H(9B)	109.0
C(8)-C(9)-H(9B)	109.0
H(9A)-C(9)-H(9B)	107.8

Table A-14. Bond lengths [Å] and angles [°] for DRB091030_G ((±)-**4.60**) (continued).

O(3)-C(10)-C(5)	124.32(16)
O(3)-C(10)-C(9)	123.08(16)
C(5)-C(10)-C(9)	112.60(15)
O(4)-C(11)-C(7)	110.19(14)
O(4)-C(11)-H(11A)	109.6
C(7)-C(11)-H(11A)	109.6
O(4)-C(11)-H(11B)	109.6
C(7)-C(11)-H(11B)	109.6
H(11A)-C(11)-H(11B)	108.1
O(4)-C(12)-C(13)	110.96(14)
O(4)-C(12)-H(12A)	109.4
C(13)-C(12)-H(12A)	109.4
O(4)-C(12)-H(12B)	109.4
C(13)-C(12)-H(12B)	109.4
H(12A)-C(12)-H(12B)	108.0
C(18)-C(13)-C(14)	119.04(17)
C(18)-C(13)-C(12)	118.38(16)
C(14)-C(13)-C(12)	122.58(16)
C(13)-C(14)-C(15)	120.05(18)
C(13)-C(14)-H(14)	120.0
C(15)-C(14)-H(14)	120.0
C(16)-C(15)-C(14)	120.39(18)
C(16)-C(15)-H(15)	119.8
C(14)-C(15)-H(15)	119.8
C(15)-C(16)-C(17)	119.48(18)
C(15)-C(16)-H(16)	120.3
C(17)-C(16)-H(16)	120.3
C(18)-C(17)-C(16)	120.18(19)
C(18)-C(17)-H(17)	119.9
C(16)-C(17)-H(17)	119.9
C(17)-C(18)-C(13)	120.84(18)
C(17)-C(18)-H(18)	119.6

Table A-14. Bond lengths [Å] and angles [°] for DRB091030_G ((±)-**4.60**) (continued).

C(13)-C(18)-H(18)	119.6
C(1)-O(1)-C(3)	91.34(13)
C(12)-O(4)-C(11)	110.73(13)

Symmetry transformations used to generate equivalent atoms.

Table A-15. Anisotropic displacement parameters (Å^2x 10^3) for DRB091030_G ((±)-**4.60**). The anisotropic displacement factor exponent takes the form: $-2p^2[\,h^2\,a^{*2}U^{11} + ... + 2\,h\,k\,a^*\,b^*\,U^{12}\,]$.

	U^{11}	U^{22}	U^{33}	U^{23}	U^{13}	U^{12}
C(1)	32(1)	44(1)	35(1)	-26(1)	3(1)	-6(1)
C(2)	31(1)	29(1)	37(1)	-17(1)	2(1)	-5(1)
C(3)	27(1)	26(1)	28(1)	-12(1)	4(1)	-7(1)
C(4)	39(1)	25(1)	36(1)	-10(1)	-2(1)	0(1)
C(5)	31(1)	24(1)	25(1)	-6(1)	2(1)	-4(1)
C(6)	28(1)	22(1)	23(1)	-6(1)	4(1)	-6(1)
C(7)	33(1)	22(1)	23(1)	-5(1)	4(1)	-5(1)
C(8)	41(1)	24(1)	26(1)	-10(1)	3(1)	-1(1)
C(9)	43(1)	31(1)	25(1)	-11(1)	3(1)	-1(1)
C(10)	25(1)	31(1)	26(1)	-5(1)	0(1)	-3(1)
C(11)	37(1)	23(1)	24(1)	-8(1)	4(1)	-2(1)
C(12)	32(1)	23(1)	28(1)	-4(1)	2(1)	-3(1)
C(13)	32(1)	19(1)	26(1)	-5(1)	2(1)	-5(1)
C(14)	37(1)	25(1)	31(1)	-10(1)	0(1)	-3(1)
C(15)	42(1)	31(1)	38(1)	-17(1)	8(1)	-4(1)
C(16)	57(1)	30(1)	28(1)	-13(1)	6(1)	-9(1)
C(17)	52(1)	40(1)	29(1)	-10(1)	-8(1)	-2(1)
C(18)	36(1)	34(1)	31(1)	-9(1)	-1(1)	0(1)
O(1)	35(1)	34(1)	33(1)	-16(1)	11(1)	-12(1)
O(2)	31(1)	72(1)	61(1)	-43(1)	9(1)	-8(1)

Table A-15. Anisotropic displacement parameters ($Å^2$x 10^3) for DRB091030_G (($\pm$)-**4.60**). The anisotropic displacement factor exponent takes the form: $-2p^2[h^2 a*^2 U^{11} + ... + 2 h k a* b* U^{12}]$ (continued).

	U^{11}	U^{22}	U^{33}	U^{23}	U^{13}	U^{12}
O(3)	30(1)	37(1)	28(1)	-1(1)	2(1)	-6(1)
O(4)	33(1)	30(1)	21(1)	-8(1)	-1(1)	2(1)

Table A-16. Hydrogen coordinates (x 10^4) and isotropic displacement parameters ($Å^2$x 10^3) for DRB091030_G (**4.60**).

	x	y	z	U(eq)
H(2)	7837	3785	1644	37
H(3)	5582	5851	878	32
H(4A)	7473	3629	3592	41
H(4B)	10114	3828	3427	41
H(5)	9494	6043	3007	32
H(6)	4804	5826	2728	29
H(7)	7164	8128	1971	31
H(8A)	5122	8745	3359	36
H(8B)	3735	7495	3669	36
H(9A)	8354	7505	4234	39
H(9B)	6367	7049	5113	39
H(11A)	2452	7937	1724	34
H(11B)	3538	9291	1448	34
H(12A)	2097	9854	-449	35
H(12B)	1142	8455	-92	35
H(14)	6129	7974	-1272	37
H(15)	6751	7968	-3122	43
H(16)	3958	8868	-4522	45
H(17)	499	9738	-4057	49
H(18)	-116	9756	-2225	41

Report: November 18, 2010
Structure: DR77 ((±)-**4.71**)
Operator: Dr. Joseph H. Reibenspies
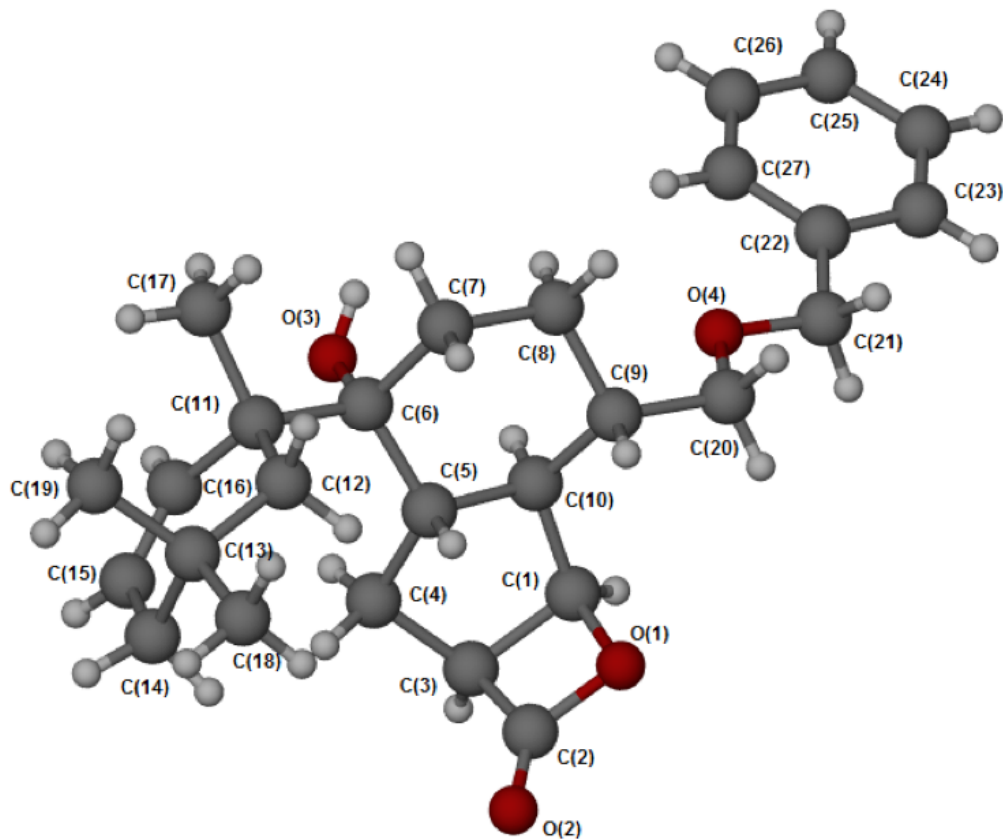
Figure A-10. Single X-ray structure of (±)-**4.71**.

Table A-17. Crystal data and structure refinement for dr77 ((±)-**4.71**).

Identification code	dr77
Empirical formula	C27 H36 O4
Formula weight	424.56
Temperature	296(2) K
Wavelength	1.54178 Å
Crystal system	Monoclinic
Space group	P2(1)/c
Unit cell dimensions	a = 8.4876(4) Å $\quad$ a= 90°.
	b = 30.4533(16) Å $\quad$ b= 108.998(3)°.
	c = 9.6704(5) Å $\quad$ g = 90°.
Volume	2363.4(2) Å^3
Z	4
Density (calculated)	1.193 Mg/m^3
Absorption coefficient	0.621 mm^{-1}
F(000)	920
Crystal size	2.00 x 0.30 x 0.01 mm^3
Theta range for data collection	5.05 to 60.00°.
Index ranges	-9<=h<=9, -34<=k<=34, -10<=l<=10
Reflections collected	16694
Independent reflections	3198 [R(int) = 0.0372]
Completeness to theta = 60.00°	90.9 %
Absorption correction	Semi-empirical from equivalents
Max. and min. transmission	0.9938 and 0.3700
Refinement method	Full-matrix least-squares on F^2
Data / restraints / parameters	3198 / 0 / 285
Goodness-of-fit on F^2	1.000
Final R indices [I>2sigma(I)]	R1 = 0.0441, wR2 = 0.1087
R indices (all data)	R1 = 0.0537, wR2 = 0.1159
Extinction coefficient	0.0045(4)
Largest diff. peak and hole	0.177 and -0.200 e.Å^{-3}

Table A-18. Atomic coordinates (x 10^4) and equivalent isotropic displacement parameters ($\mathring{A}^2$x 10^3) for dr77 (($\pm$)-**4.71**). U(eq) is defined as one third of the trace of the orthogonalized U^{ij} tensor.

	x	y	z	U(eq)
O(1)	-2339(2)	-51(1)	2552(2)	27(1)
O(2)	-4521(2)	427(1)	1818(2)	39(1)
O(3)	2242(2)	792(1)	1211(1)	25(1)
O(4)	2684(2)	-653(1)	3240(2)	26(1)
C(1)	-1289(2)	-85(1)	1571(2)	23(1)
C(2)	-3353(2)	243(1)	1631(2)	27(1)
C(3)	-2443(2)	248(1)	528(2)	23(1)
C(4)	-1423(2)	668(1)	588(2)	21(1)
C(5)	-34(2)	632(1)	2065(2)	19(1)
C(6)	1572(2)	908(1)	2355(2)	20(1)
C(7)	2774(2)	774(1)	3863(2)	25(1)
C(8)	3078(2)	281(1)	4103(2)	26(1)
C(9)	1457(2)	21(1)	3763(2)	22(1)
C(10)	379(2)	136(1)	2214(2)	20(1)
C(11)	1288(2)	1424(1)	2272(2)	24(1)
C(12)	419(3)	1571(1)	3381(2)	30(1)
C(13)	-666(3)	1985(1)	3017(3)	35(1)
C(14)	-1937(3)	1928(1)	1479(3)	39(1)
C(15)	-1139(3)	1781(1)	391(3)	34(1)
C(16)	269(3)	1554(1)	744(2)	27(1)
C(17)	3005(3)	1651(1)	2609(3)	36(1)
C(18)	-1591(4)	2027(1)	4130(3)	50(1)
C(19)	344(3)	2403(1)	3060(3)	46(1)
C(20)	1747(3)	-466(1)	4080(2)	28(1)
C(21)	2915(3)	-1109(1)	3518(2)	28(1)
C(22)	4198(2)	-1296(1)	2919(2)	27(1)
C(23)	4541(3)	-1745(1)	3091(3)	37(1)
C(24)	5701(3)	-1935(1)	2554(3)	46(1)

Table A-18. Atomic coordinates (x 10^4) and equivalent isotropic displacement parameters (Å^2x 10^3) for dr77 (($\pm$)-**4.71**). U(eq) is defined as one third of the trace of the orthogonalized U^{ij} tensor (continued).

	x	y	z	U(eq)
C(25)	6540(3)	-1681(1)	1835(3)	46(1)
C(26)	6229(3)	-1237(1)	1678(3)	39(1)
C(27)	5079(3)	-1045(1)	2233(2)	30(1)

Table A-19. Bond lengths [Å] and angles [°] for dr77 (($\pm$)-**4.71**).

O(1)-C(2)	1.356(2)
O(1)-C(1)	1.501(2)
O(2)-C(2)	1.201(2)
O(3)-C(6)	1.443(2)
O(3)-H(3)	0.8200
O(4)-C(21)	1.415(2)
O(4)-C(20)	1.427(2)
C(1)-C(10)	1.507(3)
C(1)-C(3)	1.537(3)
C(1)-H(1)	0.9800
C(2)-C(3)	1.507(3)
C(3)-C(4)	1.534(3)
C(3)-H(3A)	0.9800
C(4)-C(5)	1.531(3)
C(4)-H(4A)	0.9700
C(4)-H(4B)	0.9700
C(5)-C(6)	1.547(3)
C(5)-C(10)	1.547(2)
C(5)-H(5)	0.9800
C(6)-C(7)	1.538(3)
C(6)-C(11)	1.587(3)

Table A-19. Bond lengths [Å] and angles [°] for dr77 ((±)-**4.71**) (continued).

C(7)-C(8)	1.529(3)
C(7)-H(7A)	0.9700
C(7)-H(7B)	0.9700
C(8)-C(9)	1.527(3)
C(8)-H(8A)	0.9700
C(8)-H(8B)	0.9700
C(9)-C(20)	1.518(3)
C(9)-C(10)	1.520(3)
C(9)-H(9)	0.9800
C(10)-H(10)	0.9800
C(11)-C(16)	1.502(3)
C(11)-C(17)	1.548(3)
C(11)-C(12)	1.553(3)
C(12)-C(13)	1.532(3)
C(12)-H(12A)	0.9700
C(12)-H(12B)	0.9700
C(13)-C(19)	1.528(3)
C(13)-C(18)	1.530(3)
C(13)-C(14)	1.537(3)
C(14)-C(15)	1.494(3)
C(14)-H(14A)	0.9700
C(14)-H(14B)	0.9700
C(15)-C(16)	1.326(3)
C(15)-H(15)	0.9300
C(16)-H(16)	0.9300
C(17)-H(17A)	0.9600
C(17)-H(17B)	0.9600
C(17)-H(17C)	0.9600
C(18)-H(18A)	0.9600
C(18)-H(18B)	0.9600
C(18)-H(18C)	0.9600
C(19)-H(19A)	0.9600

Table A-19. Bond lengths [Å] and angles [°] for dr77 ((±)-**4.71**) (continued).

C(19)-H(19B)	0.9600
C(19)-H(19C)	0.9600
C(20)-H(20A)	0.9700
C(20)-H(20B)	0.9700
C(21)-C(22)	1.503(3)
C(21)-H(21A)	0.9700
C(21)-H(21B)	0.9700
C(22)-C(27)	1.382(3)
C(22)-C(23)	1.396(3)
C(23)-C(24)	1.381(3)
C(23)-H(23)	0.9300
C(24)-C(25)	1.382(3)
C(24)-H(24)	0.9300
C(25)-C(26)	1.378(3)
C(25)-H(25)	0.9300
C(26)-C(27)	1.387(3)
C(26)-H(26)	0.9300
C(27)-H(27)	0.9300
C(2)-O(1)-C(1)	90.63(14)
C(6)-O(3)-H(3)	109.5
C(21)-O(4)-C(20)	110.64(14)
O(1)-C(1)-C(10)	112.36(15)
O(1)-C(1)-C(3)	89.30(13)
C(10)-C(1)-C(3)	106.75(15)
O(1)-C(1)-H(1)	115.2
C(10)-C(1)-H(1)	115.2
C(3)-C(1)-H(1)	115.2
O(2)-C(2)-O(1)	126.0(2)
O(2)-C(2)-C(3)	137.7(2)
O(1)-C(2)-C(3)	96.26(15)
C(2)-C(3)-C(4)	113.24(16)
C(2)-C(3)-C(1)	83.82(15)

Table A-19. Bond lengths [Å] and angles [°] for dr77 ((±)-**4.71**) (continued).

C(4)-C(3)-C(1)	107.08(15)
C(2)-C(3)-H(3A)	116.1
C(4)-C(3)-H(3A)	116.1
C(1)-C(3)-H(3A)	116.1
C(5)-C(4)-C(3)	103.30(15)
C(5)-C(4)-H(4A)	111.1
C(3)-C(4)-H(4A)	111.1
C(5)-C(4)-H(4B)	111.1
C(3)-C(4)-H(4B)	111.1
H(4A)-C(4)-H(4B)	109.1
C(4)-C(5)-C(6)	119.75(15)
C(4)-C(5)-C(10)	103.79(14)
C(6)-C(5)-C(10)	110.74(15)
C(4)-C(5)-H(5)	107.3
C(6)-C(5)-H(5)	107.3
C(10)-C(5)-H(5)	107.3
O(3)-C(6)-C(7)	110.94(15)
O(3)-C(6)-C(5)	105.80(14)
C(7)-C(6)-C(5)	107.57(15)
O(3)-C(6)-C(11)	107.08(14)
C(7)-C(6)-C(11)	110.67(15)
C(5)-C(6)-C(11)	114.71(15)
C(8)-C(7)-C(6)	115.52(16)
C(8)-C(7)-H(7A)	108.4
C(6)-C(7)-H(7A)	108.4
C(8)-C(7)-H(7B)	108.4
C(6)-C(7)-H(7B)	108.4
H(7A)-C(7)-H(7B)	107.5
C(9)-C(8)-C(7)	112.39(16)
C(9)-C(8)-H(8A)	109.1
C(7)-C(8)-H(8A)	109.1
C(9)-C(8)-H(8B)	109.1

Table A-19. Bond lengths [Å] and angles [°] for dr77 ((±)-**4.71**) (continued).

C(7)-C(8)-H(8B)	109.1
H(8A)-C(8)-H(8B)	107.9
C(20)-C(9)-C(10)	115.49(17)
C(20)-C(9)-C(8)	112.78(16)
C(10)-C(9)-C(8)	107.69(15)
C(20)-C(9)-H(9)	106.8
C(10)-C(9)-H(9)	106.8
C(8)-C(9)-H(9)	106.8
C(1)-C(10)-C(9)	119.14(16)
C(1)-C(10)-C(5)	104.11(15)
C(9)-C(10)-C(5)	111.23(15)
C(1)-C(10)-H(10)	107.3
C(9)-C(10)-H(10)	107.3
C(5)-C(10)-H(10)	107.3
C(16)-C(11)-C(17)	106.89(16)
C(16)-C(11)-C(12)	110.62(16)
C(17)-C(11)-C(12)	110.61(17)
C(16)-C(11)-C(6)	109.90(15)
C(17)-C(11)-C(6)	108.30(16)
C(12)-C(11)-C(6)	110.43(15)
C(13)-C(12)-C(11)	117.65(17)
C(13)-C(12)-H(12A)	107.9
C(11)-C(12)-H(12A)	107.9
C(13)-C(12)-H(12B)	107.9
C(11)-C(12)-H(12B)	107.9
H(12A)-C(12)-H(12B)	107.2
C(19)-C(13)-C(18)	108.78(18)
C(19)-C(13)-C(12)	112.94(19)
C(18)-C(13)-C(12)	108.38(18)
C(19)-C(13)-C(14)	109.30(19)
C(18)-C(13)-C(14)	109.3(2)
C(12)-C(13)-C(14)	108.07(17)

Table A-19. Bond lengths [Å] and angles [°] for dr77 ((±)-**4.71**) (continued).

C(15)-C(14)-C(13)	112.24(19)
C(15)-C(14)-H(14A)	109.2
C(13)-C(14)-H(14A)	109.2
C(15)-C(14)-H(14B)	109.2
C(13)-C(14)-H(14B)	109.2
H(14A)-C(14)-H(14B)	107.9
C(16)-C(15)-C(14)	123.6(2)
C(16)-C(15)-H(15)	118.2
C(14)-C(15)-H(15)	118.2
C(15)-C(16)-C(11)	124.98(19)
C(15)-C(16)-H(16)	117.5
C(11)-C(16)-H(16)	117.5
C(11)-C(17)-H(17A)	109.5
C(11)-C(17)-H(17B)	109.5
H(17A)-C(17)-H(17B)	109.5
C(11)-C(17)-H(17C)	109.5
H(17A)-C(17)-H(17C)	109.5
H(17B)-C(17)-H(17C)	109.5
C(13)-C(18)-H(18A)	109.5
C(13)-C(18)-H(18B)	109.5
H(18A)-C(18)-H(18B)	109.5
C(13)-C(18)-H(18C)	109.5
H(18A)-C(18)-H(18C)	109.5
H(18B)-C(18)-H(18C)	109.5
C(13)-C(19)-H(19A)	109.5
C(13)-C(19)-H(19B)	109.5
H(19A)-C(19)-H(19B)	109.5
C(13)-C(19)-H(19C)	109.5
H(19A)-C(19)-H(19C)	109.5
H(19B)-C(19)-H(19C)	109.5
O(4)-C(20)-C(9)	111.04(15)
O(4)-C(20)-H(20A)	109.4

Table A-19. Bond lengths [Å] and angles [°] for dr77 ((±)-**4.71**) (continued).

C(9)-C(20)-H(20A)	109.4
O(4)-C(20)-H(20B)	109.4
C(9)-C(20)-H(20B)	109.4
H(20A)-C(20)-H(20B)	108.0
O(4)-C(21)-C(22)	111.91(16)
O(4)-C(21)-H(21A)	109.2
C(22)-C(21)-H(21A)	109.2
O(4)-C(21)-H(21B)	109.2
C(22)-C(21)-H(21B)	109.2
H(21A)-C(21)-H(21B)	107.9
C(27)-C(22)-C(23)	118.44(19)
C(27)-C(22)-C(21)	123.16(17)
C(23)-C(22)-C(21)	118.38(18)
C(24)-C(23)-C(22)	120.7(2)
C(24)-C(23)-H(23)	119.6
C(22)-C(23)-H(23)	119.6
C(23)-C(24)-C(25)	120.2(2)
C(23)-C(24)-H(24)	119.9
C(25)-C(24)-H(24)	119.9
C(26)-C(25)-C(24)	119.5(2)
C(26)-C(25)-H(25)	120.2
C(24)-C(25)-H(25)	120.2
C(25)-C(26)-C(27)	120.4(2)
C(25)-C(26)-H(26)	119.8
C(27)-C(26)-H(26)	119.8
C(22)-C(27)-C(26)	120.68(19)
C(22)-C(27)-H(27)	119.7
C(26)-C(27)-H(27)	119.7

Symmetry transformations used to generate equivalent atoms.

Table A-20. Anisotropic displacement parameters $(\text{Å}^2 \times 10^3)$ for dr77 $((\pm)$-**4.71**). The anisotropic displacement factor exponent takes the form: $-2p^2[h^2 a^{*2}U^{11} + ... + 2 h k a^* b^* U^{12}]$.

	U^{11}	U^{22}	U^{33}	U^{23}	U^{13}	U^{12}
O(1)	26(1)	28(1)	32(1)	-2(1)	16(1)	-3(1)
O(2)	23(1)	46(1)	52(1)	-6(1)	19(1)	3(1)
O(3)	19(1)	30(1)	27(1)	-1(1)	10(1)	1(1)
O(4)	33(1)	22(1)	26(1)	4(1)	13(1)	8(1)
C(1)	26(1)	21(1)	26(1)	-4(1)	14(1)	-1(1)
C(2)	18(1)	27(1)	35(1)	-7(1)	8(1)	-6(1)
C(3)	17(1)	27(1)	24(1)	-6(1)	5(1)	-2(1)
C(4)	18(1)	22(1)	24(1)	-1(1)	7(1)	1(1)
C(5)	19(1)	19(1)	19(1)	-1(1)	8(1)	2(1)
C(6)	18(1)	24(1)	21(1)	-2(1)	8(1)	0(1)
C(7)	18(1)	31(1)	25(1)	-5(1)	5(1)	-2(1)
C(8)	20(1)	34(1)	21(1)	2(1)	5(1)	6(1)
C(9)	23(1)	25(1)	22(1)	2(1)	11(1)	6(1)
C(10)	18(1)	20(1)	24(1)	-2(1)	10(1)	1(1)
C(11)	28(1)	22(1)	25(1)	-2(1)	11(1)	-3(1)
C(12)	40(1)	23(1)	32(1)	-2(1)	16(1)	-4(1)
C(13)	49(1)	20(1)	46(2)	-3(1)	29(1)	0(1)
C(14)	39(1)	25(1)	54(2)	4(1)	18(1)	4(1)
C(15)	42(1)	23(1)	35(1)	3(1)	9(1)	0(1)
C(16)	35(1)	20(1)	29(1)	1(1)	14(1)	-4(1)
C(17)	35(1)	30(1)	44(2)	-3(1)	11(1)	-10(1)
C(18)	72(2)	26(1)	68(2)	-4(1)	46(2)	3(1)
C(19)	64(2)	22(1)	61(2)	-6(1)	33(2)	-4(1)
C(20)	30(1)	29(1)	29(1)	5(1)	14(1)	7(1)
C(21)	29(1)	21(1)	31(1)	2(1)	6(1)	1(1)
C(22)	25(1)	24(1)	27(1)	-1(1)	1(1)	3(1)
C(23)	39(1)	25(1)	47(2)	2(1)	14(1)	2(1)
C(24)	49(2)	26(1)	64(2)	1(1)	20(1)	13(1)

Table A-20. Anisotropic displacement parameters (Å^2x 10^3) for dr77 (($\pm$)-**4.71**). The anisotropic displacement factor exponent takes the form: $-2p^2[h^2 a^{*2}U^{11} + ... + 2 h k a^* b^* U^{12}]$ (continued).

	U^{11}	U^{22}	U^{33}	U^{23}	U^{13}	U^{12}
C(25)	46(2)	38(1)	62(2)	-3(1)	27(1)	12(1)
C(26)	39(1)	37(1)	47(2)	3(1)	21(1)	5(1)
C(27)	33(1)	23(1)	32(1)	1(1)	8(1)	4(1)

Table A-21. Hydrogen coordinates (x 10^4) and isotropic displacement parameters (Å^2x 10^3) for dr77 (($\pm$)-**4.71**).

	x	y	z	U(eq)
H(3)	3210	711	1576	30
H(1)	-1256	-376	1153	27
H(3A)	-3068	140	-451	28
H(4A)	-968	677	-211	26
H(4B)	-2096	928	549	26
H(5)	-520	708	2824	22
H(7A)	3837	917	4006	30
H(7B)	2338	885	4607	30
H(8A)	3697	176	3483	31
H(8B)	3752	229	5112	31
H(9)	877	132	4417	27
H(10)	1031	71	1568	24
H(12A)	-273	1330	3502	37
H(12B)	1275	1617	4318	37
H(14A)	-2768	1714	1518	47
H(14B)	-2502	2206	1161	47
H(15)	-1656	1853	-587	41
H(16)	655	1468	-12	32
H(17A)	3610	1517	2036	55

Table A-21. Hydrogen coordinates (x 10^4) and isotropic displacement parameters (Å^2x 10^3) for dr77 ((±)-**4.71**) (continued).

	x	y	z	U(eq)
H(17B)	3624	1618	3629	55
H(17C)	2845	1957	2370	55
H(18A)	-2277	2285	3918	74
H(18B)	-798	2050	5097	74
H(18C)	-2278	1773	4074	74
H(19A)	1233	2419	3976	69
H(19B)	-368	2654	2959	69
H(19C)	799	2399	2273	69
H(20A)	2344	-508	5113	34
H(20B)	683	-615	3850	34
H(21A)	1864	-1259	3078	33
H(21B)	3264	-1159	4565	33
H(23)	3982	-1919	3573	44
H(24)	5918	-2235	2676	55
H(25)	7309	-1810	1460	56
H(26)	6793	-1065	1198	47
H(27)	4898	-743	2142	36

NMR spectra
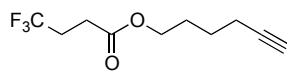
hex-5-yn-1-yl 4,4,4-trifluorobutanoate (**2.7a-2**)
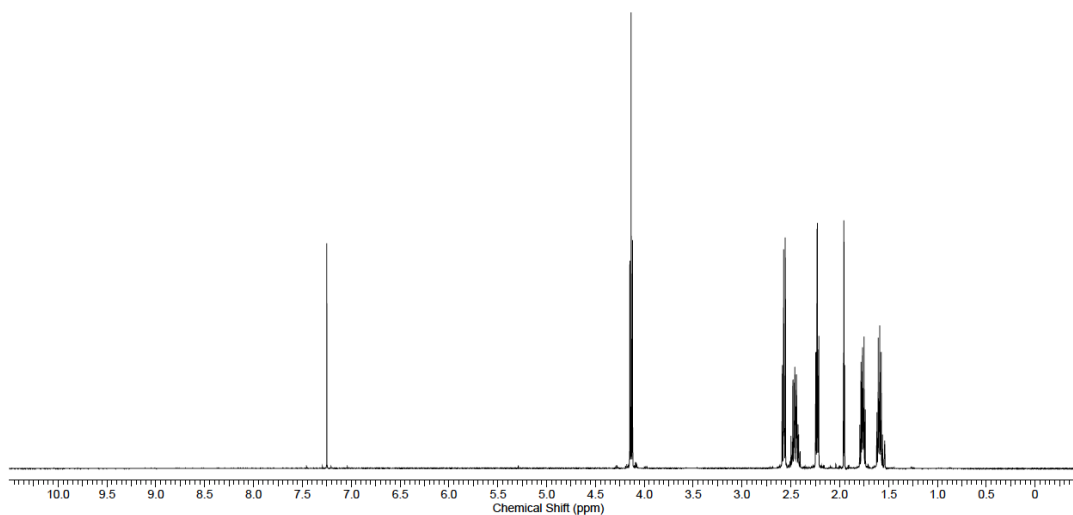
¹H-NMR (500 MHz) of hex-5-yn-1-yl-4,4,4-trifluorobutanoate (**2.7a-2**) in CDCl₃
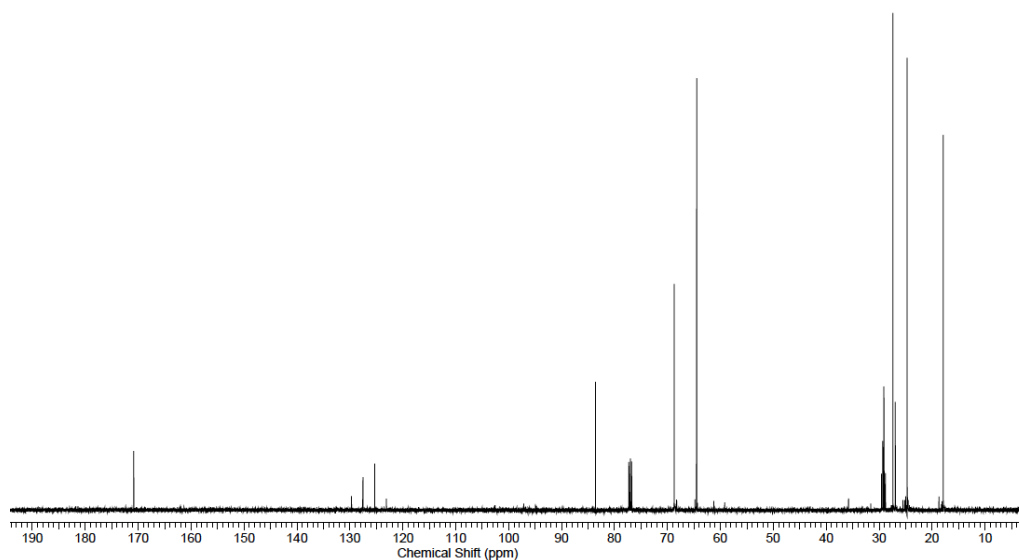
¹³C-NMR (125 MHz) of hex-5-yn-1-yl-4,4,4-trifluorobutanoate (**2.7a-2**) in CDCl₃
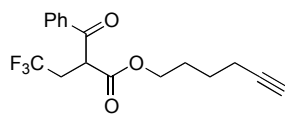
hex-5-yn-1-yl 2-benzoyl-4,4,4-trifluorobutanoate (**2.7a-3**)
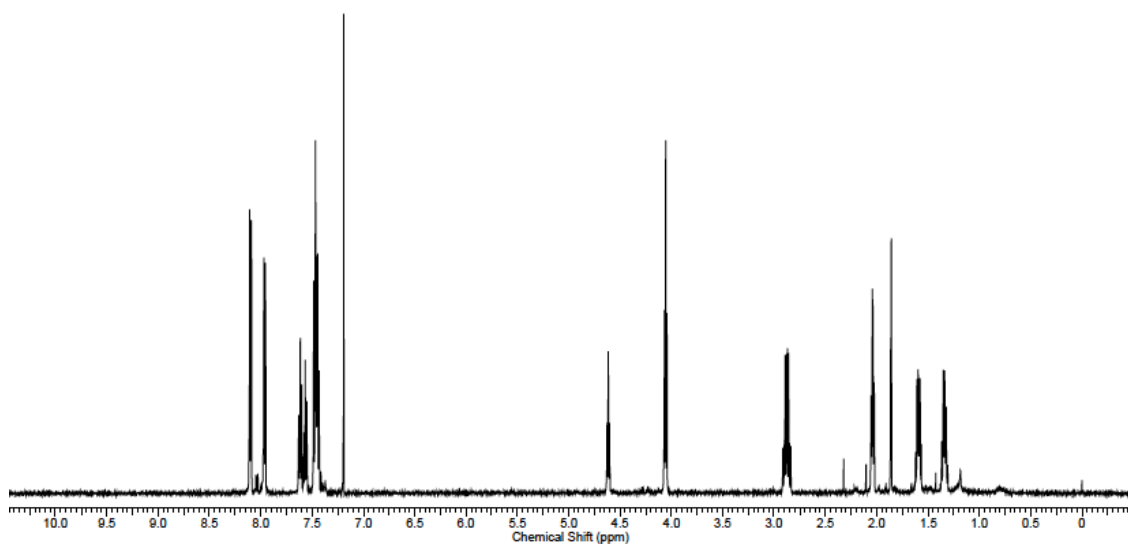
^{1}H-NMR (500 MHz) of hex-5-yn-1-yl 2-benzoyl-4,4,4-trifluorobutanoate (**2.7a-3**) in CDCl$_3$
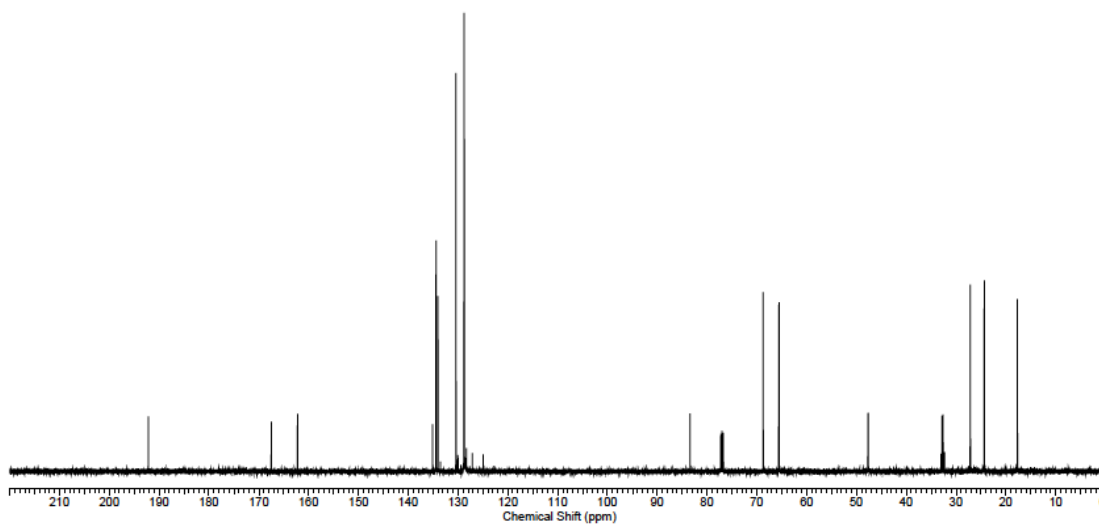
^{13}C-NMR (125 MHz) of hex-5-yn-1-yl 2-benzoyl-4,4,4-trifluorobutanoate (**2.7a-3**) in CDCl$_3$
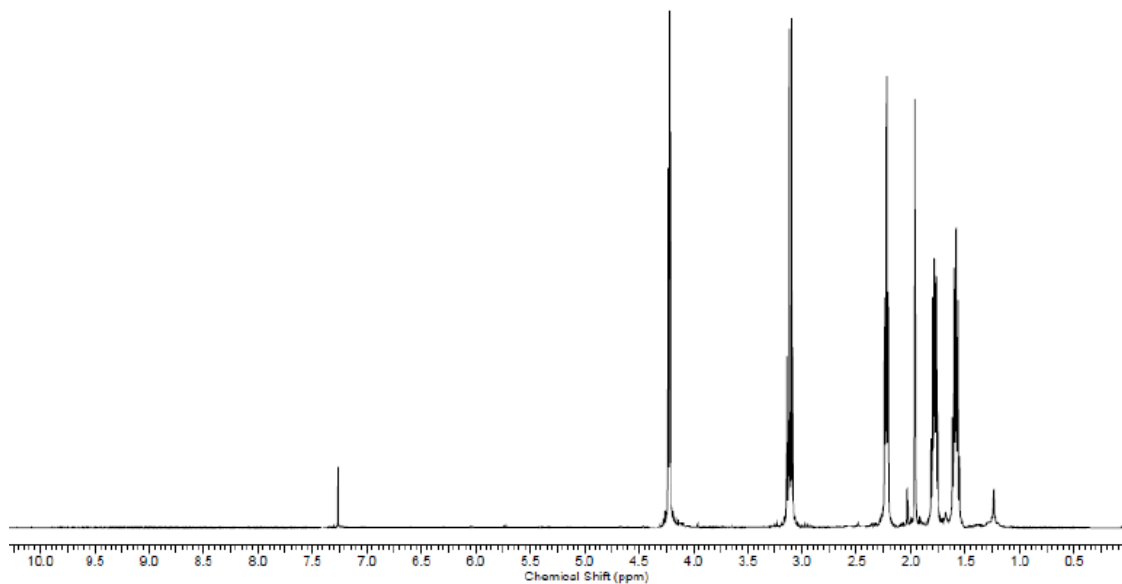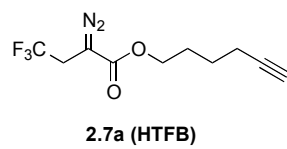
^{1}H-NMR (500 MHz) of hex-5-ynyl 2-diazo-4,4,4-trifluorobutanoate (**2.7a**, HTFB) in CDCl$_3$
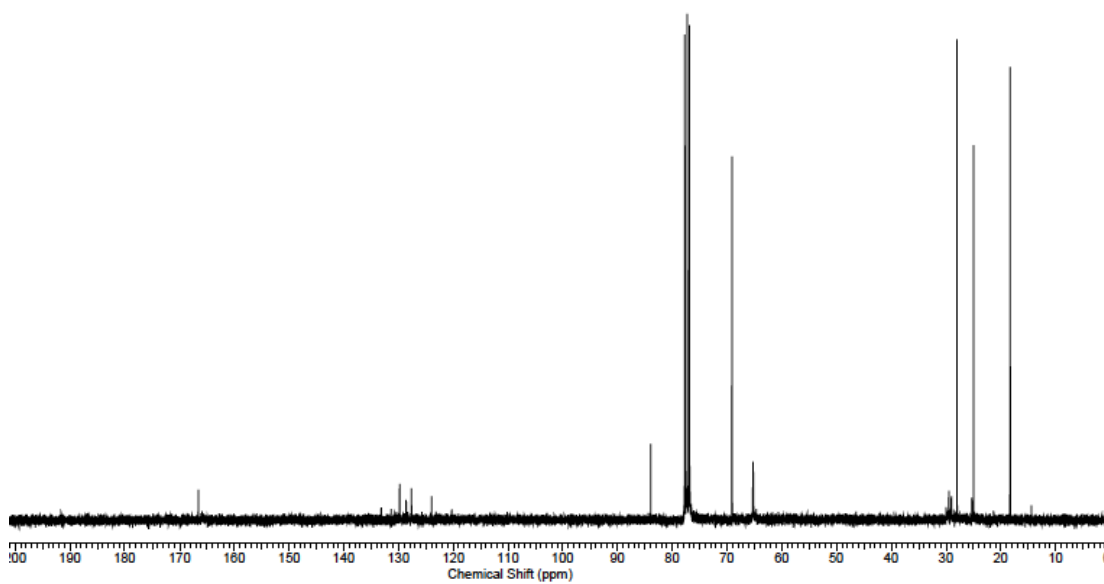
^{13}C-NMR (125 MHz) of hex-5-ynyl 2-diazo-4,4,4-trifluorobutanoate (**2.7a**, HTFB) in CDCl$_3$
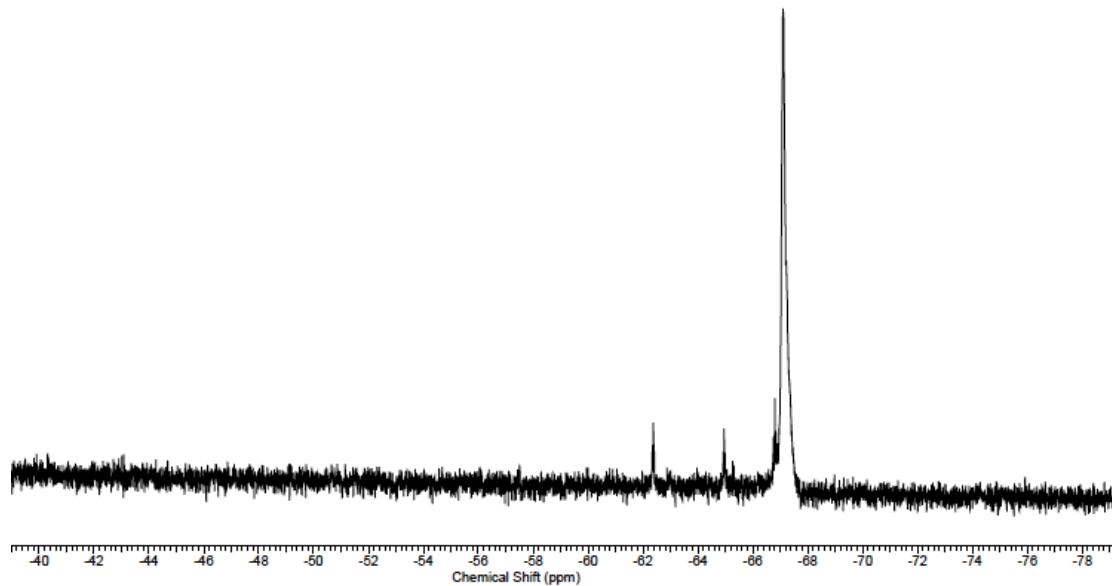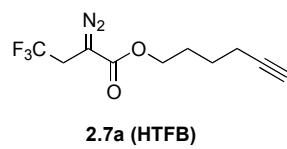
2.7a (HTFB)

^{19}F NMR (300 MHz) of hex-5-ynyl 2-diazo-4,4,4-trifluorobutanoate (**2.7a**, HTFB) in CDCl$_3$ (Trifluoroacetic acid was used as a standard; -76.55 ppm)
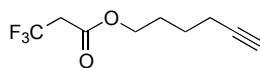
hex-5-yn-1-yl 3,3,3-trifluoropropanoate (**2.7b-2**)
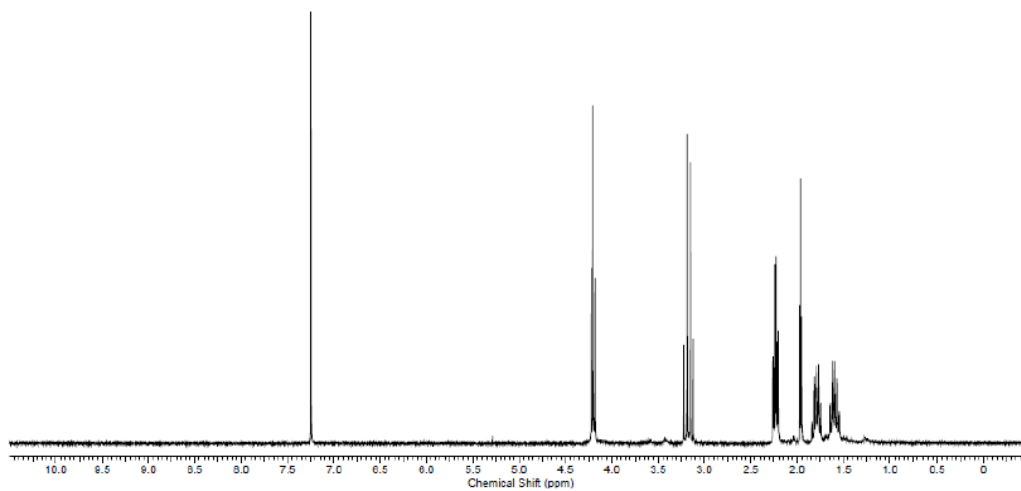
^{1}H-NMR (500 MHz) of hex-5-yn-1-yl 3,3,3-trifluoropropanoate (**2.7b-2**) in CDCl$_3$
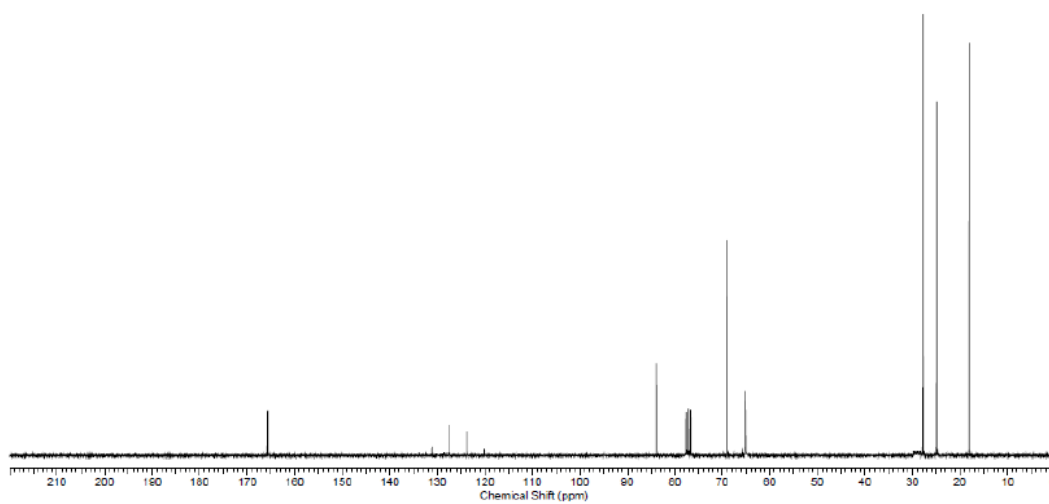
^{13}C-NMR (125 MHz) of hex-5-yn-1-yl 3,3,3-trifluoropropanoate (**2.7b-2**) in CDCl$_3$
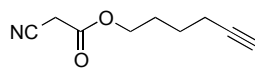
hex-5-yn-1-yl 2-cyanoacetate (**2.7c-2**)
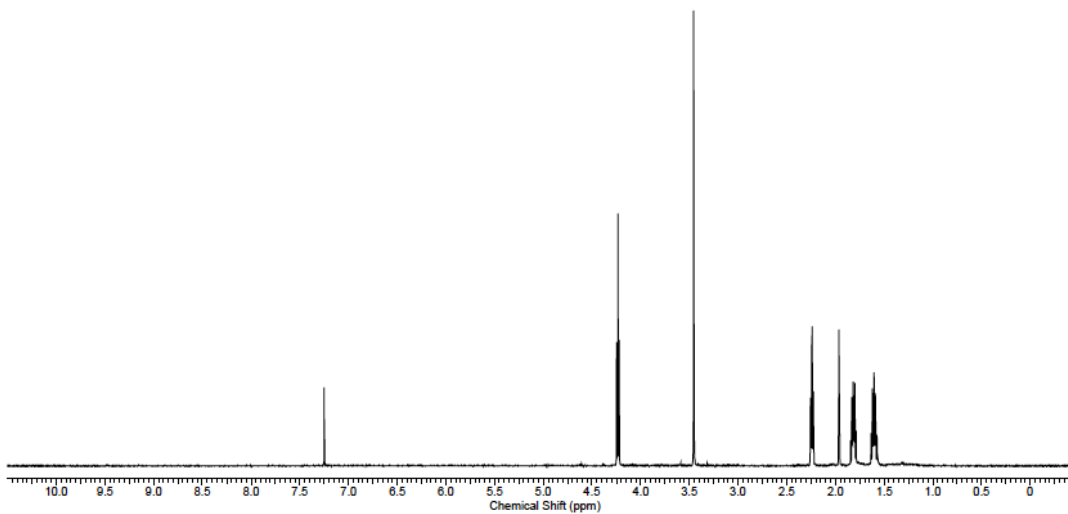
^{1}H-NMR (500 MHz) of hex-5-yn-1-yl 2-cyanoacetate (**2.7c-2**) in CDCl$_3$

^{13}C-NMR (125 MHz) of hex-5-yn-1-yl 2-cyanoacetate (**2.7c-2**) in CDCl$_3$

2.7c
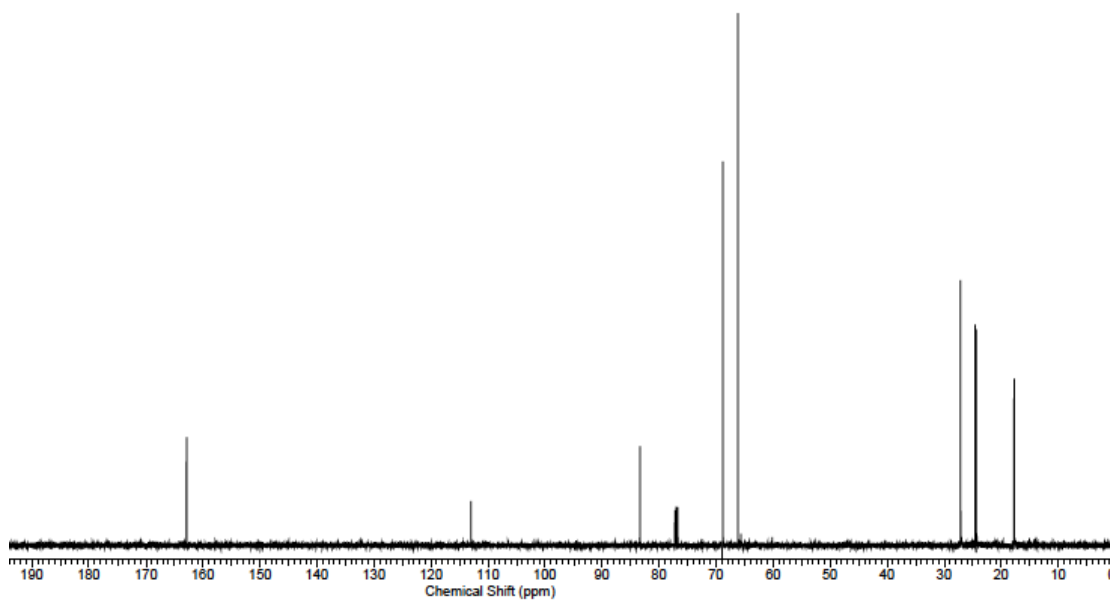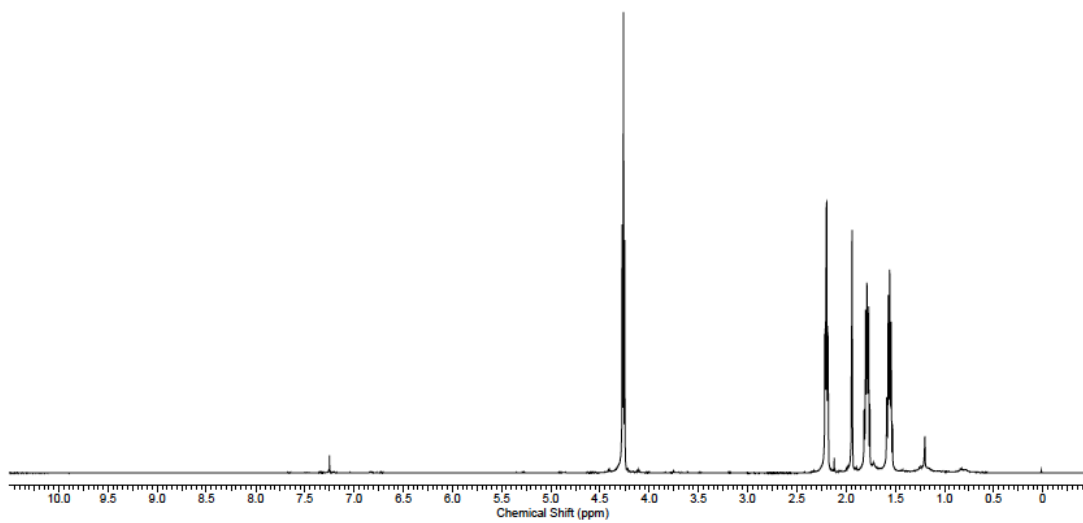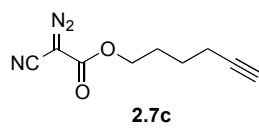
^{1}H-NMR (500 MHz) of hex-5-ynyl 2-cyano-2-diazoacetate (**2.7c**) in CDCl$_3$
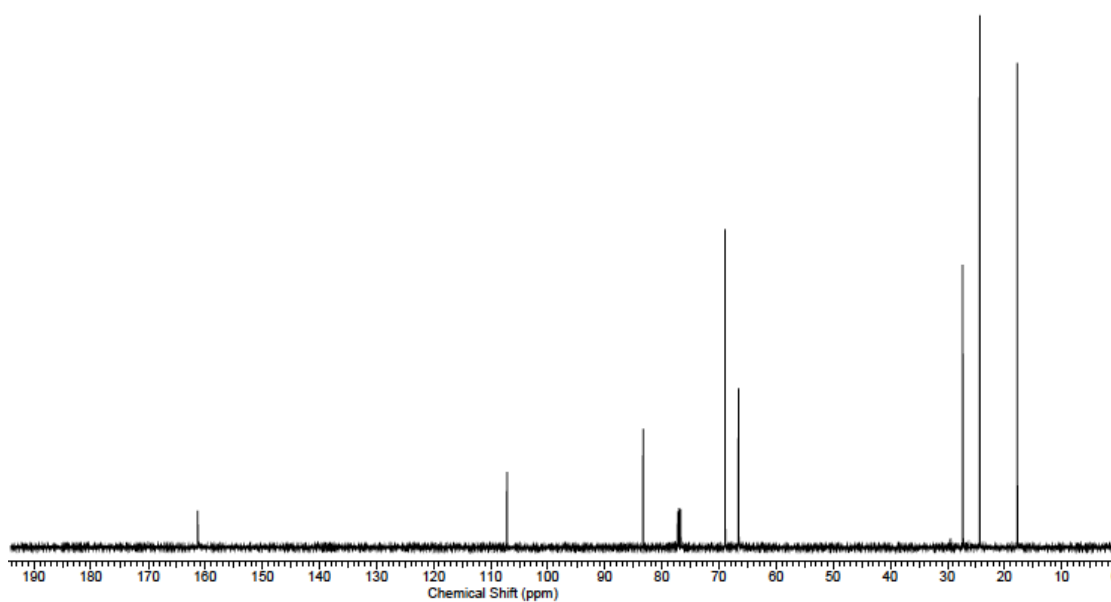
^{13}C-NMR (125 MHz) of hex-5-ynyl 2-cyano-2-diazoacetate (**2.7c**) in CDCl$_3$
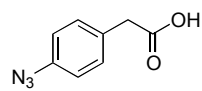
2-(4-azidophenyl)acetic acid (**2.7d-2**)
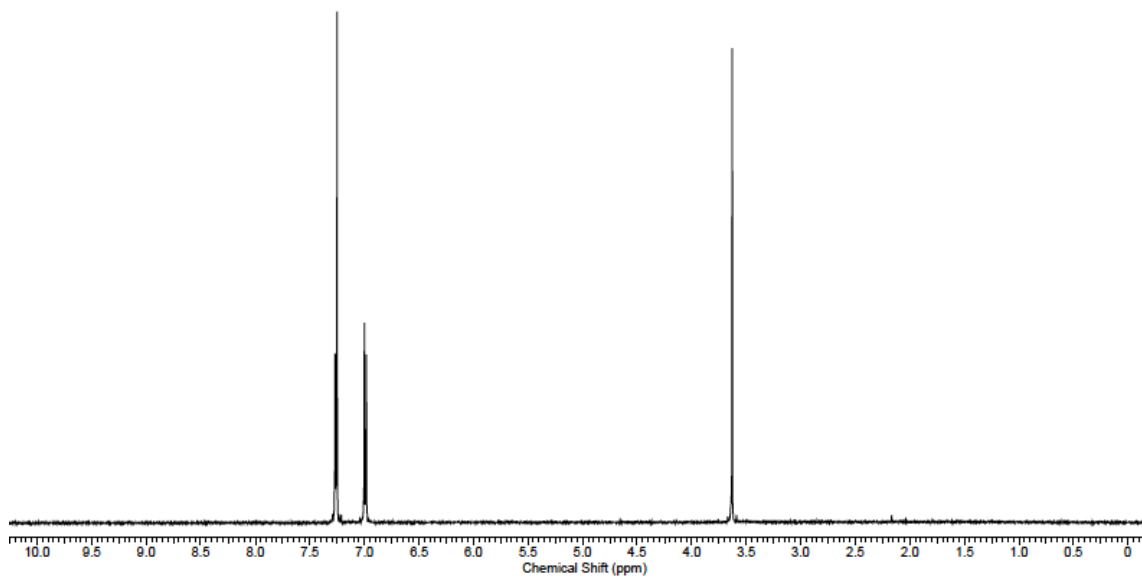
¹H-NMR (500 MHz) of 2-(4-azidophenyl)acetic acid (**2.7d-2**) in CDCl₃
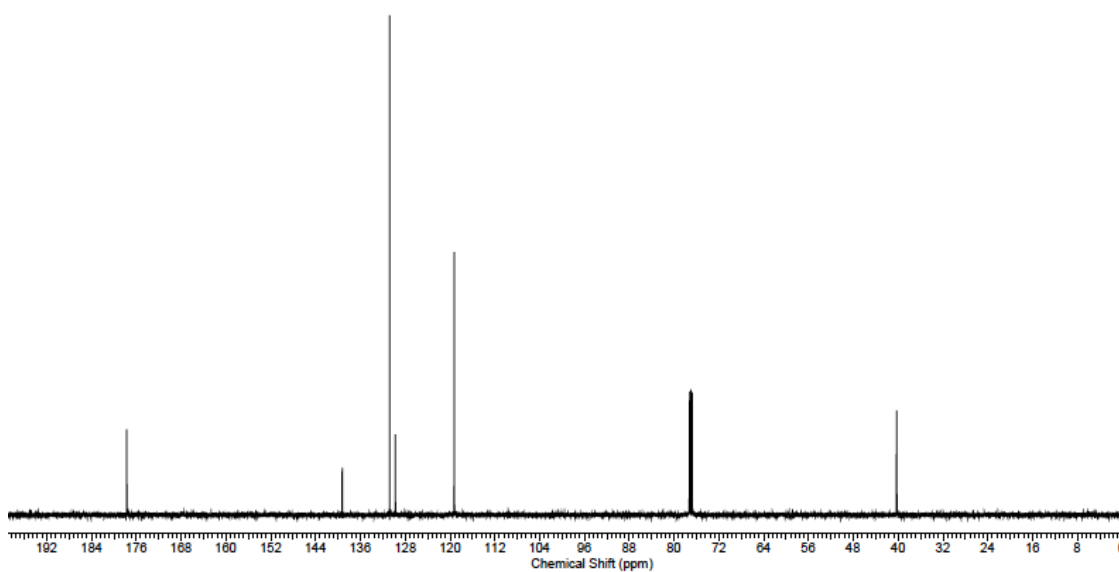
¹³C-NMR (125 MHz) of 2-(4-azidophenyl)acetic acid (**2.7d-2**) in CDCl₃
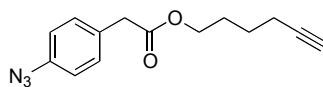
hex-5-yn-1-yl 2-(4-azidophenyl)acetate (**2.7d-3**)
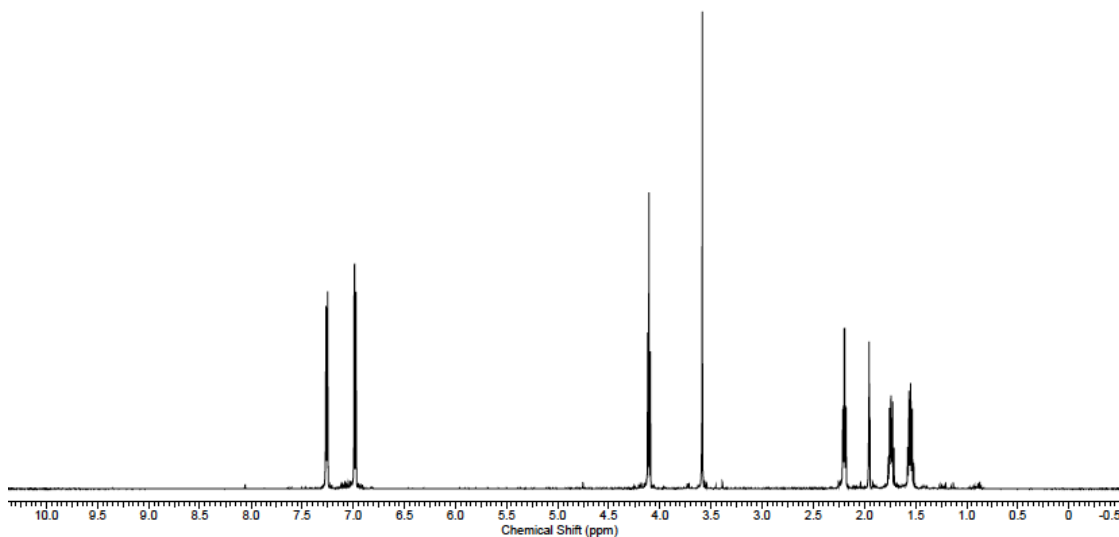
^{1}H-NMR (500 MHz) of hex-5-yn-1-yl 2-(4-azidophenyl)acetic acid (**2.7d-3**) in CDCl$_3$
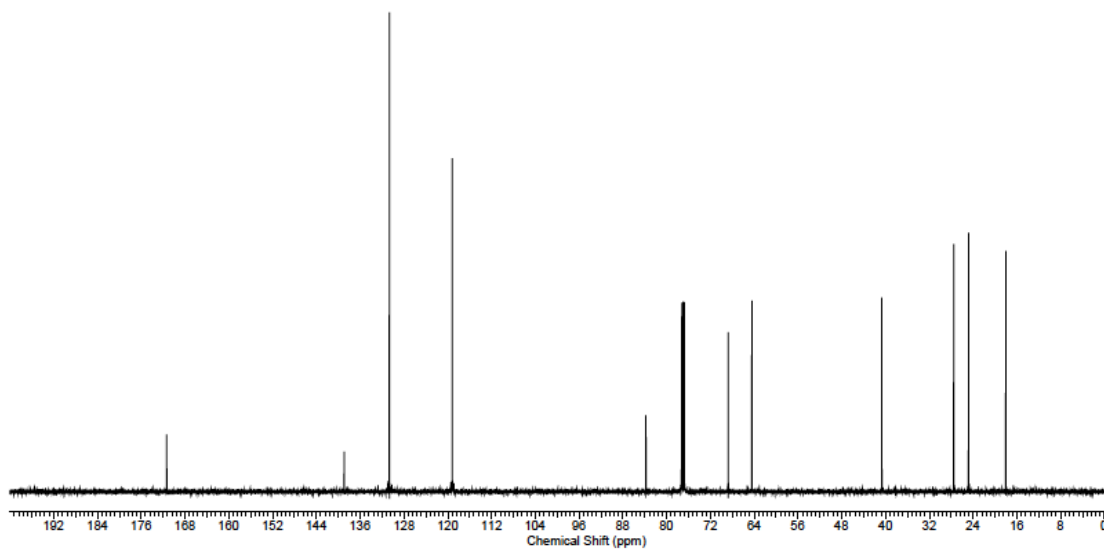
^{13}C-NMR (125 MHz) of hex-5-yn-1-yl 2-(4-azidophenyl)acetic acid (**2.7d-3**) in CDCl$_3$
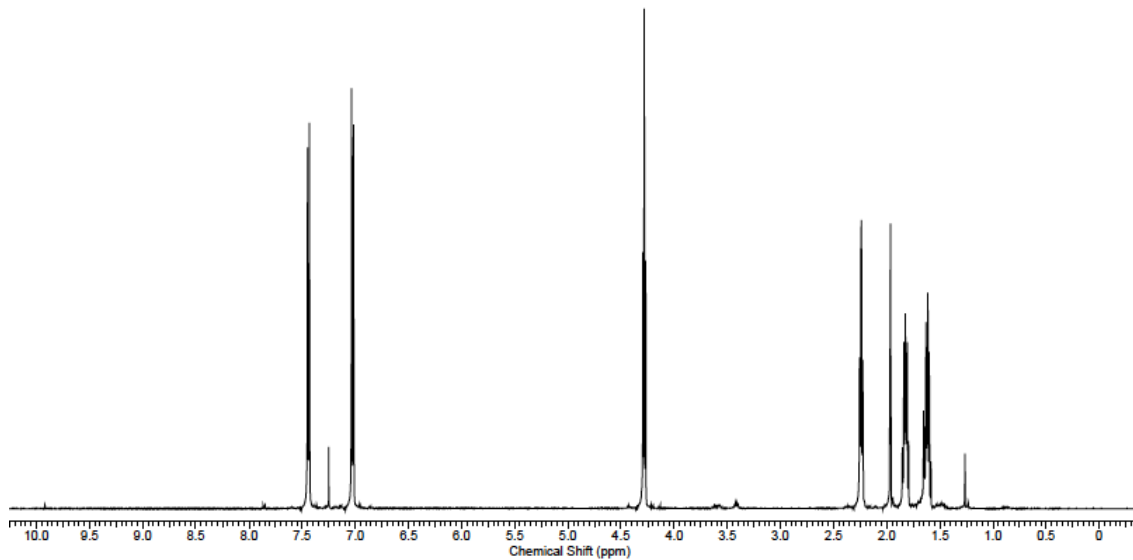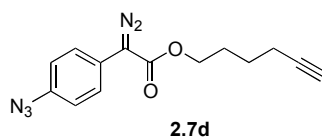
^{1}H-NMR (500 MHz) of hex-5-ynyl 2-(4-azidophenyl)-2-diazoacetate (**2.7d**) in CDCl$_3$
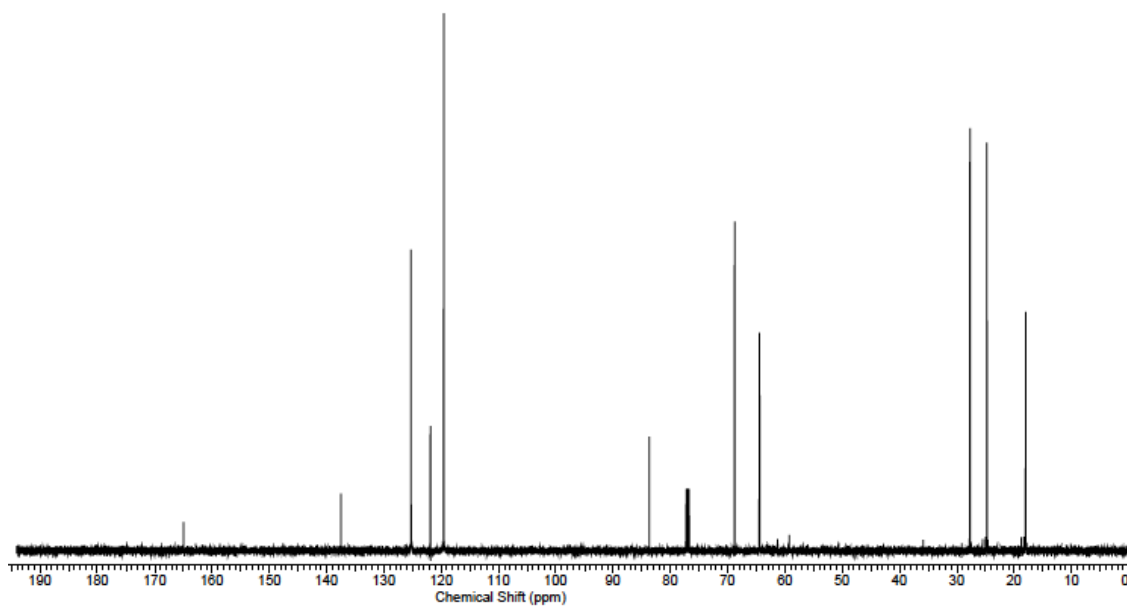
^{13}C-NMR (125 MHz) of hex-5-ynyl 2-(4-azidophenyl)-2-diazoacetate (**2.7d**) in CDCl$_3$
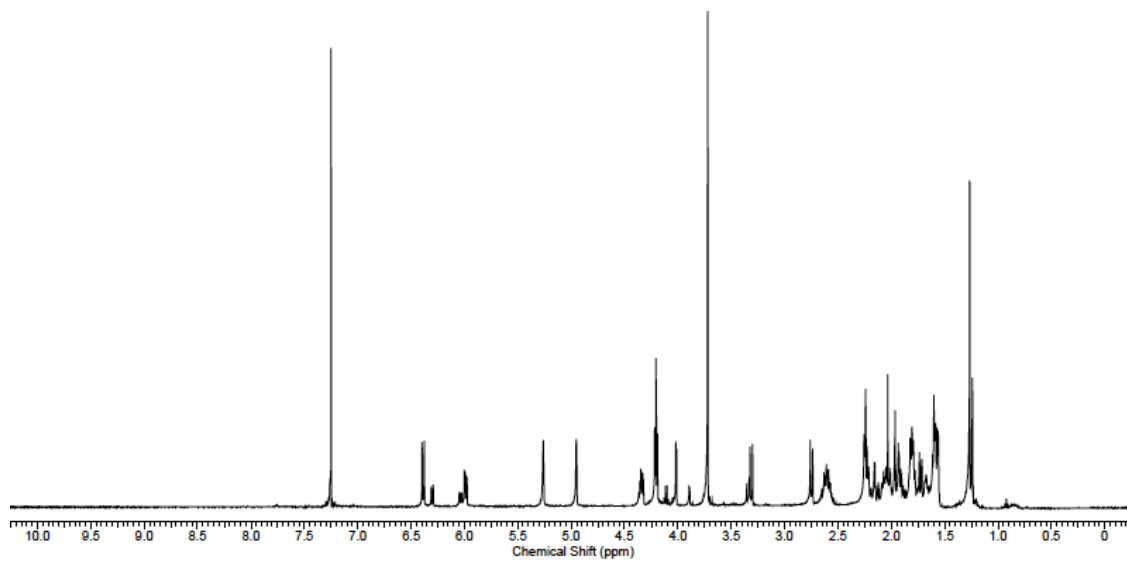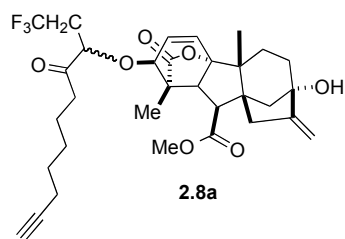
^{1}H-NMR (500 MHz) of gibberellic acid methyl ester 3-HTFB ether (**2.8a**) in CDCl$_3$
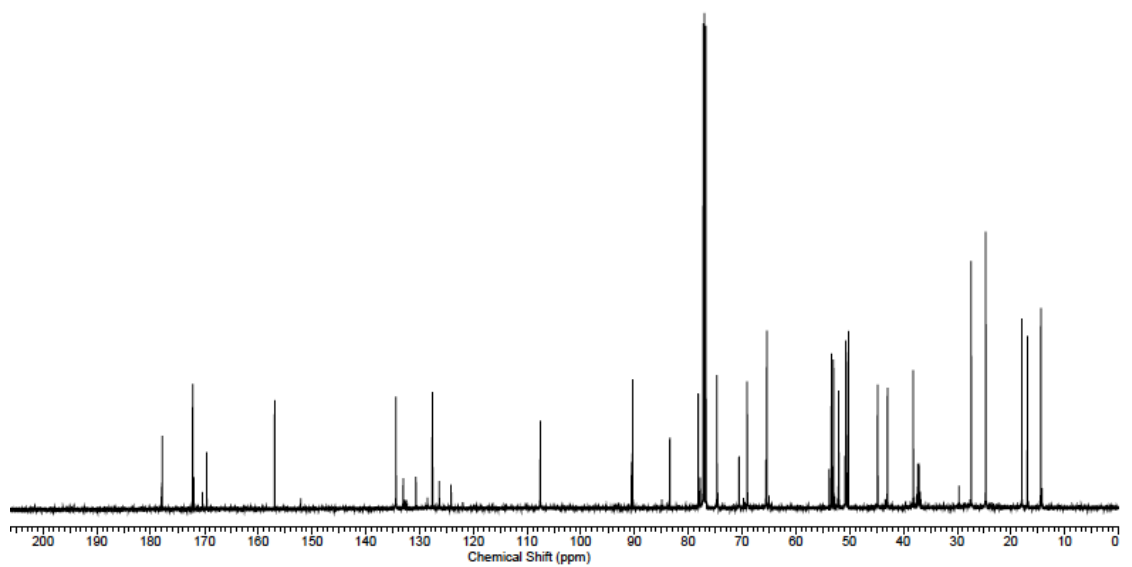
^{3}C-NMR (125 MHz) of gibberellic acid methyl ester 3-HTFB ether (**2.8a**) in CDCl$_3$
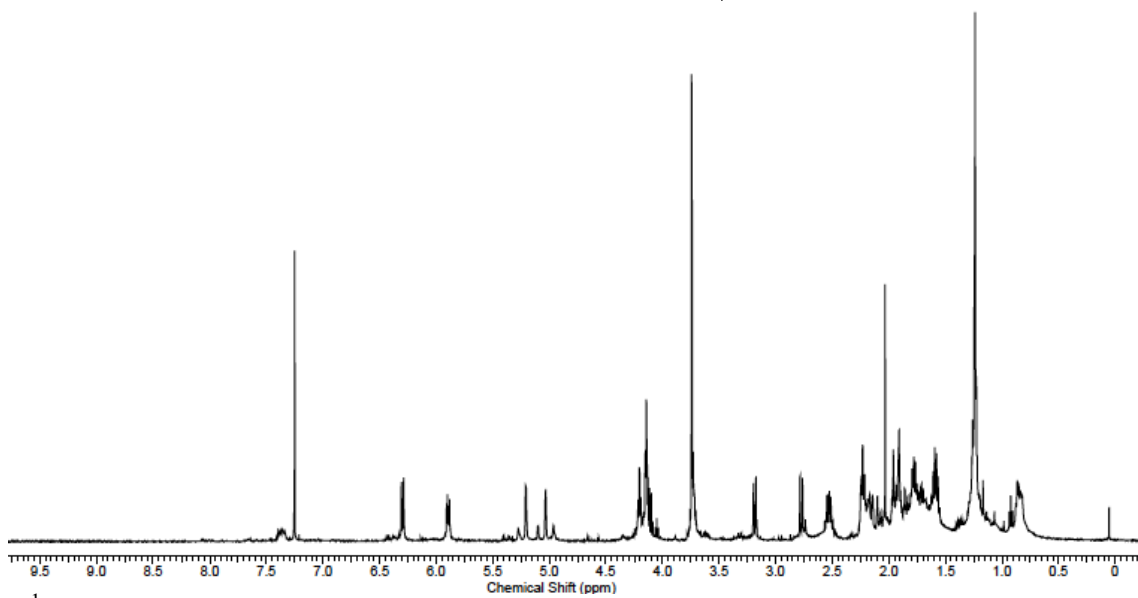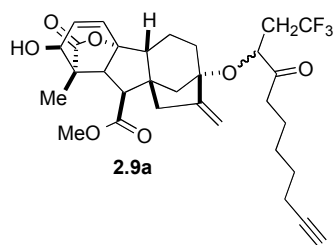
^{1}H-NMR (500 MHz) of gibberellic acid methyl ester 13-HTFB ether (**2.9a**) in CDCl$_3$
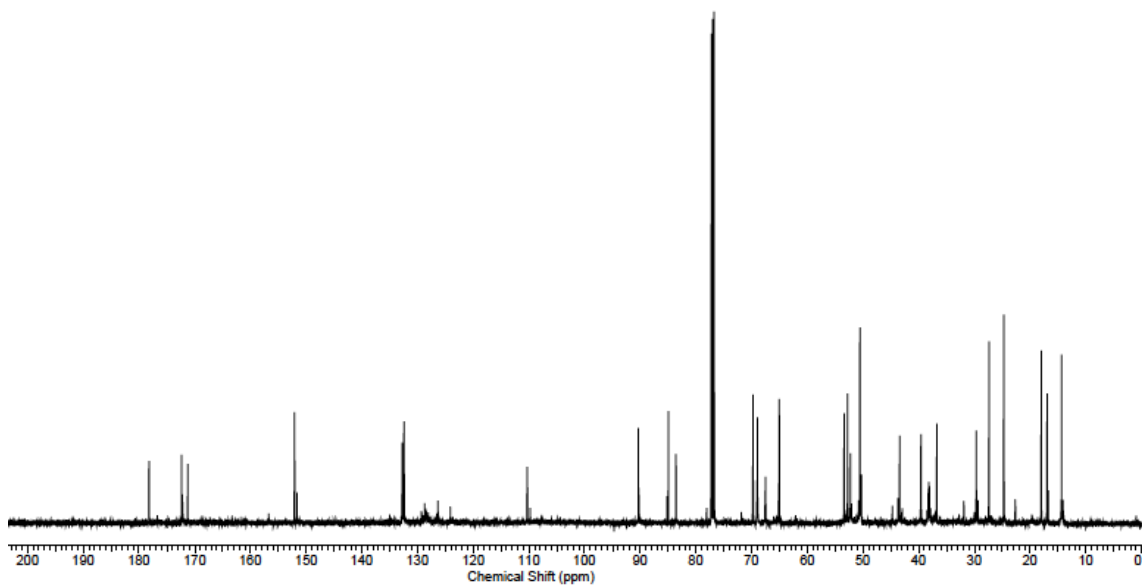
^{13}C-NMR (125 MHz) of gibberellic acid methyl ester 13-HTFB ether (**2.9a**) in CDCl$_3$
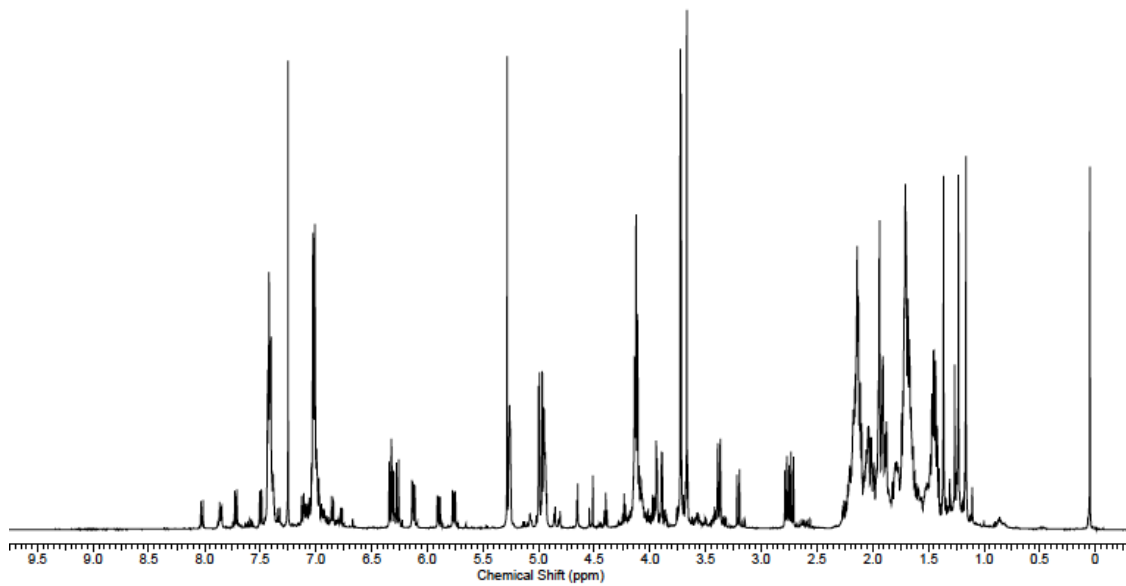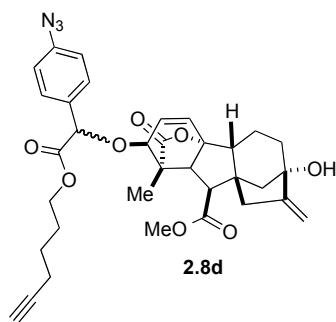
^{1}H-NMR (500 MHz) of gibberellic acid methyl ester 13-**2.7d** ether (**2.8d**) in CDCl$_3$
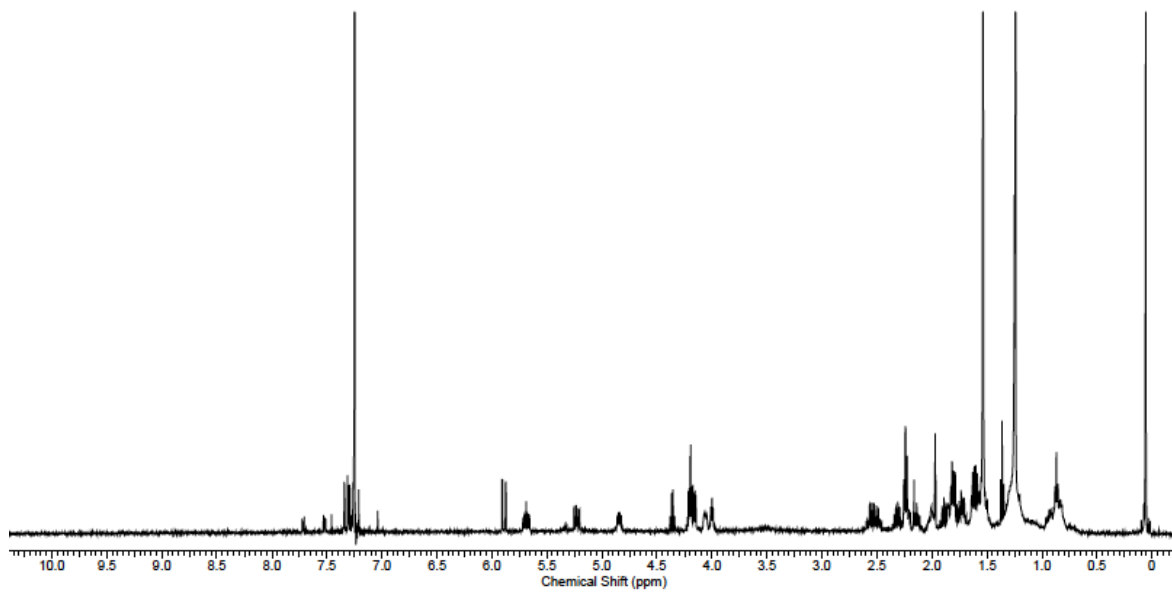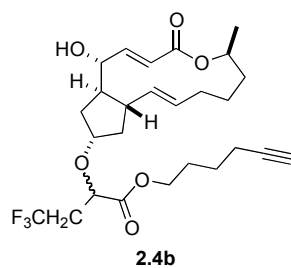
2.4b

^{1}H-NMR (500 MHz) of brefeldin A 13-HTFB ether (**2.4b**) in CDCl$_3$
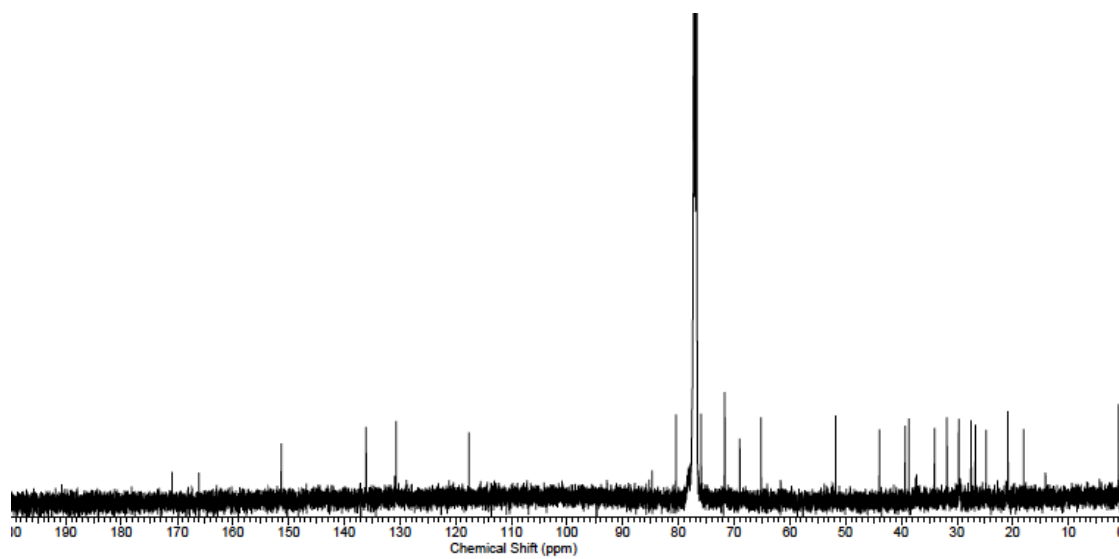
^{13}C-NMR (125 MHz) of brefeldin A 13-HTFB ether (**2.4b**) in CDCl$_3$
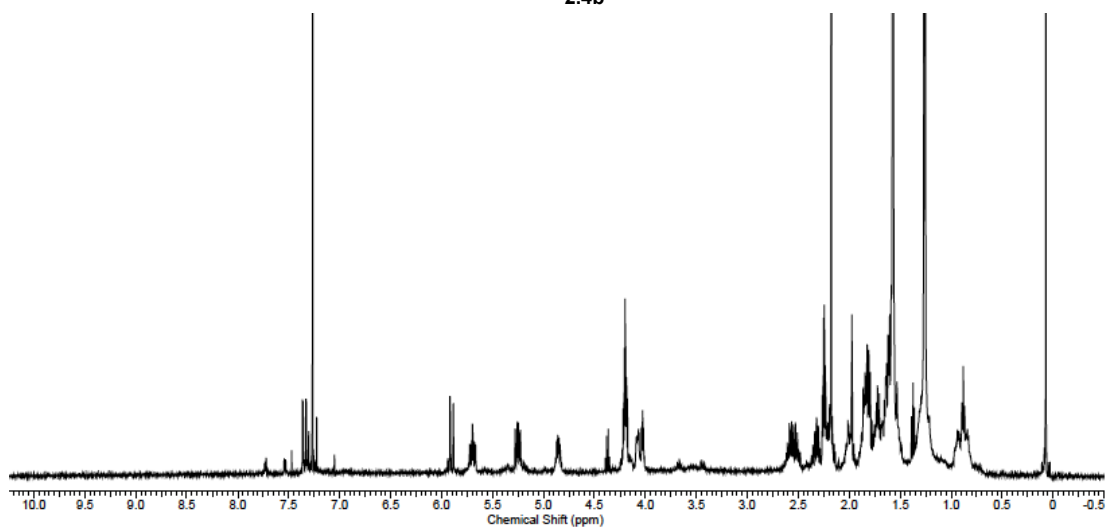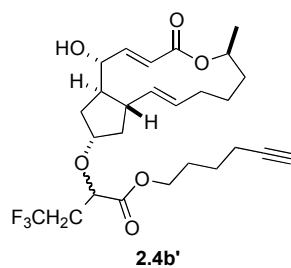
^{1}H-NMR (500 MHz) of brefeldin A 13-HTFB ether (**2.4b′**) in CDCl$_3$
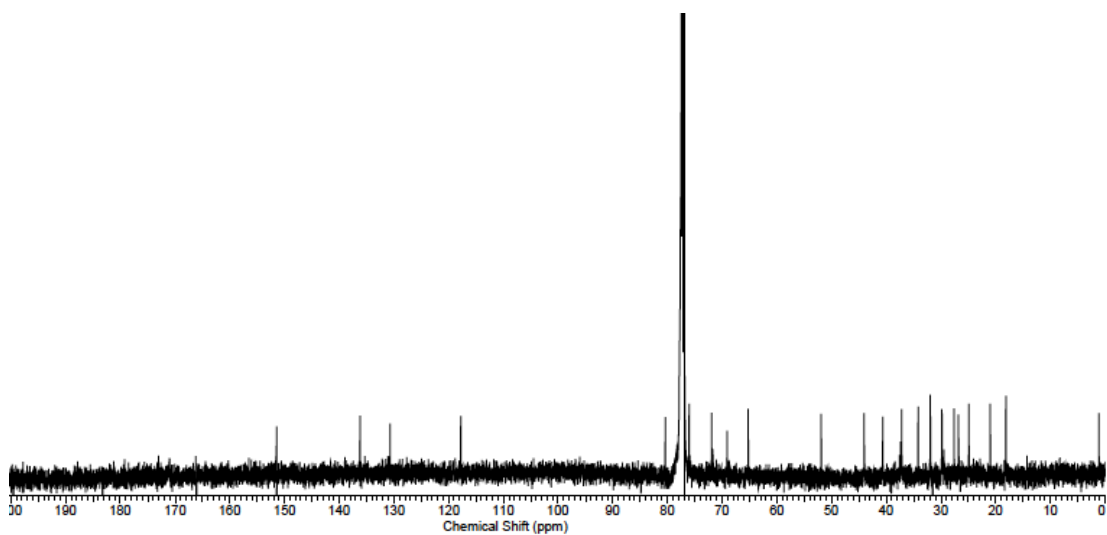
^{13}C-NMR (125 MHz) of brefeldin A 13-HTFB ether (**2.4b′**) in CDCl$_3$
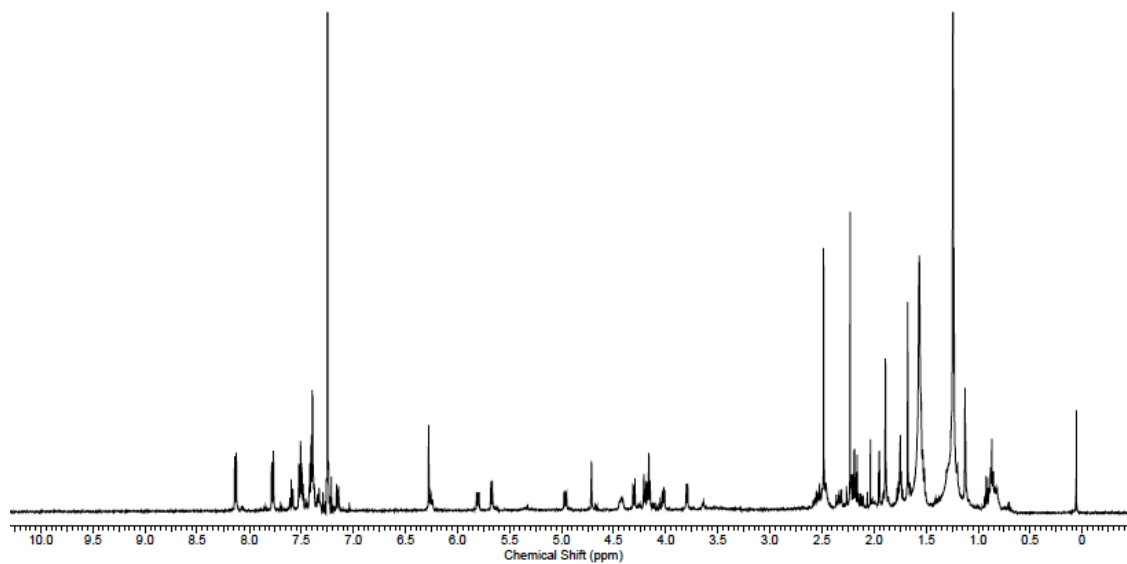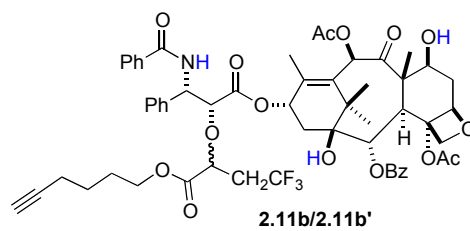
^{1}H-NMR (500 MHz) of paclitaxel 2'-HTFB ether (**2.11b/2.11b′**) in CDCl$_3$
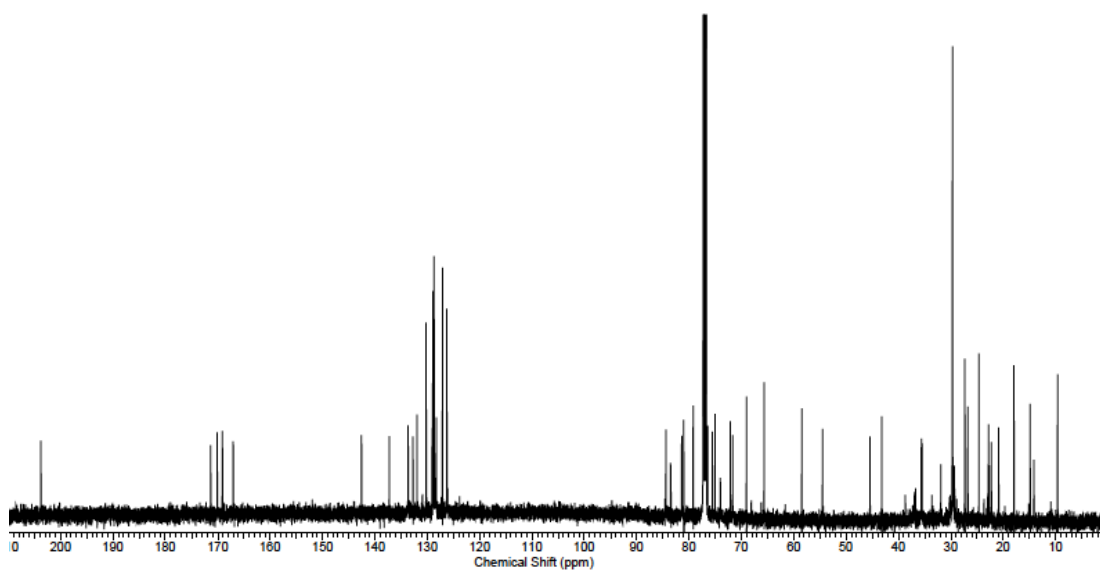
^{13}C-NMR (125 MHz) of paclitaxel 2'-HTFB ether (**2.11b/2.11b′**) in CDCl$_3$
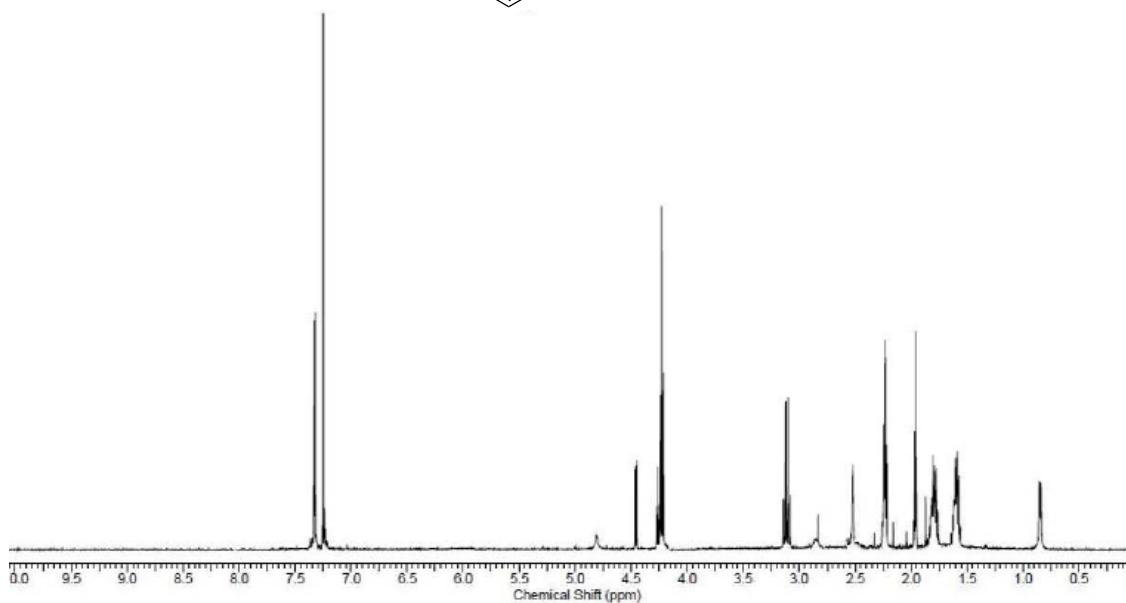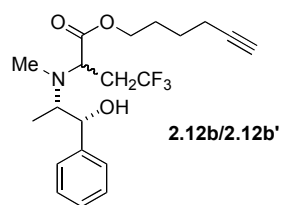
2.12b/2.12b'

^{1}H-NMR (500 MHz) of ephedrine 2-HTFB ether (**2.12b/2.12b′**) in CDCl$_3$
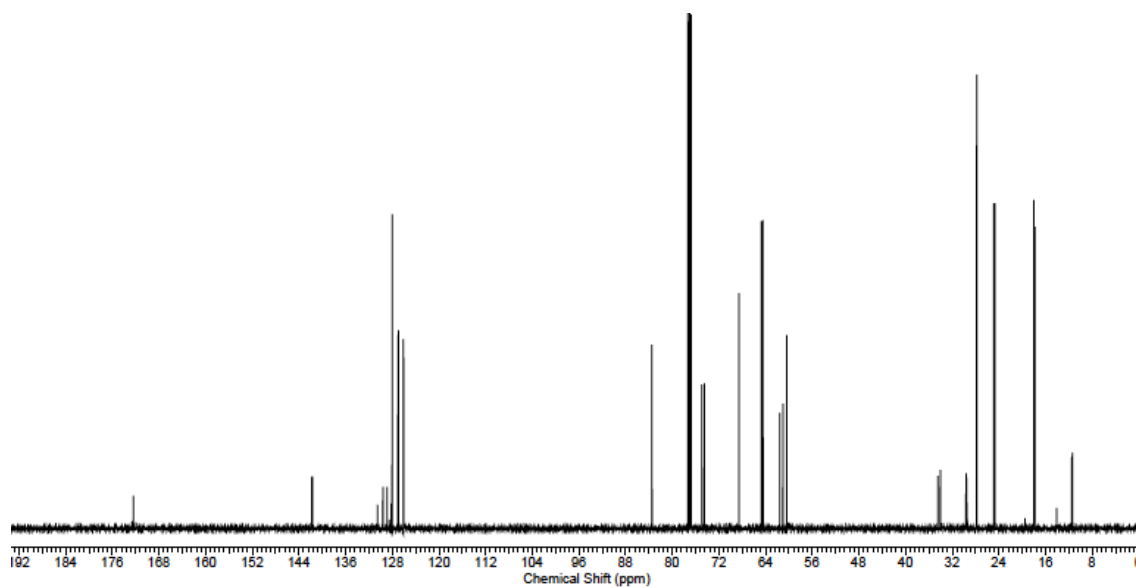
^{13}C-NMR (125 MHz) of ephedrine 2-HTFB ether (**2.11b/2.11b′**) in CDCl$_3$
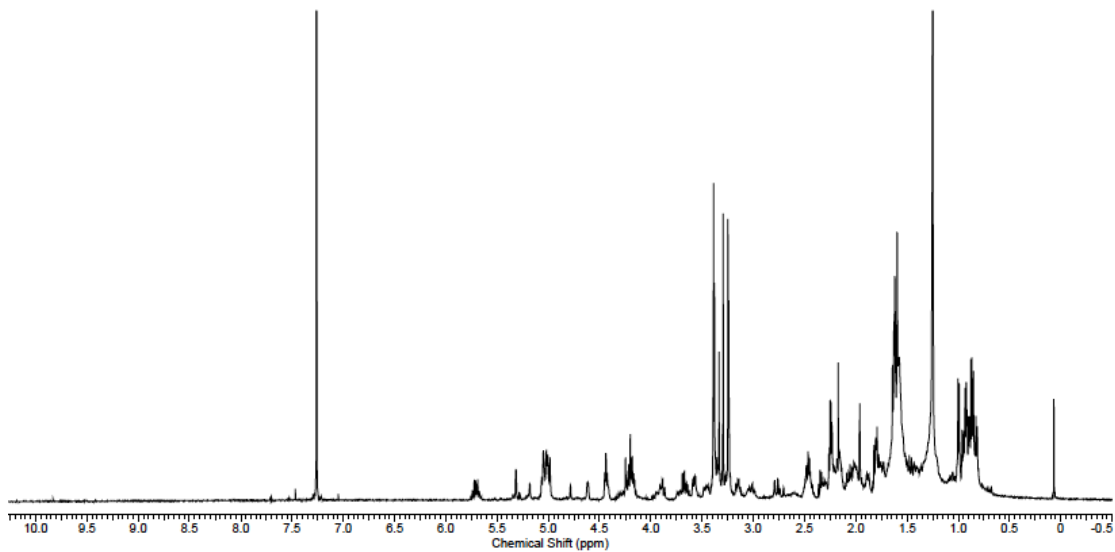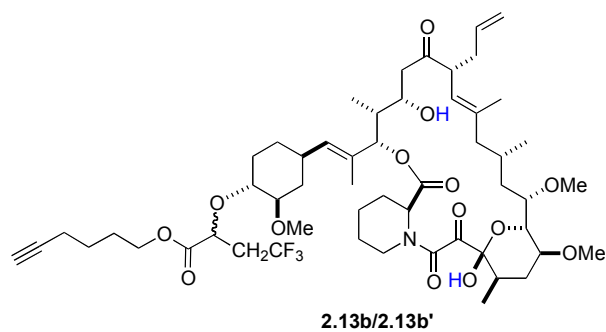
2.13b/2.13b'

^{1}H-NMR (500 MHz) of FK506 32-HTFB ether (**2.13b/2.13b′**) in CDCl$_3$
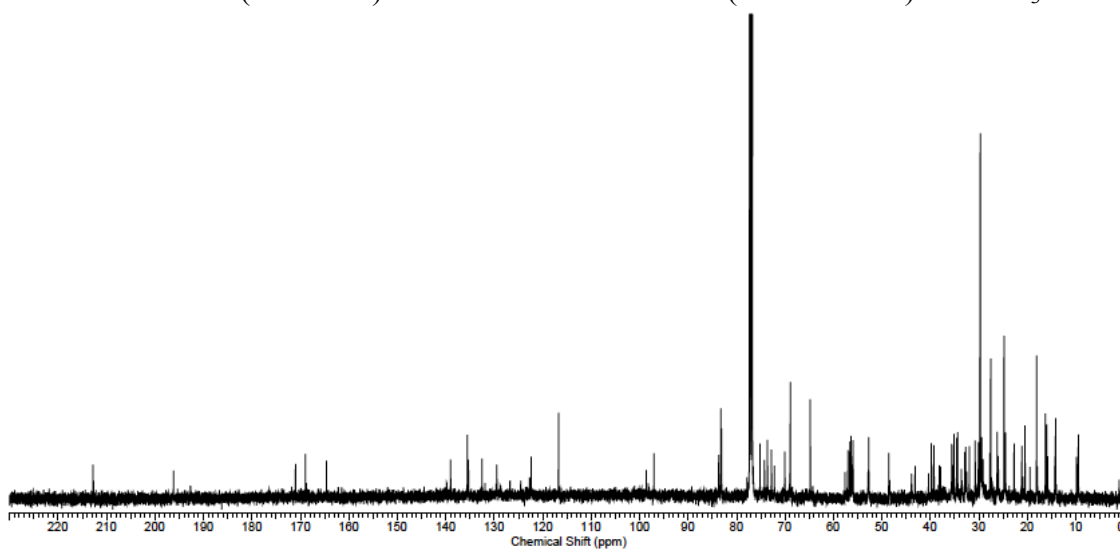
^{13}C-NMR (125 MHz) of FK506 32-HTFB ether (**2.13b/2.13b′**) in CDCl$_3$

~ 2 mg reaction

2.14b and 2.14b'

a

b

c

d

6.5 6.0 5.5 5.0 4.5 4.0 3.5 3.0 2.5 2.0 1.5 1.0 ppm
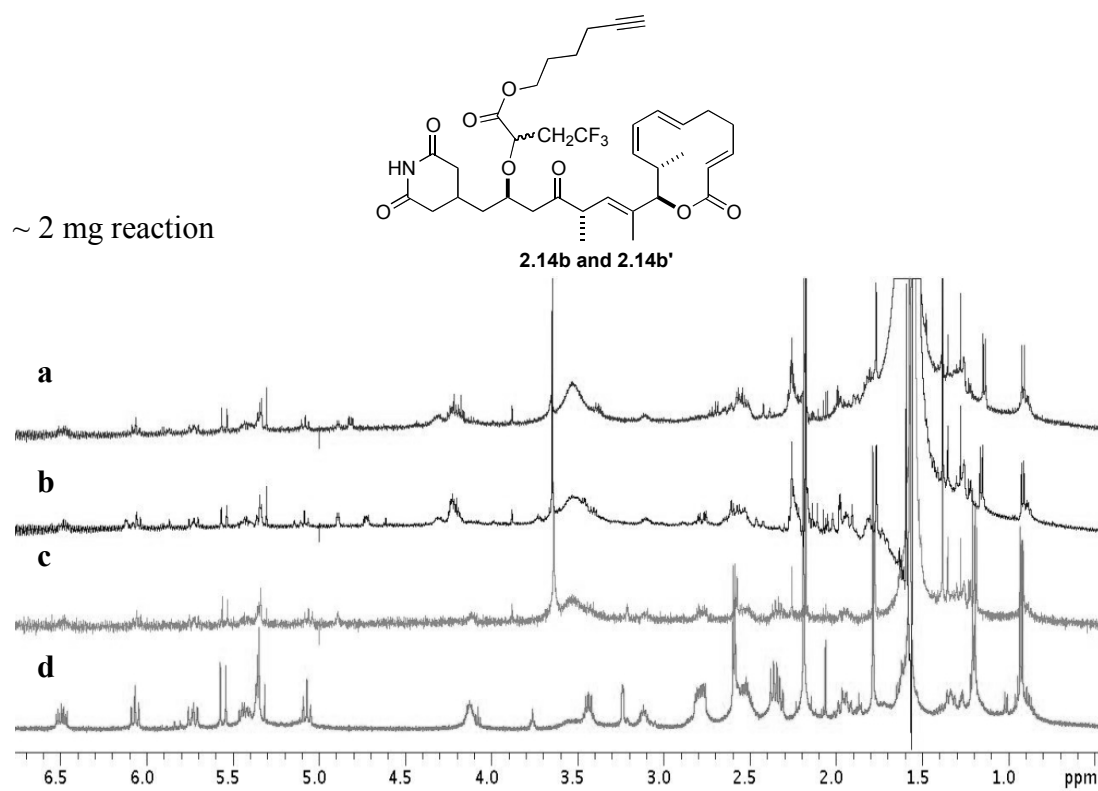
^{1}H-NMR (500 MHz) of Lactimidomycin 7-HTFB ether (**2.14b and 2.14b′**) in CDCl$_3$ (a) purified **2.14b′**; (b) purified **2.14b**; (c) recovered lactimidomycin (**2.14a**); (d) lactimidomycin (**2.14a**)
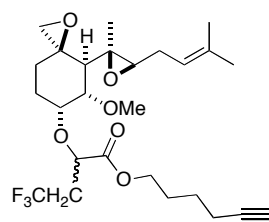
2.15/2.15'
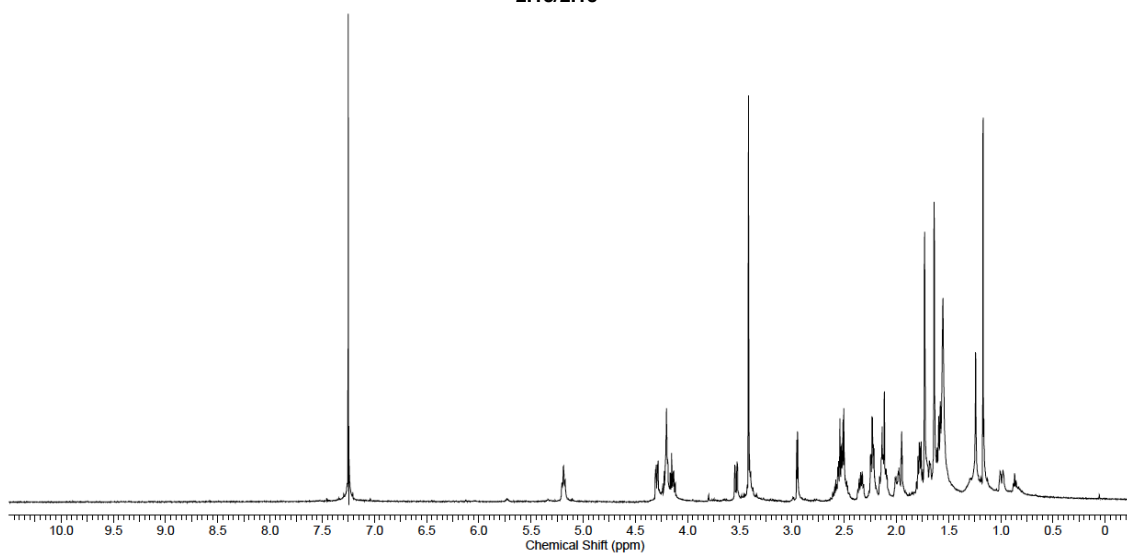
^{1}H-NMR (500 MHz) of fumagillol 6-HTFB ether (**2.15/2.15′**) in CDCl$_3$
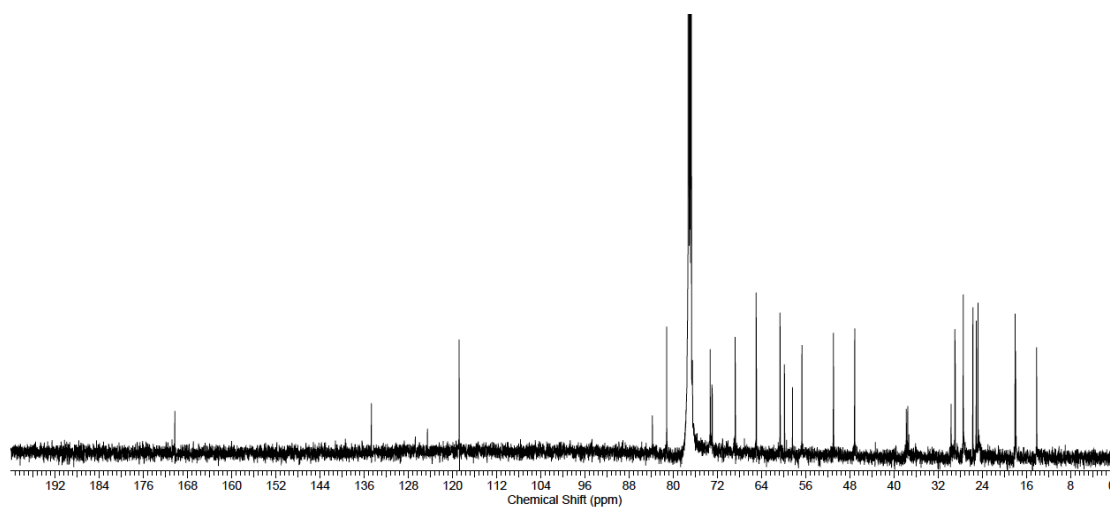
^{13}C-NMR (125 MHz) of fumagillol 6-HTFB ether (**2.15/2.15′**) in CDCl$_3$
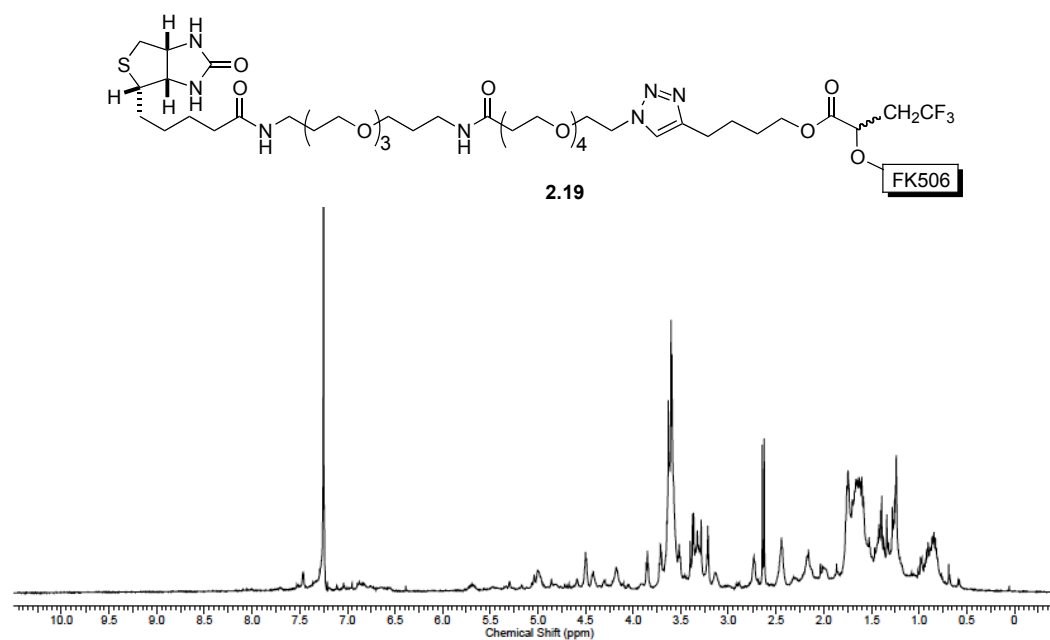
^{1}H-NMR (500 MHz) of FK506-HTFB-Biotin Probe (**2.19**)
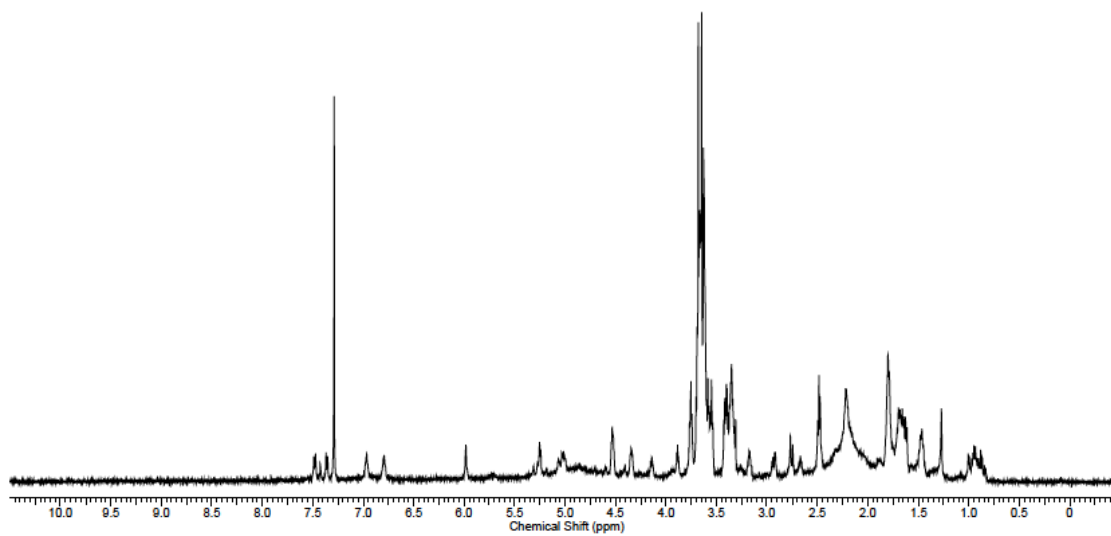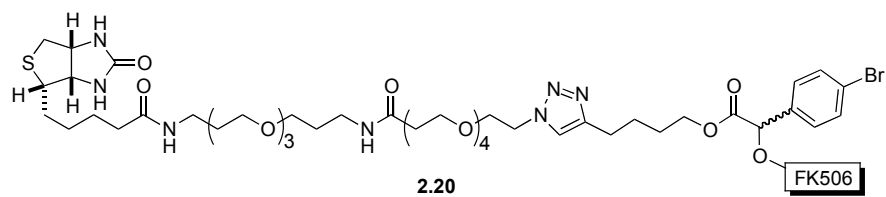
^{1}H-NMR (500 MHz) of FK506-HBPA-Biotin Probe (**2.20**)
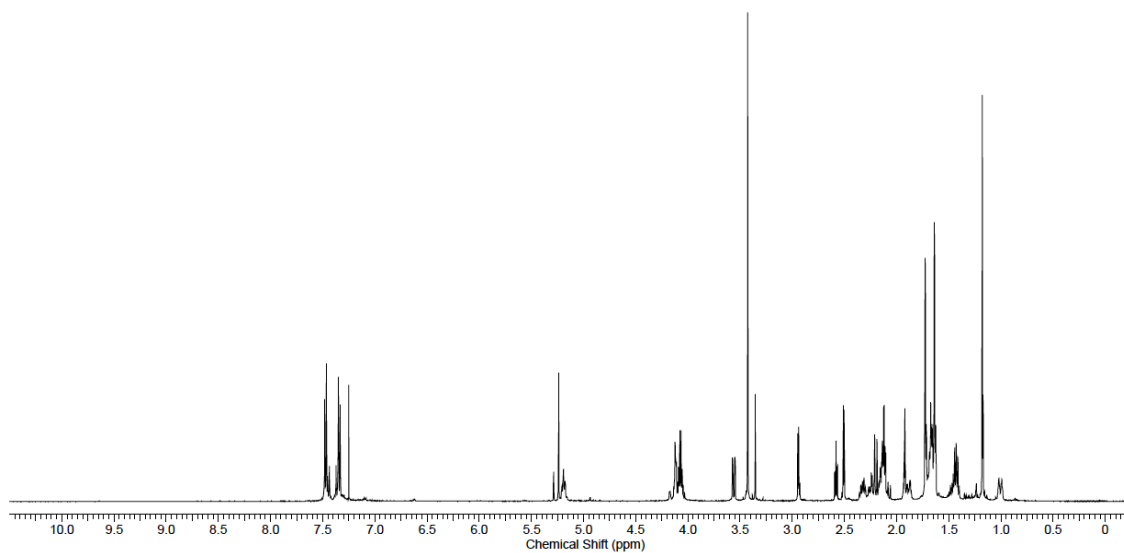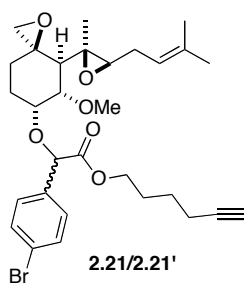
^{1}H-NMR (500 MHz) of fumagillol 6-HBPA ether (**2.21/2.21′**) in CDCl$_3$
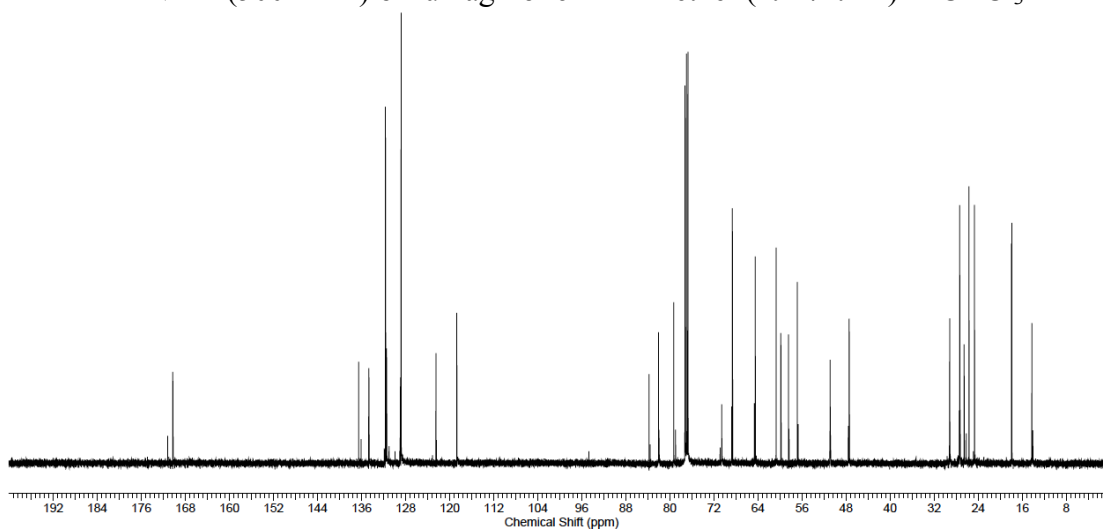
^{13}C-NMR (125 MHz) of fumagillol 6-HBPA ether (**2.21/2.21′**) in CDCl$_3$
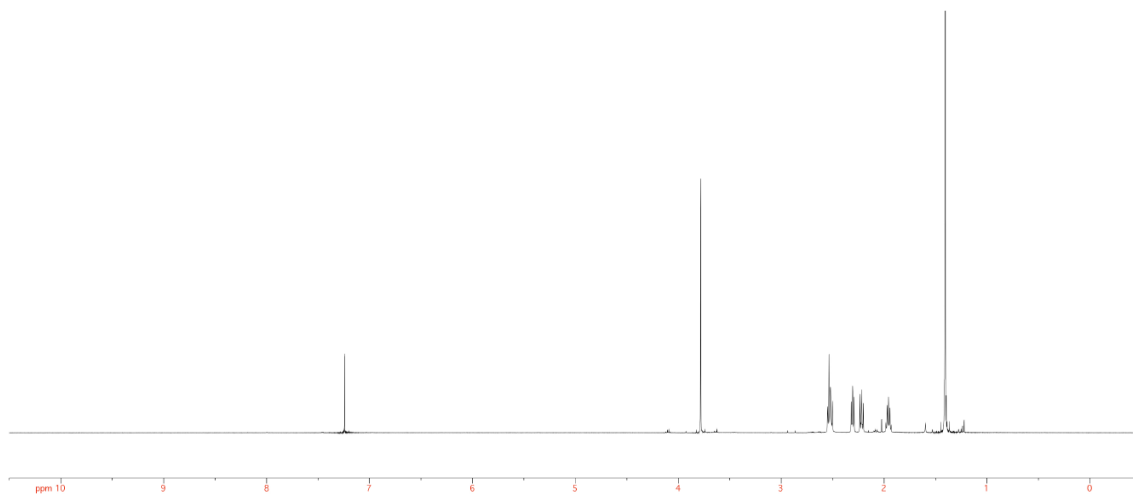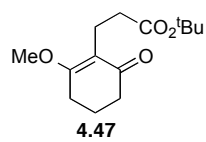
^{1}H-NMR (500 MHz) of vinylogous ester **4.47** in CDCl$_3$
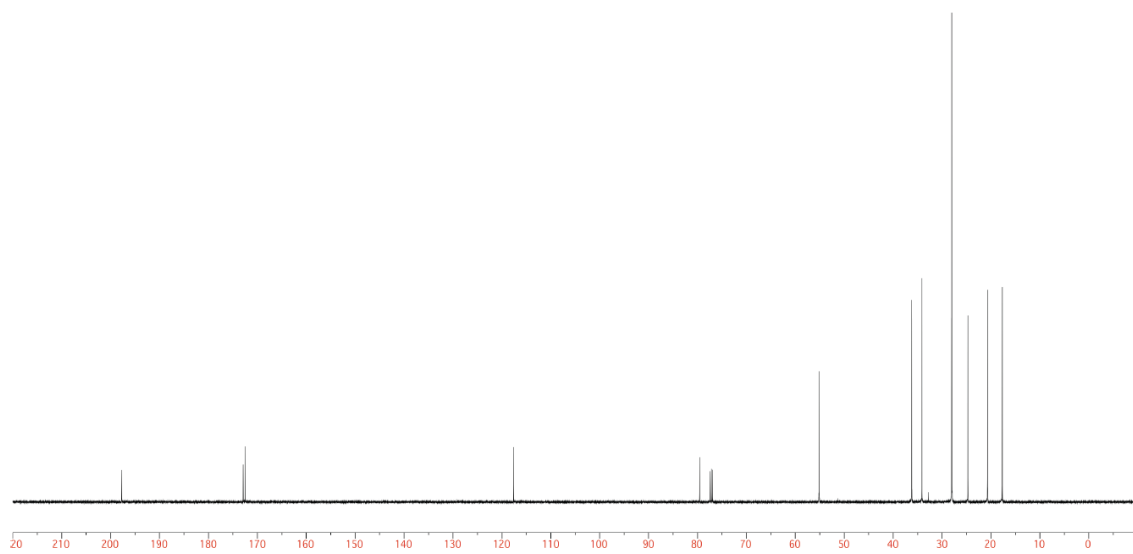
^{13}C-NMR (125 MHz) of vinylogous ester **4.47** in CDCl$_3$
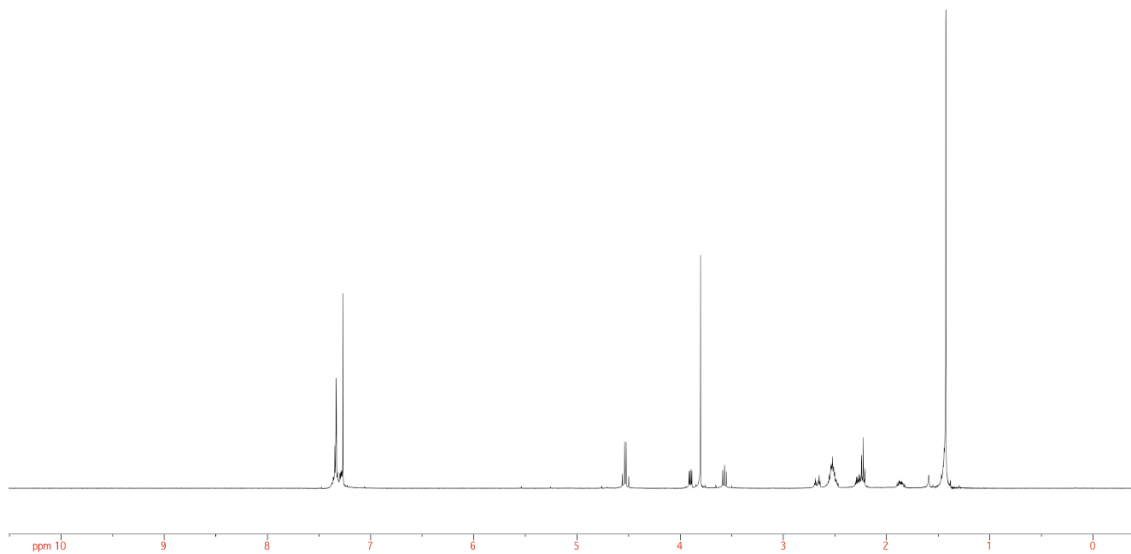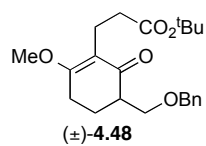
^{1}H-NMR (500 MHz) of α-Substituted ketone (±)-**4.48** in CDCl$_3$
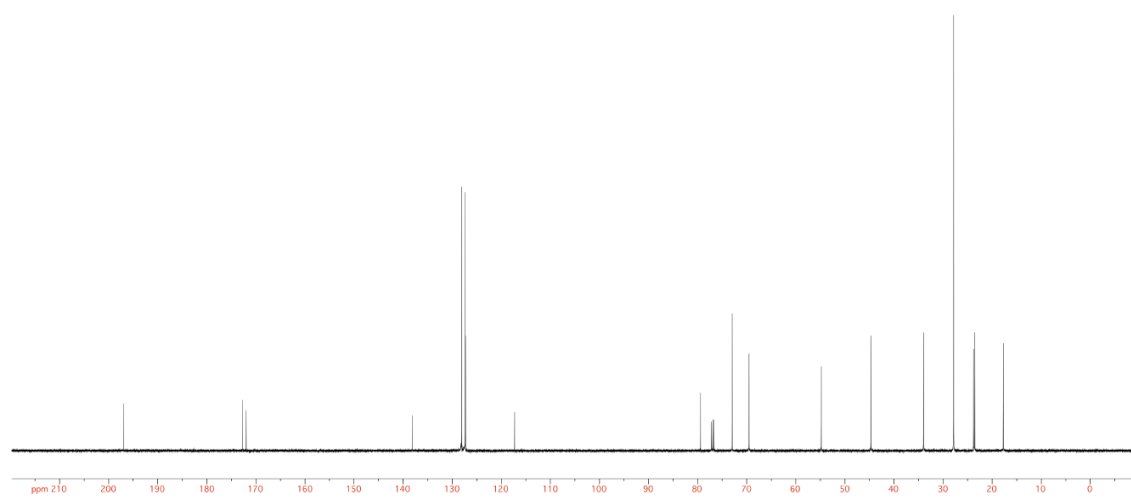
^{13}C-NMR (125 MHz) of α-Substituted ketone (±)-**4.48** in CDCl$_3$

(±)-**4.49**
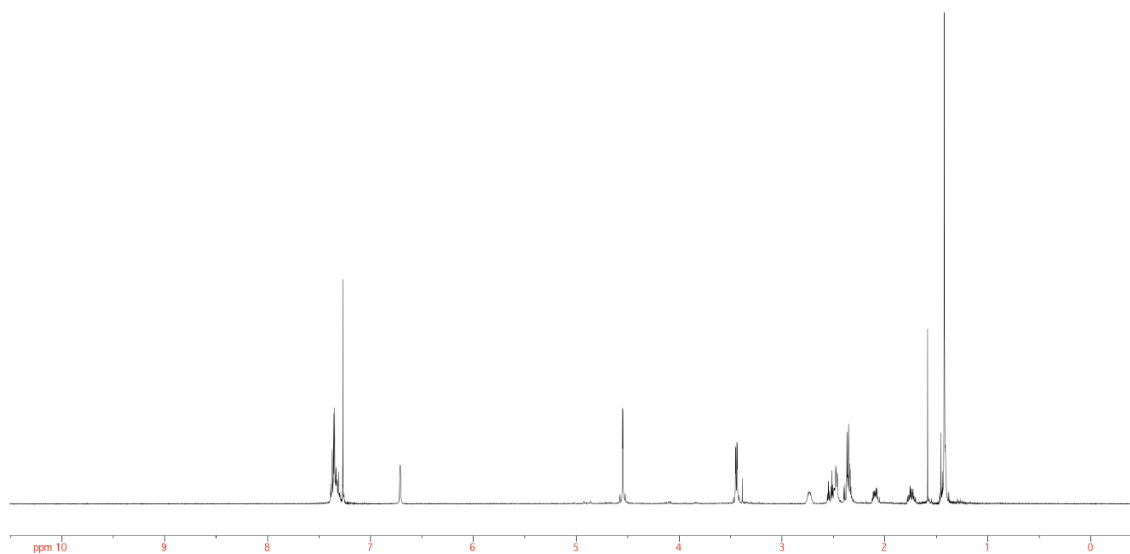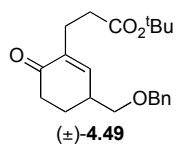
^{1}H-NMR (500 MHz) of α,β-Unsaturated ketone (±)-**4.49** in CDCl$_3$
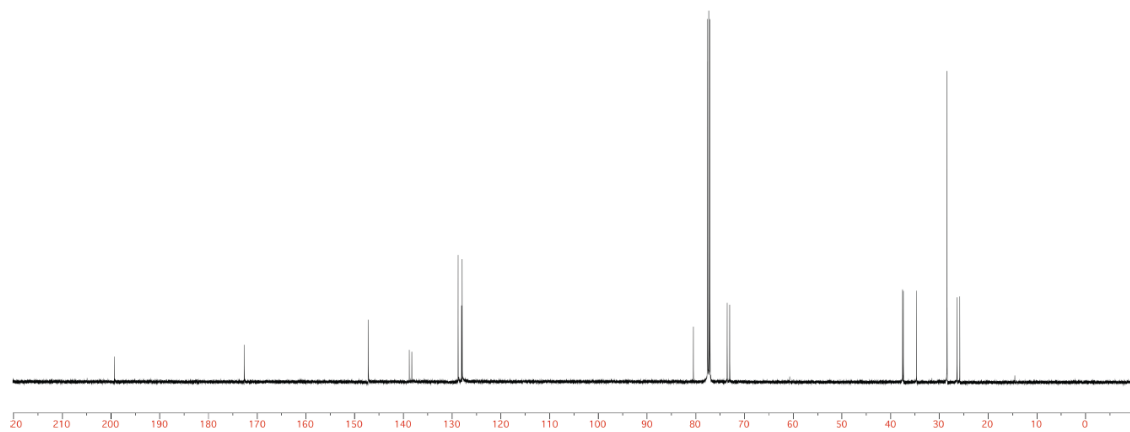
^{13}C-NMR (125 MHz) of α,β-Unsaturated ketone (±)-**4.49** in CDCl$_3$
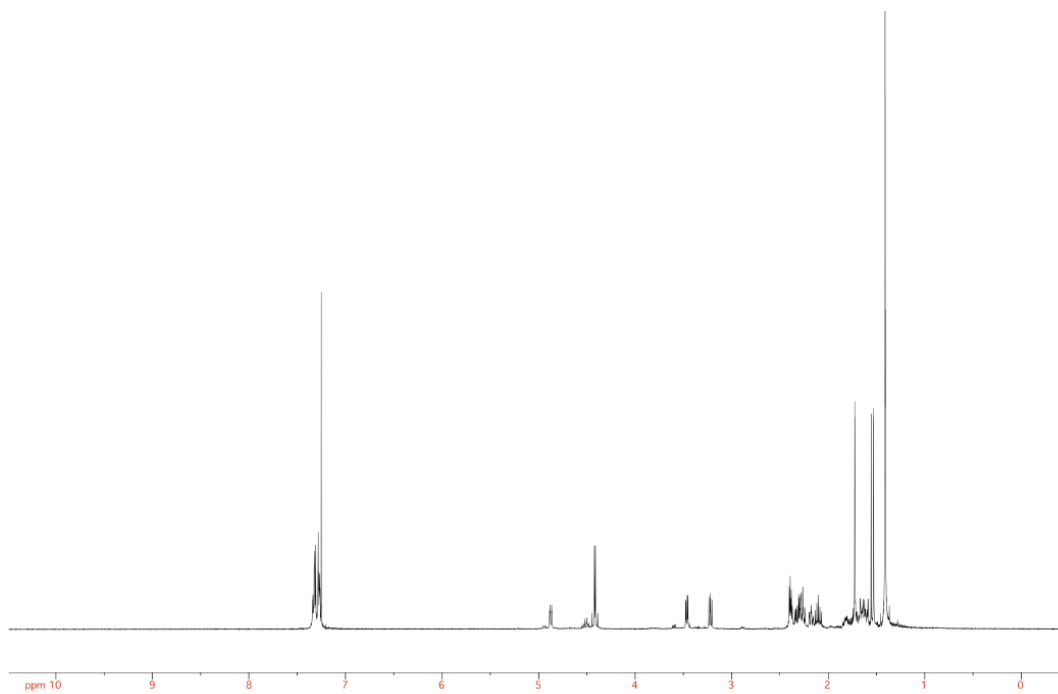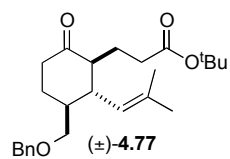
^{1}H-NMR (500 MHz) of Alkene (±)-**4.77** in CDCl$_3$
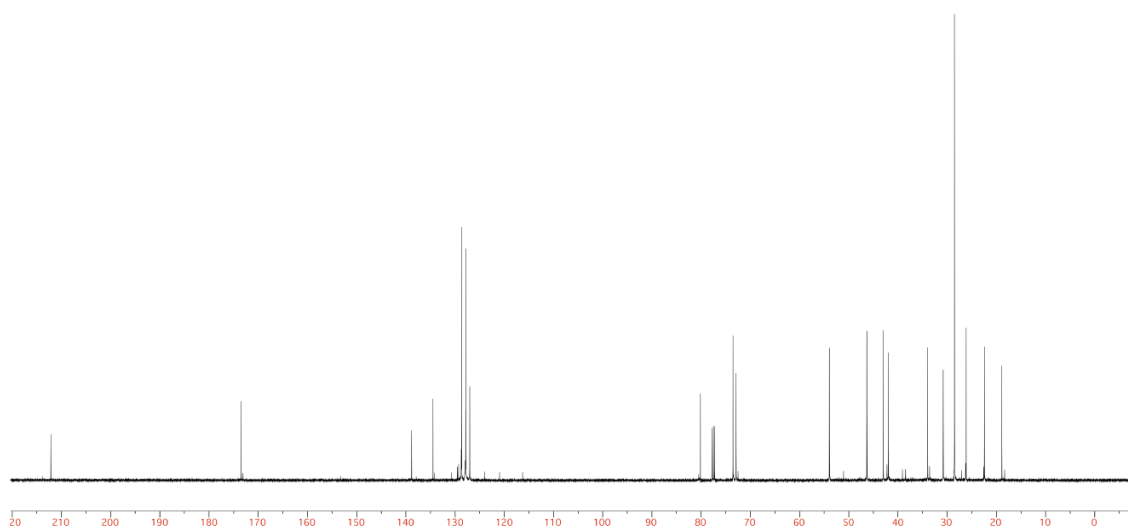
^{13}C-NMR (125 MHz) of Alkene (±)-**4.77** in CDCl$_3$
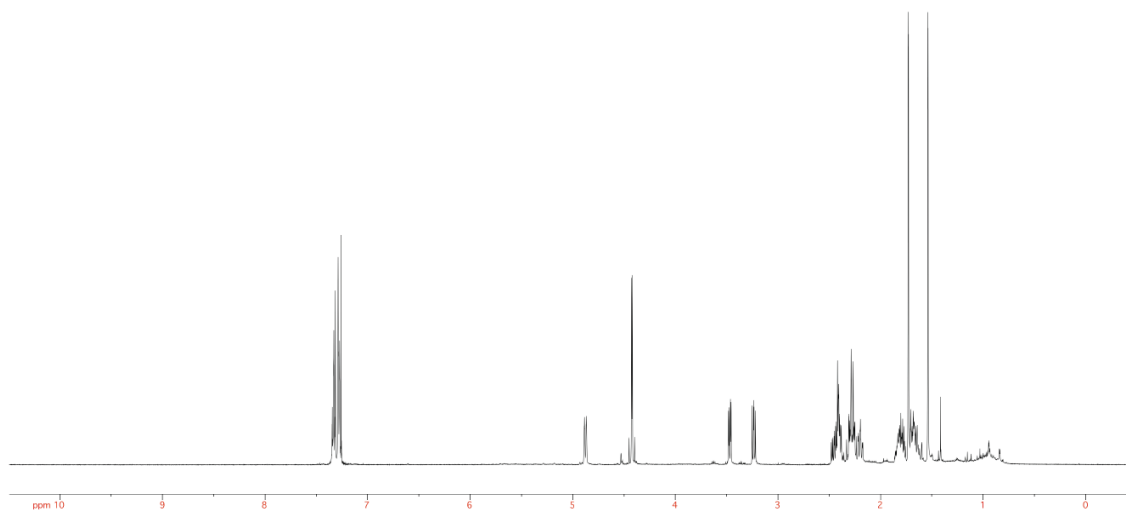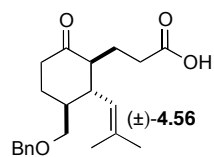
^{1}H-NMR (500 MHz) of Alkenyl acid (±)-**4.56** in CDCl$_3$
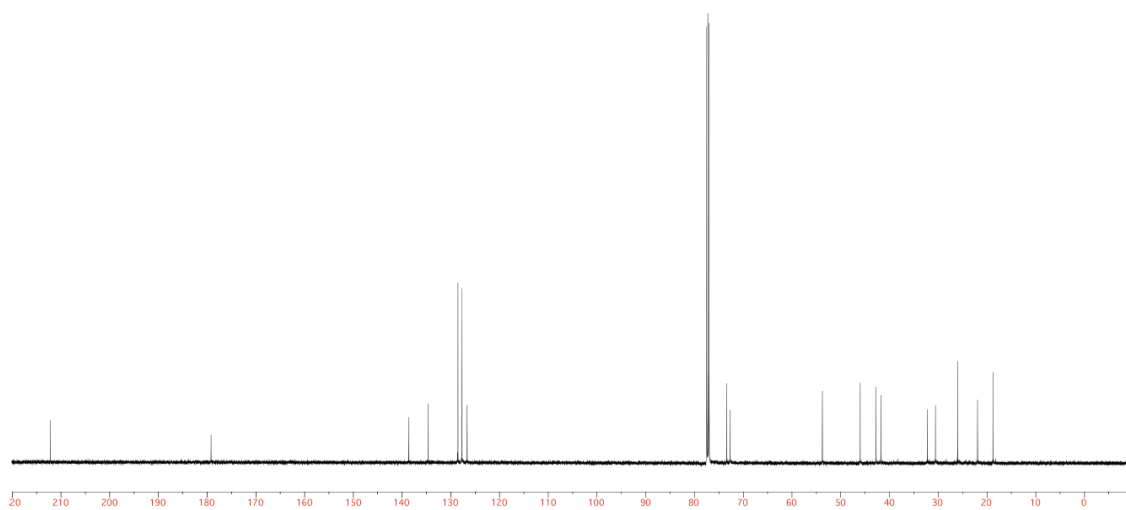
^{13}C-NMR (125 MHz) of Alkenyl acid (±)-**4.56** in CDCl$_3$
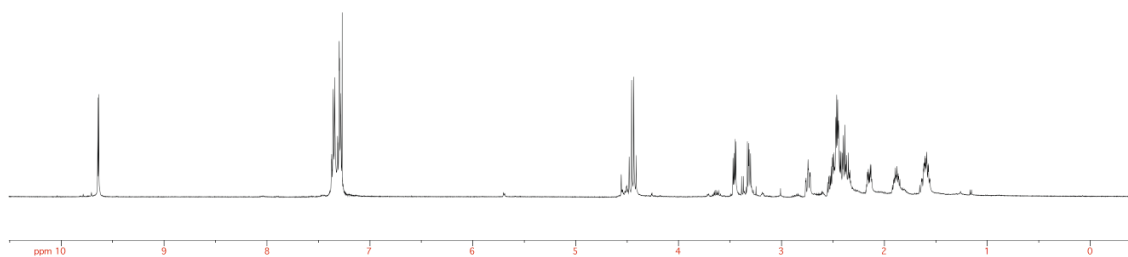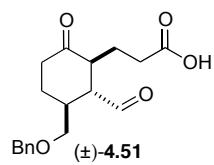
^{1}H-NMR (500 MHz) of Aldehyde acid (±)-**4.51** in CDCl$_3$
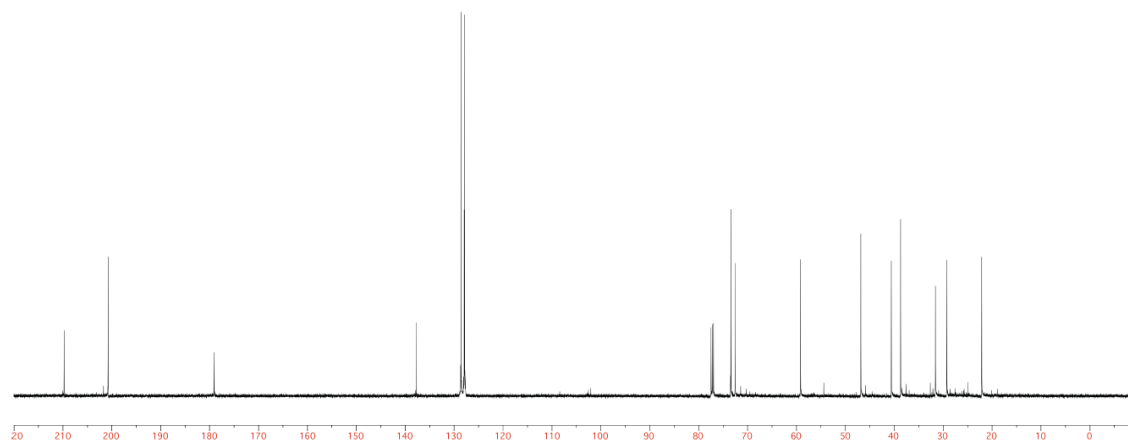
^{13}C-NMR (125 MHz) of Aldehyde acid (±)-**4.51** in CDCl$_3$
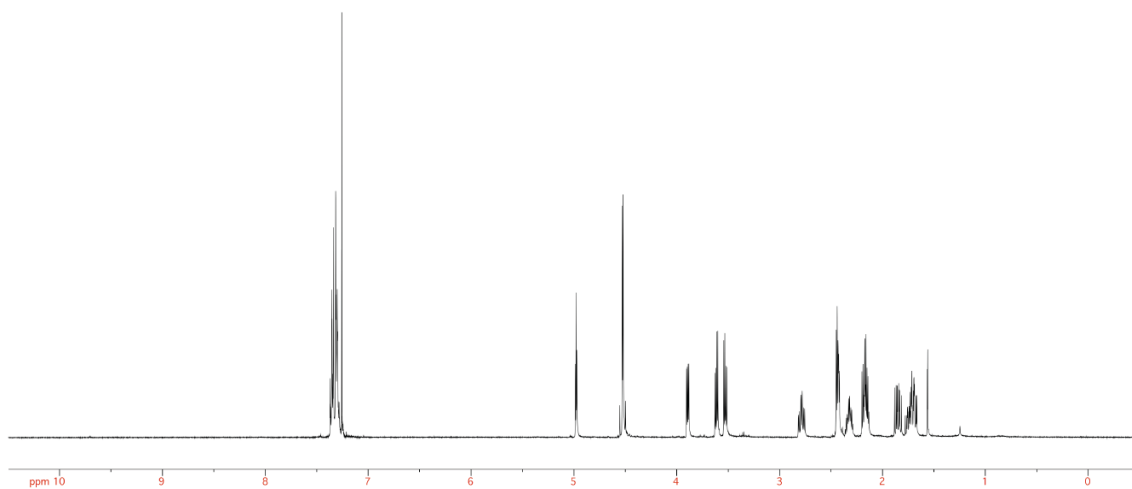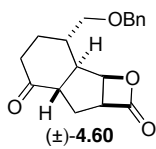
^{1}H-NMR (500 MHz) of Fused tricyclic β-lactone (±)-**4.60** in CDCl$_3$
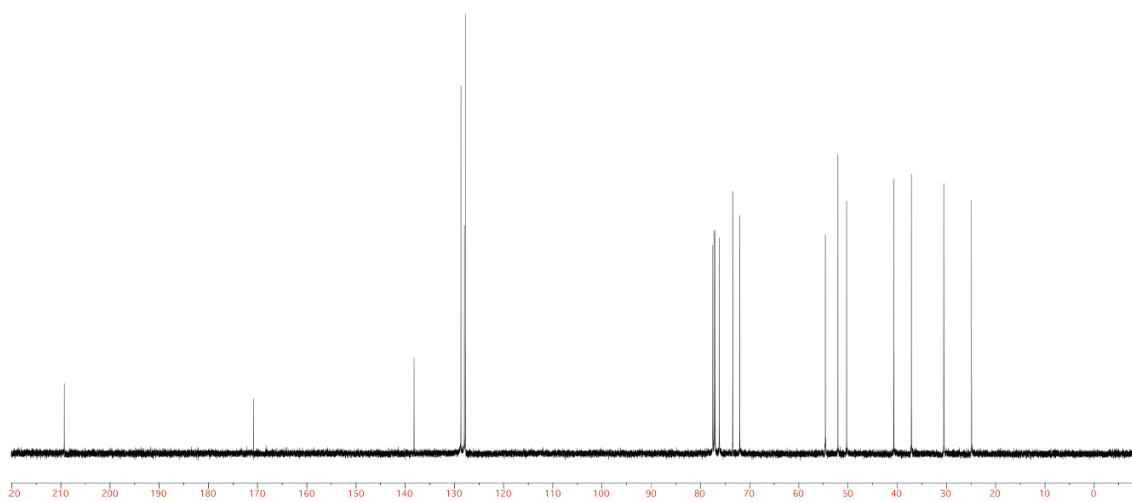
^{13}C-NMR (125 MHz) of Fused tricyclic β-lactone (±)-**4.60** in CDCl$_3$

(+)-**4.52**
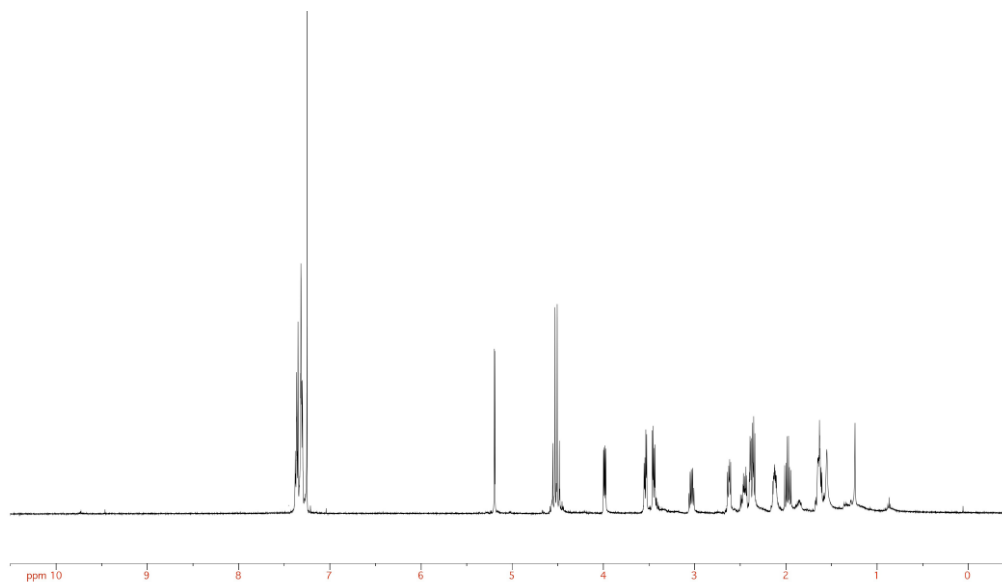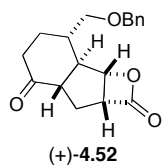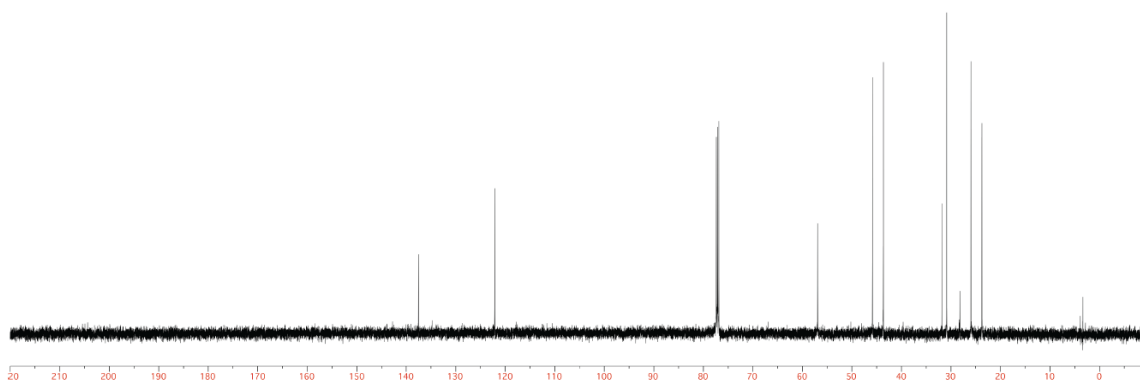
^{1}H-NMR (500 MHz) of Fused tricyclic β-lactone (+)-**4.52** in CDCl$_3$
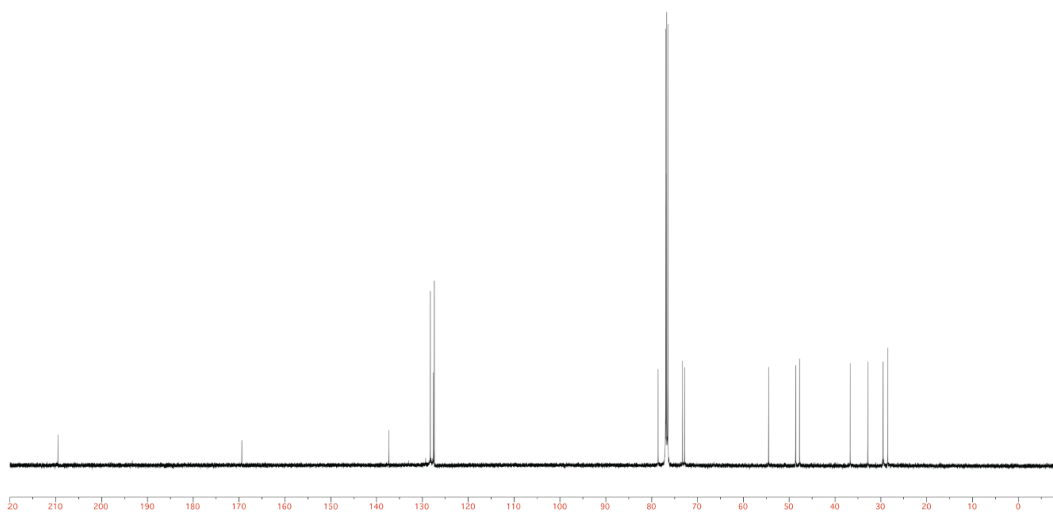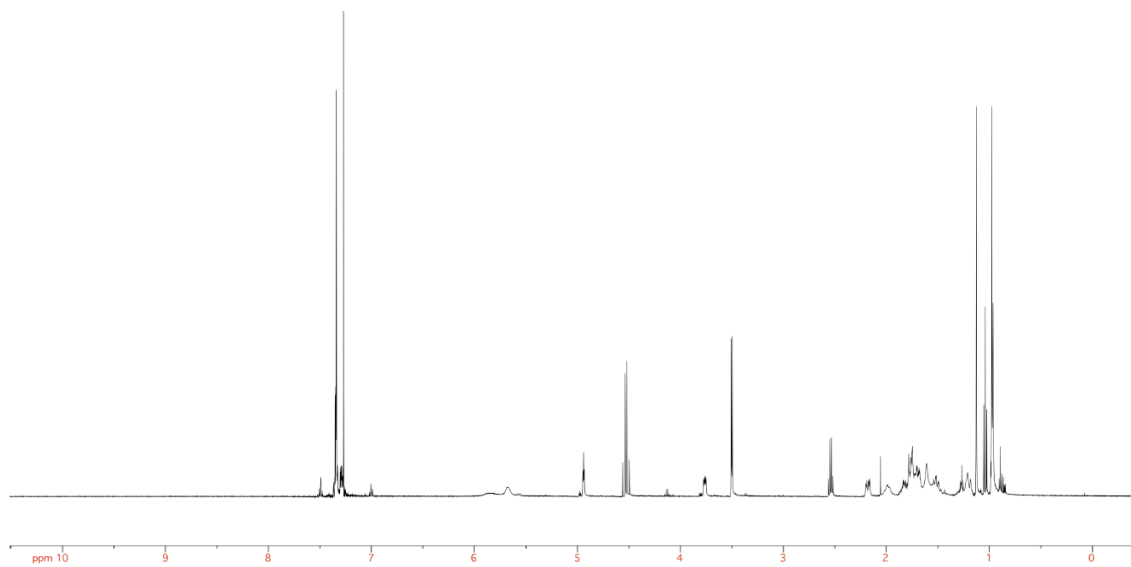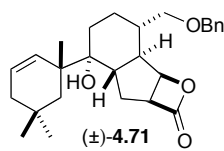

^{13}C-NMR (125 MHz) of Fused tricyclic β-lactone (+)-**4.52** in CDCl$_3$
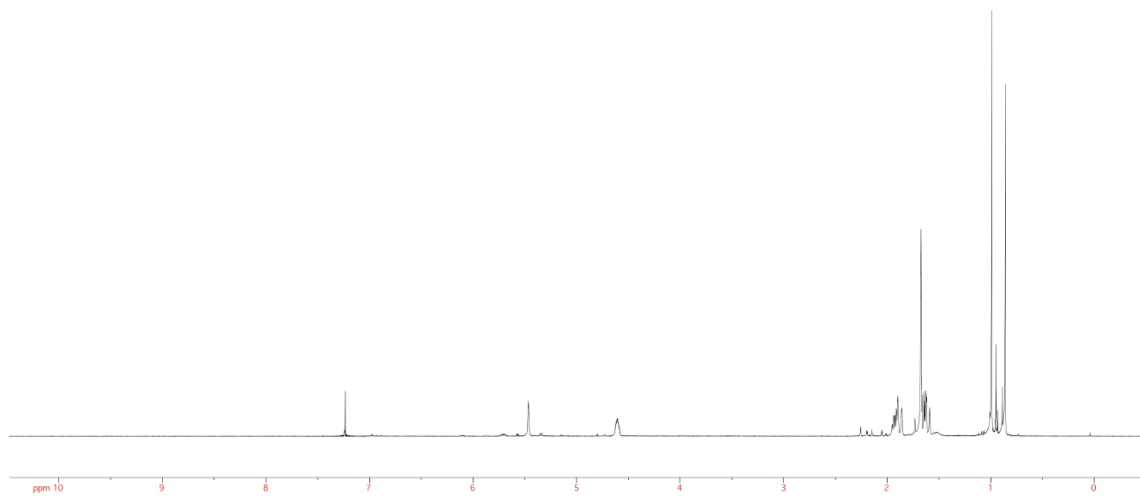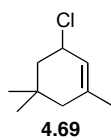
^{1}H-NMR (500 MHz) of 3-chloro-1,5,5-trimethylcyclohex-1-ene **4.69** in CDCl$_3$

^{13}C-NMR (125 MHz) of 3-chloro-1,5,5-trimethylcyclohex-1-ene **4.69** in CDCl$_3$

^{1}H-NMR (500 MHz) of Homoallylic alcohol (±)-**4.71** in CDCl$_3$
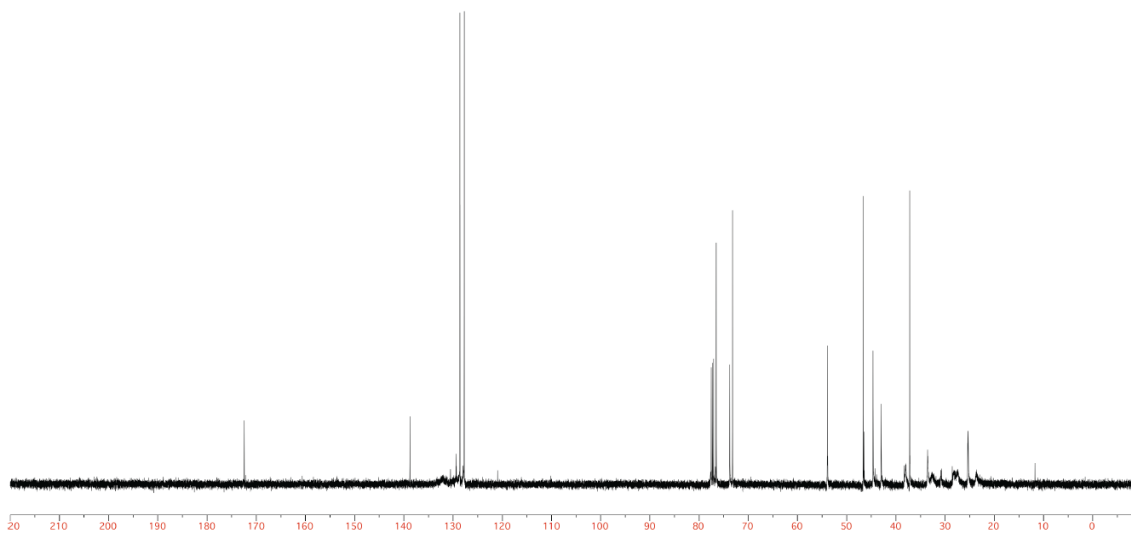
^{13}C-NMR (125 MHz) of Homoallylic alcohol (±)-**4.71** in CDCl$_3$

(±)-**4.73**
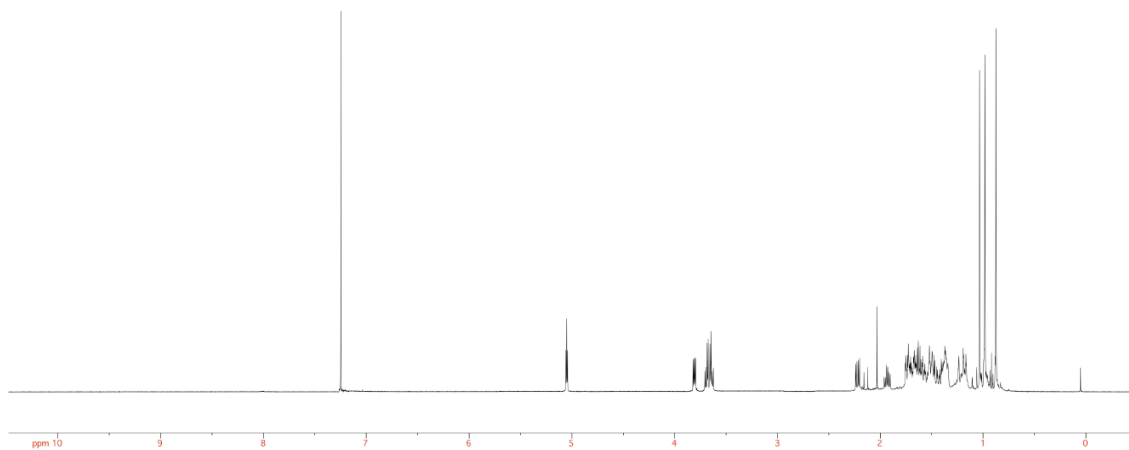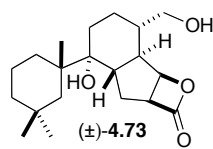
^{1}H-NMR (500 MHz) of Alcohol (±)-**4.73** in CDCl$_3$
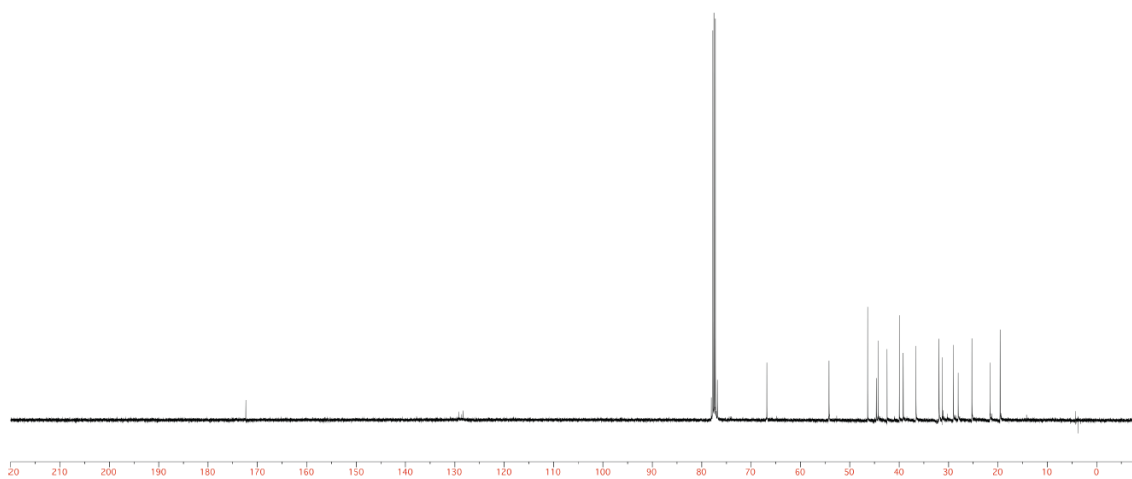
^{13}C-NMR (125 MHz) of Alcohol (±)-**4.73** in CDCl$_3$
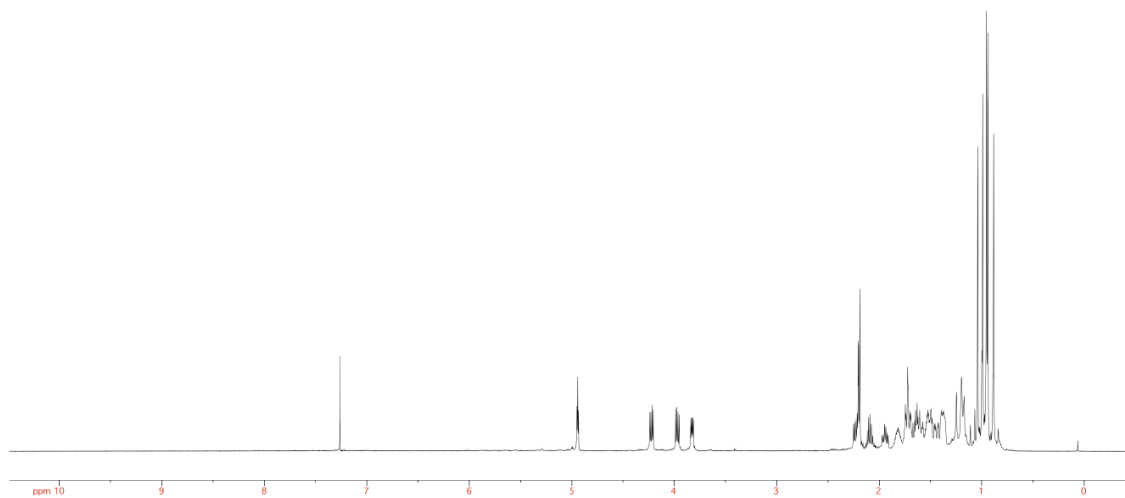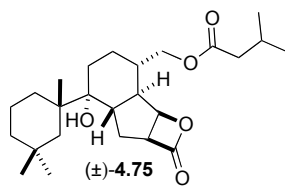
^{1}H-NMR (500 MHz) of Ester (±)-**4.75** in CDCl$_3$
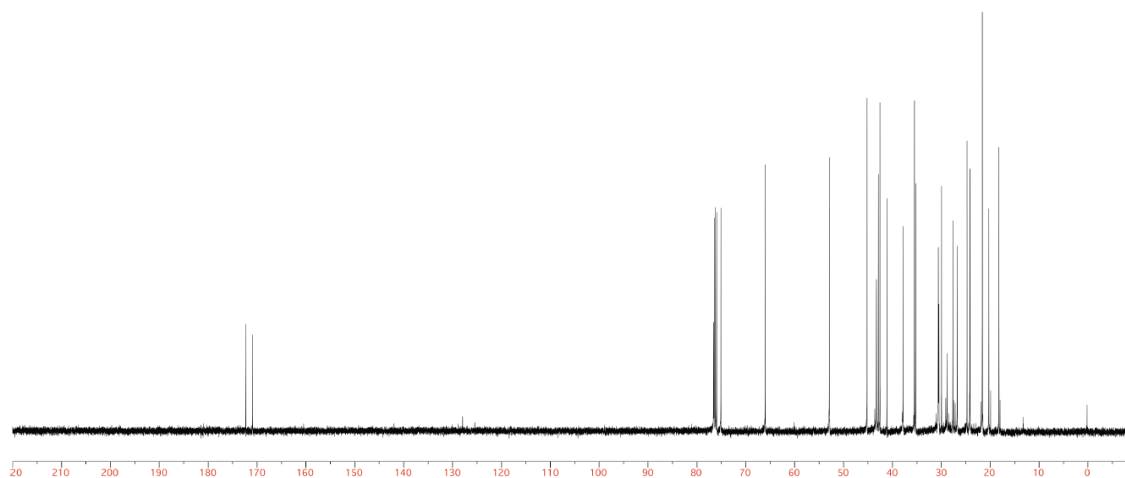
^{13}C-NMR (125 MHz) of Ester (±)-**4.75** in CDCl$_3$
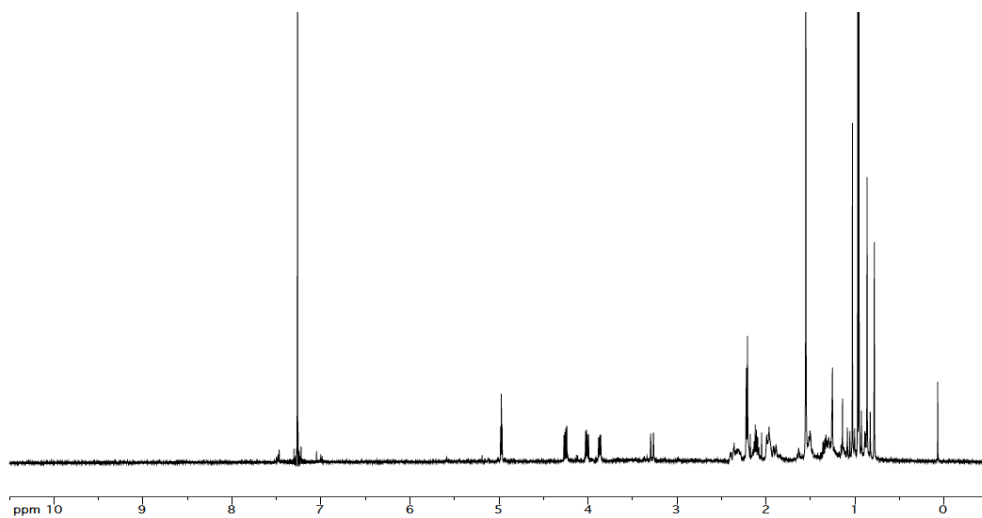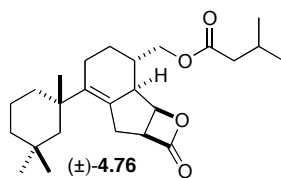
^{1}H-NMR (500 MHz) of 6,15-Bis-*epi*-spongiolactone (±)-**4.76** in CDCl$_3$
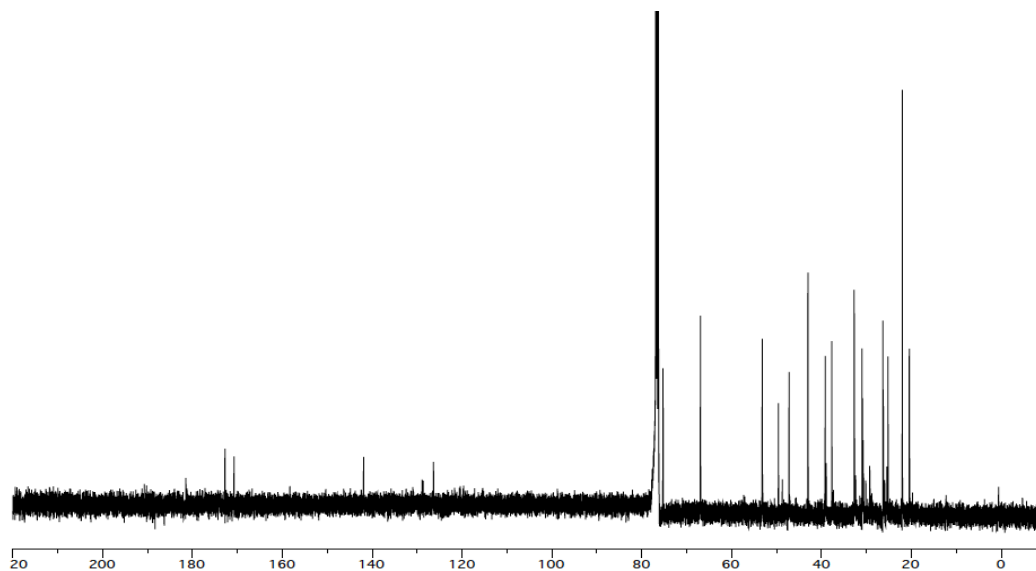
^{13}C-NMR (125MHz) of 6,15-Bis-*epi*-spongiolactone (±)-**4.76** in CDCl$_3$

(±)-**4.77**
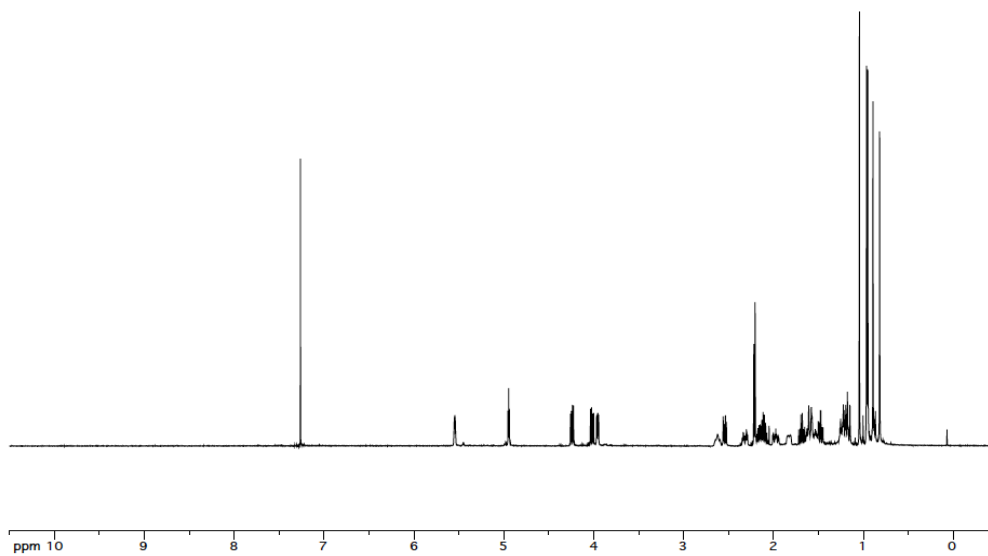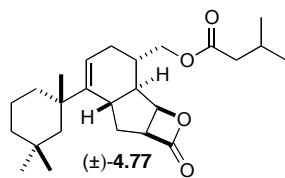
^{1}H-NMR (500 MHz) of spongiolactone derivative (±)-**4.77** in CDCl$_3$
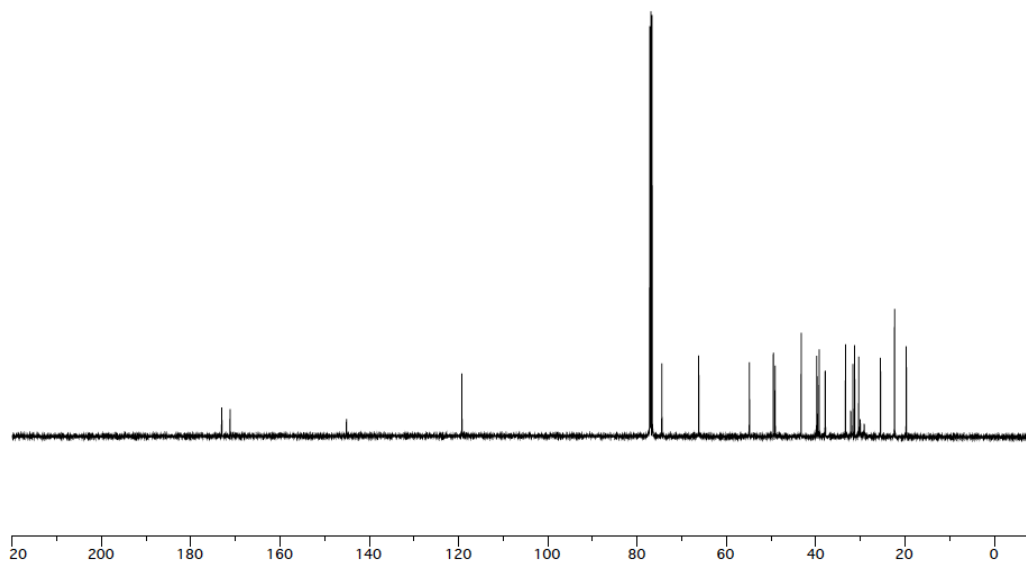
^{13}C-NMR (125 MHz) of spongiolactone derivative (±)-**4.77** in CDCl$_3$

APPENDIX B

LETTERS OF PERMISSION

ELSEVIER LICENSE
TERMS AND CONDITIONS

Oct 08, 2011

This is a License Agreement between Supakarn Chamni ("You") and Elsevier ("Elsevier") provided by Copyright Clearance Center ("CCC"). The license consists of your order details, the terms and conditions provided by Elsevier, and the payment terms and conditions.

All payments must be made in full to CCC. For payment instructions, please see information listed at the bottom of this form.

Supplier	Elsevier Limited The Boulevard, Langford Lane Kidlington,Oxford,OX5 1GB,UK
Registered Company Number	1982084
Customer name	Supakarn Chamni
Customer address	400 Nagle St. College Station, TX 77840
License number	2763471508301
License date	Oct 07, 2011
Licensed content publisher	Elsevier
Licensed content publication	Bioorganic & Medicinal Chemistry Letters
Licensed content title	β-Lactam congeners of orlistat as inhibitors of fatty acid synthase
Licensed content author	Wei Zhang, Robyn D. Richardson, Supakarn Chamni, Jeffrey W. Smith, Daniel Romo
Licensed content date	1 April 2008
Licensed content volume number	18
Licensed content issue number	7
Number of pages	4

Start Page	2491
End Page	2494
Type of Use	reuse in a thesis/dissertation
Portion	full article
Format	both print and electronic
Are you the author of this Elsevier article?	Yes
Will you be translating?	No
Order reference number	
Title of your thesis/dissertation	New Diazo Reagents and Applications of β-Lactones for Synthesis and Biological Evaluation of Natural Products
Expected completion date	Dec 2011
Estimated size (number of pages)	250
Elsevier VAT number	GB 494 6272 12
Permissions price	0.00 USD
VAT/Local Sales Tax	0.0 USD / 0.0 GBP
Total	0.00 USD

Terms and Conditions

INTRODUCTION

1. The publisher for this copyrighted material is Elsevier. By clicking "accept" in connection with completing this licensing transaction, you agree that the following terms and conditions apply to this transaction (along with the Billing and Payment terms and conditions established by Copyright Clearance Center, Inc. ("CCC"), at the time that you opened your Rightslink account and that are available at any time at http://myaccount.copyright.com).

GENERAL TERMS

2. Elsevier hereby grants you permission to reproduce the aforementioned material subject to the terms and conditions indicated.

3. Acknowledgement: If any part of the material to be used (for example, figures) has appeared in our publication with credit or acknowledgement to another source, permission must also be sought from that source. If such permission is not obtained then that material may not be included in your publication/copies. Suitable acknowledgement to the source must be made, either as a footnote or in a reference list at the end of your publication, as follows:

"Reprinted from Publication title, Vol /edition number, Author(s), Title of article / title of chapter, Pages No., Copyright (Year), with permission from Elsevier [OR APPLICABLE SOCIETY COPYRIGHT OWNER]." Also Lancet special credit - "Reprinted from The Lancet, Vol. number, Author(s), Title of article, Pages No., Copyright (Year), with permission from Elsevier."

4. Reproduction of this material is confined to the purpose and/or media for which permission is hereby given.

5. Altering/Modifying Material: Not Permitted. However figures and illustrations may be altered/adapted minimally to serve your work. Any other abbreviations, additions, deletions and/or any other alterations shall be made only with prior written authorization of Elsevier Ltd. (Please contact Elsevier at permissions@elsevier.com)

6. If the permission fee for the requested use of our material is waived in this instance, please be advised that your future requests for Elsevier materials may attract a fee.

7. Reservation of Rights: Publisher reserves all rights not specifically granted in the combination of (i) the license details provided by you and accepted in the course of this licensing transaction, (ii) these terms and conditions and (iii) CCC's Billing and Payment terms and conditions.

8. License Contingent Upon Payment: While you may exercise the rights licensed immediately upon issuance of the license at the end of the licensing process for the transaction, provided that you have disclosed complete and accurate details of your proposed use, no license is finally effective unless and until full payment is received from you (either by publisher or by CCC) as provided in CCC's Billing and Payment terms and conditions. If full payment is not received on a timely basis, then any license preliminarily granted shall be deemed automatically revoked and shall be void as if never granted. Further, in the event that you breach any of these terms and conditions or any of CCC's Billing and Payment terms and conditions, the license is automatically revoked and shall be void as if never granted. Use of materials as described in a revoked license, as well as any use of the materials beyond the scope of an unrevoked license, may constitute copyright infringement and publisher reserves the right to take any and all action to protect its copyright in the materials.

9. Warranties: Publisher makes no representations or warranties with respect to the licensed material.

10. Indemnity: You hereby indemnify and agree to hold harmless publisher and CCC, and their respective officers, directors, employees and agents, from and against any and all claims arising out of your use of the licensed material other than as specifically authorized pursuant to this license.

11. No Transfer of License: This license is personal to you and may not be sublicensed, assigned, or transferred by you to any other person without publisher's written permission.

12. No Amendment Except in Writing: This license may not be amended except in a writing signed by both parties (or, in the case of publisher, by CCC on publisher's behalf).

13. Objection to Contrary Terms: Publisher hereby objects to any terms contained in any purchase order, acknowledgment, check endorsement or other writing prepared by you, which terms are inconsistent with these terms and conditions or CCC's Billing and Payment terms and conditions. These terms and conditions, together with CCC's Billing and Payment terms and conditions (which are incorporated herein), comprise the entire agreement between you and publisher (and CCC) concerning this licensing transaction. In the event of any conflict between your obligations established by these terms and conditions and those established by CCC's Billing and Payment terms and conditions, these terms and conditions shall control.

14. Revocation: Elsevier or Copyright Clearance Center may deny the permissions described in this License at their sole discretion, for any reason or no reason, with a full refund payable to you. Notice of such denial will be made using the contact information provided by you. Failure to receive such notice will not alter or invalidate the denial. In no event will Elsevier or Copyright Clearance Center be responsible or liable for any costs, expenses or damage incurred by you as a result of a denial of your permission request, other than a refund of the amount(s) paid by you to Elsevier and/or Copyright Clearance Center for denied permissions.

LIMITED LICENSE

The following terms and conditions apply only to specific license types:

15. **Translation**: This permission is granted for non-exclusive world **English** rights only unless your license was granted for translation rights. If you licensed translation rights you may only translate this content into the languages you requested. A professional translator must perform all translations and reproduce the content word for word preserving the integrity of the article. If this license is to re-use 1 or 2 figures then permission is granted for non-exclusive world rights in all languages.

16. **Website**: The following terms and conditions apply to electronic reserve and author websites:
Electronic reserve: If licensed material is to be posted to website, the web site is to be password-protected and made available only to bona fide students registered on a relevant course if:
This license was made in connection with a course,
This permission is granted for 1 year only. You may obtain a license for future website posting,
All content posted to the web site must maintain the copyright information line on the bottom of each image,
A hyper-text must be included to the Homepage of the journal from which you are licensing at http://www.sciencedirect.com/science/journal/xxxxx or the Elsevier homepage for books at http://www.elsevier.com, and
Central Storage: This license does not include permission for a scanned version of the material to be stored in a central repository such as that provided by Heron/XanEdu.

17. **Author website** for journals with the following additional clauses:

All content posted to the web site must maintain the copyright information line on the bottom of each image, and the permission granted is limited to the personal version of your paper. You are not allowed to download and post the published electronic version of your article (whether PDF or HTML, proof or final version), nor may you scan the printed edition to create an electronic version. A hyper-text must be included to the Homepage of the journal from which you are licensing at http://www.sciencedirect.com/science/journal/xxxxx, As part of our normal production process, you will receive an e-mail notice when your article appears on Elsevier's online service ScienceDirect (www.sciencedirect.com). That e-mail will include the article's Digital Object Identifier (DOI). This number provides the electronic link to the published article and should be included in the posting of your

personal version. We ask that you wait until you receive this e-mail and have the DOI to do any posting. Central Storage: This license does not include permission for a scanned version of the material to be stored in a central repository such as that provided by Heron/XanEdu.

18. **Author website** for books with the following additional clauses:
Authors are permitted to place a brief summary of their work online only.
A hyper-text must be included to the Elsevier homepage at http://www.elsevier.com

All content posted to the web site must maintain the copyright information line on the bottom of each image. You are not allowed to download and post the published electronic version of your chapter, nor may you scan the printed edition to create an electronic version.
Central Storage: This license does not include permission for a scanned version of the material to be stored in a central repository such as that provided by Heron/XanEdu.

19. **Website** (regular and for author): A hyper-text must be included to the Homepage of the journal from which you are licensing at http://www.sciencedirect.com/science/journal/xxxxx. or for books to the Elsevier homepage at http://www.elsevier.com

20. **Thesis/Dissertation**: If your license is for use in a thesis/dissertation your thesis may be submitted to your institution in either print or electronic form. Should your thesis be published commercially, please reapply for permission. These requirements include permission for the Library and Archives of Canada to supply single copies, on demand, of the complete thesis and include permission for UMI to supply single copies, on demand, of the complete thesis. Should your thesis be published commercially, please reapply for permission.

21. **Other Conditions**:

If you would like to pay for this license now, please remit this license along with your payment made payable to "COPYRIGHT CLEARANCE CENTER" otherwise you will be invoiced within 48 hours of the license date. Payment should be in the form of a check or money order referencing your account number and this invoice number RLNK500641396.
Once you receive your invoice for this order, you may pay your invoice by credit card. Please follow instructions provided at that time.

Make Payment To:
Copyright Clearance Center
Dept 001
P.O. Box 843006
Boston, MA 02284-3006

For suggestions or comments regarding this order, contact RightsLink Customer Support: customercare@copyright.com or +1-877-622-5543 (toll free in the US) or +1-978-646-2777.

Gratis licenses (referencing $0 in the Total field) are free. Please retain this printable license for your reference. No payment is required.

Copyright
Clearance
Center

RightsLink®

Home | Account Info | Help

ACS Publications
High quality. High impact.

Title: Diazo Reagents with Small Steric Footprints for Simultaneous Arming/SAR Studies of Alcohol-Containing Natural Products via O–H Insertion

Author: Supakarn Chamni et al.

Publication: ACS Chemical Biology

Publisher: American Chemical Society

Date: Sep 1, 2011

Copyright © 2011, American Chemical Society

Logged in as:
Supakarn Chamni

LOGOUT

PERMISSION/LICENSE IS GRANTED FOR YOUR ORDER AT NO CHARGE

This type of permission/license, instead of the standard Terms & Conditions, is sent to you because no fee is being charged for your order. Please note the following:

- Permission is granted for your request in both print and electronic formats.
- If figures and/or tables were requested, they may be adapted or used in part.
- Please print this page for your records and send a copy of it to your publisher/graduate school.
- Appropriate credit for the requested material should be given as follows: "Reprinted (adapted) with permission from (COMPLETE REFERENCE CITATION). Copyright (YEAR) American Chemical Society." Insert appropriate information in place of the capitalized words.
- One-time permission is granted only for the use specified in your request. No additional uses are granted (such as derivative works or other editions). For any other uses, please submit a new request.

BACK | CLOSE WINDOW

VITA

Name: Supakarn Chamni

Address: Department of Pharmacognosy and Pharmaceutical Botany, Faculty
                    of Pharmaceutical Sciences, Chulalongkorn University, Pathumwan,
                    Bangkok, 10330, Thailand

Email Address: atomic_ta@yahoo.com

Education: B.S., Chemistry, Thammasat University, Thailand, 2005
                    Ph.D., Chemistry, Texas A&M University, U.S., 2011

Scholarship: The Royal Thai Government Scholarship for Ph.D. program

Current Position: Faculty position at Department of Pharmacognosy and
                    Pharmaceutical Botany, Faculty of Pharmaceutical Sciences,
                    Chulalongkorn University, Thailand in January 2012

Publications: "β-Lactam Congeners of Orlistat as Inhibitors of Fatty Acid
                    Synthase" by Zhang, W.; Richardson, R. D.; Chamni, S.; Smith, J.
                    W.; Romo, D. *Bioorg. Med. Chem. Lett.* **2008**, *28*, 2491-2494.

                    "Diazo Reagents with Small Steric Footprints for Simultaneous
                    Arming/SAR Studies of Alcohol-Containing Natural Products via
                    O–H Insertion" by Chamni, S.; Dang, Y.; He, Q-L.; Bhat, S.; Liu, J.
                    O.; Romo, D. *ACS Chem. Biol.* **2011**, ASAP.

Presentations: Poster presentation, 237th ACS National Meeting, Salt Lake City,
                    Utah, U.S., 2009; "Simultaneous Arming and SAR Studies of Natural
                    Products for Chemical Genetics"

                    Poster presentation and 3-min oral introduction, 2010 Marine Natural
                    Products, Gordon Research Conferences, Ventura, California, U.S.,
                    2010; "Simultaneous Arming and SAR Studies of Natural Products
                    for Chemical Genetics"

                    Oral presentation, 241st ACS National Meeting, Anaheim, California,
                    US., 2011; "Total Synthesis of Spongiolactone *via* a Nucleophile-
                    Catalyzed, Aldol-Lactonization Displaying Double
                    Diastereoselectivity and Kinetic Resolution"